A novel role for macrophages in peripheral nerve regeneration

Lucie Van Emmenis

Thesis submitted for the degree of Doctor of Philosophy

MRC Laboratory for Molecular Cell Biology

University College London

Funded by

CANCER
RESEARCH
UK

Declaration

I, Lucie Van Emmenis, confirm that the work presented in this thesis is my own. Where information has been derived from other sources, I confirm that this has been indicated in the thesis.

Signed……..... Date…….

Abstract

Peripheral nerves are one of the few adult tissues which can regenerate following injury, and macrophages have many important roles in this multicellular process. Following nerve injury, regrowing axons must traverse tissue termed the 'nerve bridge', which forms spontaneously between the nerve stumps (proximal and distal), to reconnect with their original tissue target. Previously, we found that hypoxic macrophages in the bridge induce the formation of a polarised vasculature which dedifferentiated Schwann cells subsequently use as a scaffold to migrate along, taking axons with them into the distal stump. Here, macrophages together with Schwann cells function to clear debris and remodel the environment to facilitate axonal regeneration, demonstrating distinct functions for macrophages within discrete areas of the regenerating nerve. This thesis aims to characterise nerve macrophage populations and to determine whether there is a specific Schwann cell chemoattractant within the bridge.

Resident nerve macrophages displayed a distinct gene expression pattern compared to other resident macrophage populations. Moreover, we found two distinct nerve resident populations which can be distinguished by CX_3CR1 expression and physiological location. In the injured nerve, the origin and phenotype of macrophage populations is currently unknown. We determined that the majority of macrophages in the bridge and distal stump are monocyte-derived. In further characterisation of bridge macrophages, we have identified an intrinsic ability to differentially sense hypoxia.

Here we show data to support a novel role for hypoxic bridge macrophages in promoting Schwann cell migration. Using *in vitro* chemotaxis assays, we found that hypoxic macrophages are able to induce Schwann cell migration and an unbiased screen identified the chemoattractant factor as CCL3. CCL3 is able to induce Schwann cell migration in chemotactic assays, and knockdown studies showed that CCL3 is the primary chemoattractant secreted by hypoxic macrophages. We also present preliminary *in vivo* experiments investigating the role of CCL3 following injury, as well as in models of nerve repair. A Schwann cell chemoattractant factor has wide therapeutic implications in peripheral nerve injury, as well as potential uses in the treatment of aberrant nerve growth and tumour spread.

Acknowledgements

I would first like to thank Alison for allowing me to work on this project, and for her perseverance throughout the multiple rounds of editing which she endured to arrive at the final product.

Thanks also to members of the Lloyd lab who, despite our reputation, have proved to be some of the kindest, most helpful, supportive and intelligent people I have encountered in the world of science. In particular, thanks to Anne-Laure who helped me find my feet in the lab, and who has provided day to day support and advice ever since. Thanks also to Julian and Elizabeth never fail to cheer me up and provide support and encouragement when I need it most. To the LMCB community, especially my fellow students, and our kindly neighbours in the Riccio lab for creating such a wonderful working environment.

Special thanks to the people who have contributed to the work presented here: James Phillips (Eastman Dental Institute, UCL) who provided invaluable advice on creating nerve conduits and provided surgical training, Heather West (Bennett lab, Department of Infection and Immunity, UCL) who conducted the flow cytometry experiments, Matthew Wedlich (Masters student) who completed repeats of qPCRs and Western blots, as well as providing me with a chemical burn scar which will serve as a lasting memory of his time in the lab.

To my committee members Clare Bennett, Dan Cutler and Ewa Paluch, as well as honorary committee member Julie Pitcher, who have provided all helpful advice and guidance on my project.

To my family, and all of my friends who have been my biggest cheerleaders and provided unwavering support of me over the last four years. Thank you for sticking with me despite my inability to be on time for anything, retreating from social events for the past 6 months and for humouring me by asking about my project; I know you don't really care.

And finally, to my Aleks; my flame, my muse. You have barely complained when you've had to bear the brunt of my near constant stresses and worries, and there's been minimal crying (from you), which is always a bonus. Thank you for always being there and for always knowing the right thing to say. I truly could not have done this without you, and I'm glad I didn't have to.

Table of Contents

List of Figures and Tables

List of Abbreviations and Acronyms

BBB	Blood brain barrier
BDNF	Brain derived neurotrophic factor
BMT	Bone marrow transplant
BNB	Blood nerve barrier
BSA	Bovine serum albumin
Cabo	Cabozantinib
CCL2	Monocyte chemoattractant protein-1
CCL3	Monocyte inflammatory protein-1 alpha/MIP-1α
CIL	Contact inhibition of locomotion
cMoP	Common monocyte progenitor
CMT	Charcot-Marie-Tooth disease
CNS	Central nervous system
CSF-1	Colony stimulating factor-1
CXCL12	Stromal derived factor-1/SDF-1
E(n)	Embryonic day (n)
ECM	Extracellular matrix
EM	Electron microscopy
FAC	Focal adhesion complex
FACS	Fluorescence-activated cell sorting
FAK	Focal adhesion kinase
GDNF	Glial cell line-derived neurotrophic factor
GMP	Granulocyte-macrophage progenitor
HIF-1α	Hypoxia-inducible factor-1 alpha
HSC	Haematopoietic stem cell
HUVECs	Human umbilical venous endothelial cells
KD	Knocked down
MAT	Mesenchymal-amoeboid transition
MDP	Macrophages and dendritic cell precursor

MPNSTs	Malignant peripheral nerve sheath tumours
NF1	Neurofibromatosis 1
NRG	Neuregulin
P(n)	Post-natal day (n)
P0	Protein 0
PFA	Paraformaldehyde
PLP	Proteolipid protein
PNI	Perineural invasion
PNS	Peripheral nervous system
PNS	Peripheral nervous system
RAGs	Regeneration-associated genes
rCCL3	Recombinant rat CCL3
RT-qPCR	Quantitative reverse transcription PCR
SCP	Schwann cell precursor
Scr	Scrambled siRNA
siRNA	Small interfering RNA
TAMs	Tumour associated macrophages
VEGF	Vascular endothelial growth factor
VEGFR2	Vascular endothelial cell growth factor receptor 2

Chapter One: Introduction

1.1. The peripheral nervous system

1.1.1. Structure

The peripheral nervous system (PNS) consists of neurons and supporting cells which allows the transmission of sensory and motor signals between the central nervous system (CNS, consisting of the brain and spinal cord) and the periphery (Catala and Kubis, 2013). The PNS can be divided into the somatic and autonomic nervous systems which regulate voluntary and involuntary nerve function respectively (Catala and Kubis, 2013). Each tissue is innervated by axons, which as they travel towards the spinal cord become organised into fascicles and larger nerve structures until reaching the spinal cord (Figure 1.1). Spinal nerves enter the spinal cord via the dorsal root, and leave via the ventral root, which is where the cell bodies of sensory and motor neurons reside (Catala and Kubis, 2013). Peripheral nerves vary greatly in size in humans, ranging from the cranial trochlear nerve which innervates a single muscle, to the sciatic nerve which extends out from the lower back to the thigh and innervates multiple muscles in the leg as well as the skin (Geuna, 2015, Catala and Kubis, 2013).

For all nerves, large and small, the mechanism of transmitting signals is the same: via the propagation of action potentials (Barnett and Larkman, 2007). First described in squid neurons in the 1950s (Hodgkin and Huxley, 1952), an action potential refers to a transient (<1 millisecond) reversal in polarity of the neuronal transmembrane which is propagated along the length of axons to axon terminals (Barnett and Larkman, 2007, Kress and Mennerick, 2009). The change in membrane polarity is caused by voltage gated sodium channels, which activate and subsequently inactivate, together with potassium channels to form the characteristic electrophysiological up- and downstroke of the action potential (Kress and Mennerick, 2009).

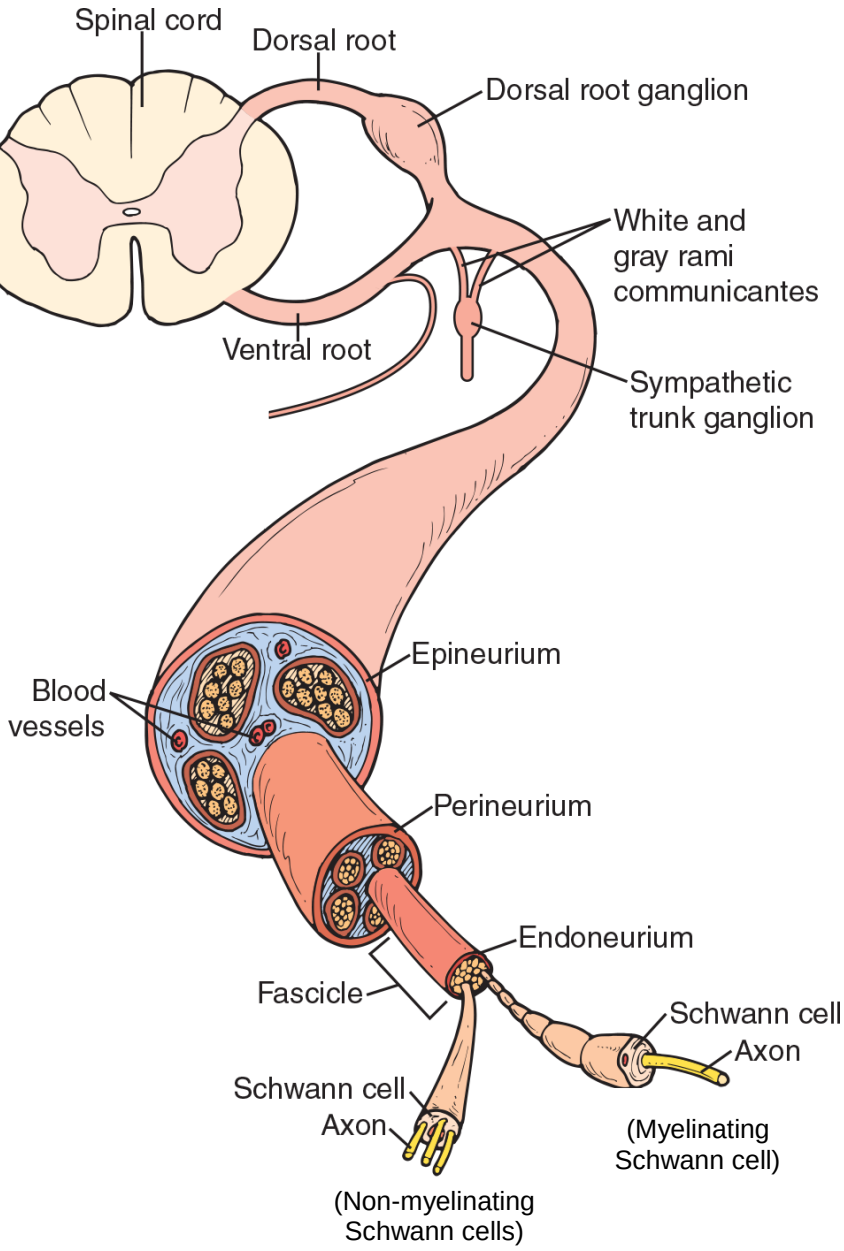

Adapted from (Kisner and Colby, 2012).

Figure 1.1 | Structure of the peripheral nervous system

Schematic showing the structure of a peripheral nerve. Single axons are grouped and organised into bundles to form fascicles, which may be further grouped to form larger nerves. All nerves enter the spinal cord via the dorsal roots, which are where the axon cell bodies are located.

Sodium channels are located on the soma, dendrites and axons, and the variations in ion channels contribute to the various action potential waveforms which can be observed in neurons (Kress and Mennerick, 2009).To carry out certain motor and sensory functions, the PNS requires the rapid transmission of action potentials. This is achieved by insulating axons with multiple layers of glial membrane (myelin) provided by oligodendrocytes in the CNS, and Schwann cells in the PNS (Barnett and Larkman, 2007, Nave and Werner, 2014). Action potentials are propagated along the length of nerves by the presence of Na^+ channels at high density in gaps in the myelin sheath known as Nodes of Ranvier, which allow the signals to jump from node to node via 'saltatory conduction' (Catala and Kubis, 2013, Barnett and Larkman, 2007). The presence of myelin surrounding axons allows nerve conduction to occur 20-100X faster compared to unmyelinated nerves (Nave and Werner, 2014). The ratio of myelin sheath thickness to axon diameter is crucial to ensure appropriate signal conduction, with the optimal ratio of axon diameter to myelin fibre diameter, or g-ratio, being on average 0.6-0.7 in humans (Kidd et al., 2013). Any significant changes from these values may indicate pathologies such as neuropathies (Nave and Werner, 2014).

Peripheral nerves have an organised structure which is intended to protect and support the axons and thus ensure the successful transmission of action potentials. Peripheral nerves consist of bundles of axons which are closely associated with Schwann cells, the main glial cell type within the PNS. To exert their function of providing insulation and/or support for axons, Schwann cells can either myelinate axons by associating in a 1:1 ratio with large diameter axons, or group together smaller diameter axons to form Remak bundles (Figure 1.2) (Bhatheja and Field, 2006, Kidd et al., 2013). Surrounding the individual axon and Schwann cell units is a matrix structure known as the endoneurium. The nerve fibres and endoneurium are further grouped into fascicles which are surrounded by a layer of fibroblast like cells, termed the perineurium. Peripheral nerves may consist of single or multiple fascicles, depending on the size of the nerve, which are surrounded by the epineurium. The epineurium consists of two distinct layers: the inner layer composed of densely structured collagen fibrils and elastic fibres, and the outer layer is composed of areolar connective tissue and collagen bundles which are arranged in a loose structure (Stolinski, 1995). The epineurium also contains vascular and lymphatic vessels.

Similarly to the blood brain barrier (BBB), the blood nerve barrier (BNB) functions to regulate and restrict the exchange of material between the privileged nerve microenvironment and the

extracellular space (Weerasuriya and Mizisin, 2011, Nakatsuji, 2017, Napoli et al., 2012). The BNB consists of the perineurium which contains zona occludens tight junctions between the cells to prevent the exchange of material, as well as the endoneurial vascular endothelium. The BNB interface is highly complex and regulated, and the integrity of this structure is important for ensuring the nerve is protected from harmful blood-borne materials and to maintain the homeostatic exchange of molecules necessary for correct nerve function (Nakatsuji, 2017). There are also blood vessels located within the space between the perineurium and the epineurium, which do not have a barrier function, and together with blood vessels in the endoneurium provide the nerve with oxygen and nutrients.

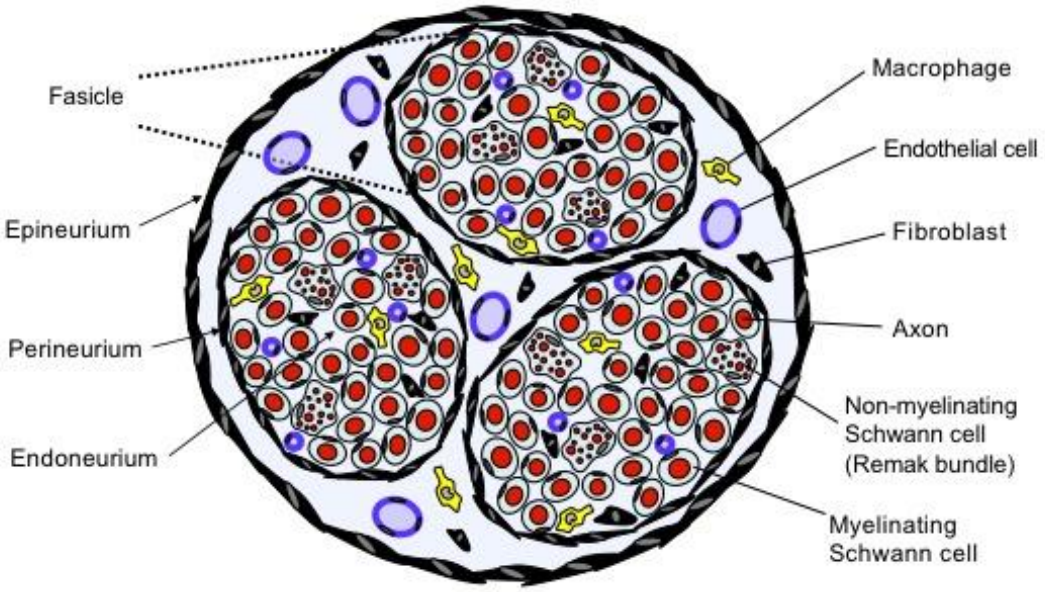

Figure 1.2 | Structure of the peripheral nerve
Schematic of a cross section of a peripheral nerve. There are multiple layers of organisation, including the outer epineurium which can enclose multiple fascicles. Each fascicle consists of bundles of myelinated axons, and Remak bundles, together with blood vessels, and resident populations of fibroblasts and macrophages, which are surrounded by the perineurium.

Within individual fascicles there are also resident populations of fibroblasts (Jessen and Mirsky, 2005) and macrophages (Griffin et al., 1993, Ydens et al., 2012). In particular the resident macrophages are thought to play an important role in peripheral nerve homeostasis as well as contributing to the PNS injury response which will be discussed further in later sections (Mueller, 2003). The roles of macrophages in the nerve during health and disease will be discussed in more detail in later sections of this thesis.

In its homeostatic state, the adult nerve is a quiescent tissue compared to many others in the body such as the intestine or the skin, which have populations of epithelial cells which have a high turnover (Richardson et al., 2014). Recent unpublished data from our lab using long term labelling studies have shown that within the stable, quiescent nerve environment, cells have extremely slow rates of turnover (Stierli et al., in preparation), which is perhaps beneficial for the stable transmission of signals between the periphery and the brain. Despite this highly complex structure and quiescent state, the PNS is one of the few tissues in the adult mammal which has the ability to extensively regenerate following injury. This is in contrast to the central nervous system (CNS) which is unable to recover substantially after damage is sustained. In part, this ability to regenerate is due to Schwann cells and their highly plastic nature which allows them to dedifferentiate following injury, and coordinate a repair response.

1.1.2.Schwann cell biology and development

Schwann cells are main glial cell type of the PNS and are the most prevalent cell type (~70%) in the sciatic nerve (Salonen et al., 1988) (Stierli et al., in preparation). Schwann cells in the quiescent adult nerve can exist in one of two types: myelinating or non-myelinating (Nave and Werner, 2014, Monk et al., 2015, Jessen and Mirsky, 2016). Myelinating Schwann cells associate in a 1:1 ratio with large calibre axons and function to insulate the axons through the formation of a myelin membrane (Bhatheja and Field, 2006, Nave and Werner, 2014, Monk et al., 2015). Non-myelinating Schwann cells group together bundles of small calibre axons to form Remak bundles (Armati and Mathey, 2013). The main functions of Schwann cells are to protect and support axons by providing nutrients, as well as being responsible for the myelin production required for salutatory conduction, which forms in response to axonal-derived signals (Nave and Werner, 2014, Catala and Kubis, 2013, Kidd et al., 2013).

1.1.2.1. Schwann cell development

Neurulation occurs from embryonic day 8 (E8) in mice and during this time the neural tube is formed, with the neural groove deepening before folding and closing, and subsequently forming the CNS (Copp et al., 2003). Crucially, a subpopulation of cells from the neural tube known as neural crest cells migrate to form the PNS, giving rise to multiple cell types such as neurons, endocrine cells and Schwann cells (Figure 1.3) (Bhatheja and Field, 2006, Monk et al., 2015, Catala and Kubis, 2013).

Neural crest cells differentiate into a number of intermediate cell types (such as neural crest-derived progenitors) before differentiating into Schwann cells, a process which involves endothelin and Notch signalling, and is controlled by the transcription factor Sox10 (Bhatheja and Field, 2006, Jessen and Mirsky, 2005, Finzsch et al., 2010). Sox10 is highly expressed in the developing PNS, specifically within Schwann cells, and genetic knockout studies have shown that without Sox10, Schwann cells are absent from axons, indicating the essential requirement of this transcription factor for Schwann cell identity (Finzsch et al., 2010, Bhatheja and Field, 2006).

Forming one of the transient, intermediate stages between neural crest cells and mature Schwann cells are Schwann cell precursors (SCP) which are present at E12-13 in mice, and require trophic support from sensory and motor neurons in order to survive (Jessen and Mirsky, 2005). SCPs are defined as migratory $Sox10^{+}$, neural crest-derived cells which are associated with neuronal projections, and are able to migrate the length of developing nerves (Monk et al., 2015, Adameyko et al., 2009). Contact with axons is crucial for Schwann cell fate, as well as their survival, proliferation and differentiation. These signals are mediated partly by neuronal Neureguin-1 (NRG1) and Schwann cell ErbB2/3 receptor signalling (Adameyko et al., 2009). Upon contact with axons, SCPs upregulate markers such as protein 0 (P0) and proteolipid protein (PLP) as they mature into Schwann cells (Jessen and Mirsky, 2005). Schwann cells function to support axonal outgrowth through a number of Schwann cell derived growth factors such as nerve growth factor (NGF), brain-derived neurotrophic factor (BDNF) and glial cell line-derived neurotrophic factor (GDNF) (Kidd et al., 2013, Jessen and Mirsky, 2005).

SCPs also have the capacity to differentiate into melanoblasts, which give rise to melanocytes in the skin (Adameyko et al., 2009), however it is their association with axons which induces maturation into a Schwann cell (Adameyko et al., 2009, Jessen and Mirsky, 2005). SCPs are able to comigrate along with developing axons, and are dependent on axons for survival, proliferation and migratory signals (Monk et al., 2015). Intermediate Schwann cells are generated from SCPs from E13-15, which coincides with a major stage in the development of peripheral nerves (Jessen et al., 2015, Jessen and Mirsky, 2005). Intermediate Schwann cells are easily distinguishable from SCPs due to their lack of migration, the dependence on autocrine, rather than axonal-derived, survival signals, as well as the deposition of an organised basal lamina (Monk et al., 2015).

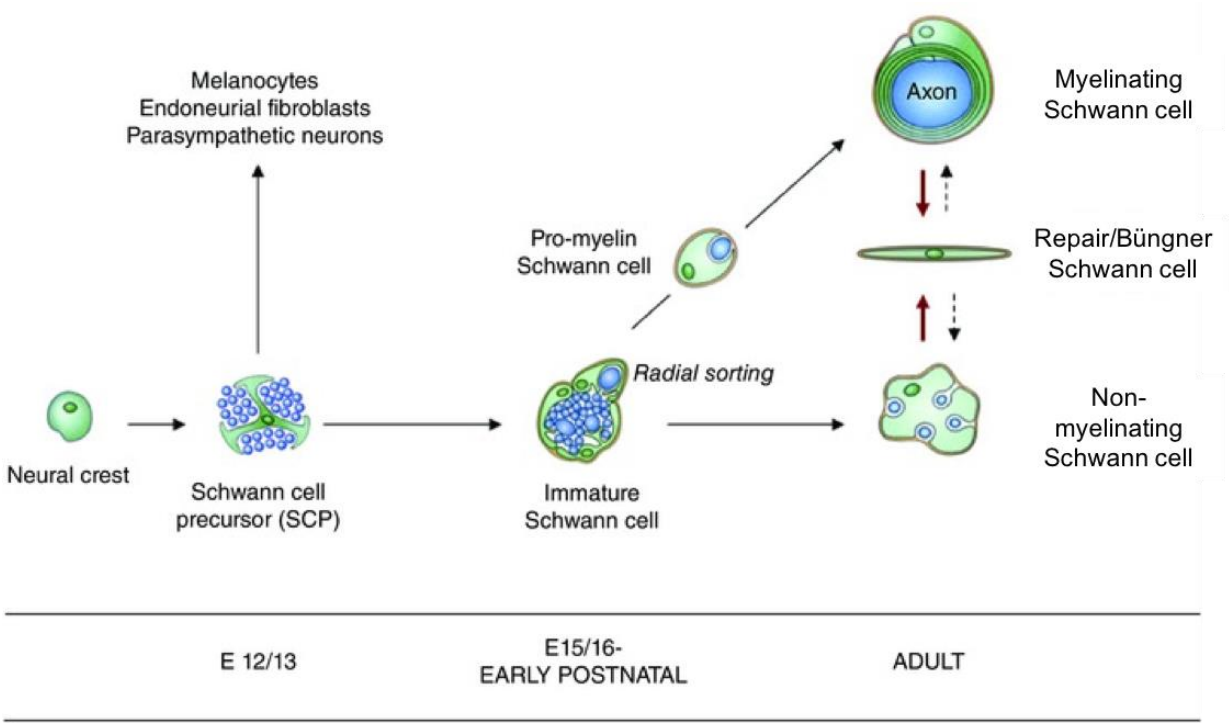

Adapted from (Jessen and Mirsky, 2016).

Figure 1.3 | Schwann cell development
The differentiation stages of Schwann cell development. Neural crest cells differentiate into SCPs, which can also produce melanocytes and endoneurial fibroblasts. Immature Schwann cells develop, and radial sorting results in Schwann cells associating in a 1:1 manner with axons in the nerve, or the formation of Remak bundles. Following injury, mature Schwann cells may dedifferentiate into a 'repair' phenotype which may proliferate and migrate, and have key roles in nerve regeneration.

The association of Schwann cells with axons during this time determines whether mature Schwann cells will be myelinating or non-myelinating in the adult nerve, and occurs via a process known as radial sorting, which begins during development and continues until approximately post-natal day 10 (P10) in mice (Feltri et al., 2016). In the process of radial sorting, bundles of axons are progressively sorted and segregated by Schwann cells which subdivide the axons until the larger calibre axons remain in contact with a single Schwann cell, and any remaining groups of axons form Remak bundles (Feltri et al., 2016). The ability of Schwann cells to sort axons in this manner is dependent on the formation of cytoplasmic protrusions which can extend into the bundles of axons, as well as many molecular components such as cell surface receptors (e.g. Gpr126 (Mogha et al., 2013)), adhesion molecules (e.g. β-integrin) and extracellular matrix (ECM) components (e.g. laminins) (Jessen and Mirsky, 2005, Feltri et al., 2016).

Myelinating Schwann cells associate in a 1:1 manner with large calibre (>1μm diameter) axons. For large diameter axons, Schwann cells wrap many layers of tightly packed myelin cell membrane around a section of axon, this is unlike in the brain where a single oligodendrocyte may enwrap several adjacent axons (Nave and Werner, 2014, Monk et al., 2015, Catala and Kubis, 2013). Wrapped sections of axon are termed internodes which can be >2mm in length, which requires 20mm^2 myelin membrane (Nave and Werner, 2014). In between these wrapped sections are the nodes of Ranvier, which contain large numbers of sodium ion channels which help to potentiate action potentials along the length of the axon, and ensure correct signal propagation (Catala and Kubis, 2013).

Immature and mature Schwann cells can also support their own survival in an autocrine manner through the release of survival factors such as insulin-like growth factor 2, neurotrophin 3 and platelet derived growth factor-β (Jessen and Mirsky, 2005). Once Schwann cells have associated with axons and differentiated into their mature form, there must be a regulated exit from the cell cycle, which results in a loss of proliferative capacity and a switch to a quiescent cell state (Feltri et al., 2016, Woodhoo et al., 2009). The transcription factor Krox20/Egr2 (expressed from E16 in mice) together with Sox10, a nuclear transcription factor, is critical for the differentiation of immature Schwann cells into mature, myelinating cells (Monk et al., 2015).This transition out of the cell cycle is regulated by a number of factors including Jun, the cAMP/PKA signalling axis, as well as neuregulins (Monk et al., 2015). Premature exit from the cell cycle and differentiation has been associated with polyaxonal myelination, where multiple axons are myelinated by a single Schwann cell (Jessen and Mirsky, 2005).

1.1.2.2. Schwann cell myelination

Schwann cells provide key nutritional and metabolic support for axons, and myelin/lipid homeostasis is a key factor in maintaining the stability of myelinating axons (Nave, 2010, Monk et al., 2015). Schwann cells increase lipid production, and decrease lipid oxidation which results in the lipid content (cholesterol and sphingolipids) of myelin membranes being higher than that found in most other cell membranes (Barrette et al., 2013). The high concentration of lipid in the myelin sheath is important to ensure neuron integrity is retained, as well as allowing fast saltatory conduction to occur (Barton et al., 2017).

Following Schwann cell association with an axon, as the Schwann cell wraps a single axon, it differentiates into a myelin-forming cell through changes to gene expression mediated by Krox-20, a

transcription regulator, and this begins a process where myelin membranes are wrapped in a spiral shape around the axon (Kidd et al., 2013). Krox-20 interacts with Sox-10 to promote myelin gene induction and lipid biosynthesis pathways, which are crucial for myelination (Jacob et al., 2014, Monk et al., 2015). In Krox-20 null mice, although Schwann cells are able to successfully associate in a 1:1 manner with axons, they are not myelinated, which highlights the important transcriptional role of Krox-20 in this process (Topilko et al., 1994, Parkinson et al., 2004). Additionally, expression of Krox-20 in non-Schwann cells is sufficient to induce transcriptional programs to leave the cell cycle and induce myelin gene expression, and therefore can be termed a 'master regulator' (Parkinson et al., 2004).

Interactions between axons and Schwann cells are key for inducing the transcriptional programming that is essential for myelination to occur. In particular NRG1 type III expression by axons, which binds to ErbB2/3 receptors on Schwann cells (Newbern and Birchmeier, 2010, Raphael and Talbot, 2011), is a key determinant in the switch to the myelinating Schwann cell fate as well as regulating myelin thickness. Moreover, this pathway has also been linked to the formation of Remak bundles (Fricker et al., 2009, Taveggia et al., 2005). Overexpression of NRG1 type III *in vivo* leads to a significant increase in myelin sheath thickness and the myelination of axons that normally would not be myelinated (Monk et al., 2015). Moreover, genetic studies in mice have shown that deficiencies in either NRG1 type III or ErbB receptors leads to a failure to myelinate (Kidd et al., 2013). The myelination process is also controlled by factors such as BDNF which act via neurotrophin receptors as a pro-myelination signal, and Notch signalling which acts as a myelin inhibitor (Woodhoo et al., 2009).

The G-protein coupled receptor (GPCR) GPR126 has also been described to be essential for Schwann cell myelination (Mogha et al., 2013). GPR126 drives the differentiation of Schwann cells through an increase of cAMP, and subsequent phosphorylation of PKA which causes Oct6 and Krox-20 transcription and therefore promotes myelin gene activity (Mogha et al., 2013). Elevated cAMP levels also repress the expression of proteins implicated in maintaining Schwann cells in an immature state, which further promotes differentiation into a mature, myelinating state (Liebscher et al., 2014, Monk et al., 2015).

Non-myelinating Schwann cells sort small calibre (<1μm diameter) axons and bring them together to form Remak bundles (Monk et al., 2015, Feltri et al., 2016). Remak bundles consist of a single Schwann cell, which does not form myelin, which has multiple axons embedded within invaginations in the plasma membrane (Armati and Mathey, 2013, Catala and Kubis, 2013). A single

non-myelinating Schwann cell may enwrap different kinds of axons such as mixtures of sensory and autonomic axons. Additionally, unmyelinated axons may interchange between different Remak bundles along the length of the nerve which means that the same axons are not likely to remain surrounded by the same neighbouring axons for any significant distance (Kidd et al., 2013, Feltri et al., 2016).

Both myelinating and unmyelinating Schwann cells contribute to the stable and quiescent environment in the healthy, adult nerve. An important feature of Schwann cells however, is their phenotypic plasticity, which allows dedifferentiation from their mature phenotype back into a progenitor-like cell, which has the ability to proliferate and migrate; a property which is particularly significant following nerve injury (Jessen et al., 2015).

1.2. Cell migration

1.2.1. Principles of cell migration

Cell migration is required for many different physiological processes in both health and disease (Scarpa and Mayor, 2016, Paul et al., 2017, te Boekhorst et al., 2016). For many cell types, migration is limited to periods during development or morphogenesis, however for some cells such as leucocytes, the ability to migrate is required for their biological function (Friedl and Wolf, 2010). The immune system relies on monocytes to migrate and patrol the vascular system as an immunosurveillance mechanism (Trepat et al., 2012, Das et al., 2015) and in response to inflammation or injury, the rapid recruitment of immune cells initiates the healing process (Trepat et al., 2012). The ability of tumour cells to migrate and metastasise results in an increase the morbidity of most cancer types (Paul et al., 2017).

Different cells may use different mechanisms to migrate, however the basic principles remain similar across all types. For cells to migrate in a particular direction, a front-rear axis of polarity is established which enables a cell to orientate itself and to organise the migration machinery to specific locations, depending on the mechanism of migration (Mayor and Etienne-Manneville, 2016, Theveneau et al., 2010, Jin et al., 2008). Cells may also migrate in response to an extracellular cue such as a gradient of chemoattractant, or another cell or cells (Theveneau et al., 2010, Trepat et al., 2012). Upon sensing an external cue, cells are able to repolarise and undergo intracellular reorganisation to allow directional migration. The surface upon which a cell migrates may also influence the mechanism of migration in 2D whereas the interactions with the surrounding matrix in 3D situations can affect the formation of focal adhesion complexes and their mode of migration (Liu et al., 2015). The surrounding

environment also affects the traction forces which are exerted, and the extent to which the environment is remodelled to permit cell migration (Liu et al., 2015, Trepat et al., 2012).

The mechanism of cell migration is dependent on many different variables such as cell type, whether migration is occurring singly or as part of a group of cells, as well as the migration substrate (Charras and Sahai, 2014, Liu et al., 2015, Theveneau et al., 2010). Broadly however, cells may be classified as migrating either as an individual cell, in a mesenchymal or amoeboid manner, or as a collective, cohesive group of cells (Trepat et al., 2012). Cells such as fibroblasts can migrate in a mesenchymal manner which involves the formation of specialised cell-matrix focal adhesion complexes (Trepat et al., 2012). Cells which migrate in this way display high levels of attachment and cytoskeletal contractility (Liu et al., 2015). This tends to be a slower mechanism of migration with cells achieving 0.1-1μm/min (Friedl and Wolf, 2010, Liu et al., 2015). Amoeboid migration is typically described as occurring in the absence of focal adhesions or stress fibres, and is classically adopted by rounded cells (Liu et al., 2015). Amoeboid migration may also be divided into two subtypes of migration. The first is a blebby, rounded migration style of migration in which cells, such as Zebrafish macrophages, do not adhere to substrates and instead push or propel themselves in order to move (Bergert et al., 2015). The second type involves the generation of actin-rich filopodia at the leading cell edge which weakly adhere to the substrate and allow cells, such as leucocytes, to pull themselves forward (Lämmermann et al., 2008). Using this method, cells may migrate at up to 10μm/min which in the context of cell migration is quite fast; amoeboid migration typically has a higher velocity compared to mesenchymal migration (Friedl and Wolf, 2010, Liu et al., 2015).

Many cell types, including Schwann cells and fibroblasts, also exhibit a degree of migration plasticity, and are able to change their mechanism of migration based on environmental variables and factors such as cellular contractility and cell adhesion (Charras and Sahai, 2014, Liu et al., 2015, Theveneau et al., 2010, Cattin et al., 2015). Cells can either undergo mesenchymal-amoeboid transition (MAT), or epithelial to mesenchymal transition which represents a change in the mechanism of migration (Liu et al., 2015). Cancer cells in particular exhibit changes to their migration which enables them to detach from a primary tumour site, and metastasise (Jin et al., 2008, Paul et al., 2017). Cancer cells *in vitro* have been observed to display multiple different modes of migration, and *in vivo* a similar variable phenotype is observed as the cancer cells metastasise, remodel the local environment and infiltrate new tissues (Clark and Vignjevic, 2015).

It is well established that collective cell migration relies on the same principles as single migrating cells (Mayor and Etienne-Manneville, 2016). Groups of cells adopt a front to rear polarity which is mediated by cell substrate interactions, such as focal adhesion complexes, as well as extracellular signals such as chemoattractants (Mayor and Etienne-Manneville, 2016, Theveneau et al., 2010). In order to migrate, cells within the middle of the cluster maintain homotypic cell-cell adhesions and are inhibited from migrating, whilst cells at the outer edge of the group display homotypic cell-cell repulsion properties (Scarpa and Mayor, 2016, Friedl and Wolf, 2010, Trepat et al., 2012). As a result, groups of cells may migrate in sheets, for example epithelial cells, or as cords, for example Schwann cells following injury (Parrinello et al., 2010, Cattin et al., 2015). Collective cell migration is more effective than single cell migration at generating directed migration towards a stimulus, and therefore is often seen in development (Mayor and Etienne-Manneville, 2016, Friedl and Wolf, 2010). Collective cell migration is a fundamental part of development and morphogenesis, and aids processes such as tissue remodelling, as well as contributing to local tissue cancer cell invasion (Scarpa and Mayor, 2016, Liebig et al., 2009). Collective cell migration is clearly an important process which occurs during nerve regeneration, and how Schwann cells collectively migrate is one of the research areas of the Lloyd lab.

1.2.2. Cell migration towards a stimulus: chemotaxis

For most cells, non-directional migration is an inefficient way of migrating, whereas directional migration towards a particular stimulus or to a find a specific interacting cell or molecule forms a part of key physiological processes (Kay et al., 2008). Chemotaxis is the ability of the movement or migration of a cell or cells to be directed in response to an extracellular gradient (Roussos et al., 2011, Kay et al., 2008). Chemotaxis was first described in bracken fern spermatozoa in 1884 (Pfeffer, 1884), and in the following years, in leucocytes which migrated toward the site of irritation in a rabbit cornea (Leber, 1888), and the slime mould *Dictyostelium discoideum* which was observed to migrate towards the source of diffusible signals (Bonner, 1947). Subsequently, chemotaxis has been described in a wide variety of cell types and in many different processes such as the recruitment of inflammatory cells to sites of infection, organ development during embryogenesis, would healing as well as contributing towards cancer cell metastasis (Jin et al., 2008, Roussos et al., 2011, Kay et al., 2008, Weavers et al., 2016).

Cells respond to gradients by sensing the difference between the front and the rear of the cell, which gives spacial information regarding the source of the chemoattractant (Van Haastert and Devreotes, 2004). In response to a chemoattractant gradient, cells then orientate themselves through actin repolarisation and migrate towards the source of the chemoattractant for a sustained period of time (Van Haastert and Devreotes, 2004, Roussos et al., 2011, Jin et al., 2008). Chemotaxis can occur in single cells, as well as in groups of cells, which is often seen during developmental processes and organogenesis as well as during regeneration. The direction of migration often occurs in response to a particular stimulus, for example well characterised chemoattractants for endothelial cells and fibroblasts are vascular endothelial growth factor (VEGF) (Cattin et al., 2015, Hobson et al., 2000) and platelet-derived growth factor (PDGF) (Wu et al., 2012) respectively.

1.3. Peripheral nerve injury and regeneration

1.3.1. Injury response

Despite the cellular complexity of the peripheral nerve, it displays the remarkable ability to regenerate following injury (Figure 1.4) (Dolenc and Janko, 1976, Fawcett and Keynes, 1990, Ide, 1996, Chen et al., 2007, Huebner and Strittmatter, 2009, Fex Svennigsen and Dahlin, 2013, Cattin and Lloyd, 2016). Peripheral nerve regeneration is a coordinated, multicellular process which requires directed migration, new tissue formation and remodelling as well as vascularisation (Zochodne, 2012, Cattin and Lloyd, 2016, Lundborg, 2003, Fawcett and Keynes, 1990, Fex Svennigsen and Dahlin, 2013). This ability to regenerate is even more extraordinary given the quiescent nature of many of the PNS cell types involved.

Following a full nerve transection, the distal portion of the injured axons degenerate in a process known as Wallerian degeneration, and contact with the nerve target is lost. The two nerve stumps (proximal and distal) initially retract but are then reconnected by the formation of new tissue, termed the ‘nerve bridge’, that spontaneously forms as the result of an unknown mechanism between the two stumps (Figure 1.4a-b). The loss of contact between the nerve and target is the main problem following nerve injury, and therefore the primary aim of regeneration is to facilitate the repair of contact between

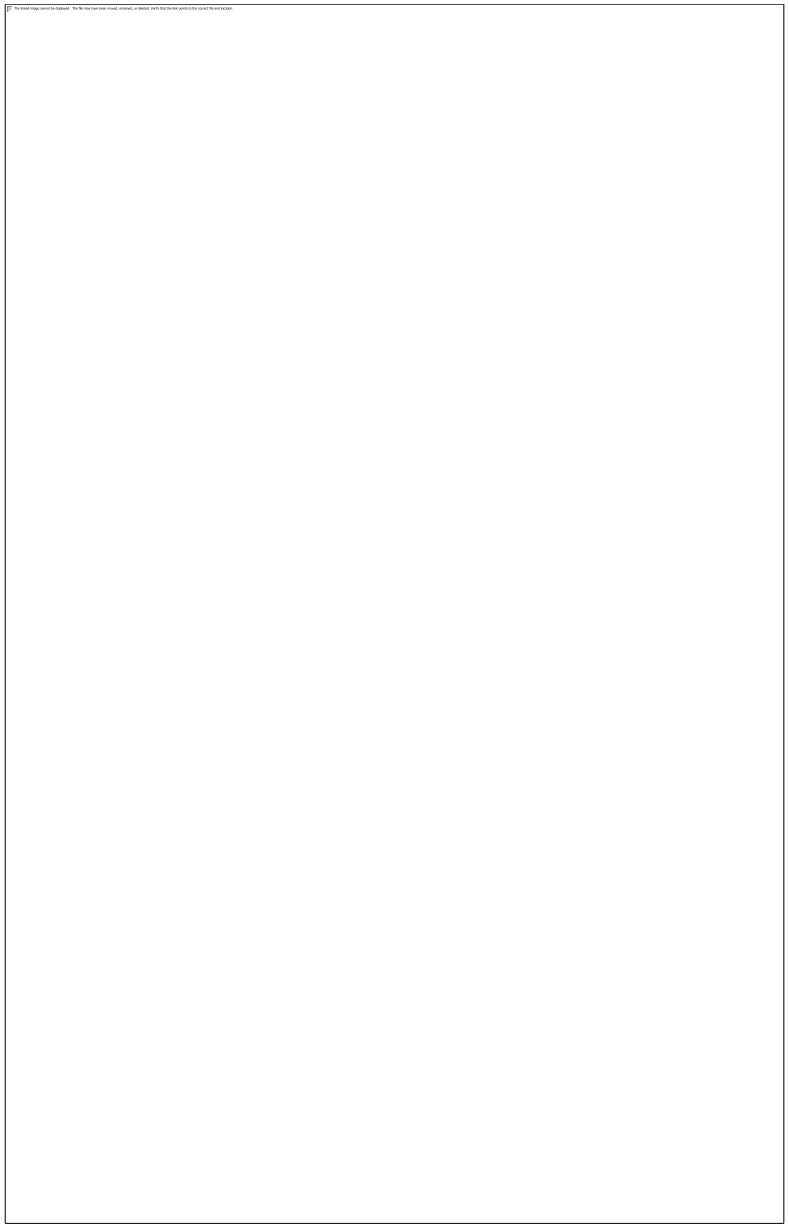

Adapted from (Cattin and Lloyd, 2016)

Figure 1.4 | The peripheral nerve can regenerate following injury.
Schematic of peripheral nerve regeneration following full transection. Following transection of a peripheral nerve, the stumps initially retract (a) but are reconnected by new tissue known as the nerve bridge (b). Initially the bridge is hypoxic due to lack of vascularisation. This is specifically sensed by macrophages, which secrete VEGF that promotes angiogenesis. Downstream of the transection in the distal stump, the axons degenerate in an active process known as Wallerian degeneration. In response to the injury, Schwann cells disassociate from the degenerating axons and dedifferentiate to a progenitor-like state that orchestrates many aspects of the regenerative process, including macrophage recruitment, clearance of axonal and myelin debris and remodelling of the environment to create a permissive environment for axonal regrowth. It also involves the formation of the bands of Büngner (c) that result from Schwann cells elongating along the length of their original basement membrane to create directional tubes, which occurs in the distal stump. Meanwhile, the bridge has become vascularised in response to the macrophage-induced VEGF signal and SCs migrate along the vasculature, taking the regrowing axons across the bridge and into the distal stump. Here, the axons re-innervate their targets and the Schwann cells recognising the axons, redifferentiate from the progenitor state, and the inflammatory response resolves to complete the regeneration process.

the damaged axon and its original tissue target (Cattin and Lloyd, 2016). A major challenge for the regrowing axons is to cross the nerve bridge, a tissue which appears to be a non-directional hostile environment lacking the directionality signals that guide growing axons during development.

Schwann cells are central organisers of this multicellular regeneration process. Immediately following injury, Schwann cells dissociate from axons and dedifferentiate to a progenitor-like state and as a result re-acquire many of the properties from early developmental stages such as proliferation, growth factor production and the ability to migrate (Scheib and Hoke, 2013, Napoli et al., 2012). The dedifferentiated Schwann cells have major roles in the regeneration process. Firstly, Schwann cells play an important role in aiding axonal outgrowth across the bridge (Figure 1.4c). Following the injury, they emerge from both stumps, cluster and form cords which migrate across the bridge, with the Schwann cells from the proximal stump guiding the regrowing axons. Schwann cell-axon interactions are necessary to ensure directional outgrowth from the proximal stump, it has been observed that axons migrating without a Schwann cell guide show restricted growth of only a few microns into the nerve bridge (Parrinello et al., 2010, McDonald et al., 2006). It was shown that without the guidance of Schwann cells, axons are unable to successfully traverse the nerve bridge and return to their tissue target, making Schwann cell migration a key mediator of axonal regrowth (Parrinello et al., 2010).

In order to cross the bridge, we have recently found that Schwann cell cords use newly formed blood vessels as a scaffold to migrate along (Cattin et al., 2015). Without the support of a blood vessel structure, we have observed that Schwann cells are unable to migrate within an *in vitro* 3D gel environment. Additionally, when blood vessel formation is prevented *in vivo*, Schwann cell migration is inhibited, which shows a requirement of blood vessels for Schwann cell migration. The blood vessels form as a result of the release of vascular endothelial growth factor (VEGF) which is released by macrophages in the bridge as a result of the hypoxic bridge environment. Importantly, the vascularisation of the bridge occurs parallel to the nerve axis providing a polarised track for the cords of Schwann cells to find their way across the bridge.

Secondly, following nerve injury, Schwann cells induce an inflammatory and regenerative response that functions to clear cellular debris and remodel the injured nerve area to provide a conducive environment for axonal regrowth (Napoli et al., 2012). The tissue environment in the distal stump must be remodelled in order to facilitate axonal regrowth, due to the inhibitory nature of myelin for axonal regrowth. This process is particularly important as removal of debris reduces the likelihood

of remyelination causing nerve compression, and in addition any potential inhibitors of axonal outgrowth are also removed (Kidd et al., 2013). Upon entering the distal stump, the regenerating axons locate the bands of Büngner, tube-like structures consisting of specialised Schwann cells within their basement membranes, which provide a substrate and a directionality to the regrowing axons, leading them back towards their original targets to ensure injury resolution (Figure 1.4c-d) (Fawcett and Keynes, 1990). Despite this remarkable ability of axons to regenerate and enter the distal stump, in humans axonal regrowth is often delayed and incomplete (Boerboom et al., 2017). If regeneration is delayed, chronic denervation of the distal stump presents a barrier for successful repair as the environment becomes less able to support axonal regrowth and regeneration is inhibited. It is important therefore that in humans following injury, that the environment is conducive for successful axonal regrowth. Schwann cells play a major role in ensuring that the regenerating environment is supportive and permits axonal regrowth (Jessen and Mirsky, 2016).

The normal, healthy nerve is a quiescent tissue, as previously mentioned many cell types within the nerve have a slow turnover, including non-myelinating Schwann cells, whilst myelinating Schwann cells appear not to divide in adulthood under homeostatic conditions. Following injury however, Schwann cells display highly plastic qualities, as they dedifferentiate to a progenitor-like phenotype in response to the injury environment and dissociate from axons (Napoli et al., 2012, Jessen et al., 2015, Woodhoo et al., 2009, Harrisingh et al., 2004). This dedifferentiation process enables Schwann cells to migrate, which is important during the nerve regeneration process.

The dedifferentiation process in Schwann cells involves activation of the Raf/MEK/ERK signalling cascade which induces a reprogramming of the Schwann cells, which is observed in both the tip of the proximal stump, as well as the distal stump (Figure 1.5) (Harrisingh et al., 2004, Napoli et al., 2012, Sheu et al., 2000). Other pathways important for the dedifferentiation-state of Schwann cells include c-Jun, which is induced by ERK and has a role in the dedifferentiation process as a negatively regulator of the transcription of the myelin genes (Woodhoo et al., 2009). In addition, c-Jun has a role in axonal regeneration, by promoting axonal survival through regulating expression of the secreted neurotrophic factors GDNF and Artemin in Schwann cells (Fontana et al., 2012, Arthur-Farraj, 2012). Notch signalling expression is sufficient to revert the myelinating Schwann cells to a demyelinating state (Woodhoo et al., 2009). Acting cell-autonomously, Ras activation induces Schwann cell dissociation

from axons, which is mediated by a loss of Sema4F expression by the Schwann cells which indirectly mediates hyper proliferation (Parrinello et al., 2010).

Dedifferentiated Schwann cells upregulate proteins which are downregulated during the myelination differentiation program, such as Sox 2, EphB2, glial fibrillary acidic protein (GFAP) and neural cell adhesion molecule 1 (NCAM1) (Deborde et al., 2016, Chen et al., 2007). Conversely, key myelin proteins such as P0 and myelin basic protein (MBP), as well as periaxin are downregulated (Chen et al., 2007, Jessen and Mirsky, 2008). Neuregulin and notch signalling are also upregulated, and these pathways aid Schwann cell proliferation during injury (Mei and Xiong, 2008, Woodhoo et al., 2009). Dedifferentiated Schwann cells secrete laminin, fibronectin, glypican, collagens II, IV and V, which are all important factors in promoting axonal outgrowth and guidance (Zochodne, 2012, Boerboom et al., 2017, Fex Svennigsen and Dahlin, 2013).

The dedifferentiated Schwann cells act to clear the myelin and axonal debris through phagocytic processes, trigger the opening of the blood nerve barrier and induce an inflammatory response, in which monocytes, neutrophils and mast cells are recruited to the nerve. Together this results in an environment that contributes to the repair of the damaged nerve (Napoli et al., 2012). Myelin breakdown occurs by first creating small fragments of myelin. The myelin pieces are next transported to the lysosome for selective digestion via mTOR-independent autophagy (Gomez-Sanchez et al., 2015). Autophagy is observed to be highly upregulated in Schwann cells following injury, and moreover, inhibition of autophagy pathways leads to a reduction in myelin clearance and a decreased rate of regeneration (Gomez-Sanchez et al., 2015).

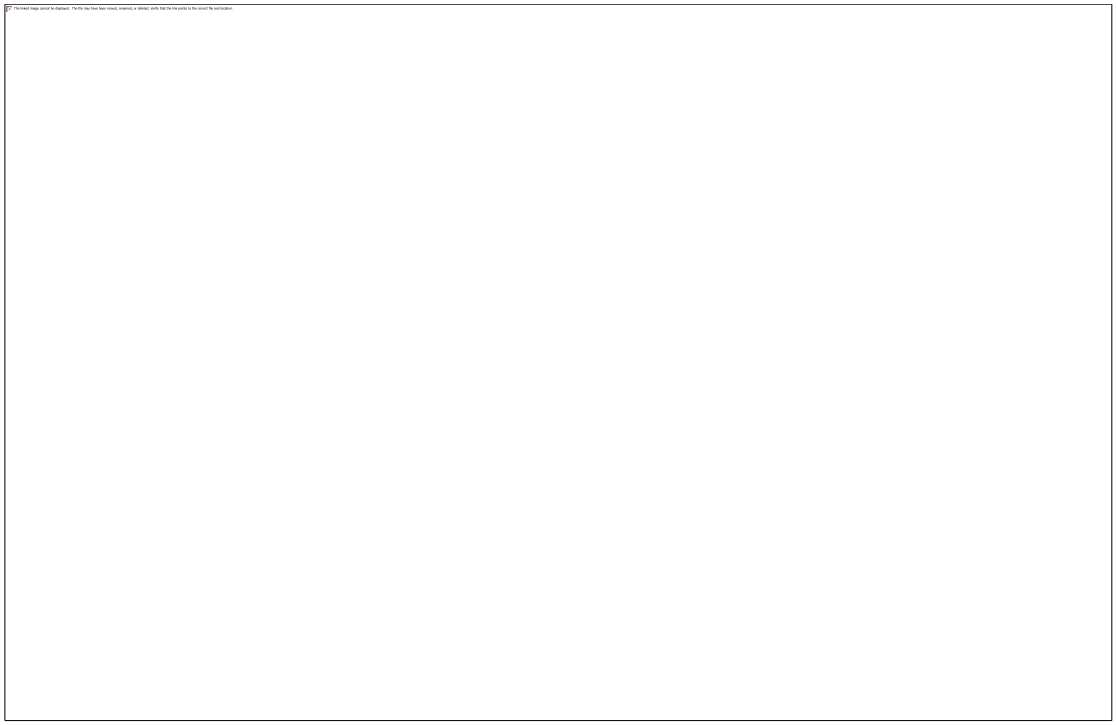

Figure 1.5 | Schwann cells orchestrate the nerve regeneration process.
Following injury, Ras activation in Schwann cells promotes dedifferentiation to a progenitor-like state. These Schwann cells perform multiple crucial roles during nerve regeneration including opening the BNB, inducing an inflammatory response, and the secretion of neurogenic factors.

The dedifferentiation of Schwann cells to this progenitor-like state is only a transient step in regeneration, when axons have regrown Schwann cells differentiate again to a mature myelinating or non-myelinating phenotype, and return to carry out their normal function. The switch in Schwann cells to differentiate back into a mature phenotype occurs in response to NRG1 type III, which is upregulated in neurons and DRGs after injury (Fex Svennigsen and Dahlin, 2013). In addition, following injury, Schwann cells have been observed to upregulate NG1 type I which acts in a paracrine manner to aid remyelination of the regrowing axons (Stassart et al., 2013) The expression of neuronal NRG1 type III has been shown to decrease with age, and together with an age-related decrease in myelin clearance, may impede axonal regeneration and slow remyelination in aged animals (Kang and Lichtman, 2013, Fex Svennigsen and Dahlin, 2013).

1.3.2.Schwann cell migration following injury

During nerve regeneration, dedifferentiated Schwann cells collectively migrate in cords out of the nerve stumps and into the nerve bridge. Schwann cells from the proximal stump guide regrowing axons across the nerve bridge to ensure successful contact with the distal stump is made, a crucial step in nerve regeneration. On a 2D surface *in vitro*, when two Schwann cells make contact, they exhibit contact inhibition of locomotion (CIL) and change migration direction (Parrinello et al., 2010). Following injury however, Schwann cells undergo a change in the mode of migration whereby they exhibit attractive rather than repulsive behaviours, and instead migrate as cords (Parrinello et al., 2010). The mechanism by which Schwann cells form cords and migrate has previously been described by our laboratory (Parrinello et al., 2010, Cattin and Lloyd, 2016). At the site of injury, fibroblasts expressing Ephrin B repulse Schwann cells via EphB2 (Figure 1.6A) (Parrinello et al., 2010). This repulsion signal results in the activation of Sox2 in Schwann cells which in turn induces the relocalisation of N-cadherin to the cell surface which causes a change in cell behaviour from repulsion, to attraction. This causes the cells to cluster through homotypic interactions and this results in Schwann cells collectively migrating as cords. The importance of this mechanism whereby Ephrin B-EphB2 signalling controls the mode of Schwann cell migration was shown following the inhibition of this signal *in vivo* which led to misdirected axonal regrowth (Figure 1.6B) (Parrinello et al., 2010).

As a result of this observed switch in cell behaviour, the migrating cords of Schwann cells are able to perform the function during nerve regeneration of guiding the regrowing axons from the proximal stump across the nerve bridge and into the distal stump. *In vivo*, many different cell types are often observed to adapt their mechanism of migration depending on the local environment, and this has been described as a mechanism by which cancer cells can migrate within diverse tissue environments (Liu et al., 2015, Tozluoğlu et al., 2013). Specifically, this change in migration refers to mesenchymal-amoeboid transition (MAT) which is dependent on variables such as cellular contractility, cell adhesion and geometry, as well as the local microenvironment (Liu et al., 2015).

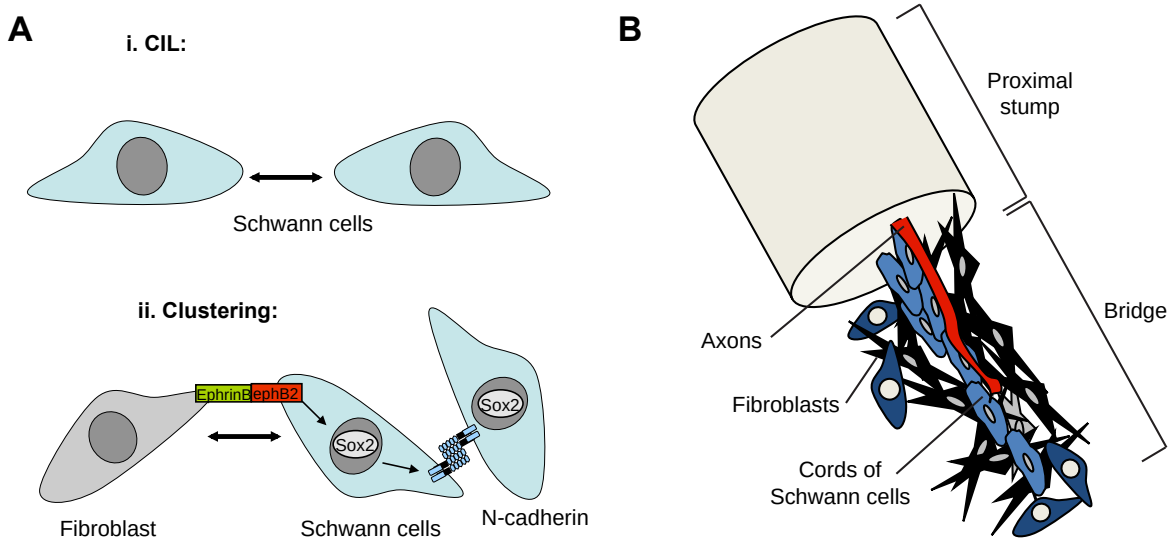

Figure 1.6 | Fibroblast sorting causes a change in Schwann cell behaviour
A. *In vitro*, Schwann cells display CIL and repulse each other upon contact (i). Upon contact with fibroblasts in the bridge *in vivo*, Schwann cells undergo a change in behaviour from repulsive to attractive (ii), which is mediated through EphrinB-EphB2 signalling (Parrinello et al., 2010). The activation of the transcription factor Sox2 in Schwann cells causes an accumulation of N-cadherin at the cell membrane, where they form cell-cell junctions, and induce clustering. B. Schwann cells migrate in cords out of the proximal stump and into the bridge, which aids regrowing axons.

In vitro on a 2D surface, individual Schwann cell migration is integrin-dependent (Cattin et al., 2015) and resembles classical mesenchymal-like migration which requires adhesion and lamellipodia-like structures (Liu et al., 2015). To facilitate adhesion, cells form focal adhesion complexes (FAC) which aid cells in sensing their environment and migration through protein and receptor interactions between the actin cytoskeleton and the extracellular matrix (Geiger et al., 2009). FAC typically comprise of combinations of integrins, talin, and focal adhesion kinase (FAK) which enable cell migration through actin polymerisation and contraction (Iskratsch et al., 2014). When key adhesion molecules (talin and β1 integrin) were knocked out in Schwann cells or the actin polymerisation inhibitor latrunculin B was applied, migration in 2D was inhibited which confirms that Schwann cells migrate in a mesenchymal manner in 2D (Afshari et al., 2010, Cattin et al., 2015, Wang et al., 2012).

In contrast in 3D *in vitro* fibrin gels, in which endothelial tubules are formed from embedded endothelial cells, Schwann cells are unable to migrate within the matrix alone, however, upon contact with an endothelial tubule exhibit integrin-independent migration in a more amoeboid-like manner with a characteristic forward extension, followed by a rear contraction which involved discrete points of contact between the Schwann cell and the endothelial cell (Cattin et al., 2015); this finding was in

contrast to fibroblasts which are able to migrate within the matrix without any additional support. Within the context of a 3D gel matrix, knockdown of focal adhesion complex proteins did not affect Schwann cell migration, consistent with amoeboid-like migration (Yamauchi et al., 2004, Cattin et al., 2015). Instead, amoeboid-like migration relies on myosin II dependent contractility from the rear of the cell (Friedl and Wolf, 2010), and the use of the Rho-kinase inhibitor Y27632 prevented rear contraction of the cells, whilst latrunculin B prevented forward cell extensions confirming that the Schwann cells were migrating in an actomyosin-driven manner (Cattin et al., 2015). The amoeboid mechanism of migration also appears to rely on direct cell:cell contact between the Schwann cells and endothelial cells. Using electron microscopy techniques, analysis of the interface between Schwann cells and endothelial cells *in vivo* showed the presence of blebs which protruded from both cell types (Cattin et al., 2015). This suggests that the blood vessel provide a non-continuous surface for the Schwann cell to migrate along, with the blebs providing direct points of contact which provide sufficient traction to propel the Schwann cells forward (Cattin et al., 2015). Theoretically, this mode of migration may not need specific molecular interactions between the two cell types but it remains to be determined whether this is the case. Moreover, whether the cells produce the protrusions constitutively and if they are required for the migration also needs to be clarified.

This difference in cell migration between the two environments, 2D and 3D may be due to the differing forces exerted on the cell during migration. In 2D, cells experience high levels of adhesion (due to the formation of FAC) and low confinement (due to the lack of a surrounding tissue matrix) and migrate in a mesenchymal-like manner. In contrast, in a 3D environment such as *in vitro* within an extracellular matrix (e.g. fibrin) gel or *in vivo,* cells experience low levels of adhesion and high levels of physical confinement which can induce a switch in cell migration behaviour to a more amoeboid-like mechanism (Liu et al., 2015, Tozluoğlu et al., 2013). Many physical variables affect a cells ability to migrate, including rigidity, adhesion, confinement and topology (Charras and Sahai, 2014). These signals, transmitted through integrins and adaptor proteins such as talin, allow the cell to respond and alter the mechanism of migration accordingly (Liu et al., 2015). The force that a cell exerts on its surroundings will alter depending on the physical environment. We have shown that the mechanism of Schwann migration differs between 2D and 3D environments, and that the requirements of cell signalling changes; i.e. in 2D β1 integrin is required for migration, whilst it is dispensable in 3D.

It is currently unknown whether there is a specific Schwann cell chemoattractant present in the

bridge which either stimulates the migration along blood vessels or attracts Schwann cells out of the stumps. Endothelial cells migrate into the bridge to form blood vessels which alleviate the hypoxia in the newly formed tissue (Hobson et al., 2000). The hypoxia in the bridge is sensed by macrophages which then upregulate hypoxia response genes and release VEGF. In previous experiments using knock out animals as well as pharmacological inhibition, we found that VEGF was necessary and sufficient to induce the formation of blood vessels within the nerve bridge following injury (Cattin et al., 2015). Using the *Vegfa*$^{fl/fl}$ *Tie2-Cre* mouse model in which *Vegfa* is inactivated in all haematopoietic and endothelial cells, we showed that vascularisation in the bridge was inhibited with only a few detectable blood vessels. Importantly, the loss of blood vessels led to a reduction in Schwann cell migration, with the majority of Schwann cells being present still in the nerve stumps and not migrating into the bridge. This showed that VEGF was required to induce blood vessel formation in the bridge. Additional experiments using the VEGF receptor 2 (VEGFR2) inhibitor Cabozantinib (Cabo) showed that when it was administered *in vivo* prior to blood vessel formation, blood vessel formation was inhibited, and similarly to the knock out studies, no Schwann cell migration was observed. However, when Cabo was administered after vascularisation had occurred in the bridge, Schwann cell migration still occurred. This *in vivo* data suggested that whilst endothelial cells migrate in a VEGF-dependent manner, Schwann cell migration occurs via VEGF-independent mechanisms (Cattin et al., 2015).

Blood vessel formation occurs prior to Schwann cell migration in the bridge, and the observation that Schwann cell migration is limited to when blood vessels have been formed may be a mechanism to ensure that Schwann cell migration occurs in a controlled manner and only in a specific direction (i.e. out of the nerve stumps and into the bridge. This was most convincingly demonstrated by the experiments in which we found that when blood vessel formation was redirected using VEGF-coated beads placed perpendicular to the nerve axis, Schwan cell migration still followed blood vessels and used them as a migration scaffold (Cattin et al., 2015). The collective migration of many different cell types relies on the presence of a chemoattractant, therefore it is likely that within the regenerating nerve there is a factor which is able to promote Schwann cell migration. The work presented in this thesis investigates whether a Schwann cell specific chemoattractant is present in the nerve bridge following injury.

1.4. Pathologies

Due to the high incidence of peripheral nerve injury, affecting ~1 million people in the UK and USA annually (Campbell and Meyer, 2006, Grinsell and Keating, 2014), and the impact it has on patient quality of life, the importance of understanding the mechanisms of nerve regeneration is clear. In particular, owing to the central role that Schwann cells play in orchestrating nerve regeneration, elucidating their mechanism of migration would be beneficially, particularly in the development of therapeutics. Modifications to the nerve regeneration process have the potential to be therapeutically beneficial to patients suffering from nerve injury in the future.

Elucidating the mechanism by which Schwann cells migrate along blood vessels is also important, as this mechanism of migration may be relevant to tumour cells. There are a number of tumours which have been reported to utilise blood vessels as a scaffold as a means of spreading however the mechanisms behind this migration remain unclear (Bovetti et al., 2007, Cuddapah et al., 2014). Characterising this process may therefore help to understand how these tumours metastasise and could ultimately lead to therapeutic agents which may halt the metastatic process.

1.4.1. Peripheral nerve neuropathies

Peripheral nerve neuropathies are relatively common and affect around 1% of the general population, rising to 7% in the elderly (Hanewinckel et al., 2016). Neuropathies primarily occur as a result of myelination defects, which eventually leads to axonal degeneration. Such defects can arise from inherited conditions (e.g. Charcot-Marie-Tooth) as well as acquired disease (e.g. diabetes) (Feldman et al., 2017), although in many cases the cause remains unknown (Hanewinckel et al., 2016). Neuropathies are often associated with neuroinflammation due to axonal degradation and demyelination which leads to the activation and recruitment of macrophages (both resident and circulating) to the damaged nerve (Barrette et al., 2013).

Due to the recent increase in obesity rates within the general population, there has also been an associated rise in the incidence of diabetes and therefore many of the secondary conditions associated with diabetes such as diabetes-associated neuropathies (Feldman et al., 2017). Neuropathies may also originate from traumatic injuries in which damage done to the nerve is sufficient to prevent efficient regeneration (Klein and Martini, 2016, Hughes, 2002).

As discussed in the previous sections, Schwann cells are important regulators of the development and maintenance of the PNS. It is not surprising therefore that a number of neuropathies are underpinned by abnormal Schwann cell/axon communication (Juarez and Palau, 2012). For example, neuropathies may occur following a bacterial infection such as *Mycobacterium leprae*, which activates the ErbB2 receptor on Schwann cells and leads to demyelination and therefore myelination defects (Nave and Werner, 2014). Guillain-Barré syndrome is an autoimmune disorder, often triggered by infections such as Zika (Parra et al., 2016) or *Campylobacter jejuni* (Wakerley and Yuki, 2013), in which the body mounts an immune attack on Schwann cells or myelin. In this condition, sites of neuroinflammation within peripheral nerves are observed which drive demyelination and axonal death, as well as demyelination-dependent pain. This condition is somewhat reversible, however the extent of axonal loss will determine the ability of a patient to recover and the long term disability.

One common heritable neuropathy is Charcot-Marie-Tooth (CMT) syndrome which is a complex, heterogeneous collection of disorders which are characterised by progressive muscular atrophy (Nicholson and Myers, 2006, Juarez and Palau, 2012). Disease onset occurs within early adulthood, with symptoms including weakness, sensory loss and muscle atrophy, first appearing in the feet before progressing upwards to include the legs and then upper limbs (Baets et al., 2014). There are different types of CMT which can be characterised by the affected cell type. CMT Type I encompasses Schwann cell demyelinating phenotypes which result in a reduction of nerve conduction velocity, and segmental demyelination and remyelination, and is the most frequently occurring peripheral neuropathy (Nicholson and Myers, 2006, Juarez and Palau, 2012). CMT Type I results from autosomal dominant or X-linked mutations in myelin genes including PMP22 (which encodes myelin protein 22) and P0 (Juarez and Palau, 2012, Lupski et al., 1991). In contrast, in CMT Type II the defect is primarily in axons, due to defects found in axon specific genes and leads to a mild reduction in nerve conduction as well as a loss of axons (Lupski et al., 1991). Further investigation into the molecular mechanisms and the disease pathophysiology of CMT may therefore lead to the discovery of novel therapeutics, using drug, cell or gene approaches, which are able to target the affected nerve architecture and provide patient benefit.

1.4.2.NF1/Schwann cell-derived tumours

NF1 is one of the most common tumour-predisposition disorders, affecting about 0.3% of the human population (Gutmann et al., 2017). NF1 is caused by the loss of the *NF1* gene which encodes the protein neurofibromin, a Ras-GAP which acts as a negative regulator of the Ras signalling pathway (Bollag et al., 1996). The loss of *NF1* predisposes patients to the development of multiple, benign Schwann cell-derived tumours known as neurofibromas (Rubin and Gutmann, 2005). In addition, the loss of NF1 also results in other clinical manifestations such as café au lait spots, optic gliomas, skin deformation and haematopoietic neoplasias (Jett and Friedman, 2010). Treatment options for NF1 patients remain limited and usually involve surgical removal, and high doses of chemotherapy and/or radiation (Staser et al., 2012, Rubin and Gutmann, 2005, Gutmann et al., 2017).

Neurofibromas are often described as resembling 'unrepaired wounds' in the nerve and contain dedifferentiated Schwann cells which are dissociated from axons and able to proliferate, as well as fibroblasts, extracellular matrix deposition and large numbers of inflammatory cells (Figure 1.7) (Parrinello and Lloyd, 2009, Rubin and Gutmann, 2005).

Schwann cells are thought to be the cell of origin of NF1 neurofibromas (Parrinello and Lloyd, 2009). The loss of *NF1* in Schwann cells results in Ras hyperactivation due to loss of Ras inhibition (Martin et al., 1990). Ras activation leads to the activation of downstream signalling events which induce cell growth and cell survival (Gutmann et al., 2017, Ratner and Miller, 2015, Ribeiro et al., 2013). However, the loss of *NF1* alone is not sufficient to drive tumour formation, and current evidence suggests that this must happen in combination with other events such as inflammation (e.g. nerve injury/transection) in order to initiate neurofibroma growth (Prada et al., 2013, Ribeiro et al., 2013).

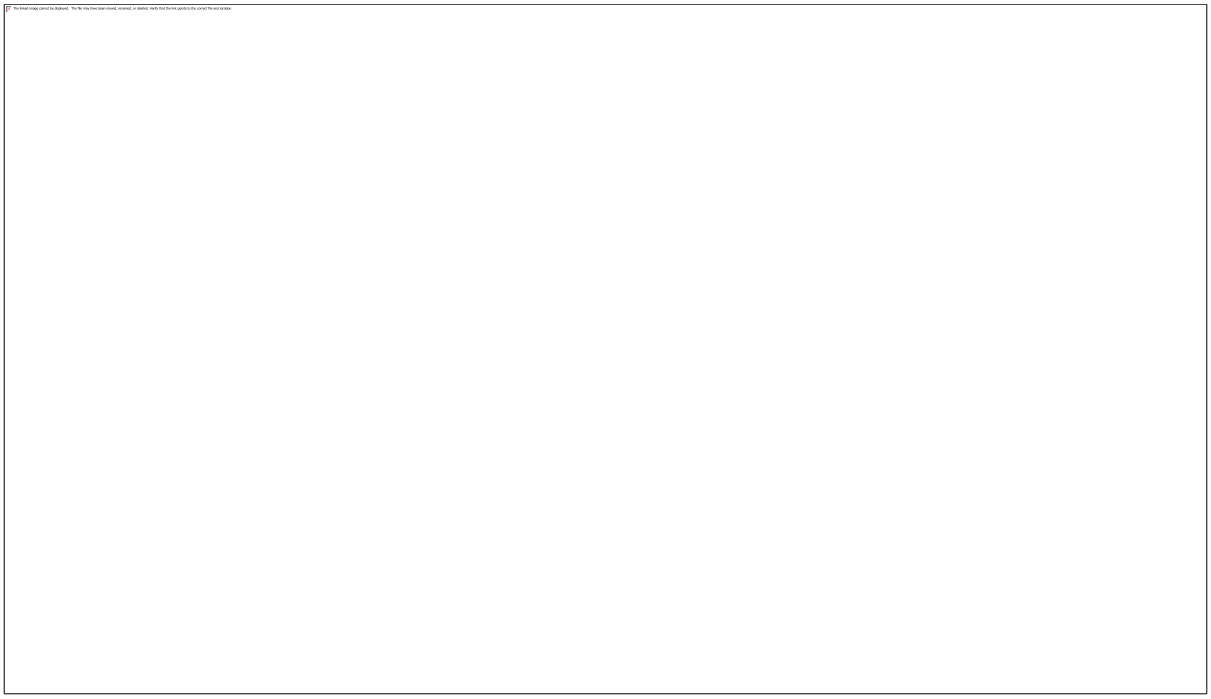

From (Parrinello and Lloyd, 2009).

Figure 1.7 | NF1 tumours resemble an injured nerve
In a normal nerve (a) the complex and ordered organisation is clearly visible. Upon formation of a neurofibroma (b), the nerve structure is disrupted. Schwann cells have dedifferentiated and dissociate from their axons, and an immune response is mounted and there is an influx of inflammatory cells.

Recent RNA-seq analysis has also confirmed that transcriptional changes observed in Schwann cells and macrophages in NF1 tumours resemble the early stages following sciatic nerve injury (Choi et al., 2017). Macrophage populations in neurofibromas are thought to contribute to the inflammatory environment of NF1 tumours by adopting a more pro-inflammatory phenotype and increasing expression of pro-inflammatory chemokines, cytokines and growth factors compared to the resting PNS (Staser et al., 2012, Choi et al., 2017). Paracrine signalling loops were also identified which demonstrated mechanisms of communication between Schwann cell and macrophage populations in NF1 tumours (Choi et al., 2017). Interestingly, unlike in nerve regeneration where a switch from pro-inflammatory to repair macrophages is observed, this is not appear to be present in neurofibromas which experience chronic inflammation (Choi et al., 2017).

Whilst benign cutaneous and subcutaneous neurofibromas form in nearly all NF1 patients, plexiform neurofibromas affect less than half (Gutmann et al., 2017, Staser et al., 2012, Ratner and Miller, 2015). Originating from cranial and large peripheral nerves, with a tendency to be located at nerve roots, plexiform tumours result in an increase in morbidity and mortality, as well as having the potential, in a small proportion of NF1 patients, to progress into malignant peripheral sheath tumours

(MPNSTs) which have a poor prognosis (Staser et al., 2012, Rubin and Gutmann, 2005). Plexiform neurofibromas are complex tumours which cause pain and discomfort through the compression of vital organs in the body (Staser et al., 2012, Ratner and Miller, 2015). Plexiform tumours have an enhanced ability to proliferate, survive as well as the ability to migrate along and escape the nerve architecture. The migration of these tumours can result in the invasion of adjacent tissues following the disruption of the perineurium, and contributes to the morbidity of this tumour type (Ratner and Miller, 2015). Oncogenic malignant peripheral nerve sheath tumours (MPNSTs) also retain migratory capabilities, which contributes to the tissue metastasis which is often observed (Ratner and Miller, 2015).

1.4.3. Tumour innervation and nerve tumour interactions

Similar to what has been observed during PNS regeneration and tissue formation, nerve innervation has also been observed in tumourigenesis. Recent work has shown that in prostate (Magnon et al., 2013) and gastric (Zhao et al., 2014) tumours, nerve innervation was necessary not only for tumour progression, but also to promote metastasis. Using animal models of cancer, these studies denervated the organ/tumour either by cutting the afferent nerve, or by using neurotoxic agents such as botulinum toxin or 6-hydroxydopamine, and when compared to control innervated animals they observed a decrease in tumour initiation and progression (Magnon et al., 2013, Zhao et al., 2014). These studies showed for the first time that nerves were crucial for inducing tumour formation and spread in an active process (Boilly et al., 2017), however the mechanisms which underlie these processes remain unclear.

The influence of the sympathetic nervous system (SNS) on the tumour microenvironment has been described to act directly through tumour innervation (Magnon et al., 2013), and indirectly through neuroeffectors or hormones which may act on distal sites such as spleen and bone marrow which will subsequently enhance the tumour microenvironment and promote tumourigenesis (Sloan et al., 2010, Cole et al., 2015). It is thought that by aiding the inflammatory tumour microenvironment, more cells are recruited and this adds to the morbidity and mortality associated with tumours. Aiding nerve-tumour interactions are Schwann cells which have been observed to directly interact with tumour cells and promote axonal guidance towards tumours (neurogenesis) (Cole et al., 2015, Bunimovich et al., 2017). The mechanisms behind the requirement of a nervous component for tumour innervation however are

not yet fully understood. Further exploration into the process of PNS regeneration may therefore allow us to find additional parallels or similarities between tumour innervation.

1.4.4.Perineural invasion

A key feature of malignant tumours is the ability to detach from the primary tumour site, and to disseminate or travel to form secondary tumour sites or metastases (Liebig et al., 2009). Solid tumours can disseminate in different ways, the three most well studied mechanisms being via direct invasion of surrounding tissues, and by lymphatic or haematogenic spread, which are well understood and characterised (Steeg, 2016). To successfully metastasise, tumours must invade the surrounding tissue, intravasate into a neighbouring lymphatic or blood vessel, extravasate out through the basement membrane and grow at a site distant from the initial lesion, processes which each involve migration and chemotaxis (Roussos et al., 2011, Steeg, 2016). Tumours may also spread along nerves in a process known as PNI, an understudied mechanism which is still not fully understood despite being first described in 1835 (Cruveilheir, 1835, Liebig et al., 2009). There have been many different descriptions of PNI in recent years, however the most commonly accepted definition of PNI is the infiltration of tumour cells within any of the three layers (epineurium, perineurium or endoneurium) of the nerve sheath. PNI may be characterised as including: cancer cell survival, an inflammatory response, chemotaxis towards the nerve, neurogenesis, tumour cell adhesion to nerve sheaths and finally invasion (Amit et al., 2016). Varying degrees of infiltration of the nerve sheath may be observed in PNI ranging from peripheral contact up to a complete encirclement (Liebig et al., 2009).

The pancreas is very well innervated by the autonomic nervous system and additionally close to 100% of pancreatic tumours exhibit perineural invasion (PNI) (Magnon, 2015). Additionally, 80% of head and neck, colon, and stomach cancers all display perineural invasion (Deborde et al., 2016). Tumour PNI leads to poor prognosis, cancer associated pain, poor outcome and decreased survival (Bunimovich et al., 2017, Amit et al., 2016, Liebig et al., 2009). For example, pancreatic cancers exhibiting PNI were associated with 23% 3-year survival rate in comparison to 49% survival rate in patients with stage-matched tumours with absence of PNI (Amit et al., 2016). Due to the infiltration into the surrounding nerves, surgery to completely remove solid tumours is rarely successful and leads to issues of nerve/sensory loss (Liebig et al., 2009).

Initially it was thought that tumour cells would spread passively along routes which would provide ‘paths of least resistance’, however in order for tumour cells to enter the nerve sheath, they must cross multiple layers of basement membrane and collagen which makes the process of PNI a much more active process, hence invasion, rather than a simple diffusion (Amit et al., 2016). PNI is the sole mechanism of dissemination for some tumours, and does not correlate with tumour spread via lymphatic or vascular systems. The reason that some cancers (e.g. pancreatic, head and neck, prostate) have a predilection for PNI whilst other types never exhibit this property remains unknown.

This precise mechanism of PNI is currently unknown, although it is likely to involve upregulation of multiple neurotrophic factors by cancer cells as well as by intratumoral nerves as well as factors to aid tissue infiltration such as proteinases, including matrix metalloproteinases (Liebig et al., 2009, Deborde et al., 2016, Ayala et al., 2008, Amit et al., 2016). In particular, the matrix metalloproteinases MMP-2 and MMP-9 have been observed to be upregulated in tumour models. It has been shown that NGF released from neural tissue caused an increase in MMP-2 expression in human pancreatic cells, and when this was replicated *in vitro* models of PNI, an increase of invasion was observed (Okada et al., 2004). There are likely many other factors involved however they are yet to be elucidated.

PNI is a complex mechanism of tumour dissemination which is still poorly understood. Issues with studying the processes which lead up to PNI come from the inability to accurately replicate the multicellular, innervated tumour environment accurately *in vitro*, as well as the failure of reliable *in vivo* models. Further investigation into PNI is therefore necessary in order to characterise the factors involved in this process, and to perhaps develop therapeutic agents to inhibit PNI and increase patient survival.

1.4.5.Stem cell niche

The haematopoietic stem cell (HSC) niche has recently been identified as having a peripheral nerve innervation component which is able to regulate the stem cell population (Morrison and Scadden, 2014, Mendelson and Frenette, 2014). The trafficking of HSCs into the bloodstream is regulated by sympathetic nerves in the bone marrow, and Schwann cells maintain the quiescent HSC cell state through the transforming growth factor-β (TGF-β)-SMAD signalling pathway, as well as potentially contributing to other currently unknown pathways (Mendelson and Frenette, 2014). Schwann cells release TGF-β activator molecules, which induces TGF-β-SMAD signalling in HSCs, and leads to the

increased phosphorylation of Smad2 and 3 which maintains HSC dormancy (Mendelson and Frenette, 2014). Following nerve injury therefore when Schwann cells exhibit a switch in cell-state and dissociate from axons, we might assume that TGF-β signalling is interrupted, allowing HSCs to re-enter the cell cycle, thus providing Schwann cells with a potentially important role within the HSC niche.

1.4.6. Tissue regeneration

Despite having the ability to regenerate and regain functions following peripheral nerve injury, mammals do not possess the ability to regenerate an entire limb, such as a hand or leg. This is in contrast to amphibians (e.g. newts), which following the loss of an appendage, such as a tail or leg, have the extraordinary ability to regenerate an entire replacement (Kragl et al., 2009, Kumar et al., 2007). The ability to regenerate results from the formation of a heterogenous blastema, which is composed of multiple cell precursors which go on to form the various new tissues (Kumar and Brockes, 2012).

It is possible however for mammals to exhibit tissue regeneration following the removal of the digit tip, at a point distal to the nail bed (Johnston et al., 2016). A process which involves the coordination of multiple different cell types, as well as the formation of distinct tissues (e.g. skin, bone, muscle) in order to regain functionality. Nerve innervation is crucial for limb regeneration in amphibians, and it was thought that innervation was also required for digit tip regeneration in mammals. In both cases, it has been found however that innervation was not strictly required, and instead that Schwann cells were essential for successful tissue regeneration (Johnston et al., 2016). It is also becoming apparent that Schwann cells play similar, and key roles both in both limb regeneration in amphibians and tissue regeneration in mammals. Following tissue damage, mature Schwann cells from the surrounding damaged nerves dissociate from their axons and dedifferentiate into a progenitor phenotype which enables them to proliferate and migrate. At the injury site, Schwann cells then release paracrine signals (oncostatin M and platelet-derived growth factor AA) which promote the expansion of mesenchymal precursor cell types to differentiate into bone and skin tissue (Johnston et al., 2016). A similar process has also been observed following skin injuries in mice, where Sox2+ Schwann cells were observed to aid repair and depletion of this cell population led to inefficient wound closure (Johnston et al., 2013).

1.4.7. Involvement of macrophages in pathologies

Macrophages clearly play important roles in many pathologies, including PNS injury (Cattin et al., 2015), and it is possible that there may be cross-talk between macrophages and Schwann cells which could both aid injury resolution, as well as progressing tumour innervation and PNI. Essential to better understanding these disease processes therefore is understanding macrophages, and characterising the specific cell populations which contribute towards nerve pathologies, which is the subject of this thesis.

1.5. Macrophages

1.5.1. Macrophage physiology

Macrophages are mononuclear myeloid immune cells, characterised by their ability to phagocytose and neutralise potentially hazardous molecules such as pathogens (Varol et al., 2015). They play a major role in maintaining tissue homeostasis, as well as contributing towards the promotion and resolution of inflammation (Varol et al., 2015, Wynn and Vannella, 2016, Ginhoux and Jung, 2014). Once thought of as solely being derived from monocytes (van Furth and Cohn, 1968), it is now clear that macrophages can also exist as distinct populations within tissues, and do not necessarily have to have a monocyte origin (Ginhoux and Jung, 2014).

Monocytes are continuously made in the bone marrow from HSCs, which differentiate through granulocyte-macrophage progenitor (GMP), macrophage and dendritic cell precursor (MDP) and common monocyte progenitor (cMoP) intermediates (Ginhoux and Jung, 2014). Monocytes require colony-stimulating factor-1 (CSF-1) to escape from the bone marrow and into the circulation (Ginhoux and Jung, 2014). Upon inflammation, monocytes are rapidly recruited to the site of injury from the bloodstream where they extravasate and differentiate into monocyte-derived macrophages, or monocyte-derived dendritic cells (Das et al., 2015, Patel et al., 2017, Ginhoux and Jung, 2014).

All organs contain resident populations of macrophages, which are specialised according to the tissue environment, both morphologically and phenotypically, and adapted to carry out tissue-specific roles (Mass et al., 2016, Yona et al., 2013, Zigmond et al., 2014). The majority of tissue resident macrophages have embryonic origins and are able to locally self-renew without contribution from bone marrow derived cells (this will be discussed in more depth in later sections). Resident macrophages play a central role in maintaining tissue homeostasis, primarily by patrolling the environment, identifying

any potential immune threats, and clearing away dying or dead cells and debris (Davies et al., 2013, Epelman et al., 2014). For example, the liver contains the highest proportion of macrophages in a solid organ, which implies that macrophages play a crucial role in liver biology (Krenkel and Tacke, 2017). Liver resident macrophages, or Kupffer cells, are one of the most well characterised tissue populations, and are required to carry out functions such as scavenging bacteria or microbial products, sensing changes in tissue health and integrity, and to commence or dampen immune responses as necessary (Scott et al., 2016, Krenkel and Tacke, 2017). To carry out these specific tissue roles, resident macrophages have a specific gene expression profile which distinguishes them from monocyte derived or circulating macrophages, as well as other tissue resident populations (Mass et al., 2016, Yona et al., 2013).

In addition to tissue resident macrophage, populations of monocyte derived macrophages have important functions in adaptive immune defence, contributing to the clearance of infection and inflammation (Ginhoux and Guilliams, 2016, Varol et al., 2015). Under normal healthy conditions, monocytes deriving from the bone marrow patrol within the circulation, and upon entry into tissues, via transmigration, differentiate into macrophages though changes in gene expression (e.g. downregulating CCR2 and Ly6C) which allows them to carry out their functions (Das et al., 2015, Patel et al., 2017, Gautier et al., 2012). These monocyte-derived macrophages are key orchestrators of inflammatory responses, and coordinate the release of chemokines and cytokines to attract neutrophils and lymphocytes, as well as growth factors, such as platelet-derived growth factor and insulin-like growth factor (Varol et al., 2015). Macrophages may also contribute to the pathophysiology of many conditions such as cancer and inflammatory disorders such as Coeliac disease or Lupus erythamatosos (Wynn et al., 2013).

1.5.2. Origin of macrophages

In mammals, macrophages are known to have either embryonic origins, in the case of tissue resident macrophages, or derive from myeloid precursors which originate from the bone marrow (Ginhoux and Jung, 2014, Epelman et al., 2014, Varol et al., 2015, Ginhoux and Guilliams, 2016). The latter can be recruited to tissues in response to particular pathological conditions such as injury and in some tissues can also replenish resident macrophage populations (Jetten et al., 2014). For a long time, it was thought that resident macrophage populations were unable to self-renew, and instead were

maintained by the constant recruitment of circulating monocytes, as a part of a linear mononuclear phagocyte system (van Furth and Cohn, 1968). Recently however, there have been many studies (Mass et al., 2016, Lavin et al., 2014, Hashimoto et al., 2013, Rantakari et al., 2016) which have challenged this long held view and proposed alternative mechanisms for how these populations are maintained and/or replenished throughout their lifetime.

In a recent review, a model for the seeding of tissue resident macrophages was proposed which involved macrophages originating from the yolk-sac and/or foetal liver based on the embryonic development of an organ (Ginhoux and Jung, 2014). For many tissues it was found that the resident tissue macrophages derived from both yolk sac haematopoiesis, which begins at E7.5 and results in cells beginning to circulate and populate tissues in the embryo at E8.5-10 when the vascular network is formed, and foetal liver haematopoiesis which begins at E11 (Figure 1.8) (Ginhoux and Jung, 2014). It was found that most adult tissues contain a mixture of macrophages from these distinct origins due to the timing of tissue formation during embryogenesis. Exceptions to this include the brain where microglia originate exclusively from the yolk sac at E9/9.5 with no contribution from the foetal liver, and also the epidermis, where the majority of resident macrophages (Langerhans cells) derive from the foetal liver (Figure 1.8) (Ginhoux and Guilliams, 2016, Ginhoux and Jung, 2014).

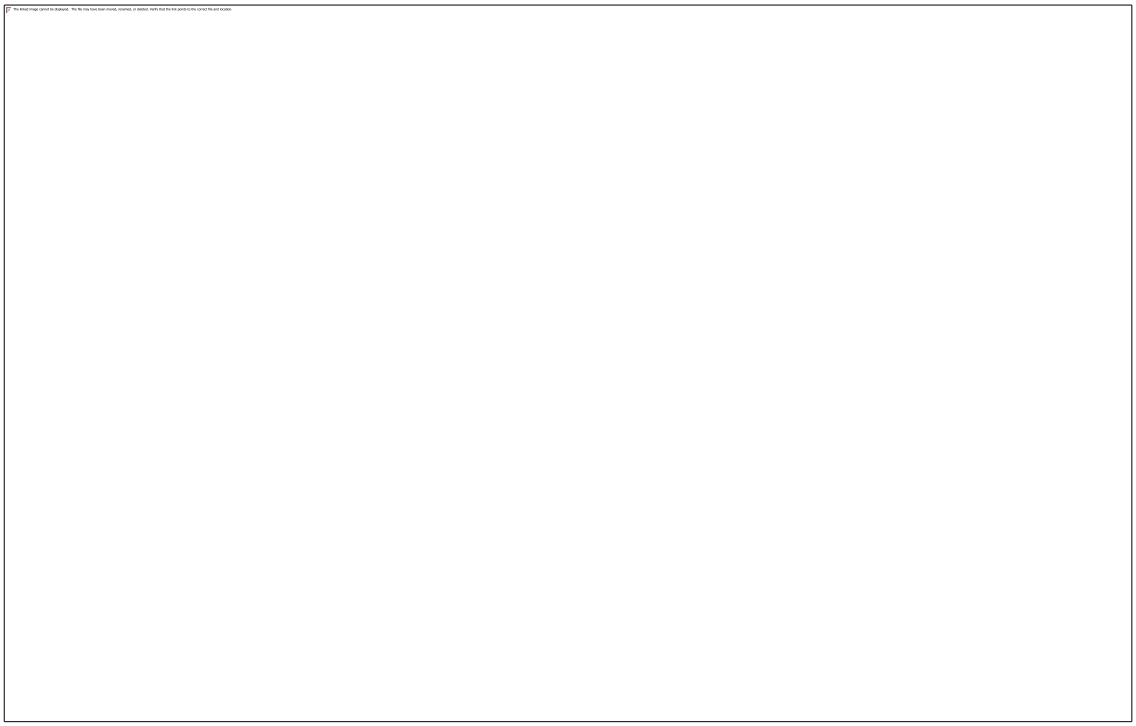

Adapted from (Ginhoux and Guilliams, 2016).

Figure 1.8 | Heterogeneous origin of tissue resident macrophages
Tissues may be classified by the turnover of their macrophages as closed, slow or fast. In a 'closed' tissue there is no contribution from monocytes to the resident macrophage population during adulthood, and the macrophages in these tissues (e.g. brain and skin) may originate from the yolk-sac or foetal liver, or a combination of both. In contrast, in tissues which are 'open', bone marrow-derived cells may be recruited during adulthood and differentiate into resident macrophages and according to a tissue specific kinetic pattern, i.e. slow (heart, pancreas) or fast (gut, dermis). It is currently unclear how the PNS should be classified within this system.

Interestingly, in some adult organs, such as the lung and the spleen, minimal yolk-sac derived macrophages remain, which indicates that during development, these cells are replaced by macrophages which originate from definitive haematopoiesis (Ginhoux et al., 2010). Moreover, in contrast to previous observations, many tissue resident macrophages can self-renew, and are able to replenish populations (for example following injury) without assistance from monocyte derived cells (Merad et al., 2002, Ajami et al., 2011, Hashimoto et al., 2013). There are however some tissue macrophage populations which do rely on circulating monocytes for replenishment, such as the pancreas and the intestine (Bain et al., 2014, Yona et al., 2013), which may be due to the nature of these tissues and the need for a high turnover of macrophages to carry out homeostatic functions.

Despite the observed differences in the origin of tissue macrophages, as well as monocyte derived cells, there has been no observed effect of these diverse origins on macrophage function (Ginhoux and Jung, 2014). Instead, it has been observed that monocyte derived cells recruited to the liver can differentiate into cells indistinguishable from the resident population (Bain et al., 2016, Scott et al., 2016). The idea that macrophages can adapt to their local tissue environment has led to an alternative theory for tissue macrophage seeding and differentiation into specific macrophage sub-types. Recent research which carried out an extensive RNA-seq on many tissue macrophage populations in mice indicated that all macrophages originate from a common precursor, the yolk sac erythro-myeloid-progenitor (EMP) (Mass et al., 2016). EMPs then generate pre-macrophages (pMacs) which are then seeded to different organs simultaneously from E9.5 during development. pMacs are recruited to tissues via chemokine signalling pathways, and upon arrival the transcriptional profile of pMacs is altered by the specific microenvironment and results in the up- or down-regulation of various genes to become tissue specific resident macrophages with characteristic functions and individual gene signatures over the course of development (Mass et al., 2016). It is these changes in gene expression which create the observed diversity of tissue macrophages which respect to their functions and

phenotypes. The idea that resident macrophages alter their gene expression depending on their tissue location has been seen multiple times using fate mapping, as well as following the adoptive transfer of macrophages into different tissues (Ginhoux et al., 2010, Bain et al., 2014, O'Koren et al., 2016), showing that the gene enhancer landscapes of tissue resident macrophages are shaped by the local environment (Lavin et al., 2014). Resident tissue macrophages therefore display distinct phenotypes which is dependent on their local environment and function.

Following the seeding of organs with macrophages, it is necessary to maintain this tissue resident population both during homeostasis, as well as following injury or infection. There had been much discussion over the contribution of monocyte-derived macrophages vs. local proliferation for the maintenance of resident tissue macrophage populations (Hume, 2006). More recently however, it has become clear that not all resident macrophage populations require monocyte-derived cells to repopulate or maintain tissue macrophage populations and instead are able to self-renew, e.g. brain and liver (Yona et al., 2013, Hashimoto et al., 2013).

Further exploration into the differences in resident macrophage populations following depletion (e.g. in monocytopenic mouse models or following whole body irradiation) have highlighted the differences in requirement for macrophage turnover in different tissues due to the nature of their function (i.e. the lung is an entry point for inhaled bacteria and pathogens) and physiological location (i.e. the brain is in a privileged environment due to the BBB) (Bain et al., 2014). For example in the intestine, embryonic-derived macrophages are almost undetectable in adulthood and a high turnover of macrophages is observed, whilst in the brain, microglia derive exclusively from the yolk-sac, have a very slow turnover and no steady state contribution from monocyte derived cells is observed (Bain et al., 2014). The brain is protected from the circulation by the BBB (Hong and Stevens, 2016), whilst there is a rich blood supply in the lungs and the intestine which is necessary for the exchange of materials (Bain et al., 2014).

In many of the original studies that investigated the origin and turnover of resident macrophages populations, bone marrow transplants (BMTs) were often used to distinguish between donor fluorescently labelled bone marrow-derived cells and non-labelled endogenous cells (Ginhoux et al., 2010). BMTs provide an easy way to identify cells which are resident and cells which have been recruited from the circulation. The major drawback with this technique however is that prior to a BMT, the recipient animals must undergo sub-lethal irradiation in order to deplete the recipient bone marrow,

and to create a ‘niche’ in which the donor bone marrow can inhabit. This process of irradiation has been found to cause difficulties when interpreting the contribution from bone marrow-derived cells. Irradiation methods ablate populations of cells which display a fast turnover, and in some tissues such as the retina, irradiation also causes a tissue injury (O’Koren et al., 2016), which results in the recruitment of bone-marrow derived cells. There are some populations of resident macrophages which are irradiation-resistant however, and it has been observed that in the absence of bone marrow-derived cells, these irradiation resistant populations may then repopulate the damaged tissue (Hashimoto et al., 2013). The process of irradiation will likely also alter the tissue microenvironment and homeostasis (i.e. cytokine and growth factor composition) which results in alterations to call turnover. All of which can contribute to an overestimation when considering the contribution of recruited cells to maintain resident populations (Ginhoux et al., 2010). Instead, methods using fate-mapping, and less commonly parabiosis, have proved to be more accurate to address the issue of determining cell origin, and distinguishing between embryonic and recruited macrophage populations (Yona et al., 2013, O’Koren et al., 2016, Epelman et al., 2014).

Recently, there has been growing support for the idea of organ or tissue ‘niches’ which influence the initial seeding of macrophages from embryonic origins, as well as the ability of bone marrow derived cells to displace embryonic-derived cells during adulthood to inhabit adult serous cavities (which line and enclose organs, e.g. the peritoneal cavity) (Bain et al., 2016, Scott et al., 2016, Guilliams and Scott, 2017). This has been observed in animal models where following depletion of resident liver macrophages, the liver ‘niche’ becomes available and therefore monocyte derived macrophages are able to populate the liver and become functional Kupffer cells (Scott et al., 2016).

There is clearly still some debate within the macrophage community with regards to the origins of macrophages. These diference may originate from the many different methodologies used to study the origins of macrophages (e.g. fate mapping, BMT), as well as the long-held hypotheses that the different research groups already subscribe to. The ability of tissues to be populated during development by the yolk-sac or foetal liver haematopoiesis is logical, and additionally, the ability of macrophages to change their transcriptional program to suit the local microenvironment, or tissue niche, and specific function fits with the diversity of macrophage subtypes. This suggests that these multiple theories are complementary, rather than exclusive when describing macrophage ontogeny.

1.5.3.Macrophage phenotypes

For a long time, macrophages have broadly been divided into two categories based on their physiology and response after injury/infection, which may be either pro- or anti-inflammatory, known as M1 and M2 subsets respectively (Murray et al., 2014, Murray, 2017). The M1 phenotype is described as having pro-inflammatory functions and can be activated by agents such as lipopolysaccharide (LPS) (Escribese et al., 2012). The M2 phenotype is associated with the resolution of inflammation, for example after injury, and by releasing high levels of anti-inflammatory mediators can turn off immune system activation. M2 macrophages also have a higher angiogenic potential when compared to M1 macrophages (Jetten et al., 2014).

More recently however, it is becoming clear that macrophage biology and function cannot be classified by such a simple two state model, and macrophages instead may exist on a continuum between pro- and anti-inflammatory function and express receptors and cytokines depending not only on macrophage origin, but also on their physiological role and tissue location (Murray, 2017). This results in many different subsets of macrophages which have important roles in tissue homeostasis and in innate and adaptive immunity which cannot be separated into the broad categories of M1 and M2 type macrophages (Murray et al., 2014). Additionally, the inflammatory state of a macrophage may change temporarily depending on multiple factors, such as age or infectious challenge (Murray, 2017).

Understanding the roles of different macrophage types and being able to apply these to human macrophage biology has the potential to aid future therapeutic intervention in cases where macrophages play a fundamental role in shaping clinical outcome, such as in nerve regeneration and cancer.

1.5.4.Tissue resident macrophages

The local tissue microenvironment of resident macrophages influences their homeostatic role, as well as their response to injury or physical damage or challenge by infection. The role of the tissue microenvironment in shaping the specific function and phenotype of macrophages is particularly apparent when looking at the specialised tissue resident macrophage populations such as those in the liver, lung and skin (Gautier et al., 2012, Epelman et al., 2014). To aid them in their local, tissue specific functions, tissue resident macrophages express a number of sensing molecules such as scavenging receptors and pattern recognising receptor, such as Toll-like receptors, as well as adhesion molecules

(Varol et al., 2015). The range of receptors that a resident macrophage expresses will vary between tissues and be dependent on the tissue specific role that they play.

In the liver, resident macrophages, or Kupffer cells, are crucial for iron homeostasis and recycle haemoglobin which is released during the turnover of aged red blood cells (Davies and Taylor, 2015). Within the lung, resident alveolar macrophages, patrol the alveolar membranes for inhaled pathogens and regulate the homeostatic function of the tissue by clearing surfactant (Maus et al., 2002, Davies et al., 2013). In the skin, the resident macrophage population, known as Langerhans cells, is specifically adapted for its role of immune surveillance by having long protrusions which are able to probe the local microenvironment and scan for pathogens (Davies et al., 2013). It is clear that the specific tissue environment contributes to the macrophage phenotype, and in turn, the resident tissue macrophages function to maintain homeostasis within the tissue as well as protecting the tissue upon injury or infection (Lavin et al., 2014).

Whilst much is known about many other resident tissue macrophages, very little has been reported about the resident population of macrophages in the PNS. Large scale RNA-seq studies analysing the different gene expression profiles of resident tissue macrophages tend to focus on the already well characterised tissue populations such as in the liver and intestine, and the PNS has not been investigated in any detail (Mass et al., 2016). Studies in the Lloyd lab as well as others have shown that in the uninjured nerve, macrophages comprise approximately 5-10% of the total cell population (unpublished data and (Griffin et al., 1993, Klein and Martini, 2016, Müller et al., 2010)). Following injury, the number of macrophages in the nerve increases dramatically, and in the nerve bridge over half of the cells, ~50%, present are macrophages (Cattin et al., 2015). The relative contribution of resident cells to the inflammatory response following injury is currently unclear, and the issue of determining the origin of macrophages in the nerve bridge will be discussed later in this work.

1.5.5.Microglia

The resident population of macrophages within the CNS are a specialised population known as microglia (Franco and Fernández-Suárez, 2015, Hong and Stevens, 2016). Unlike other resident tissue macrophages such as Kupffer and intestinal macrophages, microglia exclusively originate from yolk-sac and throughout their lifetime self-renew without any contribution from circulating monocytes (Kierdorf and Dionne, 2016, Ginhoux and Guilliams, 2016, Ajami et al., 2011, Ginhoux et al., 2010).

This is mainly due to the privileged environment of the CNS, which is separated from the extracellular environment by the BBB, which prevents the exchange of harmful materials. Following injury or inflammation however, the BBB can become compromised and inflammatory mediators such as monocytes are able to enter in order to resolve the injury (Davies et al., 2013). Recent studies have shown that following loss of BBB function, infiltrating monocytes do not remain at the injury site and differentiate into microglia, instead these infiltrating cells leave, and the resident microglia population proliferates to restore numbers (Ajami et al., 2011). Microglia numbers remain fairly constant throughout a human (or mouse) lifetime, and 0.5-2% of the microglial population is proliferating at any given time (O'Koren et al., 2016).

Apart from carrying out normal homeostatic functions such as immune surveillance and phagocytosing dead cells and debris, microglia also have emerging roles in shaping the brain environment. Microglia support brain function by pruning, remodelling and maintaining synapses, which contributes to learning and memory (Davies et al., 2013, Hong and Stevens, 2016). Recent *in vivo* studies have implicated microglia as a contributing factor for neurodegenerative disorders such as Alzheimer's disease, due to aberrant phagocytosis of healthy synaptic tissues (Hong and Stevens, 2016). However, many details surrounding their normal homeostatic role and function in disease are still unknown.

Recent microarray data analysing the transcriptome of microglia found multiple different expression profiles which were dependent on many variables such as age, brain region, sex and developmental stage, indicating distinct populations (Hong and Stevens, 2016). This suggested that microglia have a strong dependence on microenvironment, bioenergetics and immunoregulatory functions in order to drive and shape the cells particular functionality (Franco and Fernández-Suárez, 2015, Ginhoux et al., 2010).

Similarly to the CNS, the PNS is a privileged tissue environment which is maintained by a barrier: the BNB (Weerasuriya and Mizisin, 2011). The presence of the BNB suggests that PNS macrophages may have similar properties to microglia with regards to origin, turnover and function. The resident macrophage population in the PNS has not yet been as extensively characterised as microglia in the CNS however, and so further investigation into these properties may aid understanding of the role of this population during healthy and diseased states.

1.6. PNS resident macrophages

Whilst many other resident macrophage populations in the body have been well characterised, little is known about the cells which make up the resident macrophage population in the PNS. Experiments using the proliferation marker EdU for long-term labelling studies have found that the average turnover rates of macrophages within the nerve is ~6 months which suggests that within the context of the nerve, they are a relatively quiescent population (Stierli et al., in preparation).

The origin of PNS macrophages and if there is any contribution from circulating monocytes to replenish the resident population is also not fully known (Klein and Martini, 2016). Due to the level of protection that nerves experience due to the BNB, it might be expected that, similar to microglia, PNS resident macrophages are seeded at an early embryonic stage and that subsequently the population is maintained by self-renewal. The idea that macrophages fill niches when they become available, e.g. during development or following injury/depletion (Guilliams and Scott, 2017), could also be applicable in the case of the PNS. In the mouse, the PNS is first observed during development at ~E11, when nerve fascicles begins to enter limbs, however it is not fully formed until E14.5 when nerves extend into the fingertips (Catala and Kubis, 2013) providing a window of time for the niche to be populated by embryonic macrophages. Following PNS injury, the nerve bridge is also a novel tissue niche which becomes populated by macrophages, which may originate from recruited or pre-existing nerve tissue macrophages.

A recent study looking at the renewal of macrophages following injury found that in tissues where the resident macrophage population self-renews, e.g. microglia, after injury, the proportion of resident macrophages decreases as larger numbers of infiltrating monocyte derived cells enter the tissue (Davies et al., 2011). After injury resolution, fluorescence-activated cell sorting (FACS) data showed that there was increased proliferation of resident macrophages which restored numbers to homeostatic levels, and there was a minimal contribution from monocyte derived cells. It is possible that this mechanism of self-renewal and recovery following injury could be similar in the resident PNS macrophage population.

Previous experiments have found that when GFP^+ bone marrow is transplanted into GFP^- mice, there is an influx of GFP^+ cells into the sciatic nerve (in the absence of injury), both into the endoneurium and also surrounding in the epineurial space, which suggests that there are monocyte-derived populations of cells within the nerve (Müller et al., 2010, Vass et al., 1993). However, due to the caveats

associated with bone marrow transplant experiments, these results are difficult to interpret and may not be physiologically relevant. This highlights the importance of using alternative methodology, such as fate mapping, to determine nerve macrophage origin and turnover in the uncut nerve.

Resident PNS macrophages have been shown to express MHC class I (Griffin et al., 1993), and immunofluorescence data from our lab confirms that they stain positive for the pan macrophage markers CD11b, CD68, Iba1 and F4/80. PNS macrophages are found in the nerve structure between myelinated axons within the endoneurium, and here can be observed to have a longitudinal orientation (Griffin et al., 1993). Additionally, PNS macrophages are located in the epineurial space, as well as being found adjacent to blood vessels where they are often observed to have a ramified appearance (Griffin et al., 1993, Müller et al., 2010). Their location and morphology hints at the roles that the macrophages have within the PNS, which together with Schwann cells function to regulate the local immune environment of the peripheral nerve (Kieseier et al., 2006). Due to the expression of MHC Class II proteins, macrophages in the endoneurium are thought to have a homeostatic role in local surveillance of the tissue and process any proteins which are found in the endoneurial space and present to the circulating T cells in order to act as an immune defence (Griffin et al., 1993, Kieseier et al., 2006). Previous investigations into macrophage populations in the nerve have determined that the population is heterogeneous, however the multiple populations have not been fully elucidated or defined in the existing literature (Griffin et al., 1993, Kieseier et al., 2006, Müller et al., 2010).

1.6.1. The role of macrophages following PNS injury

In contrast to the lack of information regarding resident macrophages in the quiescent PNS, there has been much more progress in understanding the function of macrophages within a damaged and regenerating nerve (Rosenberg et al., 2012, Chen et al., 2015, Cattin and Lloyd, 2016). Following an injury, a large inflammatory response is mounted and macrophage numbers within the bridge and distal stump increase dramatically (Klein and Martini, 2016, Mokarram et al., 2012, Griffin et al., 1993, Cattin et al., 2015). Preliminary data from our lab using bone marrow transplant experiments has shown that the large increase in macrophage numbers in the bridge is predominantly due to macrophage recruitment from circulating monocytes, rather than the proliferation of resident PNS macrophages (Cattin et al., 2015). As a caveat to this data, as previously mentioned, experiments using BMT may be overstating the contribution of monocyte-derived macrophages. At the current time, it is unclear whether

these two macrophage populations, resident and monocyte derived, have distinct roles in the regeneration process (Das et al., 2015).

The large increase of macrophages in the damaged nerve is caused by a number of known factors. Dedifferentiated Schwann cells release monocyte chemoattractant protein-1 (CCL2) which recruits monocytes, which express the CCL2 receptor CCR2, to the site of injury to aid them in their process of debris clearance following differentiation into macrophages (Klein and Martini, 2016, Napoli et al., 2012, Perrin et al., 2005, Kwon et al., 2015). Additionally, fibroblasts release colony stimulating factor 1 (CSF1) which recruits macrophages in order to facilitate the coordinated task of remodelling the injury site (Groh et al., 2015). The various roles of macrophages following injury is summarised in Figure 1.9 and described in the following sections.

Adapted from (Cattin and Lloyd, 2016).

Figure 1.9 | Macrophages have multiple roles in nerve regeneration.
Following nerve injury, there is a huge influx of inflammatory cells to both the bridge and the distal stump. In the bridge (left panel) macrophages respond to the inflammatory environment and release VEGF-A which induces vascularisation. They may also be responsible for the release of an additional pro-migratory factor. In the distal stump (right panel), macrophages together with Schwann cells, function to remodel the environment to facilitate axonal regrowth. Schwann cells and fibroblasts release CCL2 and CSF-1 respectively which promotes the recruitment of macrophages to the injury site.

1.6.1.1. Role of macrophages in the bridge

We have recently determined a novel role for bridge macrophages in facilitating nerve regeneration following injury (Figure 1.9). Following nerve transection, a nerve bridge is formed by Day

2 (in rats) which comprises large numbers of inflammatory mediators, such as neutrophils and macrophages (Cattin et al., 2015). Analysis of the newly formed bridge in rats following sciatic nerve transection showed that macrophages were the most prevalent cell type, with half of all cells exhibiting positive staining for the macrophages marker Iba1 (Cattin et al., 2015). Other cells types present at this time point are neutrophils (24%), fibroblasts (13%) and endothelial cells (5%).

The newly formed bridge is a hypoxic environment which can be detected using hypoxyprobe-1 (pimonidazole hydrochloride), which forms irreversible immunofluorescent protein adducts when in areas of hypoxia (pO_2 <10mm Hg). Immunofluorescence analysis of the nerve bridge demonstrated that a large proportion of the cells were hypoxyprobe-1^+ and therefore hypoxic (Cattin et al., 2015). Not all of the cells in the bridge were hypoxic however, and further co-staining analysis showed that nearly all (98%) of the hypoxyprobe-1^+ cells in the bridge were macrophages, and that 80% of macrophages were hypoxic. This was a striking result, as it appeared that macrophages had a differential response to hypoxia compared to the other cell types in the bridge (e.g. fibroblasts and neutrophils).

In response to hypoxia, there is a defined hypoxic response which involves stabilisation of the transcription factor hypoxia-inducible factor-1α (HIF-1α), which is constitutively degraded under normal oxygen conditions (Semenza, 2001, Lin and Simon, 2016). HIF-1α is then translocated to the nucleus where it binds to hypoxic response elements and initiates a transcriptional response. In particular, angiogenesis is induced due to the upregulation of pro-angiogenic factors such as VEGF (Burke et al., 2003, Jetten et al., 2014). This macrophage-specific release of VEGF then induces blood vessel formation in the bridge, which, as previously described, is crucial for Schwann cell migration and subsequent axonal regrowth (Cattin et al., 2015, Cattin and Lloyd, 2016).

1.6.1.2. Role of macrophages in the distal stump

In the distal stump, macrophages are known to have a very different role to those in the bridge (Figure 1.9). Downstream of the injury site, in the distal stump, axons degenerate in a process known as Wallerian degeneration, which generates cellular axonal and myelin debris, and Schwann cells dedifferentiate into a progenitor like phenotype (Mueller, 2003, Jessen and Mirsky, 2016). Dedifferentiated Schwann cells recruit macrophages to the distal stump through the release of CCL2 (Perrin et al., 2005, Rosenberg et al., 2012, Napoli et al., 2012). Macrophages in the distal stump work together with Schwann cells to clear the myelin debris which is inhibitory for axonal regrowth and

remodel the injury environment to create a permissive environment for regeneration (Klein and Martini, 2016, Chen et al., 2015). Without this remodelling process, axonal regrowth is impaired and this has been observed in aged animals where the speed of regeneration is significantly slower than in younger controls due a slowing in the clearance of myelin debris (Kang and Lichtman, 2013).

It is thought that initially, resident PNS macrophages, together with Schwann cells, carry out this phagocytic function, however a large increase of macrophage numbers is observed in the distal stump following injury which are likely monocyte derived cells and probably contribute to the remodelling function (Mueller, 2001). The accumulation of macrophages in the distal stump following injury aids axonal regrowth due to their phagocytic function and ability to remodel the injured environment. The two populations of macrophages, resident and recruited, and the functions that they carry out have not been distinguished, and it is probable that there is a significant level of overlap.

As in the bridge, the phenotype of macrophages in the distal stump following injury is unknown. Due to the function of macrophages here, phagocytosis and tissue remodelling, which are 'pro-healing' and 'pro-repair,' we might hypothesise that macrophages here have a more M2 or anti-inflammatory phenotype. Recent work has in fact shown that following nerve injury, by augmenting the phenotype of macrophages at the injury site to an 'M2' phenotype using the chemokine IL-4, injury resolution was promoted, which included an increase in Schwann cell migration compared to non-chemokine treated nerves (Mokarram et al., 2012). Conversely, when macrophages were polarised towards a pro-inflammatory phenotype using interferon-ɣ (IFN-ɣ), there was no increase in nerve regeneration compared to the non-chemokine treated nerves. This study indicated not only that macrophages in the distal stump are likely to be polarised towards an anti-inflammatory phenotype but also, highlighted the importance of macrophages, and specifically their phenotype and function on the outcome of nerve injuries (Mokarram et al., 2012, Griffin et al., 1993). The release of IL-10 following nerve injury is also able to modulate the phenotype of macrophages to a more repair phenotype (Siqueira Mietto et al., 2015). IL-10 null mice have greater expression of pro-inflammatory macrophage markers and a decrease of repair macrophage markers. IL-10 also helps to regulate the length of time that macrophages remain in the tissue, by controlling macrophage efflux from the damaged area (Siqueira Mietto et al., 2015).

The different roles that macrophages have in the regenerating nerve emphasises the ability of macrophages to adapt their phenotype, changing over time and also physiological location to reflect

the microenvironment and biological need. By characterising the macrophage populations in the injured nerve, we may better understand the diverse functions that macrophages carry out and also develop therapeutic strategies to enhance nerve regeneration.

1.6.1.3. Role of macrophages in the ganglia

In addition to macrophages playing roles in the bridge and the distal stump following injury, macrophages at the site of the ganglia also contribute to nerve regeneration. Here, they support regrowing axons by inducing a transcriptional change which promotes migration (Niemi et al., 2013).

After PNS injury, retrograde signals transmitted to the cell bodies induce the transcription of regeneration-associated genes (RAGs), which promotes axonal regrowth (Kwon et al., 2015, Kwon et al., 2013). Macrophages are involved in this process of RAG activation, which is mediated through CCL2 release which promotes neuron-macrophage interactions (Klein and Martini, 2016, Niemi et al., 2013). The ablation of CCL2 using antibodies resulted in a reduction of nerve regeneration and neurite outgrowth (Kwon et al., 2015).

Macrophage infiltration into the ganglia has also been associated with the propagation of neuropathic pain following PNS injury through the release of pro-inflammatory mediators such as TNF-α, CCL2 and IL-1β (Krames, 2014). Following the administration of chemotherapy agents such as paclitaxel, the subsequent infiltration of macrophages into the ganglia promotes a pro-inflammatory response and an increase in chemotherapy-induced peripheral neuropathy (Zhang et al., 2016). This highlights the importance of macrophage phenotype following injury, as well as the possibility of targeting macrophages to treat neuropathic pain.

1.6.2.Macrophages in cancer

Macrophages have long been associated with cancer, and in many cases are associated with the growth and spread of tumours, which increases the severity and morbidity of many cancer types (Henze and Mazzone, 2016, Qian and Pollard, 2010). Resident populations of tumour associated macrophages (TAMs) are also known to be a marker for poor prognosis (Liu and Cao, 2015). It is known that TAMs are responsible for increasing the vascularisation of solid tumours, allowing them to maintain supplies of oxygen and nutrients which aids tumour growth and proliferation. During organogenesis, or during regeneration, macrophages promote angiogenesis through the release of VEGF in response to

the stabilisation, and nuclear relocation of HIF-1α in response to hypoxia (Hobson et al., 2000, Riboldi et al., 2012, Cattin et al., 2015). This process is also observed in tumourigenesis where TAMs attempt to resolve hypoxia and ensure nutrient delivery to the rapidly dividing tumour cells (Murdoch et al., 2008, Henze and Mazzone, 2016) To do this, TAMs release pro-angiogenic factors and vascular-modulating enzymes, such as VEGF, transforming growth factor-β (TGFβ), interleukin 1β and matrix metalloproteinases 7, 9 and 12 (Henze and Mazzone, 2016, Murdoch et al., 2008, Qian and Pollard, 2010). In addition to other roles, macrophages have critical roles not only in regulating angiogenesis in tumours, but also modulating cell migration and immune modulation (Caux et al., 2016, Qian and Pollard, 2010, Cavel et al., 2012).

Many aspects of tumour biology, in particular tumourigenesis, are similar to that of the regenerating nerve following injury. Cancer initiation has been compared with chronic wound repair as both processes involve hyperplasia and tissue remodelling, as well as the contribution of the nervous system to innervate the new tissue structures (Cole et al., 2015). In NF1 tumours, macrophages make up a large proportion of the tumour (20-40% of total cells) and reminiscent of the similarities between NF1 tumours and an injured nerve, NF1 tumours have a similar transcriptional profile to a sciatic nerve injury (Choi et al., 2017). This implies that similar to the functions following nerve injury, macrophages play important roles in tumour biology. Additionally, cross-talk between NF1 Schwann cells and macrophages has been identified as a result of RNA-seq analysis which determined paracrine signalling loops between the two cell populations (Choi et al., 2017). Schwann cells were found to release the macrophage chemoattractant colony stimulating factor 1 (CSF1) in the NF1 model, which correlates with what has already been described following sciatic nerve injury (Groh et al., 2015, Klein and Martini, 2016).

It is thought that cells such as macrophages and fibroblasts can contribute to cancer invasion in tissue microenvironments such as the nerve. In tumours which exhibit PNI, macrophages have recently been implicated in promoting the spread of tumours via the nervous system (Amit et al., 2016). Following the invasion of a tumour into the nerve tissue, macrophages are recruited to the site of PNI by Schwann cells which secrete the chemokine CCL2; macrophages express the receptor for CCL2, CCR2 (Niemi et al., 2013). After injection of cancer cells into the sciatic nerve of CCR2 deficient mice, reduced macrophage recruitment to the injection site and less PNI was observed compared to wild-

type controls (He et al., 2015, Amit et al., 2016). This shows strong evidence of macrophages, and specifically the CCL2/CCR2 axis contributing towards cancer progression along nerves.

1.7. Thesis aims

Peripheral nerves have a complex structure consisting of multiple cell types which, following injury, are able to coordinate an injury response resulting in nerve regeneration and regain of function. Whilst much is understood about the mechanisms which govern these repair mechanisms, there are questions which still remain, some of which are addressed in this thesis.

The role of the resident population of macrophages in the nerve remains poorly understood. Despite their likely roles in peripheral nerve homeostasis and following injury, this population of tissue macrophages has not been well characterised with regards to their origin, turnover or homeostatic functions within the uncut nerve. Preliminary experiments have found that the increase in macrophage numbers in the nerve bridge and distal stump following injury is due to an influx of monocyte derived macrophages, however this observation must be confirmed using alternative methodology.

Secondly, whilst it is known that Schwann cells are able to migrate out of the nerve stumps and into the nerve bridge along blood vessels, it is still unclear whether there are any additional signalling mechanisms or chemoattractants within the bridge which promote their collective migration. Due to the observation that directed cell migration usually involves a chemoattractant, we hypothesise that within the nerve bridge following injury a Schwann cell chemoattractant acts to induce collective migration along blood vessels. Schwann cell migration has been observed during processes such as limb regeneration as well as tumour innervation and PNI, which despite being distinct, share similarities with nerve regeneration. The identification of a Schwann cell chemoattractant factor therefore may have wide-ranging therapeutic applications.

The aims of this thesis were to firstly characterise macrophage populations in the peripheral nerve under both normal and injury situations, where it is known that they contribute to nerve regeneration. Secondly, through the characterisation of macrophage function in nerve regeneration, this thesis aimed to identify any Schwann cell chemoattractant molecule which is present during regeneration. Due to the emerging roles that Schwann cells have in tumour biology as well as organ development, the wide ranging therapeutic applications of such a chemoattractant molecule make

identifying a factor particularly important and necessary. Over the course of this thesis I will outline the experiments performed in order to address these aims.

Chapter Two: Materials and Methods

2.1. Materials

2.1.1. Chemicals

All chemicals bought from Sigma unless stated otherwise. Additional reagents and respective sources: CCR5 inhibitor (Maraviroc; R&D Systems); CXCR4 inhibitor (Plexixafor, AMD3100; R&D Systems); Cabozantinib (Selleckchem); Recombinant rat CCL3 (R&D Systems); VEGF-A (Lonza).

2.1.2. Antibodies

Tables 2.1-4 show a full list of antibodies and concentrations used. For immunofluorescence, AlexaFluor® secondary antibodies were obtained from Invitrogen and used at the indicated concentrations for *in vitro* or *in vivo* staining. For Western blotting, horseradish peroxidase (HRP)-conjugated antibodies were obtained from GE-healthcare and used at a concentration of 1:10,000.

Table 2.1 Immunofluorescence antibodies

	Antibody	**Supplier**	**Species**	**Concentration**
Hypoxyprobe-1	4.3.11.3	Hypoxyprobe	Mouse	1:1,000
Iba-1	019-19741	Wako	Rabbit	1:500
Prolyl-hydroxylase beta		Acris		1:1,000
S100	Z0311	Dako	Rabbit	1:100
Lectin 647		Invitrogen		1:100
F4/80	MCA497	AbD Serotec	Rat	1:500
CD68	MCA5709	AbD Serotec	Mouse	1:100
Hoechst	33342	ThermoFisher Scientific		1:1,000
AlexaFluor® 488/594/647 α-rat/rabbit/mouse		Invitrogen		*In vivo*: 1:400 *In vitro*: 1:1,000

Table 2.2 Western blot antibodies

	% acrylamide gel	**Antibody**	**Supplier**	**Species**	**Concentration**
Primary antibodies					
CCL3	15	Ab25128	Abcam	Rabbit	1:2,000
VEGF	15	Ab46154	Abcam	Rabbit	1:5,000
ERK1/2	15	M5670	Sigma Aldrich	Rabbit	1:5,000
B-actin	15	Ab8227	Abcam	Rabbit	1:5,000
CD68	15		Biorad	Mouse	1:5,000

Secondary antibodies					
Anti-rabbit			GE Healthcare		1:10,000

Table 2.3 Antibodies used for FACS

Instrument: BD Fortessa				
Marker	**Fluorochrome**	**Clone**	**Supplier**	**Concentration**
CD45	BV711	30-F11	Biolegend	1:15,000
CD24	AF488	M1/69	Biolegend	1:1000
CD11b	V450	M1/70	eBioscience	1:200
CD64	PE	X54-5.7.1	Biolegend	1:200
Ly6C	PE-Cy7	AL-21	BD Biosciences	1:400
CCR2	APC	475301	R&D Systems	1:25
MHC II	V500	M5/114	BD Biosciences	1:800
CD3e	APC-Cy7	145-2C11	BD Biosciences	1:50
Ly6G	APC-Cy7	1A8	BD Biosciences	1:50
CD19	APC-Cy7	1D3	BD Biosciences	1:400
NK1.1	APC-Cy7	PK136	Biolegend	1:200

Table 2.4 Antibodies used for immunopanning

	Antibody	**Supplier**	**Species**	**Concentration**
Primary antibodies				
CD11b/c	Clone 42	Harlan sera lab	Rabbit	1:1,000
Fibroblasts	Thy1 clone Ox7	In house	Rabbit	1:500
Secondary antibodies				
Anti-rabbit IgG	P0488	Dako		1:10,000

2.1.3.qPCR oligos

Primers were designed to target mRNA by annealing to sequences in exons spanning at least 1 or more intron/s used Primer3Plus. Please see Table 2.5 for primer sequences.

Table 2.5 RT-qPCR primers

Gene	**Forward primer (5'-3')**	**Reverse primer (5'-3')**
Rat		
Arginase1	TATCGGAGCGCCTTTCTCTA	ACAGACCGTGGGTTCTTCAC
b2m	CAGTCTCAGTGGGGGTGAAT	ATGGGAAGCCGAACATACTG
CD11b	TTACCGGACTGTGTGGACAA	AGTCTCCCACCACCAAAGTG
CXCL12	ACACTCCAAACTGTGCCCTT	GCCTCTTGTTTAAGGCTTTGTCC

CXCR4	TGACCCTCTGAGGCGTTTGG	TTCATCCCGGAAGCAGGGTT
Iba1	CCAGCGTCTGAGGAGCTATG	CGTCTTGAAGGCCTCCAGTT
iNOS	CTCACTGGGACTGCACAGAA	GCTTGTCTCTGGGTCCTCTG
CCL3	CTGTTACCTGCTCAGCACCA	GGGGTGTCAGCTCCATATGG
VEGF-A	GAGTTAAACGAACGTACTTGCAGA	TCTAGTTCCCGAAACCCTGA
Mafb	TATTCCAAGGAGTCGCCAAG	CTGAGAGCCAGTGTTCACCA
Fcrls	TGACAATGCAGGACTTGGTG	GGGTCACTGAACTCCCCTCT
Jun	CTCCCGTCTGGTTGTAGGAA	CACAGCGCATGCTACTTGAT
Fos	CTGAAGGCTGAACCCTTTGA	AGGTAGTGCAGCTGGGAGTG
Timd4	GGACCATCTCCAGGAAGTCA	GTTGTGGCTCTCCTCAGCTC
Fcgr4	CAAAAGGCTGTGGTGATCCT	GAAGGCTGTCTGGCATCTGT
Pparg	AGGGGACTGAGTGTGACGAC	TCACACAGTCCGGTCAGAAA
Mouse		
Arginase1	GACAGGGCTCCTTTCAGGAC	CTGTGATGCCCCAGATGGTT
B2M	CAGTCTCAGTGGGGGTGAAT	ATGGGAAGCCGAACATACTG
CD11b	ATGGACGCTGATGGCAATACC	TCCCCATTCACGTCTCCCA
CXCL12	ACAAGTGTGCATTGACCCGA	AGTTACAAAGCGCCAGAGCA
iNOS	AGTCTCAGACATGGCTTGCC	GCAGCTTGTCCAGGGATTCT
CCL3	CCATATGGAGCTGACACCCC	AAATGACACCTGGCTGGGAG
VEGF-A	AGAAGGAGAGCAGAAGTCCCA	GTCCACCAGGGTCTCAATCG

2.1.4.siRNA oligos

Double stranded RNA oligos were designed and supplied by Qiagen, scrambled siRNA was used as a control. Please see Table 2.6 for oligo target sequences and concentrations used.

Table 2.6 siRNA oligos

Gene	Oligo no.	Target sequence	Concentration
CCL3	1	5’-CTAGGTAGACATGATGACAAA-3’	62.5nM
CCL3	2	5’-TTGTGACTATTTATTCTGAAA-3’	62.5nM
CCL3	3	5’-TCGAGGGACTCTTCACTTGAA-3’	62.5nM
Scrambled/Scr		5’-AATTCTCCGAACGTGTCACGT-3’	62.5nM

2.1.5.Buffers

Table 2.7 Buffer composition

Solution	Components
RIPA lysis buffer*	1% Trition X-100, 0.5% sodium deoxycholate, 50mM Tris pH 7.5, 100 mM NaCl, 1mM EGTA pH 8, 20mM NaF, 100μg/ml PMSF, 15μg/ml aprotonin, 1mM Na_3VO_4
4x Laemmli buffer	200 mM Tris pH 7.5, 8% SDS (BioRad), 40% glycerol, 400 mM DTT, 0.25% bromophenol blue
10x Running buffer	50mM Tris pH 8, 500mM glycine, 0.1% SDS
10x Transfer buffer	200mM Tris pH 8, 1.5 M glycine, 20% methanol
20x TBS	200 mM Tris base pH 8, 3 M NaCl
20x TBS-T	200mM Tris base pH 8, 3 M NaCl, 0.02% Tween-20
5% milk/TBS-T	5% (w/v) skimmed milk powder in 1X TBS-T
MACS buffer	1X PBS, 1% 100 mM EDTA, 1% FCS
FACS blocking buffer	1:50 Rat anti-mouse BD sFc block (BD Biosciences), MACS buffer
10X Sato	BSA 100μg/ml, progesterone 60ng/ml, putrescine 16μg/ml, selenium 40ng/ml, thyroxine 50ng/ml, Triiodothyronine 50ng/ml, transferrin 100μg/ml, insulin 100ng/ml (Mathon et al., 2001)

*Add fresh 1:100 protease cocktail inhibitor mix

2.1.6.Cell culture

2.1.6.1. Preparation of tissue culture dishes

For primary rat Schwann cell culture, dishes were coated with 80μg/ml poly-L-lysine hydrobromide (PLL) for 20 min at RT, washed twice with tissue culture water (Baxter) and dried for >12 hours. Cell migration assays and seeding cells on glass coverslips required an additional coating of laminin onto the PLL coating. PLL coated dishes were incubated with 0.01mg/ml laminin in MEM (Gibco) for 1 hour at RT and aspirated just before seeding the cells.

2.1.6.2. Schwann cells

Primary rat Schwann cells were extracted from the sciatic and bronchial nerves of 10 post natal day 7 Sprague-Dawley rats. Nerves were dissected out and the external sheath removed before being chopped using a scalpel, and re-suspended in digestion buffer (7900U/ml DNase, 2mg/ml collagenase, 2.5% trypsin in EBSS) and incubated for 15 min in a +37°C water bath, agitating 5 times using a 1ml Gilson pipette. The mixture was digested for a further 10 minutes in the water bath before stopping the

reaction using 10% volume of FCS. Cells were spun for 5 min at 1500 rpm at RT, and the pellet was re-suspended in panning buffer (0.1% BSA (Invitrogen) in L15 (Gibco)) before being filtered using a 40μm cell strainer (Sigma Aldrich). The cell suspension was then immunopanned to remove macrophages and fibroblasts. Briefly, this was done by first coating bacterial plates with 1:125 rabbit anti-mouse IgG overnight at +4°C, washing with PBS and secondly coating with antibody against macrophages, mouse CD11b/c MAS 370p clone Ox42 (Harlan sera lab), or fibroblasts, Thy1 clone Ox7 (homemade). The cell suspension was incubated for 10 min at RT to remove macrophages twice, and then the suspension was moved to the fibroblast plates where the incubation was repeated three times. 0.05% BSA was added to the cells before centrifuging for 5 min at 1500 rpm. The pellet was re-suspended in DMEM-low glucose (1g/L) (Lonza) supplemented with 3% fetal bovine serum (FBS, Labtech.com) 1μM forskolin (Abcam), 200nM L-Glutamine (Gibco), glial growth factor (homemade), 100μg/ml kanamycin and 800μg/ml gentamycin (Gibco) and seeded onto a PLL and laminin coated culture dish. Cells were cultured on PLL and laminin until P3, before only being cultured on PLL. Schwann cells were maintained at +37°C and 10% CO_2. Cells were seeded at $5x10^5$ per $10cm^2$ dish or $1.4x10^6$ per $15cm^2$ dish, changing the media every other day and the day after passaging with trypsin.

2.1.6.3. Human umbilical venous endothelial cells

Human umbilical venous endothelial cells (HUVECs, Cellworks) were cultured on gelatin coated (EmbryoMax 0.1% Gelatin solution (EMD Millipore) for 10 min at +37°C) $15cm^2$ plastic tissue culture dishes in endothelial cell growth medium-2 (ECGM2, PromoCell) containing 100μg/ml kanamycin and 800μg/ml gentamycin (Gibco) at +37°C and 5% CO_2.

2.1.6.4. J774A.1 cells

The J774A.1 cell line (Sigma Aldrich) was cultured on T75 plastic tissue culture dishes in DMEM-high glucose (1g/L) containing 10% FCS, 200nM L-Glutamine, 100μg/ml kanamycin and 800μg/ml gentamycin (Gibco) at +37°C and 10% CO_2.

2.2. Methods

2.2.1. In-vivo experiments

2.2.1.1. Animals

Animal work was carried out in accordance to regulations of the UK Home Office. Adult (6- to 8-week old) Sprague-Dawley male rats and 6-week old mice were used for all experiments. Wild type C57/Black6 mice provided by the UCL Biological Services Central Unit. $CCR2^{-/-}$ mice (C57/Black6 background) for immunofluorescence staining, kindly provided by Clare Bennett and from Charles River. CX_3CR1^{GFP} mice for immunofluorescence staining were kindly provided by Dr Tamara Girbl (Queen Mary, University of London, UK).

2.2.1.2. Full sciatic nerve transection

Sciatic nerves (left nerve in rats, right nerve in mice) were exposed just below hipbone under general anaesthesia in aseptic conditions and transected at mid-thigh. The wound was closed using wound clips (Fine Science Tools) and the animals were able to recover with pain relief supplied as required. Nerves were dissected at the indicated days for analysis by immunostaining, protein extraction or RNA expression analysis. The contralateral uncut sciatic nerve was used as a control.

2.2.1.3. Preparation of nerves for immunofluorescence

Harvested nerves were fixed for 4 hours at RT in 4% PFA, incubated in 30% sucrose in PBS overnight at +4°C and then incubated for 2 hours at RT in 1:1 w/v 30% sucrose in PBS:optimal cutting temperature (OCT; VWR) solution. Nerves were then embedded in OCT in a cryosection mould and snap frozen in liquid nitrogen before storage at -80°C until needed.

2.2.1.4. Immunofluorescence of fixed tissue

PFA fixed and embedded nerves were cryosectioned either cross sectionally or longitudinally and transferred onto a frost free microscope slide (VWR).

For thin sections (~12μm) the following protocol was used:

Sections were washed once in PBS before permeabilisation in 0.3% triton in PBS for 30 min at RT. Slides were PBS washed and then blocked for 1 hour in 10% goat serum in PBS at RT. Primary antibody (see Table 2.1 for dilutions and suppliers) diluted in blocking buffer was added and incubated overnight

at +4°C before washing in PBS and incubating in secondary antibody (see Table 2.1 for dilutions and suppliers) for 1 hour at RT. Slides were finally washed in PBS and then mounted using Fluoromount-G (Southern Biotech).

For thick sections (~50μm) the following protocol was used:

Sections were washed once in PBS before permeabilisation and blocking in 10% goat serum and 0.3% triton in PBS for 2 hours at RT. Primary antibody (see Table 2.1 for dilutions and suppliers) diluted in 10% goat serum and 0.005% triton in PBS was added and incubated overnight at +4°C, followed by 1 hour at RT. Slides were then washed in PBS and incubated in secondary antibody (see Table 2.1 for dilutions and suppliers) for at least 2 hours at RT. Slides were finally washed in PBS and then mounted using Fluoromount-G.

2.2.1.5. RNA extraction from tissue and cDNA synthesis

Nerves were dissected at the indicated time following surgery, and immediately snap frozen in liquid nitrogen and stored at -80°C. The TissueLyser LT (Qiagen) was used to disrupt the frozen tissue prior to RNA extraction, following the manufacturer's protocol. RNA extraction was performed using Tri-Reagent and following the manufacturer's protocol. RNA concentration was determined using the Nanodrop and 500-1000ng of RNA was used to synthesise cDNA using the SuperScript II kit (Invitrogen) and following the manufacturer's protocol.

2.2.1.6. Flow cytometry analysis

Mouse nerves were dissected on day 5, taking equal lengths of proximal, bridge and distal, and contralateral uncut sciatic nerves. The epineurial sheath was removed and nerves were cut into approximately 1mm pieces using a razor blade. Dermis media (RPMI, 10% FCS), 1250 U collagenase IV, 4000 U DNase I and 5 mg dispase I (all in PBS) was added before incubating for 30 min at +37°C. 100mM EDTA was added and nerves were incubated for 5 min at RT and then put on ice to stop the digestion. Tubes were vortexed for 2 min before being passed through a 40 μm cell strainer (Sigma Aldrich). The volume of cell suspension was brought up to 40ml by passing MACS buffer (see Table 2.6). Cells were pelleted by spinning at 1,500 rpm for 5 min at RT, the supernatant discarded and the pellet resuspended in MACS buffer. The suspension was passed through a 70 μm cell strainer and the volume brought up to 10ml. Cells were pelleted by spinning at 1,500 rpm for 5 min at RT, the

supernatant discarded and the pellet resuspended in the residual volume. Cells were transferred to a V-bottomed plate (Corning), centrifuged at 2000 rpm for 2 min and the supernatant removed. Cell pellets were resuspended in FACS blocking buffer (see Table 2.7) and incubate for 30 min at +4°C. The following steps were completed by Heather West, Department of Infection and Immunity as outlined in Terhorst et al. (2015). Briefly, cells were immunostained for at least 20 min using antibodies listed in Table 2.3, washed in MACS buffer and then run on a BD Fortessa (BD Biosciences). Prior to analysing monocytes, macrophages, and DCs, B cells, T cells, NK cells, and neutrophils were systematically gated out using a dump channel corresponding to cells positive for B220, CD3, NK1.1, or Ly-6G cells. Analysis was performed by using FlowJo software (TreeStar Inc.) to identify monocyte derived populations based on a previously published gating strategy (Tamoutounour et al., 2013). Initially cells were gated to determine a population of live cells with the appropriate size, as well as excluding cells of the wrong lineage (NK cells, B cells and neutrophils). $Lin^{-}CD45^{+}$ cells were analysed for the expression of CD24 and CD11b. $CD11b^{+}$ $CD24^{lo}$ cells were further analysed for Ly-6C vs CD64 expression. After excluding $Ly\text{-}6C^{-}CD64^{-}CD11b^{+}$ conventional dendritic cells, the remaining fraction which was composed of Ly-$6C^{lo}$ to ^{hi} and $CD64^{lo}$ to ^{hi} cells, was then analysed for the expression of CCR2 vs CD64 and subsequently subdivided into $CCR2^{+}$ and a $CCR2^{-}$ populations. The $CCR2^{+}$ and $CCR2^{-}$ subsets were then gated on the expression of Ly-6C and MHCII to define monocytes (1), Ly-$6C^{hi}$ (2) and Ly-$6C^{lo}$ (3) monocyte-derived cells and $MHCII^{lo}$ (4) and $MHCII^{hi}$ (5) macrophage populations.

2.2.1.7. Injection of a substance into nerve following sciatic nerve transection

Sciatic nerves (left nerve in rats, right nerve in mice) were exposed just below hipbone under general anaesthesia in aseptic conditions and transected at mid-thigh. The wound was closed using wound clips and the animals was able to recover with pain relief supplied as required. On Day2/3 (as specified) the animal was anaesthetised and the wound was reopened using a scalpel. Using a glass capillary needle and needle pusher (Sutter Instrument Corp.), 5µl PBS or CCL3 (50µg/ml) was injected at a 1mm distance into the exposed proximal and/or distal stump before the wound was closed using wound clips. Nerves were dissected at the indicated days and prepared for immunofluorescence as described for analysis.

2.2.1.8. Nerve repair using engineered nerve conduit

Sprague Dawley (250–500 g) rats were deeply anaesthetised by inhalation of isoflurane, the left sciatic nerve of each animal was exposed at mid-thigh level, transected and a repair conduit consisting of a silicone tube containing fibrin gel was positioned between the stumps to produce an inter-stump distance of 10mm. Conduits were retained in place using one 10/0 epineurial suture (Ethicon) at both the proximal and distal stump, then wounds were closed in layers with a single 4/0 suture (Ethicon) reconnecting the muscle and wound clips closing the skin opening. The animals were allowed to recover. Neuronal regeneration was assessed across the 10mm inter-stump distance in the following conditions: (1) fibrin gel containing VEGFa (500ng/ml), (2) fibrin gel containing VEGFa (500ng/ml) and CCL3 (50 µg/ml), (3) fibrin gel only or (4) empty tube without fibrin gel. Animals were culled at the specified post-surgery time point using CO_2 asphyxiation and repaired nerves were excised under a dissecting microscope, and prepared for immunofluorescence as described.

2.2.1.9. Ex-vivo bridge cell isolation and culture

Rat nerve bridges at day 2 following injury were collected and digested using 1 mg/ml collagenase IV and 1 U/ml dispase I in EBSS (Life Technologies) for 45 min at +37°C. Digestion was stopped using RPMI containing 10% FCS, cells were then pelleted by centrifugation at 1500 rpm for 10 min before discarding the supernatant and washing the pellet twice in RPMI (Lonza) containing 10% FCS. Cells were seeded at the required density on fibronectin and PLL coated tissue culture dishes and centrifuged at 12,000 rpm for 5 min to ensure cell adhesion. Cells were incubated overnight at normoxia (20% O_2), +37°C and 5% CO_2 before use in cell based assays.

2.2.1.10. Macrophage and fibroblast isolation from bridge tissue

Bridge cells were isolated as above and the cell suspension was then immunopanned to isolate macrophages and fibroblasts. Briefly, this was done by first incubating bacterial plates with 1:125 dilution of rabbit anti-mouse IgG (DAKO) in 50mM Tris pH 9.5 overnight at +4°C, washes with PBS, followed by incubation with antibody against macrophages (1/1000, mouse CD11b/c MAS 370p clone Ox42, Harlan sera lab), or fibroblasts (1/500, Thy1 clone Ox7). The cell suspension was incubated for 10 minutes at RT on the dishes coated with the macrophage-specific antibody, and then the suspension was moved sequentially to three dishes coated with the fibroblast-specific antibody. The plates were

washed twice with PBS before being scraped to remove the purified macrophages or trypsinised to remove the fibroblasts, which were then plated at a density of 60,000 cells/24 well plate and incubated overnight at +37°C, 20% O2 and 5% CO2 before use in cell based assays. To generate conditioned media for chemotaxis assays, cells were washed twice in Sato (see Table 2.7) before incubating in Sato for a further 24 hours at 20%, 1.5% or 0.1% O2. The conditioned media was then filtered (0.45µm pore-size) before use.

2.2.1.11. Extraction of macrophages from organ tissues

Sciatic nerves, brain, kidney and lung tissue was harvested from 6-8-week-old adult rats. The tissue was digested and macrophages were extracted by immunopanning as described above 2.2.1.10.

2.2.2.Cell assays

2.2.2.1. siRNA transfection

For siRNA transfection, J774A.1 cells were seeded 100,000/6 well plate. The next day, cells were washed 2X 15 min with Sato before adding 600µl fresh Sato media. Test or scrambled siRNA was diluted in Sato media (see Table 2.6 for target sequence and concentrations used) before adding 6µl HiPerfect (Qiagen), and incubated for 10 min at RT to allow complexes to form. Cells were then incubated with the complexes for 48 hours at +37°C, 1.5% O_2 and 5% CO_2. Knockdown efficiency was determined using RT-qPCR and Western blot analysis. For chemotaxis assays (Boyden and Dunn chambers), the conditioned media was harvested after 48 hours and filtered (0.45 µm pore size) before use.

2.2.2.2. Generation of J774A.1 conditioned media

J774A.1 cells were seeded at 60,000 cells/24 well and incubated overnight at +37°C and 5% CO_2. The following morning, cells were washed twice in Sato and incubated in 1ml of Sato for 48 hours at either ambient oxygen levels (20% O_2) or in hypoxic conditions (1.5% O_2). The conditioned media was then collected and filtered (0.45µm pore size, Thermo Fisher Scientific) before use in subsequent assays.

2.2.2.3. Transwell migration assay (Boyden chamber)

For Boyden chamber assays (Boyden, 1962), Schwann cells or HUVECs were harvested, washed twice for 3 min in Sato and seeded at a density of 75,000 or 50,000 respectively into 8 μm pore cell culture inserts (Millipore) coated with fibronectin. Inserts were placed into 24 well plates and incubated for 15 min at +37°C and 5% CO_2 before transferring into the test conditions, Sato was used as a negative control and 3% serum culture media or 5ng/ml VEGF-A^{165} (Lonza) was used as a positive control for Schwann cells or HUVECs respectively. Cells were then allowed to migrate at +37°C and 5% CO_2 for 4 hours. Filters were fixed using 4% PFA/PBS, washed with PBS and stained using Hoechst (see Table 2.1) before washing, cleaning and mounting using Fluoromount-G® (SouthernBiotech). Cells which had migrated through the filter were quantified (5 fields of view per filter).

2.2.2.4. Dunn chamber

For Dunn chamber assays (Zicha et al., 1991) 20,000 Schwann cells were seeded onto laminin and PLL coated glass coverslips and incubated overnight in 3% serum culture media. Cells were then washed twice with Sato. The Dunn chamber was prepared by washing the reservoirs twice with Sato. The coverslip with Schwann cells was then inverted and placed onto the Dunn chamber, leaving an opening to remove the Sato from the outer reservoir using Whatmann paper. The test media was then added to the outer reservoir and the coverslip was realigned centrally to ensure both reservoirs were covered. The chamber was then imaged using time-lapse microscopy. Live-imaging was performed at 10x using a Zeiss Axiovert 200M microscope equipped with a Hamamatsu Orca AG camera controlled by Volocity software (Improvision) and an environmental chamber set at +37°C and with a humidified stream of 10% CO_2 in air. Images were taken every 10 minutes for 24 hours.

2.2.2.5. Cell tracking

Cells were tracked by their nucleus using Volocity software for 8-12 hours. Cell velocity was then measured and cell migration tracks were created using macro plugins in Excel as described in (Gorelik and Gautreau, 2014).

2.2.2.6. Hypoxyprobe incorporation assay

Using ex-bridge cells (see 2.2.1.9) seeded at 60,000 cells/well on fibronectin and PLL coated coverslips, hypoxyprobe-1 (pimonidazole HCl, Hypoxyprobe) was added to achieve a final concentration of 100 μM and the cells were incubated at +37°C and 5% CO_2 and either 20%, 1.5% or 0.1% O_2 for 5 hours. Cells were washed for 15 min in RPMI containing 10% FCS before immunostaining.

2.2.2.7. Unbiased cytokine screen

The Mouse Cytokine Array Panel A (ARY006, R&D Systems) was used to analyse cytokine expression in conditioned medium from J774A.1 cells. 10 x 10^6 J774A.1 cells were seeded on a 15cm tissue culture plate. The following morning, cells were washed twice in Sato and incubated in 5ml of Sato for 48 hours at either ambient oxygen levels (20% O_2) or in hypoxic conditions (1.5% O_2). The conditioned media was then collected and filtered (0.45μm pore size) before use in the Array, following the manufacturer's protocol.

2.2.3.Microscopy

2.2.3.1. Immunocytochemistry of cells

Cells grown on glass coverslips were fixed using 4% PFA/PBS for 10 min, permeabilised with 0.3% triton in PBS for 10 min, and then washed with PBS, with all steps occurring at room temperature (RT). Coverslips were blocked using 3% bovine serum albumin (BSA)/PBS for 1 hour at RT, before incubation with primary antibody (see Table 2.1 for dilutions and suppliers) overnight at +4°C. Coverslips were then washed with PBS and incubated with secondary antibodies conjugated to AlexaFluor® (see Table 2.1 for dilutions) and diluted in 3% BSA/PBS for 1 hour at RT. Coverslips were washed with PBS before mounting onto microscope slides using Fluoromount-G® (SouthernBiotech). For analysis of hypoxia, the hypoxyprobe-1 kit (hypoxyprobe) was used according to the manufacturer's instructions.

2.2.3.2. Confocal microscopy and image analysis

All images were acquired using an inverted Leica TCS SP confocal microscope. For each experiment, the same parameters were used (volume, Z-stack number) with the same acquisition settings. Image processing and analysis was carried out using Fiji software. Longitudinal reconstructions of nerves were

completed using the photomerge function in Photoshop CS4 and reconstructed nerve images were placed on a black background.

2.2.3.3. Time lapse movies

Live-imaging was performed at 10x using a Zeiss Axiovert 200M microscope equipped with a Hamamatsu Orca AG camera controlled by Volocity software (Improvision) and an environmental chamber set at +37°C and with a humidified stream of 10% CO_2 in the air. Images were taken every 10 minutes for 24 hours.

2.2.4.Molecular biology

2.2.4.1. RNA extraction from cells and tissues and cDNA synthesis

Cells were directly lysed in Trizol Reagent. RNA extraction was performed using Tri-Reagent and following the manufacturer's protocol. RNA concentration was determined using the Nanodrop and 500-1000ng of RNA was used to synthesise cDNA using SuperScript II Reverse Transcriptase (Invitrogen) and following the manufacturer's protocol. Tissue samples were crushed and homogenised on dry ice and then lysed in Trizol Reagent.

2.2.4.2. qPCR analysis

Quantitative PCR was performed using 2μl of template cDNA (diluted 1:4 in RNase free water) and 23 μl of MESA Blue qPCR MasterMix Plus Kit (Eurogentec) including 100nM forward and reverse primers (see Table 2.5) was used per reaction in a 96 well plate. Water was used as a negative control.

Cycle parameters:

MeteorTaq activation	5 min	95°C
Amplification (40 cycles):		
Denaturation	15 min	95°C
Annealing/extension	1 min	58°C
Dissociation curve	1 min	60°C

2.2.5.Protein Analysis

2.2.5.1. Protein extraction from cell monolayer

Media was aspirated from the cells and washed once with cold PBS before freezing at -80°C. Cell plates were thawed on ice and harvested in RIPA (see Table 2.7 for composition) including protease inhibitors, followed by 15 min incubation on ice to lyse. Cells were collected, before vortexing and incubating for a further 10 min, twice before being homogenised using a 30-gauge needle (BD Bioscience). Cell debris was pelleted by spinning at 13,000 rpm for 15 min at +4°C, the supernatant was collected and protein quantified using the BSA assay (Pierce, Thermo Scientific).

2.2.5.2. Protein extraction from cell pellet

After digesting nerves as previously described, the cell suspension was centrifuged at 1300rpm for 3 min to pellet cell material and supernatant was discarded. Pellets were snap frozen in liquid nitrogen and stored at -80°C. To lyse cells, 4X cell pellet volume of RIPA (see Table 2.7 for composition) including protease and phosphatase inhibitors were added and the protocol from 2.2.5.1 was followed.

2.2.5.3. Protein extraction from cell supernatant

Supernatant was harvested and cell debris was removed using 0.45 μm filter. 10% volume of trichloroacetic acid was added and supernatant was incubated overnight at +4°C. Protein was pelleted by spinning 10 min 13,000 rpm +4°C and washed once with 100% acetone. The supernatant was removed before drying the pellet, and resuspending in laemmli buffer (see Table 2.7 for composition) containing β-mercaptoethanol.

2.2.5.4. Western blot

Please refer to Table 2.7 for buffer compositions used herein. Western blotting was performed using Hoefer Scientific Instrument and BioRad Western Blot apparatus. 20-30 μg of protein was resolved using sodium dodecyl sulphate – polyacrylamide gel electrophoresis. As a size reference, 5 ul of PageRuler Plus Prestained Protein Ladder (Thermo Scientific) or ECL Rainbow Marker – Low Range (Amersham, GE Healthcare) was also loaded. Protein was transferred onto nitrocellulose membrane (Millipore-Immobilon), which was then blocked in 5% milk-TBST for 1 hour at RT. The membrane was

incubated overnight at +4°C with primary antibody (see Table 2.2 for dilutions and suppliers) and washed 3 times in TBS-T before incubating with a HRP-conjugated secondary antibody (see Table 2.2 for dilutions and suppliers) for 1 hour at RT. The membrane was then washed 3 times in TBS-T and proteins were detected using Pierce-ECL Western blot substrate (Thermo Scientific) or Luminata Crescendo Western HRP substrate (EMD-Millipore) and the ImageQuant LAS 4000.

2.2.5.5. Statistical analysis

All data are represented as mean values ± SEM unless indicated otherwise. During surgery, and nerve processing, the animals or nerve tissue samples were randomised and blinded by a colleague to reduce bias. The blinding was only revealed following completion of image analysis.

To analyse our data, when there were ≥3 or more experimental groups One-way ANOVA was used to compare means (assuming normal distribution). When there was 2 experimental groups, we used a two-tailed Students t-test to compare means (assuming normal distribution). p values are indicated as follows: ns $p \geq 0.05$, *$p < 0.05$, **$p < 0.01$, ***$p < 0.001$. For experiments n≤2 standard deviation (SD) is calculated, for experiments n≥3 standard error of the mean (SEM) is calculated.

Chapter Three: Characterisation of macrophages in healthy and injured peripheral nerves

3.1. Chapter introduction

Currently, very little is known about the nature of the resident macrophage population in peripheral nerves, as previous studies investigating resident macrophage population have often not included the nerve as a separate tissue (Mass et al., 2016, Epelman et al., 2014, Lavin et al., 2014). As a result, it is often assumed that resident peripheral nerve macrophages are similar to the resident macrophage population in the brain, microglia. Although the role of resident macrophages in the normal nerve is not known, there has been significant progress in understanding the function of macrophages within a damaged and regenerating nerve (Kiguchi et al., 2010, Rosenberg et al., 2012, Cattin et al., 2015, Das et al., 2015). Moreover, previous work from our lab has determined a novel role for macrophages during nerve regeneration in promoting blood vessel formation which subsequently aids Schwann cell migration (Cattin et al., 2015). It is also clear that macrophages have distinct roles depending on their physiological location following injury. For example, macrophages in the bridge have very different roles to those in the distal stump (Cattin et al., 2015, Kang and Lichtman, 2013). The aim of this chapter therefore is to characterise these different macrophage populations in the normal nerve and following injury, particularly with respect to their origins, and inflammatory phenotype.

3.2. RNA expression analysis of bridge macrophages reveals a complex pattern of pro- and anti-inflammatory markers

Macrophages have been traditionally described as existing in two broad phenotypes M1-like and M2-like (which may be further sub-divided) with the phenotypes characterised by their immune response, surface antigens and chemokine expression (Murray et al., 2014). Resident macrophages or circulating monocytes can polarise to either phenotype in response to a variety of stimuli, chemokines and immune challenges present in the microenvironment. M1-like macrophages are referred to as pro-inflammatory due to their association with innate immunity reactions and are commonly identified by iNOS and high MHC class II expression (Murray, 2017, Martinez and Gordon, 2014). M2-like macrophages are characterised by their ability to antagonise an inflammatory response, and are known as anti-inflammatory or repair macrophages; common identifiers of this phenotype are arginase1 and CD206 (Mannose receptor) expression (Murray, 2017, Martinez and Gordon, 2014). The current dogma

is that M1 or pro-inflammatory macrophages are the primary responders to injury or infection, and it is the M2 or anti-inflammatory macrophages which are recruited at a later stage to resolve the injury, due to their 'pro-healing' phenotype (Martinez and Gordon, 2014, Das et al., 2015). However, this two stage model represents an overly simplistic description of a continuum which exists between two activation states, pro- or anti-inflammatory. In reality, the phenotype of macrophages is too complex to describe in such a binary manner. Instead, macrophages exhibit a number of different cell surface antigens and receptors and release different chemokines in response to many different biological cues (Murray, 2017, Martinez and Gordon, 2014, Das et al., 2015). Due to this high level of variability, some groups now refer to macrophages in a way that reflects how the macrophage was polarised, e.g. M(IL-4) or M(IFN-γ), to better address the function of the macrophage and what caused its activation (Murray et al., 2014, Murray, 2017).

Macrophages are a highly plastic cell type, and in many cases, the phenotype and function of macrophages is influenced by the surrounding environment (Ma et al., 2017, Scott et al., 2016, Lavin et al., 2014, Murray, 2017). We, and others, have observed that following injury, macrophages carry out specific functions based on their location (Chen et al., 2015, Cattin and Lloyd, 2016, Rosenberg et al., 2012, Ydens et al., 2012). It has previously been reported that following sciatic nerve injury there appears to be an upregulation of M2 phenotype macrophages in the distal stump of the nerve (Ydens et al., 2012), however macrophages within the bridge have not yet been characterised. We therefore determined the phenotype of macrophages in the nerve bridge following injury, and whether this was distinct from macrophages in the distal stump. To do this, a full sciatic nerve transection was carried out in wild type rats, and tissue from the bridge and distal stump was harvested, as well as the contralateral uncut nerve, at Day 2, 3, 5 and 7 following injury. RT-qPCR was then carried out to determine the relative expression of the most commonly used pro- and anti-inflammatory (iNOS and arginase1 respectively) macrophage markers. To account for the likely fluctuations in macrophage proportions in the bridge and distal stump, expression levels were normalised to the pan-macrophage marker CD11b in the uncut nerve. However, we did not purify the macrophage population for these experiments and it is possible that we may be including RNA from other inflammatory cells and non-macrophage cell types which may also express iNOS or arginase1.

Prior to vascularisation of the bridge (Day 2), a large increase in CD11b RNA was observed in the bridge compared to the uncut nerve (Figure 3.1A) which is consistent with the increased numbers

of macrophages observed by immunofluorescence staining in the bridge at this time point (Cattin et al., 2015). On Day 3, there was a decrease in the levels of CD11b expression, presumably as other cell types, such as endothelial cells, entered the bridge and diluted the signal. On Days 5 and 7 the levels remained fairly constant, consistent with macrophages remaining in the bridge. In the distal stump, there was also an increase in the levels of CD11b on Day 2, but to a lower extent than seen in the bridge, consistent with the known infiltration of macrophages into the distal stump (Figure 3.2A) (Ydens et al., 2012). In both the bridge and the distal stump, we observed that iNOS expression peaked at Day 3 following injury (Figure 3.2B), and was followed by a sharp decrease. This suggested that the polarisation of macrophages in both nerve regions towards a pro-inflammatory (M1-like) phenotype was transient. Arginase1 displayed a different pattern of expression, and appeared to peak at Day 2 before undergoing a steady decline to basal levels in both the bridge and the distal stump (Figure 3.1C). This decrease in arginase1 expression is likely due to the resolution of injury following injury.

To confirm the RT-qPCR data, immunofluorescent staining of arginase1 in the distal stump showed that the majority (~80%) of macrophages present at Day 2 were of an anti-inflammatory or 'pro-repair' phenotype (Figure 3.2). In addition, we observed that the morphology of the macrophages in the distal stump compared to the uncut nerve, was very different. In the uncut nerve, the macrophages appeared to be small and have a compact cytoplasm. In contrast, in the distal stump, the macrophages appeared to be larger than those in the uncut nerve, and also have taken on a more 'foamy' appearance which indicates phagocytic activity. This obvious difference in morphology may be due to the different functions that the macrophages play following injury.

One caveat to these experiments is that neutrophils also express CD11b, and so it is possible that by using RT-qPCR primers for CD11b we may be identifying a mixed population of macrophages, monocyte-derived cells and neutrophils. Neutrophils may also express iNOS and arginase1, and so the RT-qPCR data here may be representative of a mixed inflammatory cell population. The staining data depicting arginase1^{+} macrophages however suggests that no neutrophils are expressing arginase1, as these cells would be easily identifiable by their characteristic lobed nucleus (Lindborg et al., 2017).

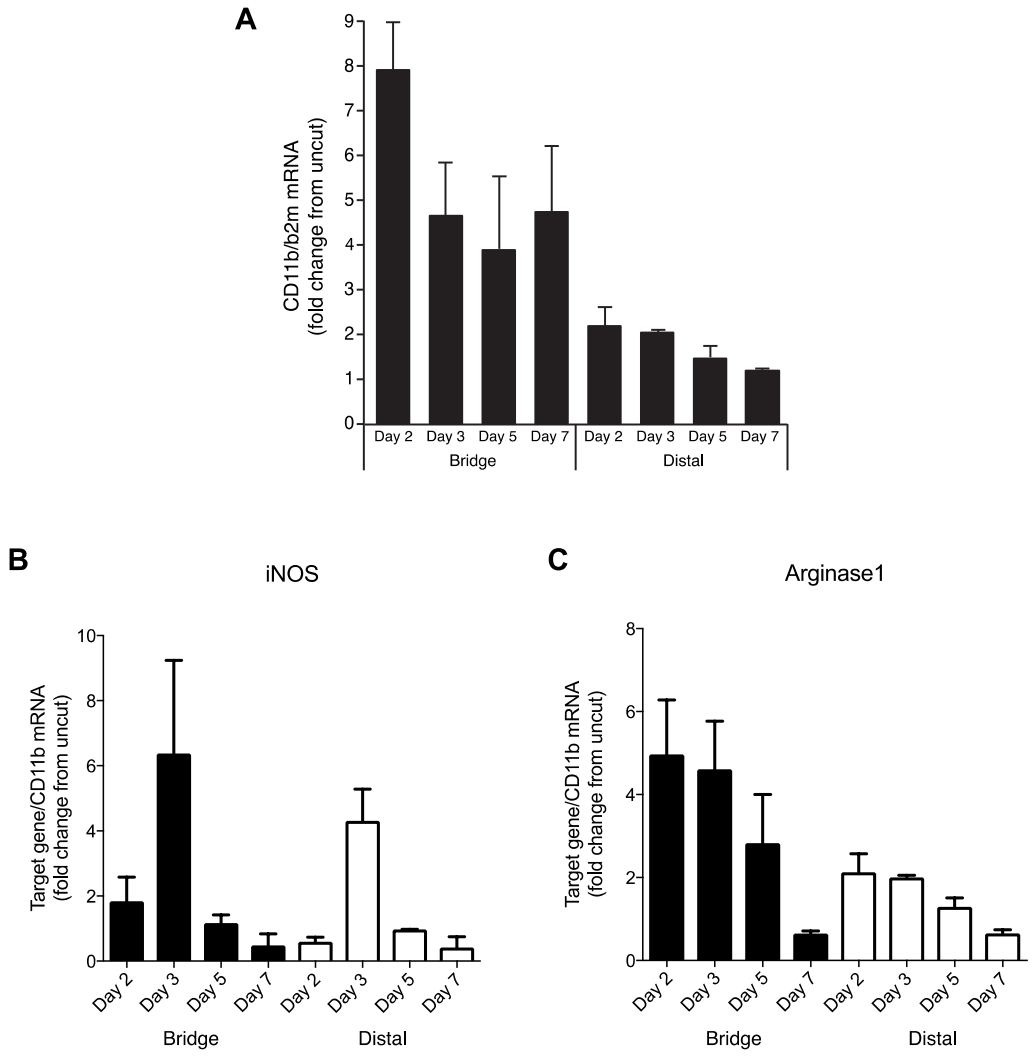

Figure 3.1 | RNA expression analysis of bridge macrophages show a complex pattern of pro- and anti-inflammatory markers

A. Quantitative RT-qPCR analysis of CD11b mRNA isolated from the bridge and the distal stump and compared to contralateral uncut sciatic nerves from rats at the specified time point following injury. Graph shows CD11b transcript levels normalised to b2m and relative to the levels in the uncut nerve (n=3 animals, graph shows mean value + SEM). B. Quantitative RT-PCR analysis of iNOS (M1) and arginase1 (M2) mRNA isolated from the bridge, the distal stump and uncut sciatic nerves after injury. Graph shows iNOS or Arginase1 transcript levels normalised to CD11b and relative to levels in the uncut nerve (n=3 animals, graph shows mean value + SEM).

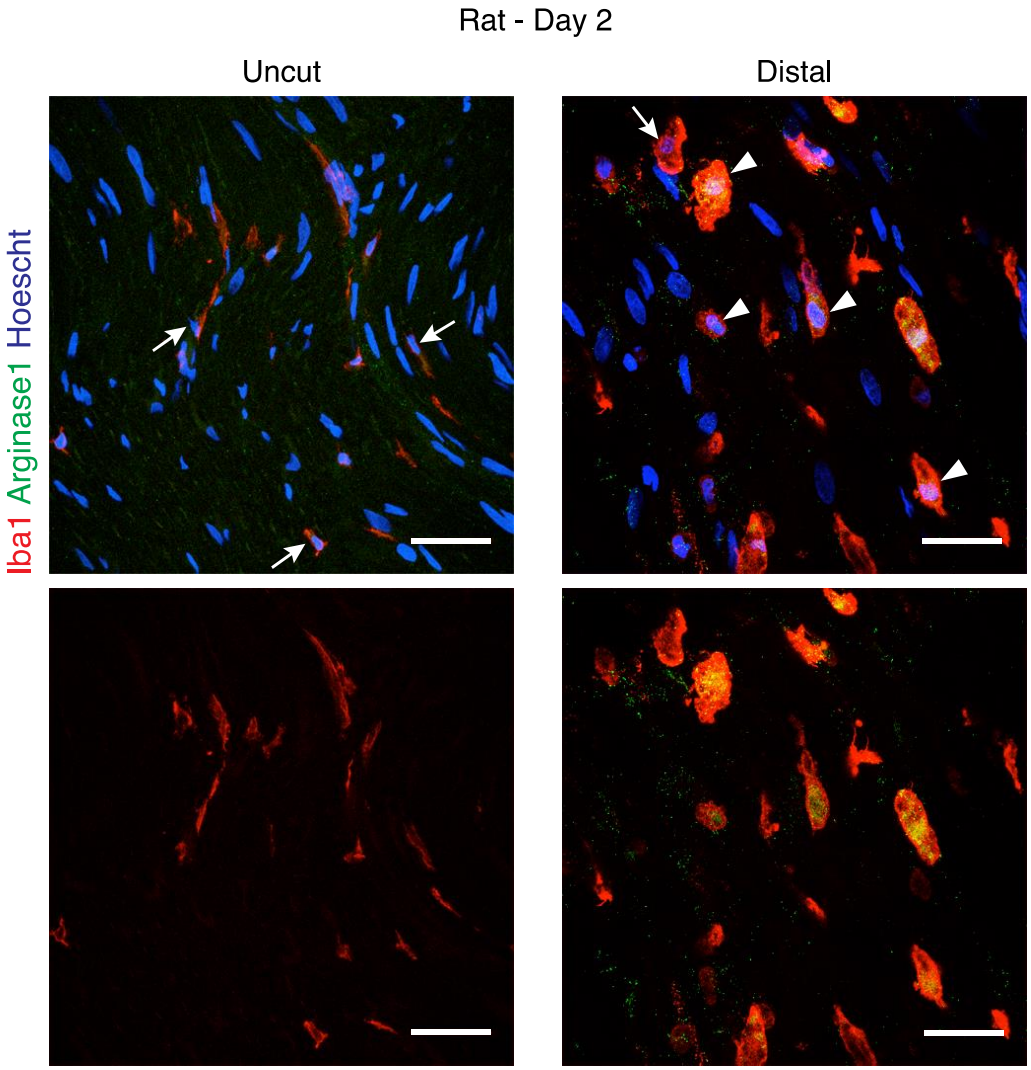

Figure 3.2 | Immunofluorescent staining confirms arginase1 expression in the distal stump
Representative images of arginase1 staining (green) in the distal stump and contralateral uncut rat nerve isolated on Day 2 following injury. Macrophages are identified by Iba1^{+} staining (red) and counterstained with Hoechst (blue). Arrows represent Iba^{+} arginase^{-} macrophages, arrowheads represent Iba1^{+} arginase^{+} macrophages. Scale bar = 30μm.

These preliminary experiments indicated that following injury, the bridge and distal stump shared expression profiles for the pro- and anti-inflammatory markers iNOS and arginase1, respectively. This RNA expression analysis indicated that the populations of myeloid cells likely changed over time as the nerve responds to injury and regenerates.

3.3. The peripheral nervous system has two distinct populations of resident macrophages which are location specific

To further investigate the nerve resident macrophage populations, we decided to first use a reporter mouse to characterise the uncut nerve and therefore the macrophage population whilst in a resting or homeostatic state. To investigate macrophage lineage, many research groups have used a mouse model in which CX_3CR1 promoter activity is coupled to GFP expression or Cre recombinase (Yona et al., 2013). CX_3CR1 is a transmembrane receptor for fractalkine, and is expressed in monocytes, dendritic cells, and NK cells (Jung et al., 2000). In the CX_3CR1^{GFP} mouse, all macrophages, as well as monocytes and monocyte-derived cells which express CX_3CR1 at that time point will also express GFP (Jung et al., 2000). GFP^+ resident macrophage populations within the CX_3CR1^{GFP} mouse include microglia and intestinal and renal macrophages, whilst GFP^- populations include Kupffer cells and skin and lung macrophages (Yona et al., 2013). The observed difference in GFP expression results from the differences in origin of the resident macrophage populations, as well as the level of recruitment of monocyte populations to replenish specific tissue populations. In the brain, microglia populations are established prenatally and originate from yolk-sac precursors, with no contribution from circulating monocytes and are long lived. Microglia retain CX_3CR1 expression and therefore the entire population is GFP^+. The intestinal population of macrophages in the mouse has a short half-life of 3 weeks (Jaensson et al., 2008) and relies on the contribution of monocyte-derived cells to replenish macrophage numbers, which results in this population also being GFP^+. In contrast, resident populations in the spleen, lung and liver are GFP^-, despite also being established prenatally and developing from CX_3CR1^+ precursors. However, these resident populations lose CX_3CR1 expression and have no contribution from monocytes as these populations maintain their numbers by self-renewal. Whilst many resident macrophage populations had been characterised in the CX_3CR1^{GFP} mouse, it was unclear whether macrophages in the nerve expressed CX_3CR1. By characterising CX_3CR1 expression in the nerve, it

may hint at the developmental or monocyte origins of this population, as well as allowing us to identify similarities with other tissue resident macrophage populations.

To investigate the expression of CX_3CR1 in peripheral nerve macrophages, we immunostained cross sections of uncut sciatic nerve and stained for the macrophage marker Iba1, as well as identifying endogenous CX_3CR1^{GFP} expression. Analysis of the nerves showed that there appeared to be two distinct populations of macrophages (Figure 3.3). Within the nerve fascicles (and within the BNB), cells stained positive for both Iba1 and GFP, whilst surrounding the endoneurium (outside of the BNB) and outside of the fascicles was a distinct population which was $Iba1^+$, yet GFP^-. The identification of these two distinct macrophage populations was an unexpected finding, as it had not previously been seen that two such populations existed within the nerve environment and additionally it hinted at differences in origin between the two different macrophage populations. Within the fascicles, and similar to microglia, macrophages are GFP^+. It is possible therefore that the resident cells of the peripheral nerve also originate from the yolk-sac and retain CX_3CR1 expression. Conversely, outside of the BNB, the macrophage population is GFP^- and therefore has lost CX_3CR1 expression. This suggests that perhaps similar to Kupffer cells, this resident population may be established prenatally, and able to self-renew without a contribution from monocytes. Apart from their different physiological location, it was unclear what the differences were between these two populations. The different expression of CX_3CR1 may hint at differences in the cell ontogeny and rates of turnover, and it may be connected to the different roles that the macrophages play within the two distinct nerve regions.

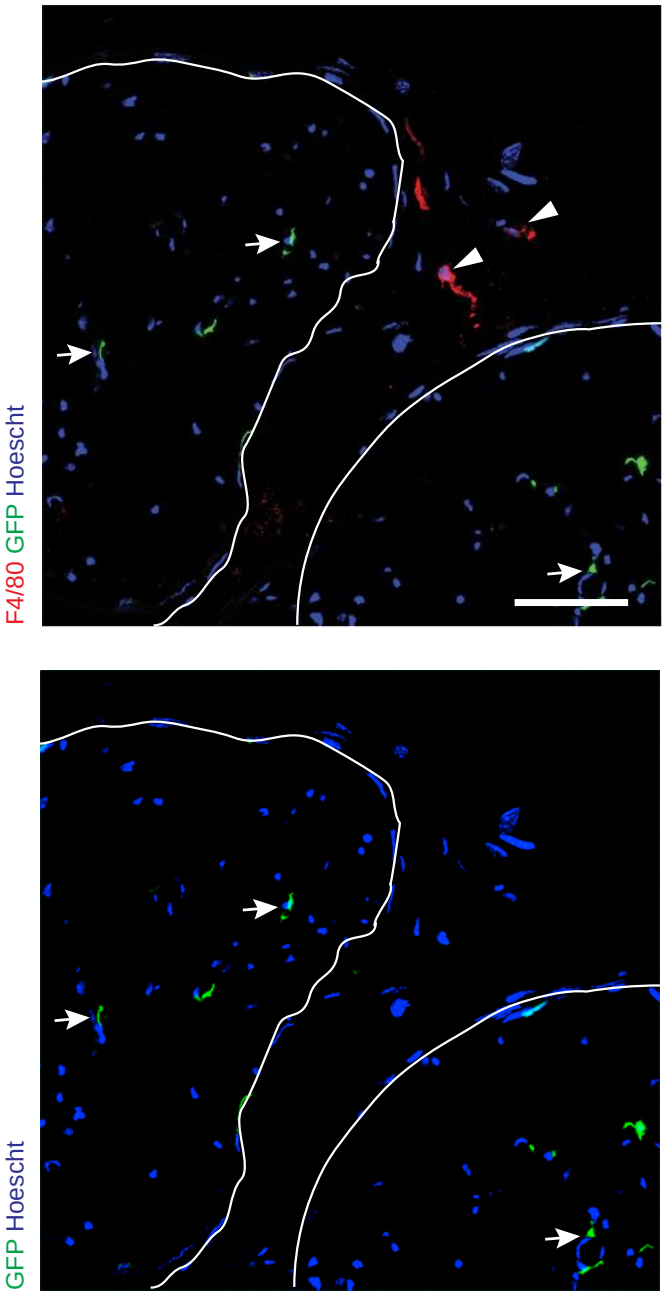

Figure 3.3 | CX_3CR1 staining in the uncut nerve
Representative images of cross sections of nerve from CX_3CR1^{GFP} mice. Immunostained for GFP (green), macrophages (Iba1, red) and nuclei/Hoechst (blue). Arrows show CX_3CR1^{+} macrophages, arrowheads show CX_3CR1^{-} macrophages. Scale bar = 50μm.

3.4. Flow cytometry analysis reveals diverse populations of monocyte-derived macrophages in the nerve following injury

Our preliminary analysis indicated an increase in macrophages in the bridge and distal stump following injury and that there are two distinct nerve resident macrophage populations, we sought to investigate how exactly the composition of these populations changed following injury. However, as several myeloid cell populations in the uncut nerve and following injury express CD11b (e.g. neutrophils), we decided to use flow cytometry using a wider range of antibodies that would allow us to better characterise the macrophages in the nerve and asses any contribution of monocyte-derived populations during homeostasis and following injury. This work was performed in collaboration with Dr Clare Bennett (Department of Infection and Immunity, UCL).

To carry out the flow cytometry experiments, nerve bridges along with proximal and distal stumps and the contralateral uncut nerve were taken from 15 mice at Day 5 following sciatic nerve transection. Care was taken to take the same length of nerve tissue from each animal without taking any surrounding muscle which may contaminate the preparation. Following harvesting, the epineurium was stripped from the nerves to ensure that only macrophages from within the nerve were analysed. Nerves were then digested with collagenase and dispase to remove extracellular matrix and to create a single cell suspension. Cells were then pelleted and incubated in blocking buffer before antibodies to detect cell surface antigens and receptors were added (for a full list see Table 2.3) and the cells were analysed by flow cytometry.

To separate out the different populations of cells, a gating scheme was designed using established protocols to identify populations of myeloid cells (Figure 3.4) (Tamoutounour et al., 2013). Initially cells were gated to determine a population of live cells of the correct size, as well as excluding cells of the wrong lineage (NK cells, B cells and neutrophils) (Figure 3.4A). Macrophages were gated by using the pan-macrophage marker CD11b, followed by CD64 which is upregulated as monocytes differentiate into macrophages to ensure that dendritic cells were excluded from this gate (Figure 3.4B). Next, to distinguish between early and mature cell populations, we gated on CCR2 expression. CCR2 is a receptor which is highly expressed on monocytes and monocyte-derived macrophages and is down regulated in mature, differentiated macrophages and resident tissue macrophage populations (Siebert et al., 2000). CCR2 is the receptor for the monocyte chemoattractant protein-1 (CCL2) which is a

chemoattractant required for monocyte egression from the bone marrow, as well as facilitating monocyte and macrophage recruitment during injury and inflammation (Patel et al., 2017, Zigmond et al., 2014).

Within the CCR2^{+} population, using Ly6C and MHCII we were able to identify populations of monocytes (Ly6C^{hi}MHCII^{-}) and monocyte-derived populations (Ly6C^{int}MHCII^{+} and Ly6C^{lo}MHCII^{+}) which represent a developmental transition of monocytes (P1) as they enter tissues, transition through an intermediate stage (P2) and differentiate into monocyte-derived macrophages (P3) (Figure 3.4B). These populations morphologically resemble blood monocytes (P1) and intermediate monocyte/macrophage populations (P2 and P3). The CCR2^{-} population could then be gated into two distinct populations based on MHCII expression, Ly6C^{lo}MHCII^{-} and Ly6C^{lo}MHCII^{+} (Figure 3.4B P4 and P5). These two populations represent tissue macrophages in morphology. (For full gating strategy, see 2.2.1.6.)

The flow cytometry data showed that there were stark differences between the healthy and injured nerve, as well as within the distinct regions of the injured nerve in regards to the contribution of myeloid cells (Figure 3.5).

3.4.1. Uncut nerve

Within the uncut nerve, we found that there were two populations of macrophages, a CCR2^{+}Ly6C^{lo}MHCII^{hi} (P3) population and a CCR2^{-}Ly6C^{lo}MHCII^{+} (P5) population, together with a more minor population of monocytes (P1). These results may be consistent with the previous staining data in the CX$_3$CR1^{GFP} mouse which indicated that there were two distinct populations of nerve resident macrophages. They also appear consistent with our long-term EdU studies that showed the turnover of macrophages is extremely slow in the nerve, as there appears to be little transition between the macrophage populations. The presence of a large CCR2^{+} population indicates this population is monocyte derived but it is unclear when they were seeded into the nerve and why they have retained CCR2 expression. Further characterisation of the CX$_3$CR1$^{-/+}$ populations should help to resolve these questions.

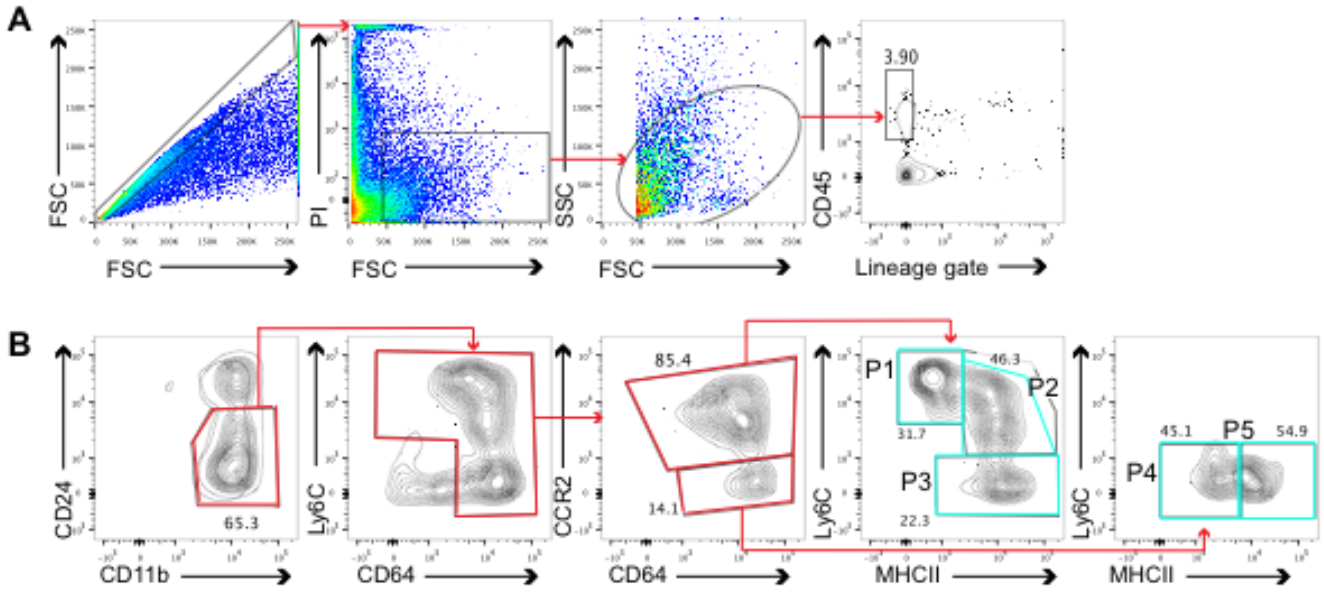

Figure 3.4 | Gating scheme for flow cytometry experiments

To determine the origin of macrophages within the nerve following injury, we used a gating strategy to determine populations of myeloid cells based on their CCR2, Ly6C and MHCII expression. A. The initial panel of gating was carried out to achieve a population of live cells of the appropriate size, as well as excluding cells of the wrong lineage (NK cells, B cells and neutrophils). B. Monocytes and macrophages were gated using LyGC and CD64 to exclude dendritic cells. CCR2 gating revealed two populations of cells which were at different stages of differentiation. A monocyte population (1) was determined as $CCR2^{+}Ly6C^{hi}MHCII^{-}$, and a developmental cascade of monocyte-derived cells (moDCs) were identified as $CCR2^{+}Ly6C^{int}MHCII^{-}$ (2) and $CCR2^{+}Ly6C^{lo}MHCII^{-}$ (3) which indicated differentiation into macrophages following entry into the tissue. $CCR2^{-}Ly6C^{lo}MHCII^{-}$ (4) and $CCR2^{-}Ly6C^{lo}MHCII^{+}$ (5) populations represent mature populations of macrophages within the tissue which have tissue macrophage characteristics, however the precise origin of these cells (monocyte-derived vs. embryonic resident) is unclear.

The population of monocytes may be due to two reasons: 1) They represent a resident populations of monocytes, which resemble blood monocytes, this has previously been observed within the dermis (Tamoutounour et al., 2013), and additional tissues (Jakubzick et al., 2013) in the absence of tissue inflammation. 2) They are the result of contamination from blood monocytes from the many blood vessels which are found within the nerve structure. Further studies should help to distinguish between these possibilities.

3.4.2. Proximal stump

In the proximal stump, we also observed a shift in the composition of myeloid populations compared to the uncut nerve, with a profile similar to the distal stump. However, there are two major differences. Firstly, the ratio of $CCR2^{+}$:$CCR2^{-}$ cells is less (80:20) and secondly, the overall number of cells entering the region is much less (Figures 3.5 and 3.6). This probably reflects the fact that the region close to the stump undergoing an inflammatory response whereas the nerve remains less infiltrated further from the cut, where the axons remain intact and the nerve requires less remodelling. Further studies using immunostaining could determine the extent of macrophage activity within this region.

3.4.3. Bridge and distal stump

Previously we have observed that in the bridge and the distal stump there is a large increase in macrophages following an injury to the nerve. It was unclear however, whether these macrophages originated from the resident population or were monocyte-derived. Previous experiments carried out using bone marrow transplants to determine the origin of macrophages in the bridge had shown that the majority of cells appeared to originate from the monocyte population rather than the resident population (Cattin et al., 2015).

Consistent with the previous findings, the flow cytometry analysis showed a dramatic change in the macrophage populations within both the bridge and the distal stump. We observed both an increase in the ratio of $CCR2^{+}$:$CCR2^{-}$ cells 95:5 (Figure 3.5), and a large increase in $CCR2^{+}$ cell numbers within these regions (Figure 3.6). Together this indicates that there is a large increase in recently entered monocytes and monocyte-derived cells, as evidenced by the emergence of a P2 population ($CCR2^{+}Ly6C^{int}MHCII^{-}$), which represents monocytes transitioning into macrophages. We also observed that as well as P5 ($CCR2^{-}Ly6C^{lo}MHCII^{+}$), there is a P4 population ($CCR2^{-}Ly6C^{lo}MHCII^{-}$), which

represents an additional, distinct population of macrophages. This large immune response is reflected in the observed increases in all myeloid populations (P1-5) (Figure 3.6B), which indicates that following nerve injury there is a strong activation of monocyte recruitment mechanisms. This data confirms what was seen previously in the bone marrow transplant experiments (Cattin et al., 2015).

The profiles of the bridge and the distal stump are similar, however we do observe that the bridge has smaller P4 and P5 populations. As these populations will contain nerve resident macrophages, it follows that the bridge would likely contain fewer of these cells due to being a newly formed tissue and lacking in resident cells. It would be interesting to conduct a time course following injury to see how the myeloid composition of the bridge changes over time, to see whether the flow cytometry profile became indistinguishable from the uncut nerve, or whether the high level of recruited monocytes and monocyte-derived cells leave the bridge tissue with a distinct pattern of macrophages populations. In the distal stump the larger P4 and P5 populations (Figure 3.6B) may represent the resident macrophages within the distal stump proliferating or changing activation state following injury. There appears to be a transition population further suggesting that the P5 population might be differentiating into the P4 population. This is not seen in the bridge, where two distinct P4 and P5 populations are seen. In the bridge there is also an additional small population within the P3 gate ($CCR2^{+}Ly6C^{lo}MHCII^{hi}$), which seems to be $MHCII^{int}$ (Figure 3.5). This population is not seen in the distal stump and it unclear what this population represents. Together these results indicate a dramatic influx of monocyte-derived cells into the bridge and distal stump following injury, which is consistent with our previous findings (Cattin et al., 2015). However, further studies are needed to further characterise the temporal behaviour of these cells and the resident populations.

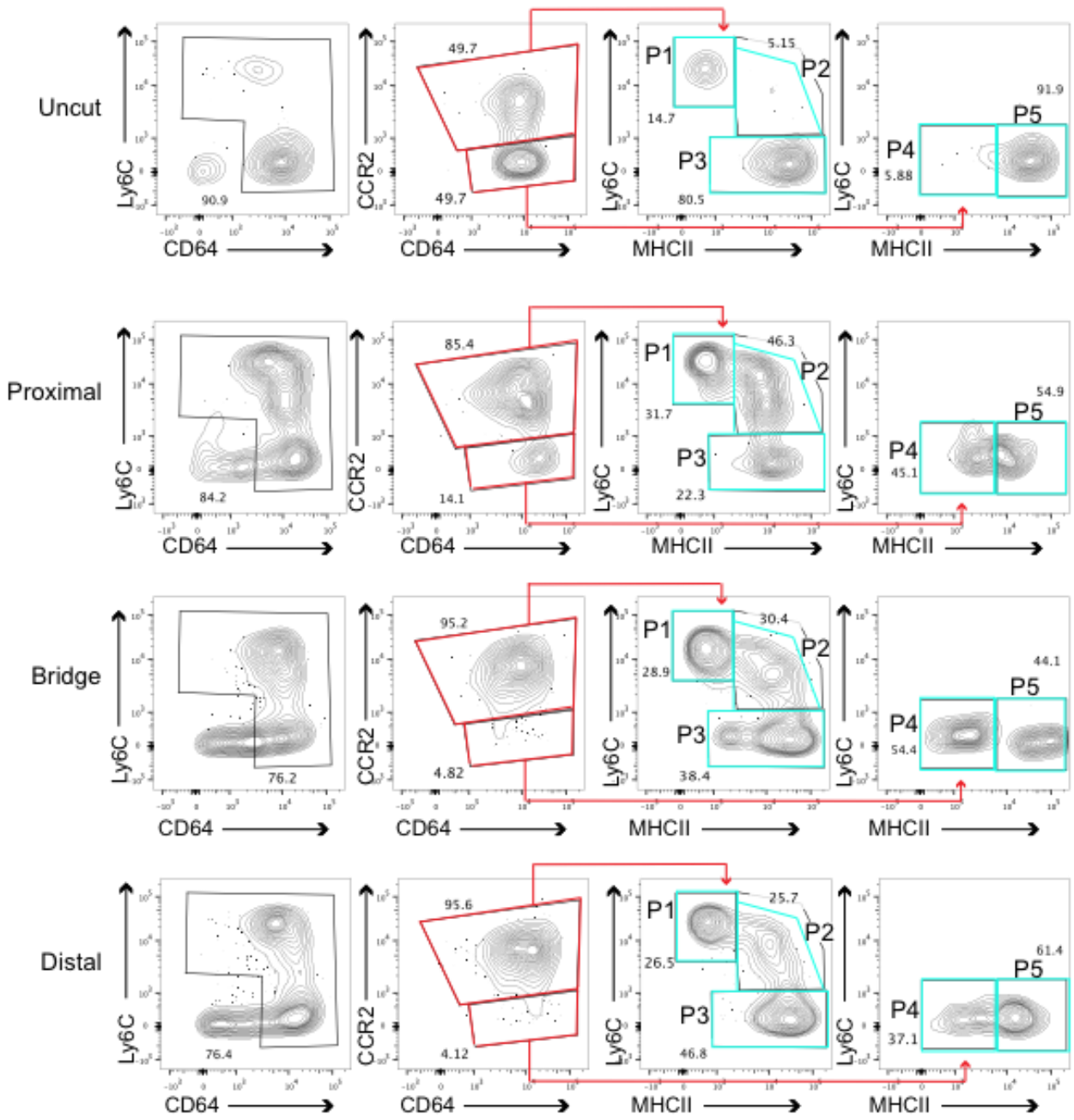

Figure 3.5 | Myeloid cells contribute to populations following injury in the peripheral nerve
Representative flow cytometry plots from the contralateral uncut nerve, proximal stump, bridge and distal stump on Day 5 following injury (n=3, sample pooled from 15 WT mice).

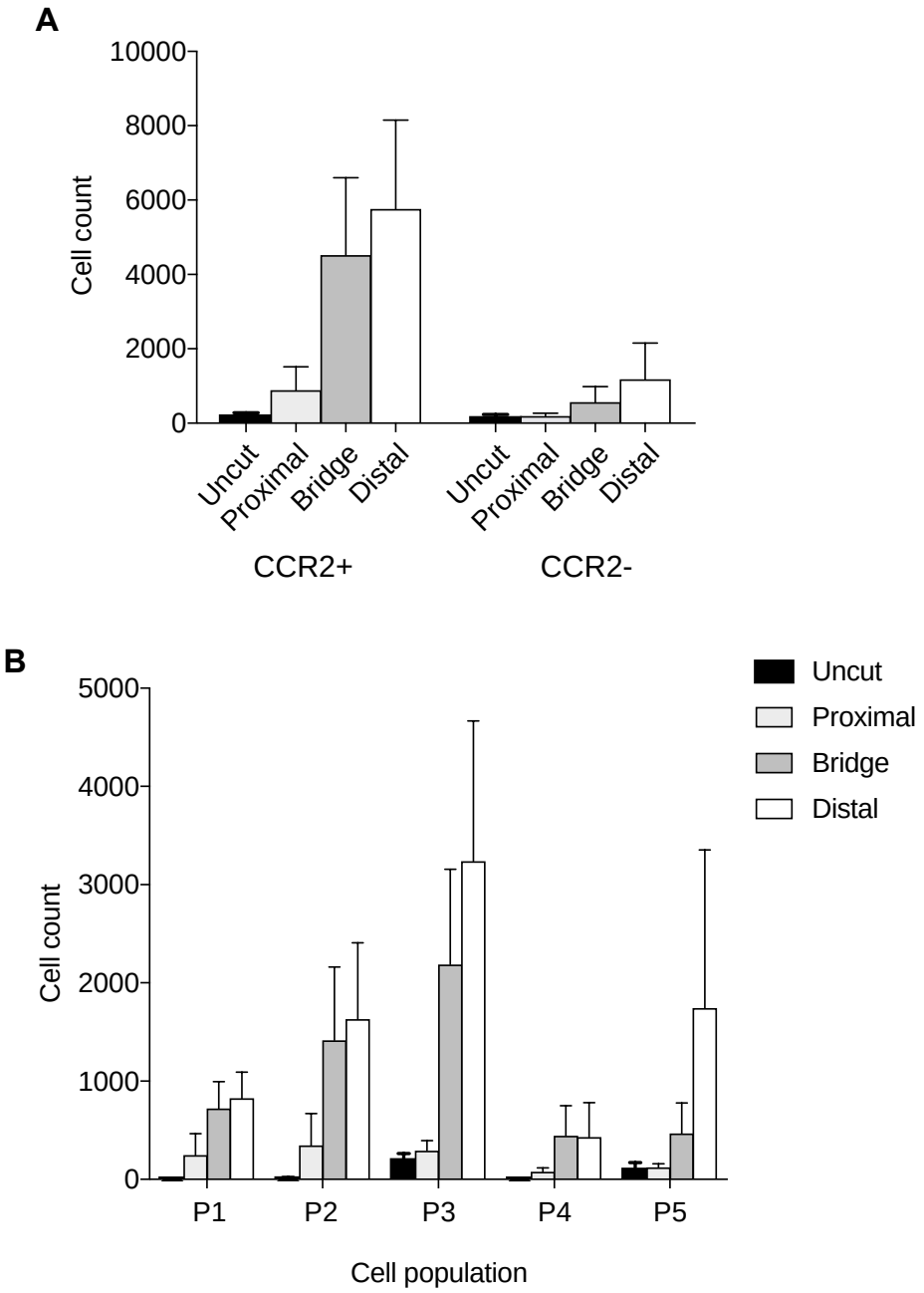

Figure 3.6 | CCR2^{+}/CCR2^{-} populations in the regenerating nerve
Cell counts from flow cytometry and extrapolated from cell populations using counting beads isolated on Day 5 following injury showing CCR2^{+} and CCR2^{-} populations (A) and monocyte-derived populations 1-5 (B). Graphs shows mean cell counts + SEM. n=3, each experiment represents cells pooled from 15 WT animals.

3.5. Contribution of monocyte-derived cells to nerve regeneration

We have observed using immunofluorescence and flowcytometry experiments that following sciatic nerve injury there is a large influx of monocytes into the nerve bridge. Using CCR2 knockout ($Ccr2^{tm1Ifc}$ (Boring et al., 1997)) mice as well as control heterozygous animals, we wanted to observe nerve regeneration following sciatic nerve injury, and to quantify the number of macrophages which were present. In the CCR2 KO animal, we were curious to test whether the nerve bridge still formed, and whether the numbers of macrophages change in the CCR2 knockout compared to control animals.

Initially, to determine whether the CCR2 KO mice had the same proportion of resident peripheral nerve macrophages that we observe in wild type animals, we quantified the numbers of macrophages present in the nerve. To do this, we took thin cross sections of uncut nerves from male and female CCR2 KO animals and heterozygous controls and stained for macrophages using the marker F4/80 and for blood vessels and perineurial cells using the marker glut1. Confocal images of the nerve sections were obtained, and macrophages (F4/80+ and Hoechst+) were quantified from at least 5 different sections per animal. In data from the lab (Stierli and Napoli et al., in preparation) as well as published data (Griffin et al., 1993, Klein and Martini, 2016) the percentage of macrophages in the quiescent nerve has been quantified as ranging between 6-10%. When the proportion of macrophages in the uncut nerve from $CCR2^{+/-}$ and $CCR2^{-/-}$ mice were quantified, we found that there were 10% and 7% respectively which indicated that there was no significant difference from wild type animals, and indicated that the CCR2 gene modification did not appear to alter the embryonic seeding or maintenance of nerve resident macrophages (Figure 3.7).

To investigate monocyte recruitment following injury, we performed a full sciatic nerve transection on both $CCR2^{-/-}$ and $CCR2^{+/-}$ animals and harvested them at Day 5 following injury, and quantified the number of macrophages ($F4/80^{+}$) present as a proportion of cells in the bridge. We observed that morphologically the control $CCR2^{+/-}$ bridges were normal and we observed that the percentage of macrophages within the nerve bridge, 43% (Figure 3.8A, left panel and quantified in 3.8B) which was an expected result, and was similar to the proportions of macrophages that have been observed previously (Cattin et al., 2015).

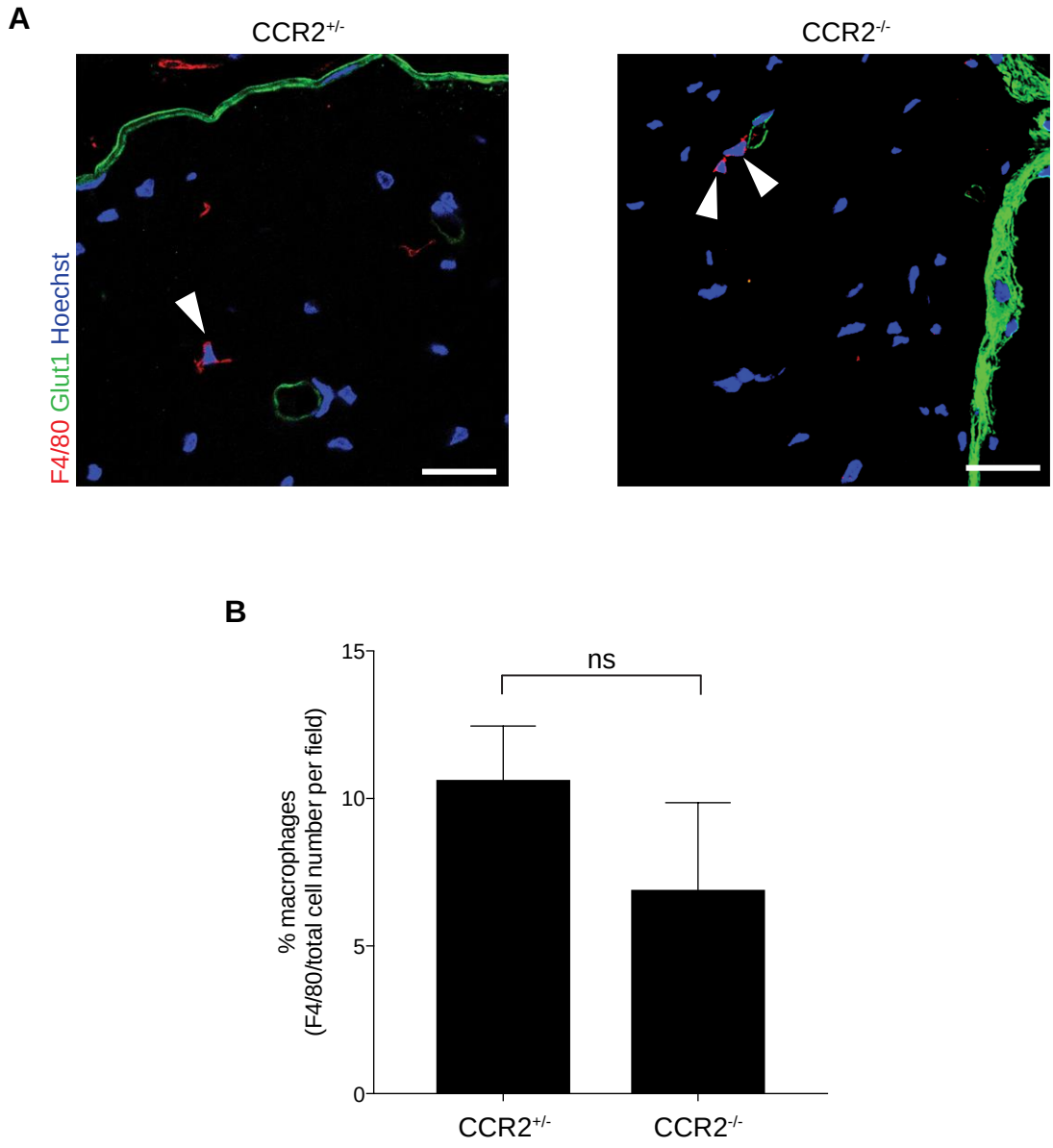

Figure 3.7 | CCR2-/- and CCR2+/- macrophage quantification in the uncut nerve
A. Representative images of cross-sections of uncut nerve from $CCR2^{+/-}$ and $CCR2^{-/-}$ animals. Nerves immunostained to detect blood vessels (glut1, green), macrophages (F4/80, red) and nuclei counterstained with Hoechst (blue). Arrowheads show F4/80+ cells. Scale bar = 50µm. B. Quantification of macrophages (F4/80+). Graph shows mean +SEM, n=3. (NB: glut1 also stains perineurial cells.)

In the CCR2$^{-/-}$ animals, we saw that at Day 5 the gross morphology of the bridge was similar to what we would observe in a control animal (Figure 3.8A, right panel). Despite the similar gross morphologies, when we quantified the macrophages in the bridge, we saw that the percentage of macrophages in the CCR2$^{-/-}$ animals was approximately half (~20%) of the numbers seen in the control animals (Figure 3.8B). This indicated that in the knockout animals, as might have been expected, there was a decrease in the recruitment of monocyte-derived macrophages. This aligns with our previous flow cytometry data which indicated that the majority of cells in the nerve bridge following injury were monocyte-derived. There were still macrophages present in the bridge following injury, and we could hypothesise that these macrophages were resident macrophages which have proliferated and migrated into the bridge or monocyte-derived cells which have been recruited to the nerve bridge in a CCR2 independent manner, which could then carry out the bridge-specific macrophage roles in regeneration.

In the CCR2$^{-/-}$, the Schwann cells did appear to be migrating in a less directional manner into the bridge, which may indicate that the CCR2$^{-/-}$ animals exhibit abnormal regeneration compared to controls. This is a potentially interesting result; however it requires further investigation to see whether the lack of CCR2^{+} macrophages has a significant effect on nerve regeneration in the short or long-term. Schwann cell and blood vessel migration into the bridge were not quantified due to time restraints, however in the future it would be desirable to quantify these parameters in the CCR2 knockout animals to determine whether macrophage recruitment is important for nerve regeneration.

This mouse model confirmed that monocyte-derived macrophages are recruited to the nerve bridge following injury, however it indicated that resident macrophages or monocyte-derived cells recruited by alternative methods may compensate for the decrease in CCR2-dependent cell recruitment.

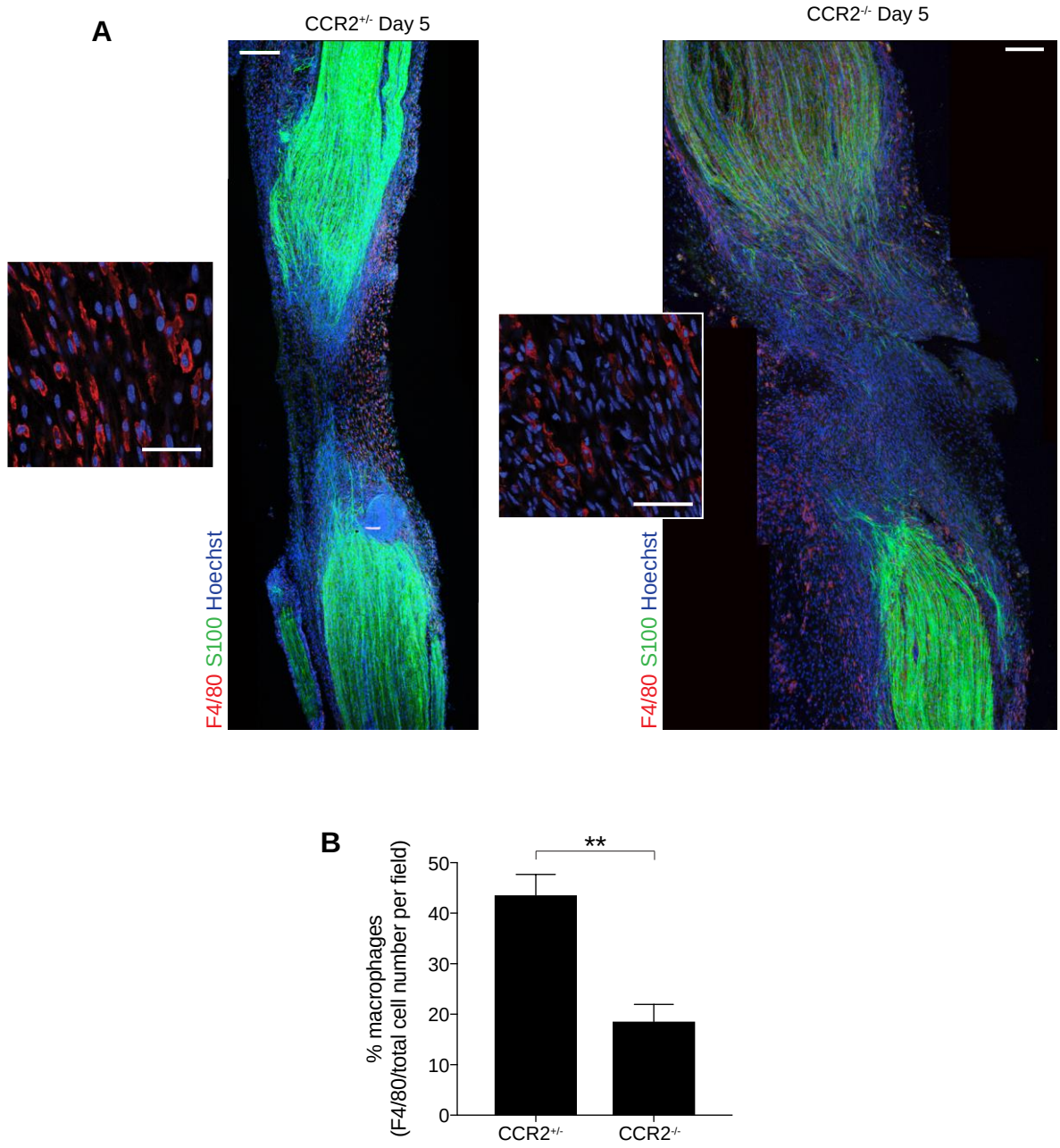

Figure 3.8 | CCR2$^{-/-}$ mice display a reduced number of macrophages in the bridge following injury
A. Representative images of CCR2$^{+/-}$ (left panel) and CCR2$^{-/-}$ (right panel) on Day 5 following injury stained for Schwann cells (S100, green), macrophages (F4/80, red) and nuclei counterstained with Hoescht (blue). Scale bar = 200µm. (Inset shows high magnification of bridge used for quantification. Scale bar = 50 µm. B. Quantification of macrophages present at Day 5 in the nerve bridge following injury. Graph shows mean % of total cells +SEM, n=3.

3.6. Nerve resident macrophages are distinct from other tissue resident macrophages

There have been many recent reports which have employed the use of transcriptomic analysis both at a single cell and whole population level to analyse and compare different tissue resident macrophage populations (Lavin et al., 2014, Ginhoux and Guilliams, 2016, Choi et al., 2017, Mass et al., 2016). Whilst this has been useful to determine the expression profile of many resident macrophage populations, peripheral nerves have not been analysed in these studies. An interesting recent study looked at how the expression profile of multiple tissue resident macrophages changed over time, from the pMac stage during embryonic development (E7) up until early adulthood (P21) when the macrophage population was established within a specific tissue microenvironment (Mass et al., 2016). We therefore used this information to characterise the adult nerve resident macrophage gene profile compared to other tissue resident macrophage populations. We were particularly interested to see how similar the nerve and brain resident macrophage populations were, as it has often been assumed that these populations are phenotypically similar.

Initially, to gain insight into the transcriptome of resident macrophages in the peripheral nerve, we carried out RNA expression analysis on tissue macrophages extracted from the nerve and compared this to well characterised populations from the brain (microglia), liver and kidney. We chose to determine the expression levels of the following genes: Mafb, Fcrls, Jun, Fos, Timd4, Fcgr4 and Pparg. These genes were highly expressed in at least one of the tissues we chose and were known to be differentially expressed by different macrophage populations. The aim of this preliminary experiment was to determine which macrophage population, if any, the peripheral nerve macrophages most closely resembled.

To isolate the macrophages, the organ tissue was harvested from adult rats and digested using collagenase and dispase. The cells were then pelleted, and washed with fresh media to remove debris. The cells were resuspended in media and macrophages were isolated using cell culture dishes coated with an antibody against CD11b. The cells were then scraped off the plate in Tri reagent and the RNA was extracted before carrying out reverse transcription. The resulting cDNA was then used to perform a qPCR with primers specific for the genes of interest, and normalised to the housekeeping gene b2m. Per tissue, the gene expression was then normalised to the highest expressing gene from the panel (Figure 3.19).

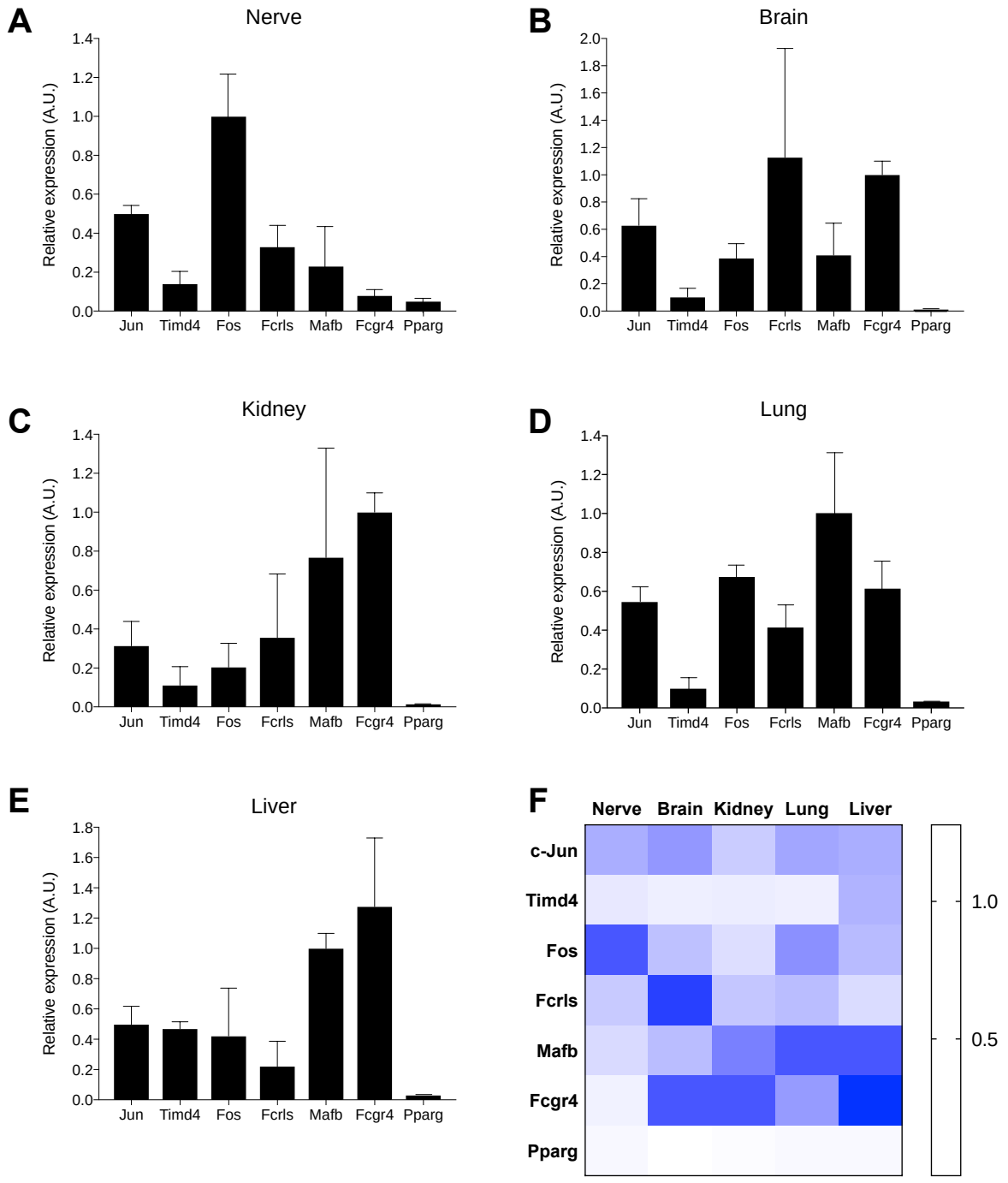

Figure 3.9 | RNA expression analysis highlights variable gene expression patterns in resident tissue macrophage populations.

RT-qPCR data for specified gene expression in nerve (A), brain (B), kidney (C), lung (D) and liver (E) CD11^{+} resident macrophage populations. Graphs show average +SEM, n=3. F. RT-qPCR data expressed as comparative heat map, n=3.

The immediate impression from the RT-qPCR results from the different tissues is that they each display very distinct expression profiles (Figure 3.9). In particular, it is interesting to note that the nerve and brain macrophage expression pattern is quite different, which suggests that these two resident populations may be more different than has been previously assumed. One of the striking differences was that the nerve macrophages had much lower expression of Fcgr4, which encodes the Fc ɣ receptor IV (FcɣRIV) compared to all of the other resident populations (Figure 3.9). Myeloid cells express various different FcgRs which enable interactions with IgGs, immune complexes or cells and may have an inactivating or activating effect on the macrophage (Guilliams et al., 2014). FcɣRIV binds IgG2 and is an activating receptor which can facilitate antibody-mediated phagocytosis in macrophages (Suwanichkul and Wenderfer, 2013). Our data is consistent with previous findings which shows that the lung (Guilliams et al., 2014), brain and kidney (Suwanichkul and Wenderfer, 2013) express Fcgr4. The lack of Fcgr4 expression in the nerve therefore suggests that another FcɣR type predominates and that immune interactions within the nerve are modulated in an alternative manner.

Nerve and brain resident macrophages did however, both display low expression of Mafb, which has recently been identified as a key transcription factor repressor for regulating the self-renewal properties of macrophages (Soucie et al., 2016). When expressed, Mafb represses self-renewal promoting genes such as Myc, Stat3 and Akt1, and the macrophage population is quiescent (Soucie et al., 2016). The loss or inhibition of Mafb therefore results in the loss of repression on these self-renewing genes, which promotes proliferation, and the ability to serially re-plate *in vitro*. Cells with low Mafb or knockout of Mafb maintain their macrophage phenotype throughout life and have been observed to last many rounds of self-renewal *in vitro*. These qPCR results therefore suggest that peripheral nerve macrophages have the ability to self-renew, a property that microglia are also known to exhibit.

Across all tissues there was low expression of the peroxisome proliferator activated receptor ɣ (PPARɣ/Pparg), a fatty acid metabolism transcriptional regulator (Chawla, 2010). In macrophages, PPARɣ has been observed to regulate activation and effector function through their metabolic state (Chawla, 2010). High expression of PPARɣ typically is associated with an alternatively activated (or M2-like) macrophage state and so in this instance, tissue-wide low expression of PPARɣ correlates with a ‘resting’ macrophage state, which has not been polarised following injury or immune response an is consistent with the resting state of the tissues.

3.7. Macrophages have an intrinsic differential response to hypoxia

One of the major roles that macrophages have during nerve regeneration is the promotion of new blood vessel growth into the bridge (Cattin et al., 2015). Immediately following injury, the newly formed nerve bridge is hypoxic due to the lack of blood vessels and the formation of new vasculature has been shown to be crucial for the regeneration process. The hypoxia response of tissues has been well characterised, and it is known that angiogenesis is promoted by the release of VEGF from cells which sense hypoxia and in turn upregulate hypoxia response genes (Burke et al., 2003, Lin and Simon, 2016). We found that in the nerve bridge, macrophage-derived VEGF was responsible for inducing blood vessel formation (Cattin et al., 2015). Through the genetic knockout of *Vegfa* specifically in myeloid cells and pharmacological inhibition of VEGF receptor 2 (VEGFR2) using Cabozantinib (Cabo), we showed that blood vessel formation in the nerve bridge was dependent on macrophage-released VEGF (Cattin et al., 2015). Additionally, it was determined that macrophages are the only hypoxic cell type (>90% total cells) within the bridge on Day 2 after injury, prior to blood vessel entry (Cattin et al., 2015).

This result was particularly interesting, as it suggested that macrophages within the bridge differentially sense hypoxia compared to other cell types in the same conditions (e.g. fibroblast, neutrophils). This could be an important property of macrophages, as we know that the hypoxia-induced release of VEGF in the bridge is crucial for blood vessel formation, however it was unclear whether the differential response of the macrophages was due to the injured nerve microenvironment, or whether this was an intrinsic property of the macrophages. The ability to act as primary responders to hypoxia has implications for the many disease states where hypoxia is present, such as following injury or in tumours (Lin and Simon, 2016, Riboldi et al., 2012, Semenza, 2012).

To address whether this observed differential hypoxia response was an intrinsic property of macrophages or due to the nerve microenvironment, we determined whether this response was maintained *in vitro*. To do this, nerve bridges were isolated from adult rats at Day 2 (prior to vascularisation) when it is known that a large proportion of the cells are macrophages, and additionally that these macrophages are hypoxic. The bridges were digested with dispase and collagenase to remove extracellular matrix components and to create a single cell suspension. Cells were then washed twice in media containing serum in order to remove any residual digestion enzymes and any remaining cellular debris, and the cells were counted using a haemocytometer. Cells were seeded in triplicate onto PLL and fibronectin coated coverslips at a concentration of 60,000 cells/well, and allowed to settle

overnight in normoxic conditions (20% O_2). The following day, hypoxyprobe was added to the bridge cell cultures before incubating for five hours at three different oxygen concentrations 20% O_2 (normal *in vitro* oxygen conditions), 1.5% O_2 (moderate hypoxia) and 0.1% O_2 (severe hypoxia). Cells were then washed twice in media and fixed in PFA before being stained for hypoxia and macrophage markers (hypoxyprobe-1 and Iba1 respectively) and quantified using confocal microscopy. From this analysis, it was observed that as the level of hypoxia increased, so did the number of hypoxic cells (Figure 3.10A and quantified in Figure 3.10B). This was an expected finding, and at the highest level of hypoxia (0.1% O_2) we saw the highest proportion of hypoxic cells. When we quantified the hypoxic cells at each oxygen level according to their cell type, we found that more than 90% of macrophages were hypoxic at 1.5% oxygen (Figure 3.10C). In contrast, non-macrophages cells in the bridge were mostly negative for hypoxyprobe at 1.5% oxygen (20% hypoxyprobe+), and only at severe levels of hypoxia were the majority of these cells hypoxic (Figure 3.10C). These results showed that when cells were isolated from the nerve bridge and cultured in varying oxygen concentrations macrophages showed a similar differential response to that observed *in vivo*. This suggested that macrophages are differentially sensitive to hypoxia in the nerve bridge, compared to the other non-macrophage cell types present such as fibroblasts and that this is an intrinsic property of macrophages however the molecular mechanisms underlying this differential response are unknown.

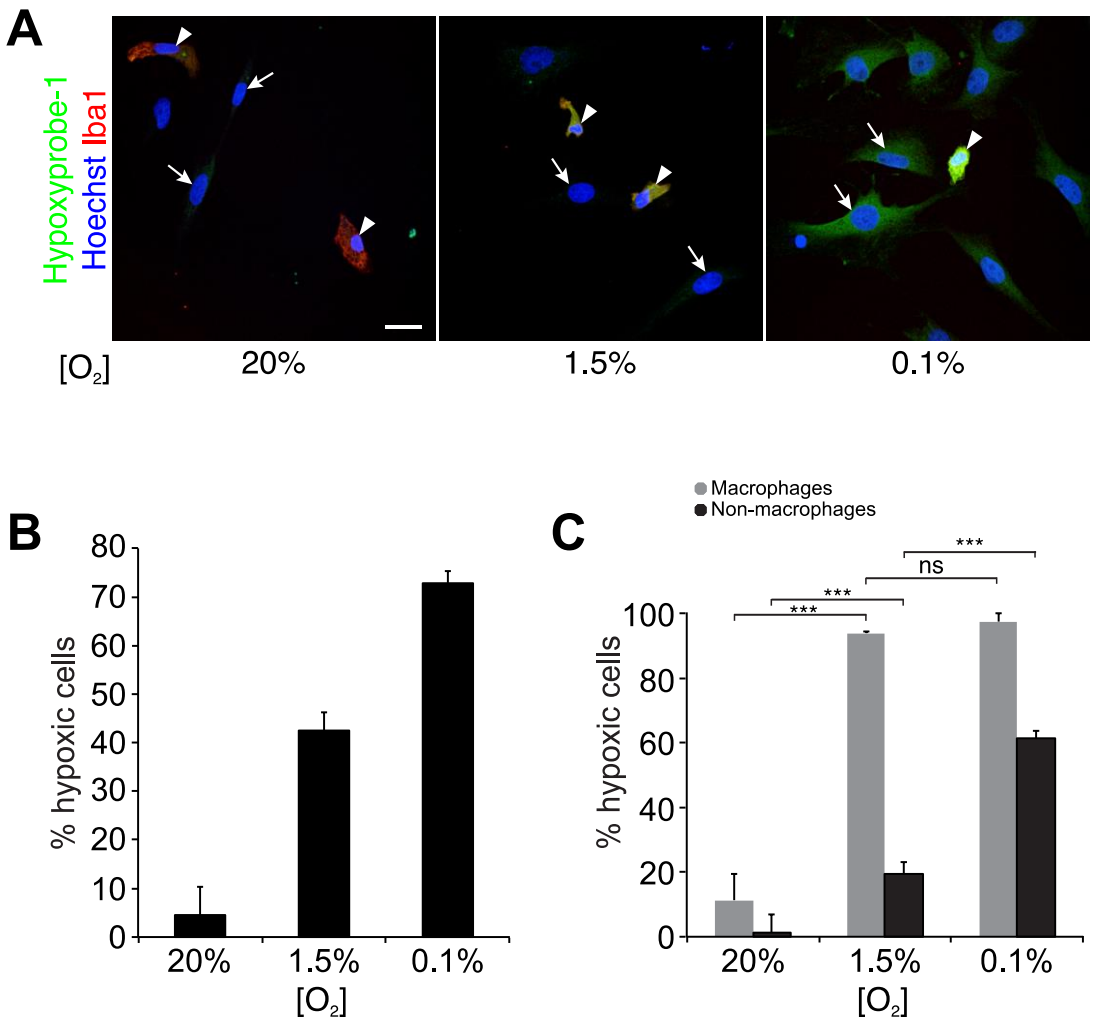

Figure 3.10 | Macrophages are selectively sensitive to hypoxia compared to non-macrophage cell types

A. Representative images of cells taken from Day 2 sciatic nerve bridges, incubated at varying levels of hypoxia and immunostained for hypoxyprobe (green), macrophages (red) and nuclei counterstained with Hoechst (blue). Scale bar = 20μm. B. Quantification of total hypoxic (hypoxyprobe$^+$) cells in rat ex-vivo nerve bridge cell preps. Graph shows mean +SEM, n=3. C. Quantification of hypoxic (hypoxyprobe$^+$) macrophage (Iba1$^+$) and non-macrophage (Iba1$^-$) cells. Graph shows mean +SEM, n=3, ***p<0.001. One-way ANOVA test was used for statistical analysis.

3.8. Chapter discussion and conclusions

Peripheral nerve macrophages remain one of the most understudied tissue resident populations in the body. Whilst multiple tissue resident macrophage populations, e.g. microglia, Kupffer cells, have been characterised, the same cannot be said for those from peripheral nerves. Here, we have performed a preliminary characterisation of this population.

RNA expression analysis of resident macrophage populations in the nerve, liver, kidney, brain and lung showed that the expression patterns were strikingly different between the tissues, which is likely to reflect not only the specific microenvironment and function, but also the differential ability of macrophage populations to self-renew. This analysis also showed that nerve macrophages are distinct from microglia; the PNS and CNS resident macrophages are usually thought of as being similar populations, however this analysis shows that there are transcriptional differences between the two populations, which are likely to be connected to their location as well as their function.

When isolating macrophages from the nerve we did not distinguish between endoneurial and epineurial macrophages, and experiments using the CX_3CR1^{GFP} reporter mouse identified that these two macrophage populations are different; macrophages within the endoneurium were CX_3CR1^{+} whilst macrophages outside of the endoneurium were CX_3CR1^{-}. This difference in CX3CR1 expression may reflect differences in the turnover of these cells; the endoneurial macrophages are long lived and might be able to renew in a manner similar to microglia, whilst the macrophages surrounding the endoneurium may instead rely on monocyte-derived cells to maintain populations. To determine whether the CX_3CR1^{+} resident macrophages require monocyte-derived cells to maintain the population, additional mouse models will need to be used. For example, by using the $CX_3CR1^{YFP-CreER/wt}$:$R26^{RFP}$ mouse (O'Koren et al., 2016) and applying a pulse dose of tamoxifen this would result in CX_3CR1^{+} YFP^{+} cells (i.e. monocytes and the population of resident nerve macrophages within the fascicles) becoming RFP^{+}. If this is then followed by a 'wash out' period of several weeks, RFP expression will be lost in monocytes due to their fast turnover, yet retained in the nerve macrophages. Analysis of the uncut nerves would then show whether the macrophages inside of the BNB rely on monocyte recruitment, as the population would contain both YFP^{+} and RFP^{+} populations.

Similar to in the brain, it is becoming apparent that there are multiple subsets of PNS macrophages, as evidenced by CX_3CR1 staining as well as the multiple myeloid cell populations present in the nerve following injury which showed heterogeneous cell populations. To fully determine the

differences between these populations it may be advisable to firstly sort CX_3CR1^+ and CX_3CR1^- nerve macrophages and subsequently to perform a single cell RNA-seq analysis which would enable us to identify transcriptional differences not only between these two defined populations, but also to identify whether there are additional subsets within these populations. Carrying out this analysis prior to injury and following injury would also allow us to identify how these subpopulations change their expression profiles to enable nerve regeneration.

Flow cytometry analysis also showed that in the uncut nerve there was a population of monocytes present, despite the lack of inflammation within the tissue; the presence of a monocyte population in the absence of infection has previously been observed in other tissues (Jakubzick et al., 2013). In the uncut nerve we also found that there appeared to be two different populations of resident cells (confirming the CX_3CR1 staining), however it is not possible to state the origins or specific composition of this population with certainty as it requires further exploration using reporter mice (Tamoutounour et al., 2013).

Following injury, RNA expression analysis and preliminary staining data determined that the phenotype or activation status of macrophages in the nerve following injury is subject to temporal changes. As expected, we saw a dramatic increase in the proportion of macrophages in the bridge and to a lesser extent in the distal stump compared to uncut controls. In both regions, we also saw that there were increases in both iNOS and arginase1, which fluctuated in the days following injury, and decreased at 7 days post-injury which we would assume is due to injury resolution with a resulting decrease in the proportion of macrophages in both the bridge and the distal stump.

The flow cytometry experiments showed that the majority of cells recruited to the bridge following injury were bone-marrow or monocyte-derived, confirming previous experiments in which bone marrow from GFP^+ mice was transplanted into GFP^- mice prior to injury. These initial experiments showed that close to 90% of macrophages in the bridge were GFP^+ and therefore bone marrow derived. However, due to the use of irradiation within these experiments, which may have altered the local turnover of macrophages in tissues; flow cytometry analysis was therefore important to confirm these results. The data presented here shows only a preliminary characterisation of peripheral nerve macrophages, due to the small sub-set of genes tested, as well as only investigating a single time-point (6 weeks). To fully investigate the peripheral nerve resident macrophage population, it would be preferable to test many different time points, from embryonic stages, through early post-natal time points

up until adulthood to observe whether the composition and expression profiles of the peripheral nerve macrophages change, as well as identifying the point during development when a nerve resident population of macrophages is established. The gene expression profile may also indicate the roles that nerve macrophages play in the homeostatic state, as well as hinting at the function following peripheral nerve injury.

Longer term experiments, using fluorescence reporter mice would provide information about resident and monocyte-derived macrophage longevity. In particular, it would be of interest to track the cells which infiltrate the nerve following injury resolution and, using flow cytometry and staining, determine changes in the macrophage populations and whether the infiltrating cell populations become indistinguishable from resident macrophages. It would be interesting to see whether the flow cytometry profile on the regenerated nerve resembled the uncut nerve with two distinct populations, or whether this was altered.

In order to look at the contribution of the $CCR2^{-}$ macrophages to the nerve regeneration process, we used the $CCR2^{-/-}$ mouse and carried out a sciatic nerve injury. Interestingly, we found that despite the decrease in macrophage numbers, the bridge was still able to form, however it seemed like Schwann cell migration was less directional in the CCR2 knockout animals compared to the controls. Schwann cell and blood vessel migration into the bridge was not quantified and so further experiments to quantify regeneration efficiency will be conducted in the future.

Experiments carried out on macrophages in the nerve bridge following injury have highlighted a novel property of macrophages, that they have a differential response to hypoxia. This had not previously been reported, and we observed this phenotype both *in vivo* and *in vitro*. This differential response of macrophages to hypoxia confers macrophages within the nerve bridge the ability to induce blood vessel growth, through the hypoxia-induced release of VEGF. We have previously seen that in the absence of VEGF release, through genetic knock out studies, that blood vessel growth is seriously impaired which leads to aberrant Schwann cell migration, and therefore nerve regeneration is compromised. The presence of hypoxia within the cells (as identified by hypoxyprobe staining) indicates that there is imbalance in the demand, compared to the supply of oxygen, i.e. demand>supply. Hypoxyprobe specifically and irreversibly binds in areas of hypoxia and therefore represents conditions where the demand for oxygen is above what is being supplied. Hypoxia is associated with inflammation as there is an increase on oxygen demand from the milieu of cells in the area which have increased

metabolic demands in order to produce the cytokines, inflammatory mediators and enzymes necessary to resolve inflammation (Taylor et al., 2016). Our data suggests that within the injured nerve, macrophages in the nerve bridge are experiencing a higher demand for oxygen compared to their demand, resulting in hypoxyprobe^{+} staining. The same was observed *in vitro* which suggests that the differential response to hypoxia is intrinsic and not due to the microenvironment. The mechanism behind this differential response of macrophages to hypoxia is still not understood, however it is possible that it represents a switch in macrophage activation state.

This chapter presents the preliminary experiments carried out to characterise PNS macrophages in the uncut nerve and following injury. To further characterise these populations, we will initially use the $CX_3CR1^{YFP-CreER/wt}$:$R26^{RFP}$ mouse which would allow us to discriminate between the various macrophage populations within the nerve (O'Koren et al., 2016). We would then conduct FACS and sort the cell populations before conducting immunofluorescence staining and single cell RNA-seq analysis. This will allow us to answer questions regarding the phenotype and gene profiles of monocyte-derived cells and the contribution of monocytes to maintain populations in the uncut nerve as well as following injury and subsequent resolution.

Chapter Four: A novel role for macrophages in inducing Schwann cell migration

4.1. Chapter introduction

We have recently found that Schwann cells use newly formed blood vessels as a scaffold in order to migrate across the new tissue that constitutes the nerve bridge (Cattin et al., 2015). The blood vessels form in response to the release of VEGF by hypoxic macrophages in the bridge. However, it has not been determined whether there is a chemoattractant present in the nerve bridge following injury, which may recruit Schwann cells and promote their collective migration.

We recently found that Schwann cells migrate in a VEGF-independent manner *in vivo* (Cattin et al., 2015). The use of a genetic knock out animal ($Tie2^{Cre}$), where VEGF is specifically knocked out in myeloid cells, confirmed that VEGF was necessary for blood vessel formation, and crucially demonstrated that Schwann cells were unable to migrate into the bridge, showing the reliance of Schwann cells on blood vessels for migration. In addition, *in vivo* experiments using the VEGFR2 inhibitor Cabozantinib administered systemically prior to blood vessel formation inhibited endothelial cell migration and therefore Schwann cell migration into the bridge. However, when Cabozantinib was administered post-blood vessel formation, we observed that Schwann cell migration was unaffected, which showed that in contrast to endothelial cell migration, VEGF signalling was not required for Schwann cell migration into the bridge.

3D electron microscopy analysis of the bridge showed that Schwann cells directly interact with endothelial cells at multiple points of contact via protrusions produced from both the Schwann cell and endothelial cell surfaces. One hypothesis is that the endothelial cells provide a discontinuous frictional surface, which provides the traction which Schwann cells require to migrate. Although the mechanism of interaction between the endothelial cells and Schwann cells is not yet fully understood, we have shown that the amoeboid-like migration observed along the blood vessels *in vivo* is in contrast to their migration *in vitro* in 2D. Additionally, despite the identification of an endothelial cell chemoattractant (VEGF) in the nerve bridge, it is not clear whether there is a factor present in the bridge, and distinct from VEGF, which attracts Schwann cells and/or promotes their collective migration along the tracks of endothelial cells. Collective migration is more efficient when directed by a chemoattractant factor (Mayor and Etienne-Manneville, 2016, Trepat et al., 2012), therefore it is highly likely that within the nerve bridge, there is a Schwann cell specific chemoattractant which promotes migration into the bridge.

There are already some known Schwann cell chemoattractants; Schwann cell precursors and neural crest cells have been reported to migrate in response to stromal derived factor-1 (CXCL12 also known as SDF-1) and Schwann cells have been observed to increase their migration in response to neurotrophins (Neurotrophin-3) (Yamauchi et al., 2004), glial cell line-derived growth factor (GDNF) and neuregulin 1 type III (Theveneau et al., 2010). The identification of a Schwann cell chemoattractant could have therapeutic potential for the treatment of peripheral nerve injury, particularly in patients who require a nerve graft or artificial nerve conduit to aid recovery. Following such peripheral nerve injuries, the regrowing axons must regain contact with their original tissue target in order to regain functionality. Over short distances, physiological regeneration may occur quickly and efficiently, however over longer distances or across an artificial nerve conduit, there is a delay in full nerve regeneration, which may lead to incomplete recovery and the inability to recover full functionality. By identifying a Schwann cell chemoattractant, the process of nerve regeneration could potentially be accelerated through the use of the factor therapeutically which may improve patient outcomes.

This chapter outlines the experiments which were carried out in order to identify a potential Schwann cell chemoattractant.

4.2. Cell culture of rat sciatic nerve bridge cells

As previously discussed, we have shown that VEGF is required for blood vessel formation in the bridge, and that subsequently Schwann cells use the newly formed vasculature in order to migrate out of the nerve stumps and across the nerve bridge (Cattin et al., 2015). It is currently unknown whether there is a chemoattractant factor present in the bridge which is able to promote Schwann cell migration. In order to determine whether cells within the bridge secrete a Schwann cell chemoattractant factor, we decided to purify the cells from the nerve bridge to determine their chemotactic activity.

We decided to culture cells from rat sciatic nerve bridges harvested on Day 2 following injury. This time point was chosen as the bridge is fully formed and macrophages in the bridge have been shown to be hypoxic and secret VEGF (Cattin et al., 2015), however endothelial cells and Schwann cells have yet to migrate into the tissue from the nerve stumps. The nerve bridge was easily identifiable from the nerve stumps at this time point, as it had a distinct morphology and could be excised from the nerve without taking any surrounding muscle or proximal or distal stump tissue which could contaminate the cell population. In order to carry out subsequent experiments, it was important that enough cellular

material could be harvested from the bridge tissue also that the cells survived and could be cultured in various conditions.

For the initial optimisation experiments, three nerve bridges were taken from adult male rats, and digested using collagenase and dispase to separate cells from the extracellular matrix (ECM) and to create a single cell suspension. Cells were then washed twice in media containing serum in order to remove any residual digestion enzymes and any remaining cellular debris, and the cells were counted using a haemocytometer. To determine the optimal conditions for plating the bridge cells, 60,000 cells/well were seeded in duplicate onto PLL coated glass coverslips in a combination of conditions. We chose to determine the effect of centrifuging the cells either immediately or the following day for 5 minutes at 12,000 rpm, as well as a number of different plate coatings (PLL only, PLL and fibronectin, PLL and laminin or PLL and Matrigel, a gelatinous protein mixture which has been previously used to analyse Schwann cell migration). After seeding, cells were cultured for a total of 48 hours and fixed using PFA, before cells were stained for Hoechst and the nuclei were quantified (10 fields counted per duplicate coverslip). The condition which yielded the highest number of total cells was the immediate centrifugation of the bridge cells following cell seeding (Figure 4.1A). Moreover, we found that both fibronectin and laminin coated coverslips resulted in slightly higher numbers of surviving cells than when using PLL coating alone and were in sufficient numbers for analysis (Figure 4.1A). The use of Matrigel was not successful however, as very few cells survived (Figure 4.1A).

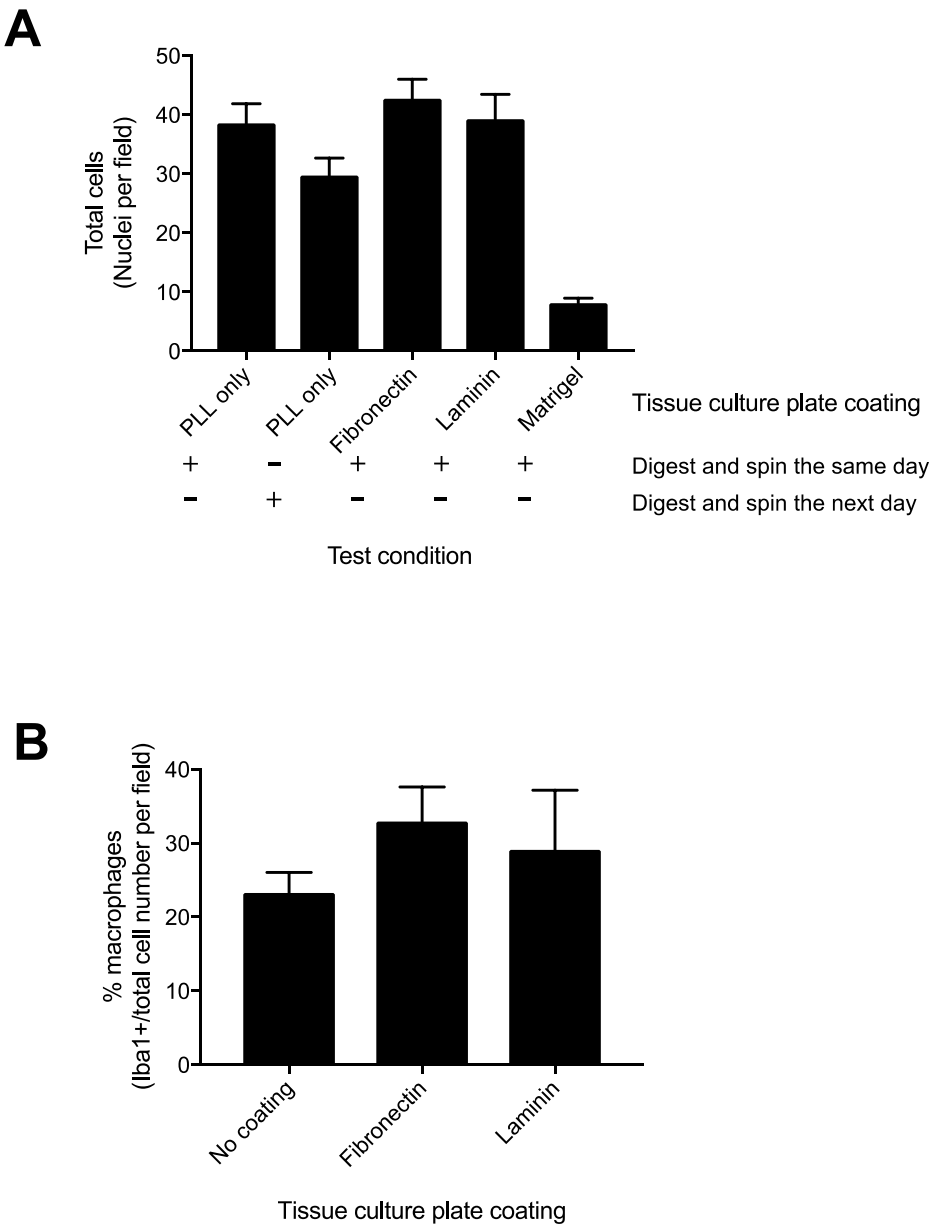

Figure 4.1 | Optimisation of macrophage cell extraction from Day 2 rat sciatic nerve bridges
A. Quantification of total cells retrieved from different cell culture conditions: 1) PLL only, centrifugation the same day 2) PLL only, cultured overnight and centrifuged the next morning, or centrifugation the same day and seeding onto 3) PLL and fibronectin (1:100), 4) PLL and laminin (1:100) or 5) PLL and Matrigel. Bar shows average from two experiments ±SD, 10 fields counted per coverslip in duplicate. B. Quantification of Iba1^{+} cells (macrophages) per condition. Graph shows average of two experiments ±SD, 10 fields counted per coverslip in duplicate.

Having optimised the conditions to purify bridge cells, it was important to quantify the cell types present in the cell preparation to ensure more than one cell type was surviving, and therefore representative of *in vivo* cell populations. Previously, we showed that in the nerve bridge on Day 2 following injury that macrophages are the majority cell type (~50% of cells) and that they selectively sense hypoxia and release VEGF. Because of this, we postulated that macrophages may also release other factors important for the regenerative process. To test the optimal conditions for the isolation of macrophages from our bridge cell preparation, 60,000 cells/well were seeded in duplicate onto coated glass coverslips in the following conditions: 1) PLL only, 2) PLL and fibronectin (1:100), 3) PLL and laminin (1:100). After seeding, cells were cultured for a total of 48 hours and fixed using PFA, cells were then stained for Iba1 (a macrophage marker) and Hoescht and the percentage of macrophages was calculated (Figure 4.1B, 10 fields counted from duplicate coverslips). We observed that the isolation of macrophages from the bridge was improved by using either laminin or fibronectin as a coating, however fibronectin seemed to perform slightly better, (>30% Iba^+ cells per field compared to <30% Iba^+ cells per field).

4.3. Do bridge cells secrete a chemotactic factor for Schwann cells?

Having successfully optimised the protocol for purifying cells from the nerve bridge in sufficient quantities containing representative cell populations, it was possible to use the bridge cells in *in vitro* migration assays to determine whether the bridge cells released a Schwann cell chemoattractant. We also wanted to address whether hypoxia played a role in the release of a potential Schwann cell chemoattractant, as prior to Schwann cell (and endothelial cell) migration into the bridge, the bridge is hypoxic (Cattin et al., 2015). It is known that hypoxic macrophages from the bridge release VEGF, however, we have recently shown that Schwann cell migration occurs in a VEGF-independent manner (Cattin et al., 2015). We therefore used VEGF and the VEGFR2 inhibitor Cabozantinib to confirm the VEGF-independent migration of Schwann cells.

To test for the presence of a chemokine, we initially used the Boyden chamber chemotaxis assay (Boyden, 1962). This assay involved seeding the migrating cells of interest into a hanging chamber containing a porous membrane at the base, which is then placed into a well containing the test chemoattractant (i.e. conditioned media or cells). The cells in the upper chamber are then incubated for four hours to allow migration to occur. Any cells which attempted to migrate from the upper

compartment into the lower well become trapped in the pores of the membrane, and can be quantified. As a control cell type, human venous endothelial cells (HUVECs) were used as it is known this cell type will increase migration in response to VEGF (Hobson et al., 2000, Cattin et al., 2015) as well as conditioned media from hypoxic macrophages.

To investigate the effect of bridge cells on Schwann cell migration, rat sciatic nerve bridge cells were purified as previously described and seeded at a density of 60,000 cells per well in a 24 well plate. The bridge cells were cultured in media containing serum for 24 hours, before the cells were washed and the medium replaced with minimal media (Sato), and the cells were placed at either normoxia (20% O_2) or hypoxia (1.5% O_2). 24 hours later, Schwann cells or HUVECs were then seeded into the upper compartments of the Boyden chambers (75,000 or 50,000 cells per well respectively) and placed into the wells containing the bridge cells and allowed to migrate at 20% O_2 in the presence or absence of 10μM Cabozantinib for four hours before cell migration was quantified (Figure 4.2). For each cell type a positive control was used to determine the ability of the cells to migrate, medium containing serum for Schwann cells, and VEGF for HUVECs.

As expected, HUVECs migrated in a VEGF dependent manner (Figure 4.2A), which was demonstrated by the increase in migration in response to VEGF as well as the hypoxic bridge cells (***$p<0.001$). Moreover, HUVEC migration was inhibited by the addition of Cabozantinib, which indicated that migration was occurring in a VEGF-dependent manner and confirmed our previous *in vivo* findings (Cattin et al., 2015).

We observed that Schwann cell migration was increased by the presence of 3% serum culture media in the lower compartment, and additionally that Cabozantinib had no effect on Schwann cell migration. In contrast to what was observed in the HUVECs, VEGF was not sufficient to induce Schwann cell migration, confirming a VEGF-independent manner of migration. Interestingly, Schwann cell migration increased in response to bridge cells cultured in hypoxic conditions (Figure 4.2B) and was also not inhibited by Cabozantinib. These experiments showed that bridge cells cultured in hypoxia were able to attract Schwann cells. Additionally, the use of the VEGFR2 inhibitor demonstrated that consistent with our *in vivo* findings, Schwann cell migration was occurring in a VEGF-independent manner.

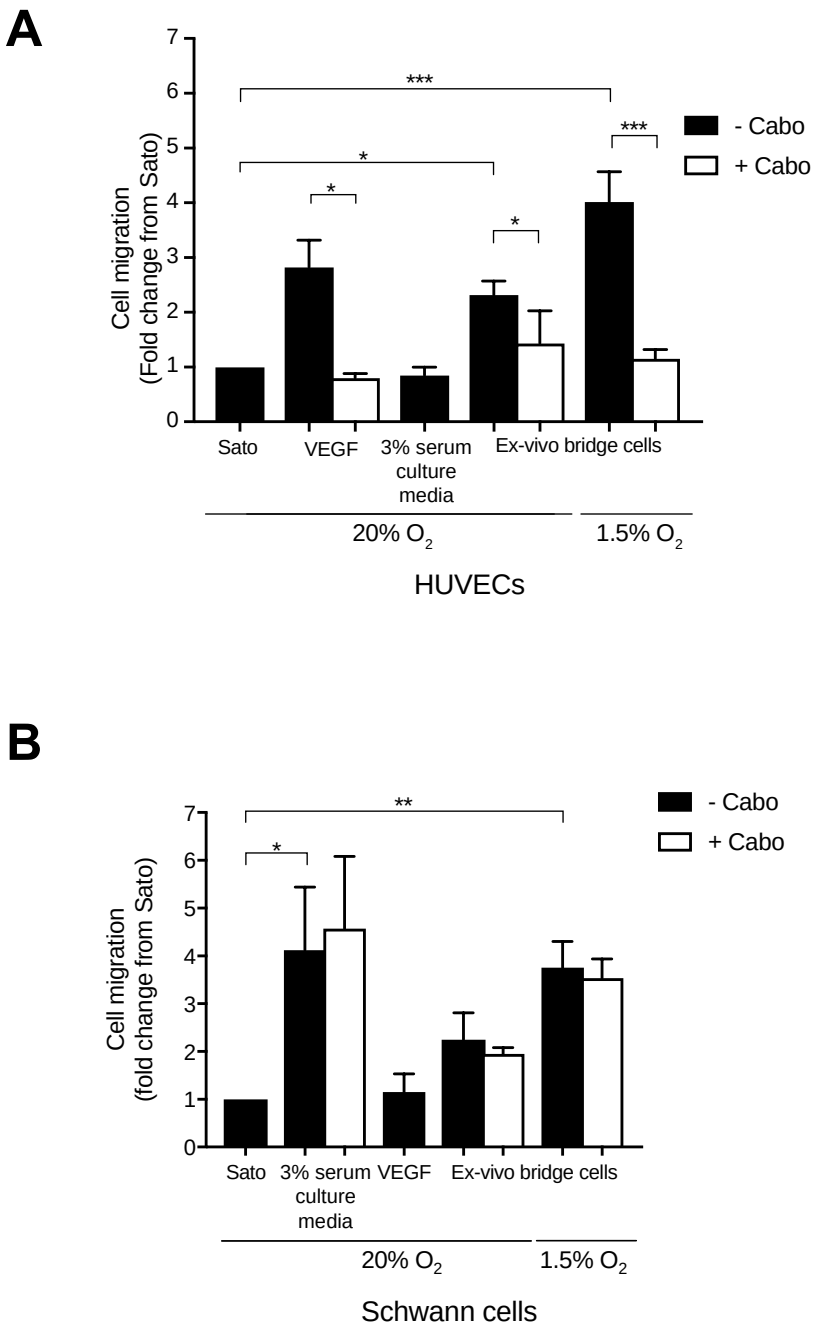

Figure 4.2 | Hypoxic ex-vivo bridge cells are able to attract Schwann cells in a Boyden chamber 50,000 HUVECs (A) or 75,000 Schwann cells (B) were placed in the upper compartment of Boyden chambers and allowed to migrate for 4 hours after addition of ex-vivo bridge cells incubated for 24 hrs at 20% or 1.5% O_2, minimal media, 5ng/ml VEGF-A^{165} or 3% serum culture media in the lower chamber in the presence or absence of 10μM Cabozantinib. (n=5 for each group, graphs show the fold change in cell migration from control Sato conditions ±SEM). One-way ANOVA test was used for statistical analysis.

4.4. Macrophages are able to promote Schwann cell migration

Having found that nerve bridge cells were able to induce Schwann cell migration *in vitro,* it was necessary to determine which cell type was responsible for the increase in migration. To do this, we purified specific cell populations from the bridge and then used them in the Boyden chamber assay. At Day 2 following injury, the two largest populations of cells within the bridge are macrophages and fibroblasts, and it is therefore likely that one of these two populations is responsible for the observed increase in Schwann cell migration. In order to purify the individual cell populations we used immunopanning, which uses antibodies to selectively capture specific cell types. To do this, bridge cells were purified as previously described, however prior to seeding the cells, the cell suspension was positively immunopanned using an antibody specific to macrophages (CD11b) or to fibroblasts (Thy1). Macrophages or fibroblasts within the cell suspension adhered to the antibodies on the corresponding cell culture plate, and following a wash with PBS were detached either by scraping (macrophages) or by trypsinisation (fibroblasts). The cells were then counted and used in subsequent cell based assays. In order to confirm the efficiency of the panning procedure, 5,000 panned cells were seeded onto laminin and PLL coated coverslips in duplicate, fixed using PFA and immunolabelled for macrophages and fibroblasts (Iba1 and prolyl hydroxylase respectively) before quantification (Figure 4.3A). For both macrophages and fibroblasts, close to 100% pure populations were recovered (Figure 4.3B).

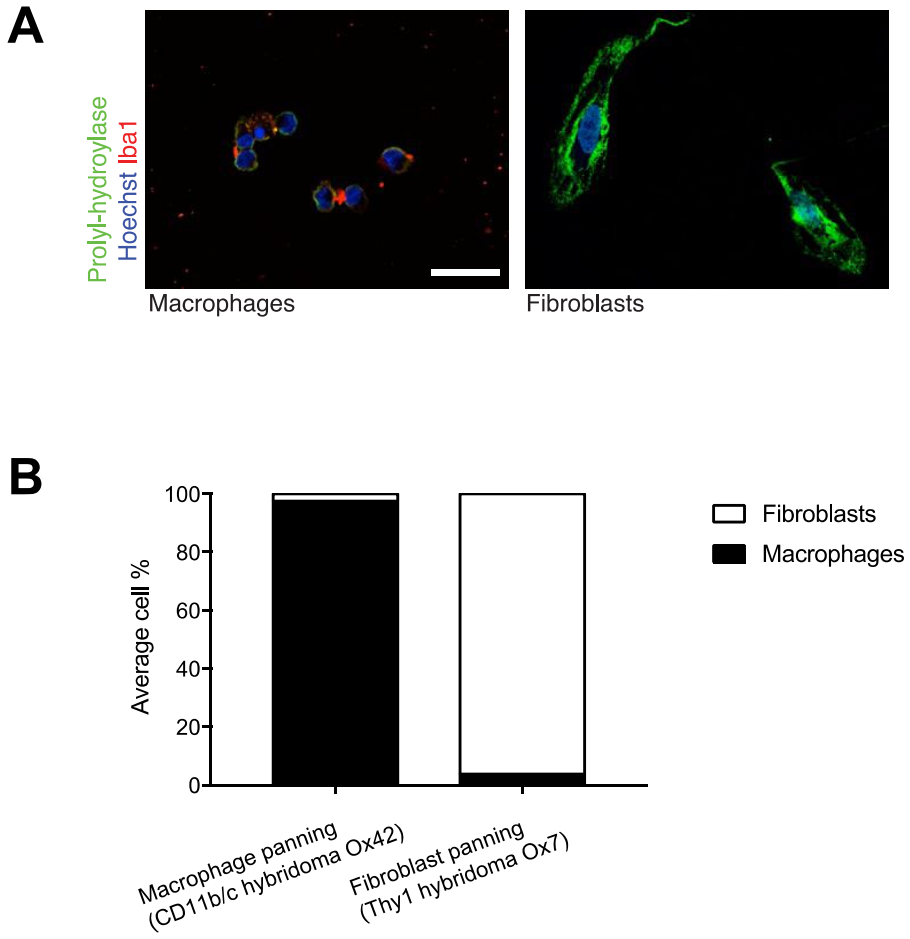

Figure 4.3 | Extraction of macrophages and fibroblasts from Day 2 sciatic nerve bridges
A. Representative images of macrophages and fibroblasts extracted from the sciatic nerve bridge on Day 2. Antibodies specific for the cell type (as indicated) were used to pan for the cells. Cells were immunolabelled to detect macrophages (Iba1, red) and fibroblasts (prolyl-hydroxylase, green). Nuclei counterstained with Hoechst (blue). Scale bar = 30μm. C. Quantification of macrophages (Iba1+) and fibroblasts (prolyl-hydroxylase+) cells per panning condition. Graph shows average cell percentage of two experiments, 20 fields were quantified from duplicate coverslips.

To identify whether macrophages or fibroblasts were responsible for the observed increase in Schwann cell migration, the immunopanned macrophages and fibroblasts were seeded into the lower compartment (50,000 cells/well) of Boyden chambers and incubated overnight at normoxia (20% O_2) or hypoxia (1.5% O_2) in minimal media. The following morning, Schwann cells and HUVECs were seeded into the upper compartment of the Boyden chamber and allowed to migrate for four hours, before fixing in PFA and quantifying the migratory cells. As in previous experiments, 3% serum culture media and VEGF were used as positive controls for Schwann cells and HUVECs respectively, and migration was normalised to migration occurring in response to Sato.

When macrophages were cultured in hypoxia, we saw that Schwann cell migration increased over 3-fold (***$p<0.001$) compared to control (Figure 4.4), which was similar to the increase observed in response to the positive control of 3% serum culture media. This result suggested that hypoxic macrophages within the nerve bridge were releasing a potent Schwann cell chemoattractant. As expected, endothelial cell migration was induced by hypoxic macrophages from the bridge (***$p<0.001$). However, we also observed that HUVECs migrated in response to macrophages cultured at normoxia, which was an unexpected result. A possible explanation for this is that when the macrophages were purified from the nerve bridge, the *in vivo* environment was hypoxic and may have 'primed' the macrophages by activating hypoxia-inducible signalling pathways, which may still be active when we culture them in our assays. Consistent with this, we also observed increased Schwann cell migration in response to macrophages cultured at normoxia. Conversely, fibroblasts cultured at either normoxia or hypoxia did not attract either Schwann cells or HUVECs, with migration rates similar to basal levels seen in minimal media.

These results show that macrophages from the bridge are responsible for the increase in Schwann cell migration induced by bridge cells, and that this response is induced by hypoxia.

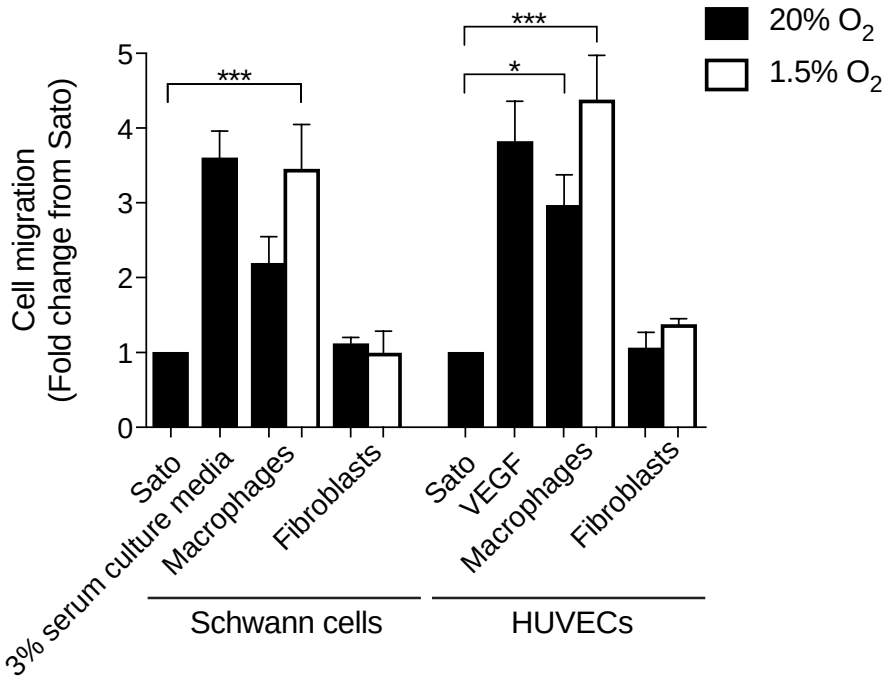

Figure 4.4 | Hypoxic macrophages from the nerve bridge are able to attract Schwann cells
Schwann cells (A) or HUVECs (B) were placed in the upper compartment of Boyden chambers and allowed to migrate for 4 hours into the lower chamber containing media with no factors (Sato), 5ng/ml VEGF-A^{165} or 3% serum culture media, or macrophages or fibroblasts cultured at 20% or 1.5% O_2. Bars show average fold change in migration from control of 4 experiments +SEM. One-way ANOVA test was used for statistical analysis.

4.5. Assessing the role of J774A.1 cells on Schwann cell migration

Up until this point, all of the experiments analysing Schwann cell migration have used cells purified from rat sciatic nerve bridges, and whilst this approach has proven successful, it is hindered by the low numbers of cells that can be purified from the nerve bridges. As it is difficult to culture primary macrophages, we tested whether the macrophage cell line, J774A.1, behaved similarly. J774A.1 cells are adherent and originate from a mouse reticulum cell sarcoma, and they are reported to display a typical immune response when subjected to inflammation or infection and are commonly used for *in vitro* studies of macrophage function (Cho et al., 2000, Cai et al., 2014). Macrophages isolated from the nerve bridge display an intrinsic differential response to hypoxia, so we were interested to test whether the J774A.1 cell line also had such a differential response. This was important to determine, in order to assess whether the cell line could act as a suitable *in vitro* model.

To test the hypoxia response, we used the hypoxyprobe staining protocol. 10,000 J774A.1 cells were seeded onto PLL and laminin coated coverslips, and incubated for four hours in the presence of hypoxyprobe-1 at 20%, 1.5% or 0.1% O_2. Cells were then fixed and immunolabelled to detect hypoxyprobe (Figure 4.5A). Immunolabelling the cells revealed that the response of the J774A.1 cell line to hypoxia was the same as primary macrophages isolated from the nerve bridge (Figure 4.5A). We observed that at 20% O_2, no cells were hypoxic whilst at 0.1% O_2 all of the J774A.1 cells were hypoxic. Importantly, at 1.5% O_2 all of the J774A.1 cells were also positive for hypoxyprobe, and therefore hypoxic, which mirrored what we had seen with the isolated bridge macrophages. This result told us that the J774A.1 cells responded to similar levels of O_2 and had a similar hypoxia-response as the bridge macrophages.

To test whether the J774A.1 cell line was able to induce Schwann cell migration in a hypoxia-dependent manner, we repeated the Boyden chamber assays. Similar to previous migration experiments, 60,000 J774A.1 cells were seeded and incubated for 48 hours in 20% or 1.5% O_2 with minimal media, before the conditioned media (CM) was collected and filtered, and placed in the lower compartment of the Boyden chamber. Schwann cells or HUVECs were seeded into the upper compartment (75,000 and 50,000 cells/well respectively) and allowed to migrate at normoxia for four hours before fixation.

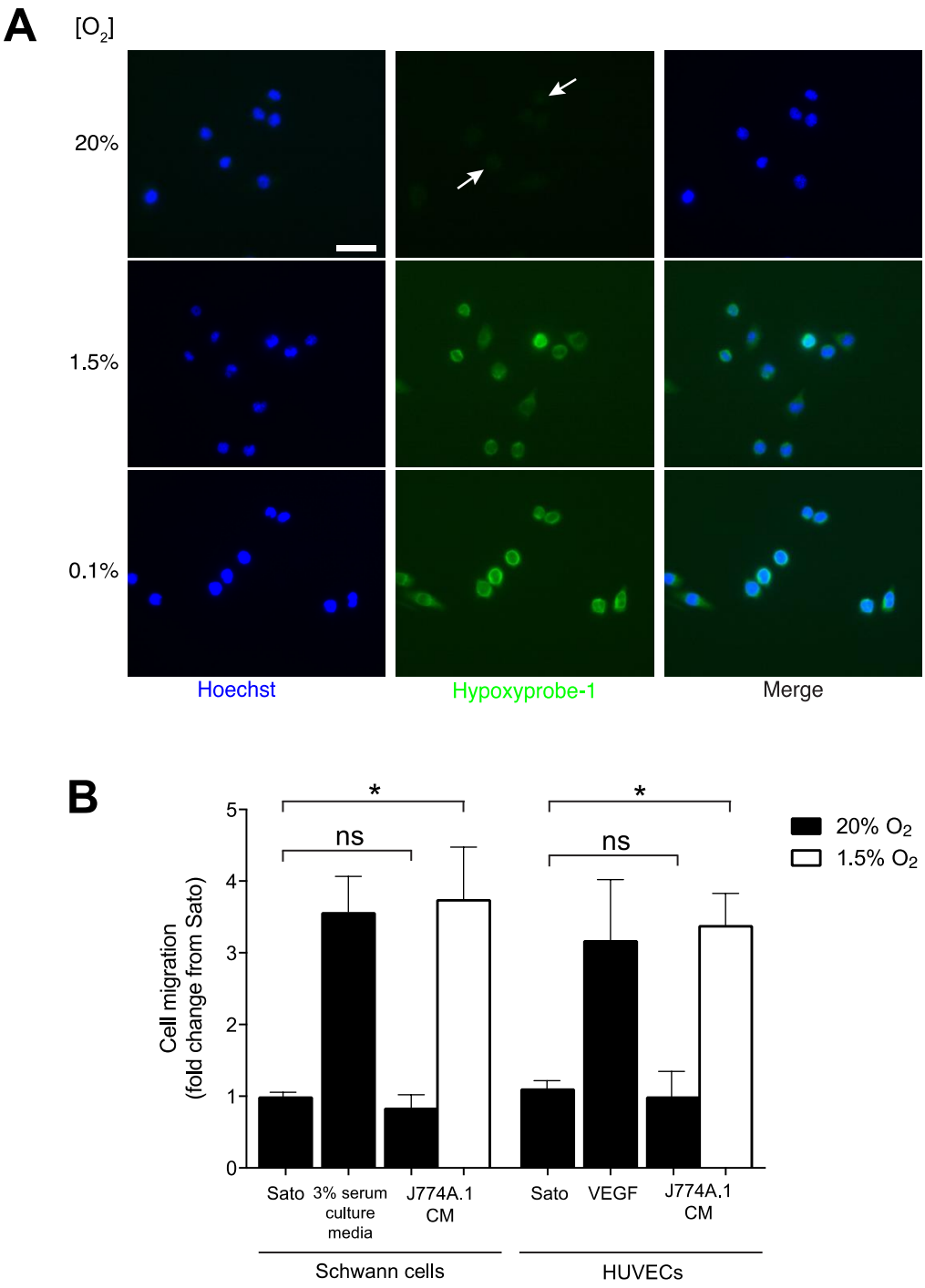

Figure 4.5 | Hypoxic J774A.1 cells are able to attract Schwann cells

A. Representative images of J774A.1 cells incubated with hypoxyprobe at varying O_2 concentrations immunostained to detect hypoxic cells (hypoxyprobe-1$^+$, green) and nuclei counterstained with Hoechst (blue). Arrows show non-hypoxic cells in the 20% O_2 condition. Scale bar is 50μm. B. Schwann cells or HUVECs were placed in the upper compartment of Boyden chambers and allowed to migrate into the lower chamber containing Sato, 3% serum culture media, VEGF or CM from J774A.1 cells cultured at 20% or 1.5% O_2. Bars show average of 3 experiments +SEM. One-way ANOVA test was used for statistical analysis.

We observed that when the J774A.1 cell line was cultured in hypoxia (1.5% O_2), there was a large increase in both Schwann cell (>3-fold *p<0.05) and HUVEC (>3-fold *p<0.05) migration compared to control medium (Figure 4.5B). This was similar to what was seen with the bridge cells and showed that the J774A.1 cells release hypoxia-inducible Schwann cell and endothelial cell chemoattractants.

4.6. The CXCL12/CXCR4 signalling axis is important for Schwann cell migration

Having identified that hypoxic macrophages release a Schwann cell chemoattractant, we aimed to identify the specific factor. Initially taking a candidate approach, we first tested the hypothesis that the hypoxia-induced factor could be CXCL12. CXCL12 is a chemotactic factor which is upregulated in development and induces the migration of neural crest cells, a Schwann cell precursor (Theveneau et al., 2010). Schwann cells also express the receptor for CXCL12 (CXCR4, (Demir et al., 2017)) which further hinted at the possibility that CXCL12 could be a chemoattractant factor and that this signalling axis could potentially play a role in Schwann cell migration following injury. In order to determine whether macrophage-derived CXCL12 was responsible for an increase in Schwann cell migration, a number of approaches were taken.

Initially, to confirm the expression of CXCR4 (Bhangoo et al., 2007, Ödemis et al., 2010), we conducted RNA expression analysis on cultured Schwann cells, which determined that CXCR4 was expressed (data not shown). Having confirmed the expression of CXCR4 in Schwann cells, this indicated therefore that CXCL12 could act on Schwann cells to modulate their migration. To test whether the CXCL12/CXCR4 axis played a part in modulating Schwann cell migration, we tested whether inhibition of CXCR4 decreased Schwann cell migration. In the first instance, we used the inhibitor in the presence of 3% serum culture media and analysed Schwann cell migration in the Boyden chamber, and in parallel time-lapse microscopy experiments. Schwann cells were allowed to migrate in 2D on laminin coated tissue culture plates in Sato, or 3% serum culture media -/+ the CXCR4 inhibitor, and recorded by time-lapse microscopy for 12 hours (Movie 4.1). Cells were tracked and the migration speed was calculated in each of the conditions. This enabled us to analyse how the CXCR4 inhibitor was affecting Schwann cell migration. In the Boyden chamber assay, Schwann cell migration in the presence of the CXCR4 inhibitor (Plerixafor, AMD3100) caused a reduction of Schwann cell migration to basal levels, which implied that by inhibiting CXCR4, Schwann cell migration was prevented (Figure

4.6A). However, the time-lapse microscopy experiments (Figure 4.6B) showed that in the presence of the CXCR4 inhibitor, the Schwann cells were less able to migrate, and had a flatter and rounder morphology (Movie 4.1). Quantification of the migration speed in each condition showed that there was a significant decrease (*$p<0.05$) with the CXCR4 inhibitor compared to both the Sato and the 3% serum culture media condition (Figure 4.6B). Together, these results suggested that the CXCR4 inhibitor blocked Schwann cell migration. The effect on Schwann cell migration was quite pronounced however, and, as these effects were seen in response to 3% serum culture media (which to our knowledge does not contain CXCL12), quite surprising. This inhibitory effect on Schwann cell motility might indicate an autonomous requirement of this pathway for migration or alternatively it could be the result of toxicity or a non-specific effect of the CXCR4 inhibitor, which meant that the results were difficult to interpret.

Next, we investigated the expression of CXCL12 in our *in vitro* and *in vivo* models. We had already observed that Schwann cell migration increased in response to a hypoxia inducible chemokine secreted by J774A.1 cells (Figure 4.5B) so we measured the transcript levels of CXCL12 by RT-qPCR to see whether there was a change in expression between the two oxygen conditions (20% vs. 1.5% O_2). This analysis showed that CXCL12 expression was unaffected by the hypoxic state, whereas the positive control VEGF (a known hypoxia-inducible factor) did increase in expression in hypoxic conditions (Figure 4.7A). As there was no change in CXCL12 mRNA expression in the hypoxic cells, this implied that CXCL12 was not the factor which was responsible for an increase in Schwann cell migration as we were specifically looking for a hypoxia inducible factor, however it remains a possibility that there could be a change in expression occurring at the post-transcriptional level.

We then analysed the transcript levels of CXCL12 following injury *in vivo*. Tissue samples were taken from the nerve bridge and distal stump on Day 2 following injury in adult rats and RNA was extracted. CXCL12 transcript expression was then measured by RT-qPCR and compared to the basal levels in the uncut nerve, and normalised to the housekeeping gene b2m (Figure 4.7B). The results showed that transcript levels of CXCL12 remained relatively unchanged between the three distinct areas of the nerve, even showing a decrease within the nerve bridge, unlike VEGF transcript levels which showed a gradient of expression. This *in vivo* data further indicated that CXCL12 was unlikely to be the signalling molecule responsible for Schwann cell migration.

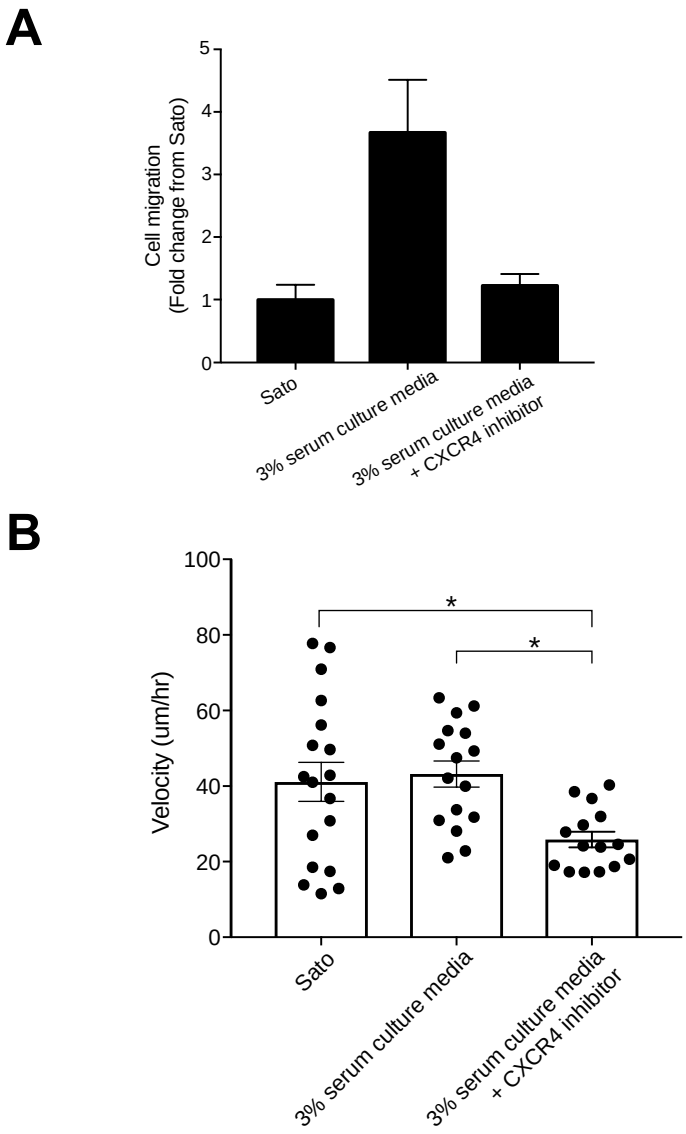

Figure 4.6 | CXCR4 inhibitor prevents Schwann cell migration

A. Quantitative RT-qPCR analysis of CXCR4 in mRNA isolated from Schwann cells, b2m was used as a positive control. Graph shows relative CXCR4 and b2m expression (n=3, graph shows mean ±SEM). B. Schwann cells were placed in the upper compartment of a Boyden chamber and allowed to migrate for 4 hours in response to Sato, 3% serum culture media or 3% serum culture media with 50μg/ml CXCR4 inhibitor (AMD3100) in the lower chamber. Graph shows fold change in cell migration from control ±SEM (n=3). C. Quantification of Schwann cell migration speed in the presence of Sato, 3% serum culture media or 3% serum culture media with 50μg/ml CXCR4 inhibitor AMD3100. Graph shows average cell velocity ±SEM (n=3). 50 cells counted per condition.

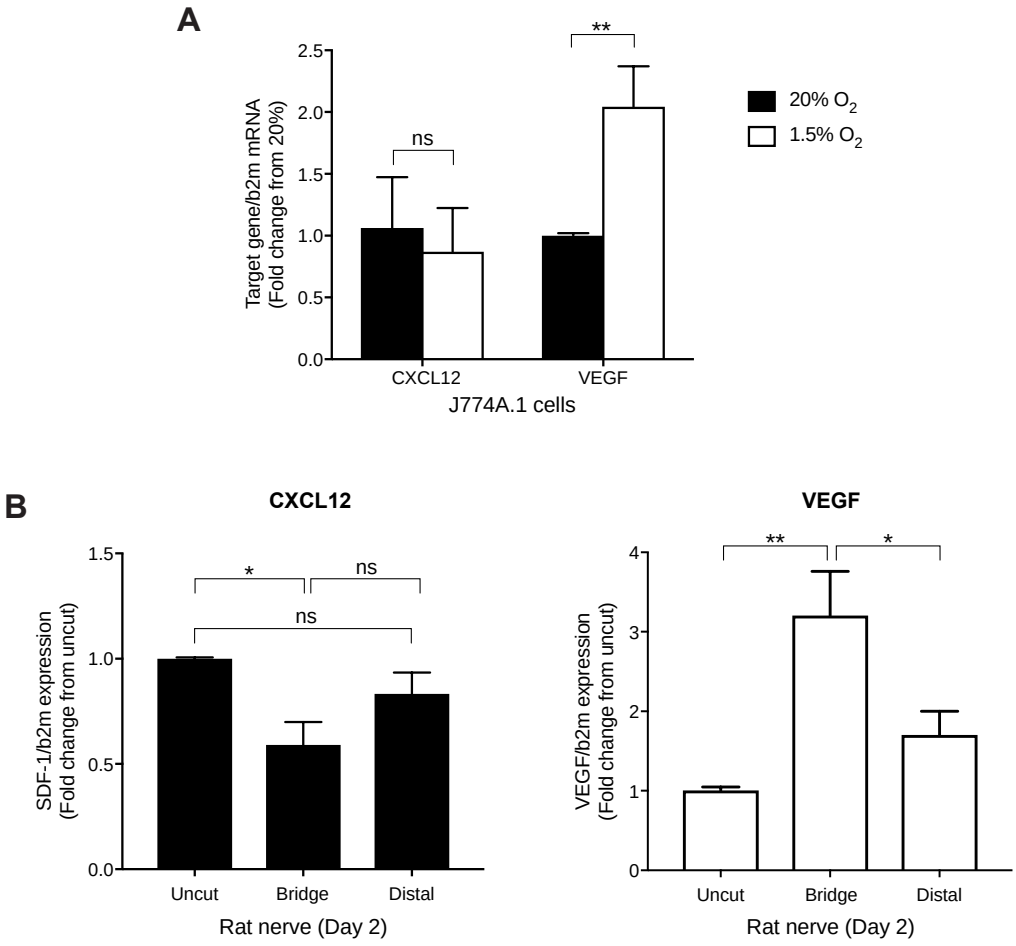

Figure 4.7 | CXCL12 expression in response to hypoxia *in vitro* and *in vivo* following injury.
A. Quantitative RT-qPCR analysis of CXCL12 mRNA isolated from J774A.1 cells after 24 hr incubation at 20% or 1.5% O_2, VEGF was used as a positive control. Graph shows CXCL12 and VEGF transcript levels relative to 20% O_2 control and normalised to b2m (n=3, graph shows mean ±SEM). B. Quantitative RT-qPCR analysis of CXCL12 (left) or VEGF (right) mRNA isolated from the bridge, distal stump and contralateral uncut rat nerves at Day 2 following injury. Graphs show transcript levels relative to the uncut nerve and normalised to b2m (n=3, graph shows mean value ±SEM).

Taken together, these data suggest that CXCL12 is unlikely to be the macrophage-secreted factor responsible for the recruitment of Schwann cells. However, it does not rule out the involvement of the CXCL12/CXCR4 signalling axis in modulating Schwann cell motility, due to the strong effects of the CXCR4 inhibitor on the ability of Schwann cells to migrate.

4.7. Unbiased cytokine screen to identify hypoxia-inducible factors secreted by macrophages

In order to identify the hypoxia-inducible Schwann cell chemoattractant, we decided to attempt to identify factors upregulated in hypoxia compared to normoxia in the conditioned media of J774A.1 cells. To do this, we used an unbiased cytokine screen to find potential candidates, which we could subsequently test using our migration assays to investigate their effects on Schwann cell migration. We used a cytokine array, which can detect the levels of 40 cytokines (including CXCL12) in conditioned medium. J774A.1 cells were seeded in $10cm^2$ cell culture plates and incubated in Sato for 48 hours at either 20% or 1.5% O_2. After 48 hours, the conditioned media from the cells was collected and filtered to remove cell debris before conducting the cytokine screen following the manufacturers protocol. The membranes were developed using ImageQuant (Figure 4.8A) and the images were quantified to determine any changes in cytokine expression between the two oxygen conditions (Figure 4.8B).

The cytokine screen resulted in two important findings. Firstly, the screen confirmed that the candidate molecule CXCL12 was not upregulated in the conditioned media of J774A.1 cells incubated at 1.5% O_2 (Figure 4.8; no. 9). This result corresponded with the RNA expression analysis which showed that there was no increase in CXCL12 RNA as a result of hypoxia in the J774A.1 cells (Figure 4.7A) and further suggested that CXCL12 was not the chemokine responsible. Secondly, the screen identified two hypoxia inducible cytokines secreted by the macrophages: CCL3 and CCL4 (or MIP-1α and MIP-1β) (Figure 4.8, no. 6 and 7 respectively). CCL3 is a known chemoattractant for macrophages; it is released by macrophages following injury and attracts macrophages to the site of inflammation thus promoting the inflammatory response (Trifilo et al., 2003, Perrin et al., 2005, Kiguchi et al., 2010, Cittera et al., 2007). Given the known chemoattractant roles of this chemokine and the hypoxia induced upregulation of CCL3, it provided us with a new candidate Schwann cell chemoattractant secreted by macrophages.

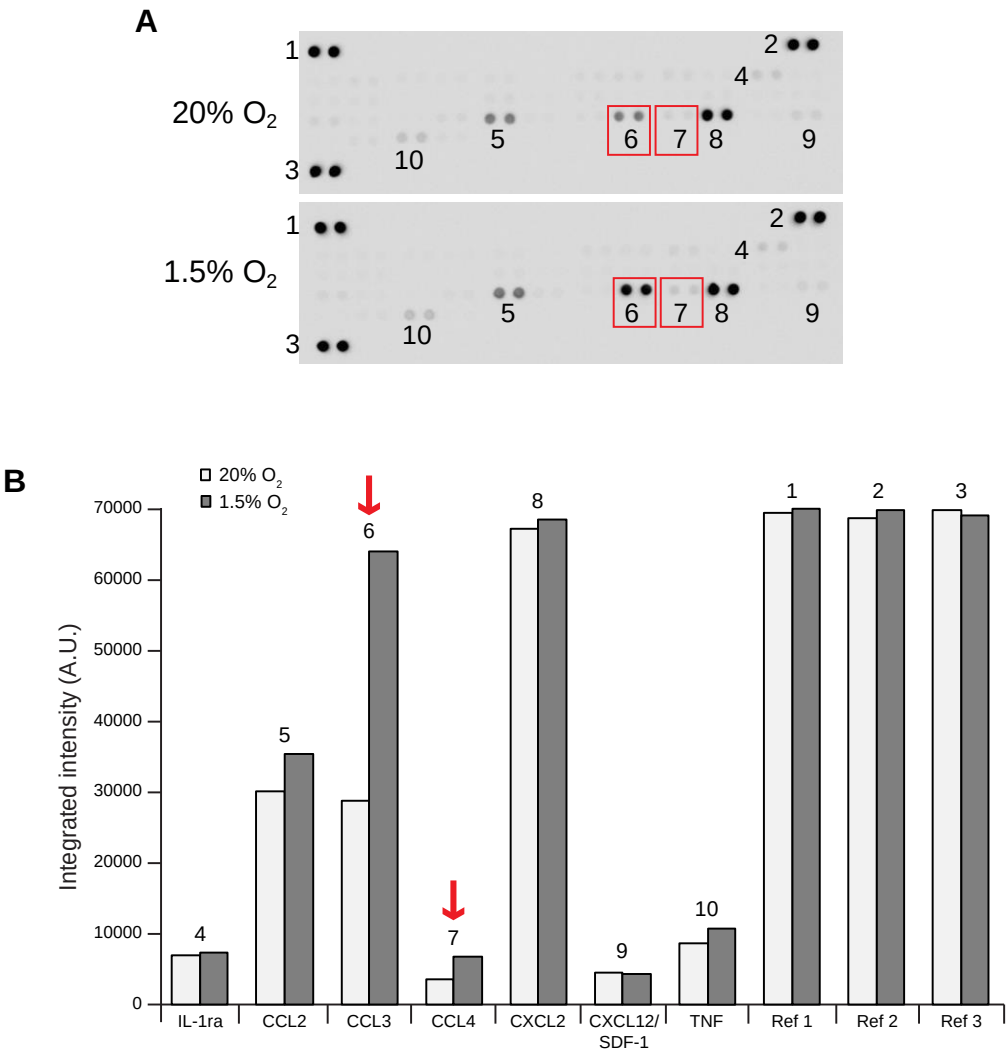

Figure 4.8 | CCL3 is identified as hypoxia induced molecule from cytokine screen
A. Cytokine and chemokine protein array membranes after incubation with conditioned media from J774A.1 cell line incubated at 20% or 1.5% O_2 for 48 hrs. Duplicate detection spots indicating cytokines present in the conditioned media are numbered to correspond with quantification bars. B. Quantification of cytokine and chemokine levels measured by the cytokine protein array. Red arrows indicate cytokines with upregulated expression in hypoxia. Graph shows mean pixel density of duplicate detection spots, n=1.

4.8. CCL3 is expressed by macrophages in a hypoxia-inducible manner

Chemokines are crucial for inducing many biological processes such as chemotaxis, angiogenesis, haematopoesis as well as tumour growth (Menten et al., 2002). CCL3 is a member of the CC chemokine subfamily, and is sometimes referred to as CCL3 (Menten et al., 2002, Davatelis G, 1988). CCL3 is known to be released by monocytes, macrophages and neutrophils in response to inflammation, and functions to recruit macrophages, and to induce the transendothelial migration of leukocytes (Cook et al., 1995). The chemotactic effects of CCL3 have been observed both *in vitro* and *in vivo* (Cook et al., 1995, Menten et al., 2002). *CCL3*$^{-/-}$ mice mostly develop normally however it has been reported that they display a reduction in inflammation and a delay in virus clearance following infection, which highlights the role CCL3 plays in macrophage recruitment (Cook et al., 1995, Trifilo et al., 2003, Perrin et al., 2005).

To confirm the findings of the cytokine screen, we analysed CCL3 protein expression in the conditioned media of J744A.1 cells. To test this, 200,000 cells were seeded in triplicate in normal culture media containing 10% serum and incubated for 24 hours. The cells were then incubated with minimal media for 48 hours in normoxic (20% O_2) or hypoxic (1.5% O_2) conditions. Equal volumes of conditioned media were taken from the dishes and the protein was extracted from the samples by TCA precipitation and analysed by Western blot. The membranes were probed for CCL3, VEGF (as a positive control), and B-actin as a loading control. This protein analysis confirmed that in the J774A.1 cell line, CCL3 was upregulated following hypoxia by approximately 12-fold (Figure 4.9A and quantified in 4.9B). An increase of approximately 1.5-fold was observed with the positive control VEGF (Figure 4.9A and quantified in 4.9B).

To analyse the RNA expression levels of CCL3 in J774A.1 cells, we seeded cells and incubated them for 48 hours in normoxic (20% O_2) or hypoxic (1.5% O_2) conditions. Cells were harvested and an RT-qPCR was conducted to look at the difference in expression between the two oxygen states, using the known hypoxia-inducible factor VEGF as a positive control. This RT-qPCR showed that there was an upregulation of CCL3 as a result of hypoxia of approximately two-fold (Figure 4.9A). We also observed an upregulation of VEGF in the hypoxic conditions. There was a discrepancy in the levels on induction between the RT-qPCR and Western blot data which suggests that there may be post-translational mechanisms acting on CCL3. Taken together, this data shows that the factor CCL3 is

upregulated in macrophages when cultured in hypoxia, which confirmed the results of the cytokine screen.

Having identified that CCL3 is upregulated in J774A.1 cells, we tested whether CCL3 expression could be detected in the nerve following injury. To do this we harvested nerve bridges, distal stumps and contralateral uncut nerves from three adult rats at Day 2 following injury, and snap froze in liquid nitrogen and then extracted the RNA. We then performed an RT-qPCR on the samples to determine the expression of CCL3, compared to housekeeping genes. We used VEGF as a positive control as we have previously observed a concentration gradient of VEGF *in vivo* between the bridge and the nerve stumps (Cattin et al., 2015).

The RNA expression analysis showed that there was a large increase of CCL3 mRNA in the nerve bridge (20-fold increase) compared to the contralateral uncut nerve (Figure 4.10A). In the distal stump, there is also an increase of CCL3 compared to the uncut control, however this was much less. At Day 2 following injury there is a large population of macrophages in the distal stump, which may release CCL3 to recruit further macrophages to aid regeneration, or to change the behaviour of Schwann cells in this region. It is also possible that there was some contamination of bridge tissue in the distal stump RNA sample, which would have been introduced when the tissue was excised following injury. The gradient of CCL3 expression between the bridge and the nerve stumps indicates that CCL3 is a potentially exciting candidate to act as a chemoattractant factor for Schwann cells following injury.

To determine the protein levels in the different regions of the nerve, we harvested sections of injured sciatic nerve, as well as the uninjured contralateral nerve, from adult rats on Day 2 following injury and snap froze in liquid nitrogen. Using a tissue homogeniser, we extracted the protein from the samples and ran a Western blot to detect CCL3, macrophage marker CD68 and total ERK (Figure 4.10B). This analysis showed that there were much higher levels of CCL3 in the bridge compared to the uncut, proximal and distal portions of the nerve, which confirmed the previous RT-qPCR results. This indicated that in the bridge following injury, there is a physiological gradient of CCL3. This suggested that similar to VEGF, which is also found in a gradient in the nerve bridge, CCL3 could also be acting as a chemoattractant.

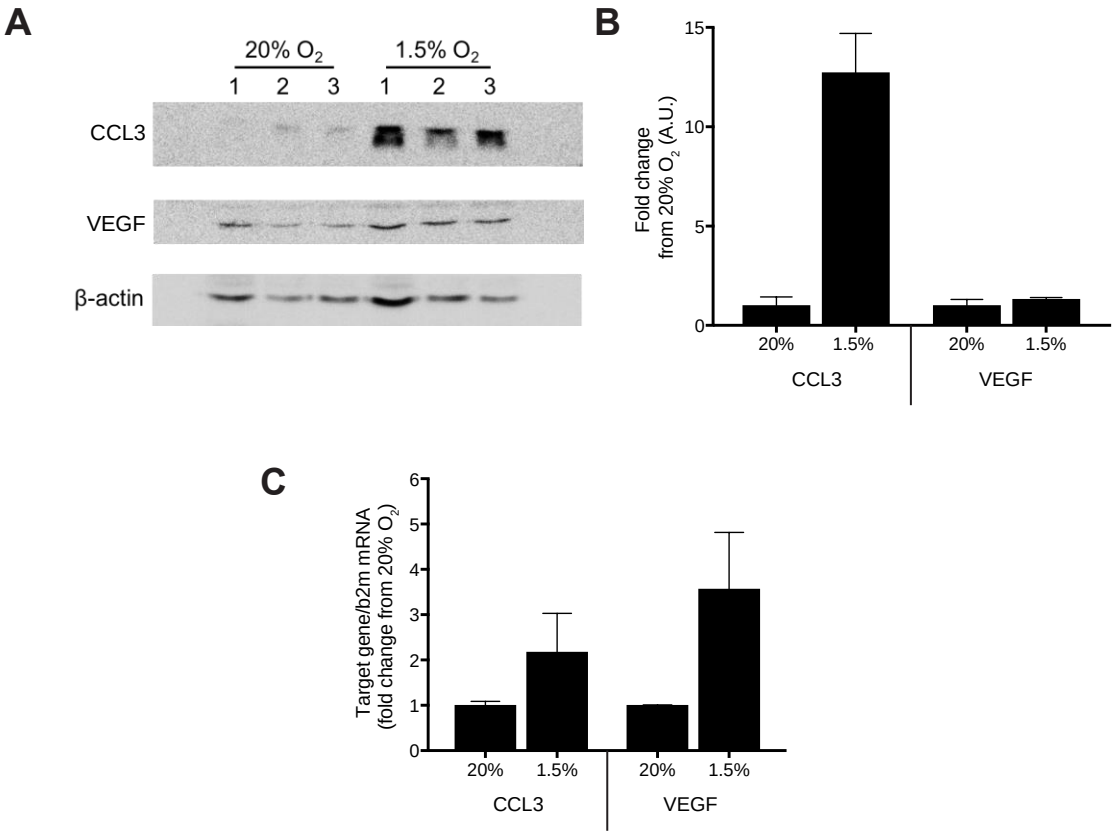

Figure 4.9 | CCL3 is expressed in the J774A.1 cell line

Representative Western blot showing 3 technical repeats (A) and quantitative densitometry (B) showing CCL3, VEGF and β-Actin expression in the J774A.1 cells incubated at 20% or 1.5% O_2 for 48 hours. Graph shows average ±SEM, n=3. C. RNA expression analysis of J774A.1 cells cultured in 20% or 1.5 O_2 for 48hrs. Bars show average of 3 repeats +SEM. One-way ANOVA test was used for statistical analysis.

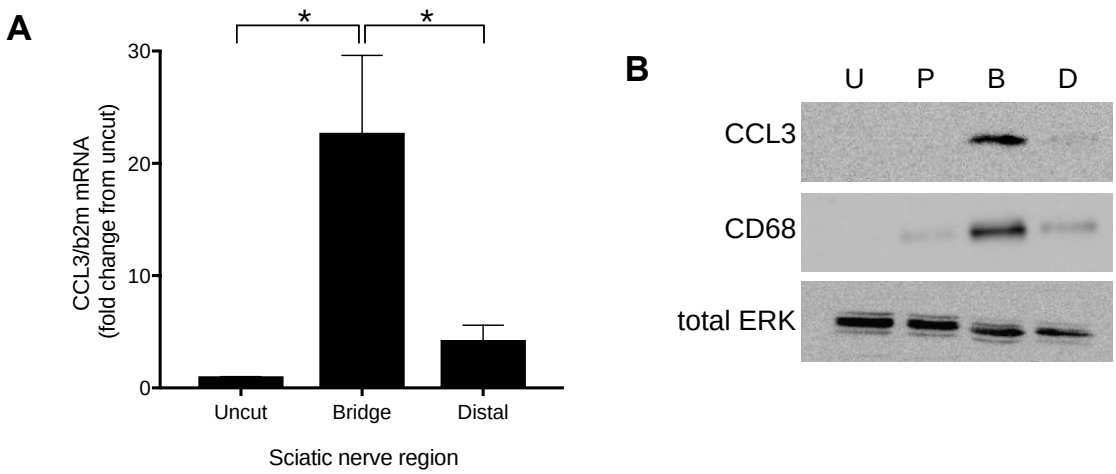

Figure 4.10 | CCL3 is expressed in the nerve bridge following injury
A. RNA expression analysis of rat nerves following injury. Bars show average of 3 animals +SEM. One-way ANOVA test was used for statistical analysis. B. Representative Western blot showing CCL3, CD68 and total ERK expression in the uncut (U), proximal (P), bridge (B) or distal (D) section of the sciatic nerve.

The macrophage marker CD68 was also upregulated in the bridge compared to the uncut nerve (Figure 4.10) which correlated with the previous RNA expression analysis and flow cytometry data which showed an increase of macrophages in the bridge following injury.

4.9. Macrophages express CCL3 in the nerve bridge following injury

Following injury there is a huge influx of monocyte-derived cells into the nerve bridge, and we have shown that they play an important role in nerve regeneration following injury (Cattin et al., 2015). We found that macrophages in the bridge are predominantly monocyte-derived, with only a small number derived from the resident nerve population. To determine which specific macrophage population was responsible for the release of CCL3 in the bridge we carried out sciatic nerve surgery on 10 mice and collected the nerves on Day 5 following injury. The cells were then flow cytometry sorted, and the F4/80^{+} CCR2^{-} (more mature/resident-like macrophages) and CCR2^{+} macrophages (recently recruited/monocyte-derived cells) were collected. RNA expression analysis was performed on these cells to determine the expression of CCL3 as well as the positive control VEGF, which we know is highly expressed in the bridge following injury (Cattin et al., 2015). This analysis showed that CCL3 was upregulated in both macrophage populations in the bridge compared to the uncut nerve as we had previously observed, but a far greater increase was observed in the monocyte-derived (CCR2^{+}) macrophages (Figure 4.11A). Consistent with previous data, CCL3 was also upregulated in the distal stump, however the increase was not as high as in the bridge.

The difference in CCL3 expression between the bridge and the distal stump was particularly interesting. Our previous data had shown that there was an influx of CCR2^{+} macrophages into both the bridge and the distal stump. However, it appears that within the CCR2^{+} population, there is a distinct expression pattern of CCL3 between these two nerve regions. This could be due to a number of reasons. Firstly, we have identified that CCL3 is a hypoxia-inducible factor, and so the upregulation seen in the bridge could be due to the hypoxic bridge environment. Secondly, the increase could be due to the phenotype of the macrophage population, which is present in the bridge compared to the distal stump and correlated to the distinct roles that the macrophages play in both physiological regions. This would be consistent with sub-populations of CCR2^{+} macrophages in the bridge and the distal stump which carry out specific temporally defined functions.

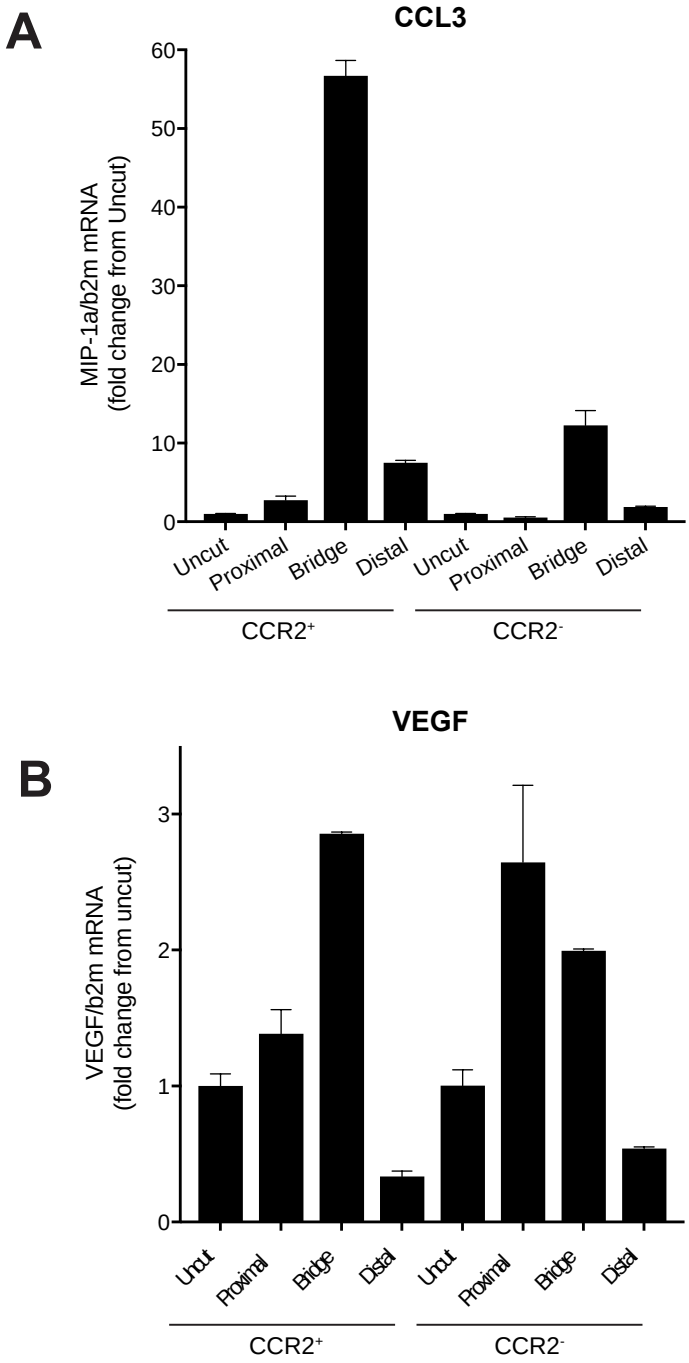

Figure 4.11 | CCL3 is expressed by CCR2$^+$ macrophages in the nerve bridge
RNA expression analysis of CCR2$^+$ and CCR2$^-$ macrophages from mouse nerves harvested on Day 5 following injury. CCL3 is highly upregulated in bridge in both CCR2$^+$ and CCR2$^-$ macrophages, which the larger increase observed in the CCR2$^+$ population. Bars show pooled data from 10 animals +SD, n=1.

Consistent with previous data (Cattin et al., 2015), VEGF transcript levels were increased in the macrophage populations in the bridge (Figure 4.13B). This RNA expression analysis implied that following injury, CCL3 is highly expressed specifically by monocyte-derived ($CCR2^+$) macrophages in the nerve bridge. This result further indicates that diverse macrophage populations are present following injury, and that these macrophages may have distinct roles.

4.10. Schwann cells express the receptors for CCL3

Although Schwann cells have previously been shown to express the receptors for CCL3, CCR1 and CCR5, *in vivo* by immunofluorescence staining (Kiguchi et al., 2010), we wanted to confirm the expression of these receptors by Schwann cells in our *in vitro* system. Schwann cells were cultured under normal conditions *in vitro*, and RNA was extracted. An RT-qPCR was performed to test for the expression of CCR1 and CCR5 as well as the positive control receptor CXCR4. The analysis showed that *in vitro*, CCR1 and CCR5 were expressed by Schwann cells at a similar level to the receptor CXCR4 (Figure 4.12).

Antibodies were acquired in order to identify CCR1 and CCR5 expression by Western blotting and immunofluorescence staining, however optimisation was not successful. In future studies therefore, alternative antibodies to detect CCR1 and CCR5 will be purchased and optimised for use in immunofluorescence staining and protein analysis studies, in both our *in vitro* Schwann cells, as well as following injury *in vivo*.

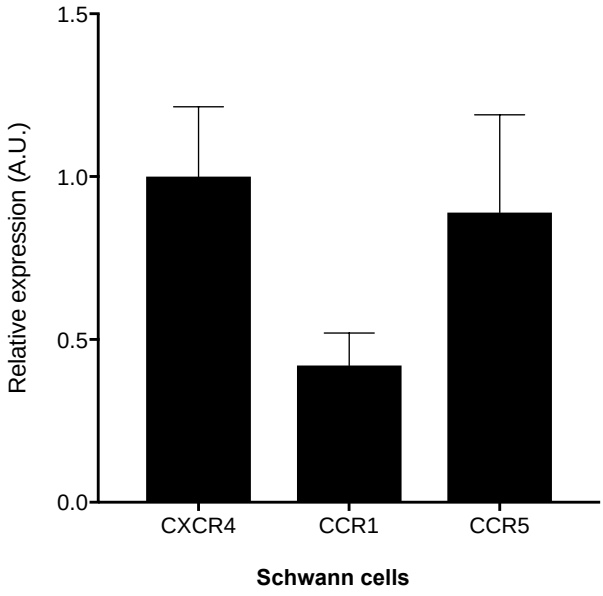

Figure 4.12 | CCR1 and CCR5 are expressed on Schwann cells *in vitro*
Expression of CCR1 and CCR5 in Schwann cells *in vitro*. Expression shown as a ratio compared to expression of CXCR4 ±SEM. n=3.

4.11. Recombinant CCL3 is a chemokine for Schwann cells

The results so far suggested that CCL3 was a strong candidate as a potential chemoattractant for Schwann cells. To test this, we used two different cell migration assays using a concentration gradient of CCL3, and analysed the response of Schwann cells.

In the first instance, we used the Boyden chamber to look at Schwann cell migration in response to increasing concentrations of recombinant rat CCL3 protein. Schwann cells were seeded in triplicate into the upper compartment of a Boyden chamber and left to migrate for four hours in response to 10, 50, 150 or 250ng/ml rCCL3 diluted in Sato, with Sato and 3% serum culture media as negative and positive migration controls respectively. Migratory cells were quantified and normalised to generate a fold change in migration compared to Sato (Figure 4.13). We observed that Schwann cell migration increased in response to 3% serum culture media (***$p<0.001$), which demonstrated that Schwann cells were migrating normally. Schwann cell migration was also increased in response to both 10ng/ml (**$p<0.01$) and 50ng/ml (***$p<0.001$) rCCL3 which confirmed that CCL3 had chemoattractant properties. Moreover, when the Schwann cells were incubated with a CCL3 receptor inhibitor (50μg/ml Maraviroc) and 50ng/ml rCCL3, migration was inhibited to near basal levels. This confirmed that CCL3 was able to induce Schwann cell migration.

At the two highest concentrations of CCL3 (150 and 250ng/ml) we observed that the concentration dependent increase in Schwann cell migration was lost, and there was a decrease compared to the 10 and 50ng/ml CCL3 conditions. The low chemotaxis at high concentrations of CCL3 may be due to receptor saturation (Tweedy et al., 2016). When a cell is exposed to high concentrations of a chemoattractant, receptors at both the front and the rear can become fully occupied, the cell can no longer resolve the external chemokine gradient, and this results in a loss of directional migration.

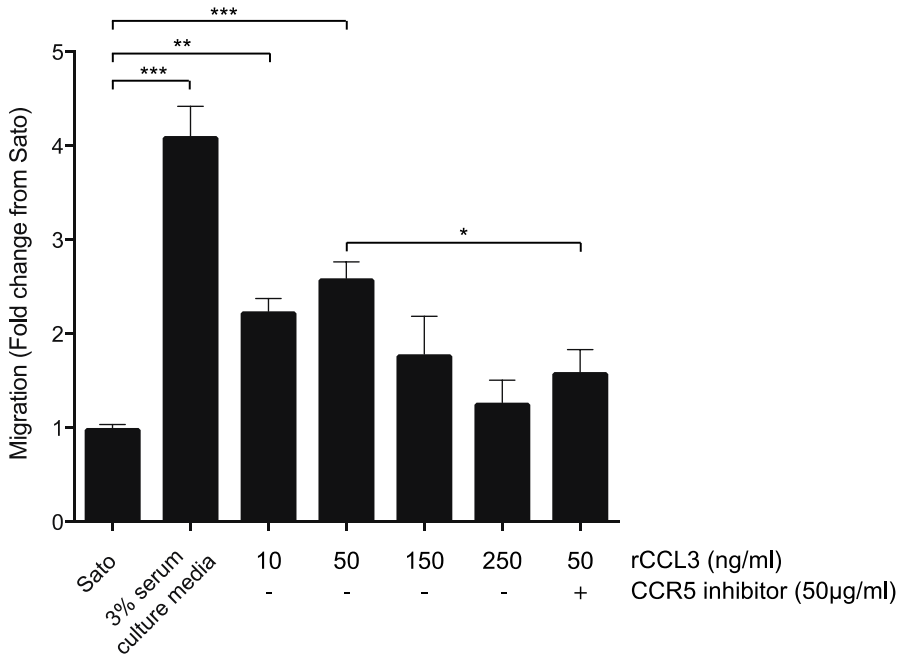

Figure 4.13 | CCL3 is able to attract Schwann cells *in vitro* using the Boyden chamber.
Schwann cells were placed in the upper compartment of Boyden chambers and allowed to migrate into the lower chamber containing media with no factors (Sato), 3% serum culture media, or rCCL3 at the indicated concentration, in the presence or absence of Maraviroc (CCR5 inhibitor). Bars show the average of 4 experiments, +SEM. One-way ANOVA test was used for statistical analysis.

The data from the Boyden chamber demonstrated that rCCL3 was able to increase the migration of Schwann cells *in vitro*. This could be due to either an increase in migration speed, or an increase in migration directionality, which due to the nature of this assay, cannot be distinguished. To test if CCL3 was having an effect on Schwann cell migration velocity, Schwann cells were seeded onto PLL and laminin coated dishes and incubated with Sato, 3% serum culture media or rCCL3 and imaged every 10 minutes using time-lapse microscopy for 12 hours. Cell migration was tracked in Volocity, and average cell velocity was calculated. Schwann cell migration velocity did not significantly increase following incubation with CCL3 when compared to migration speeds of cells in Sato or 3% serum culture media (Figure 4.14). This result indicated that the increase in Schwann cell migration seen in the Boyden chamber assay was unlikely to be due to an increase in migration speed.

To test whether CCL3 had an effect on Schwann cell migration directionality, we decided to use the Dunn chamber assay (Zicha et al., 1991). The Dunn chamber is made up of two circular wells containing medium, separated by a raised 'bridge' on which cells migrate. The smaller, inner well contains Sato to act as a neutral buffer, and the test media is added to the larger outer well. When a coverslip with adherent cells is inverted on top of the chamber, a gradient between the outer and inner wells is created across the 'bridge', and if the outer well contains a chemoattractant, cells will migrate towards it. The chamber is imaged using time-lapse microscopy and cell migration tracked, to analyse migration directionality. For our experiments, 15,000 Schwann cells were seeded onto a glass coverslip and incubated overnight in normal culture conditions, before being washed twice in Sato. The coverslip was then inverted and placed onto the Dunn chamber with Sato, 3% serum culture media or Sato containing 50 ng/ml rCCL3 (the optimal concentration for Schwann cell migration, as determined by the Boyden chamber experiments) in the outer chamber. Cells were then left to migrate for 24 hours and imaged every 10 minutes using time-lapse microscopy. Cell migration was tracked in Volocity, and cell migration tracks and directionality were calculated using a plugin in for Excel (Gorelik and Gautreau, 2014).

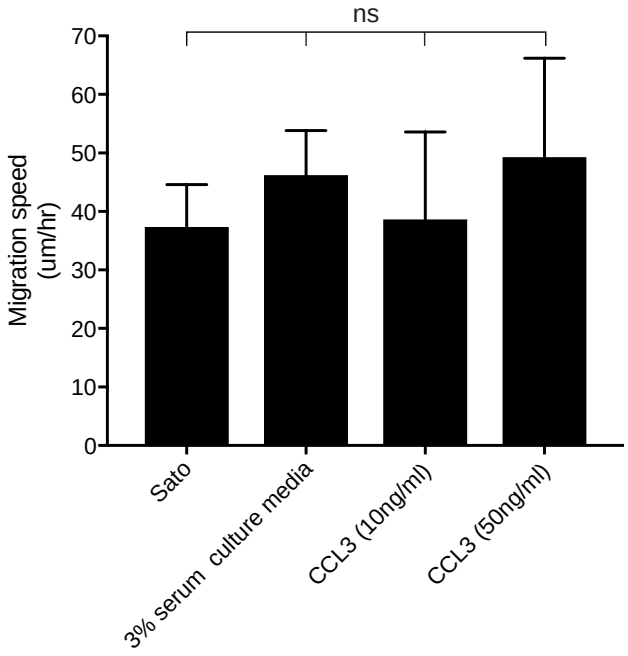

Figure 4.14 | CCL3 does not increase the speed of Schwann cell migration
Quantification of Schwann cell migration speed in the presence of Sato, 3% serum culture media or 50ng/ml rCCL3. Graph shows average. Graph shows average of 3 experiments +SEM. One-way ANOVA test was used for statistical analysis.

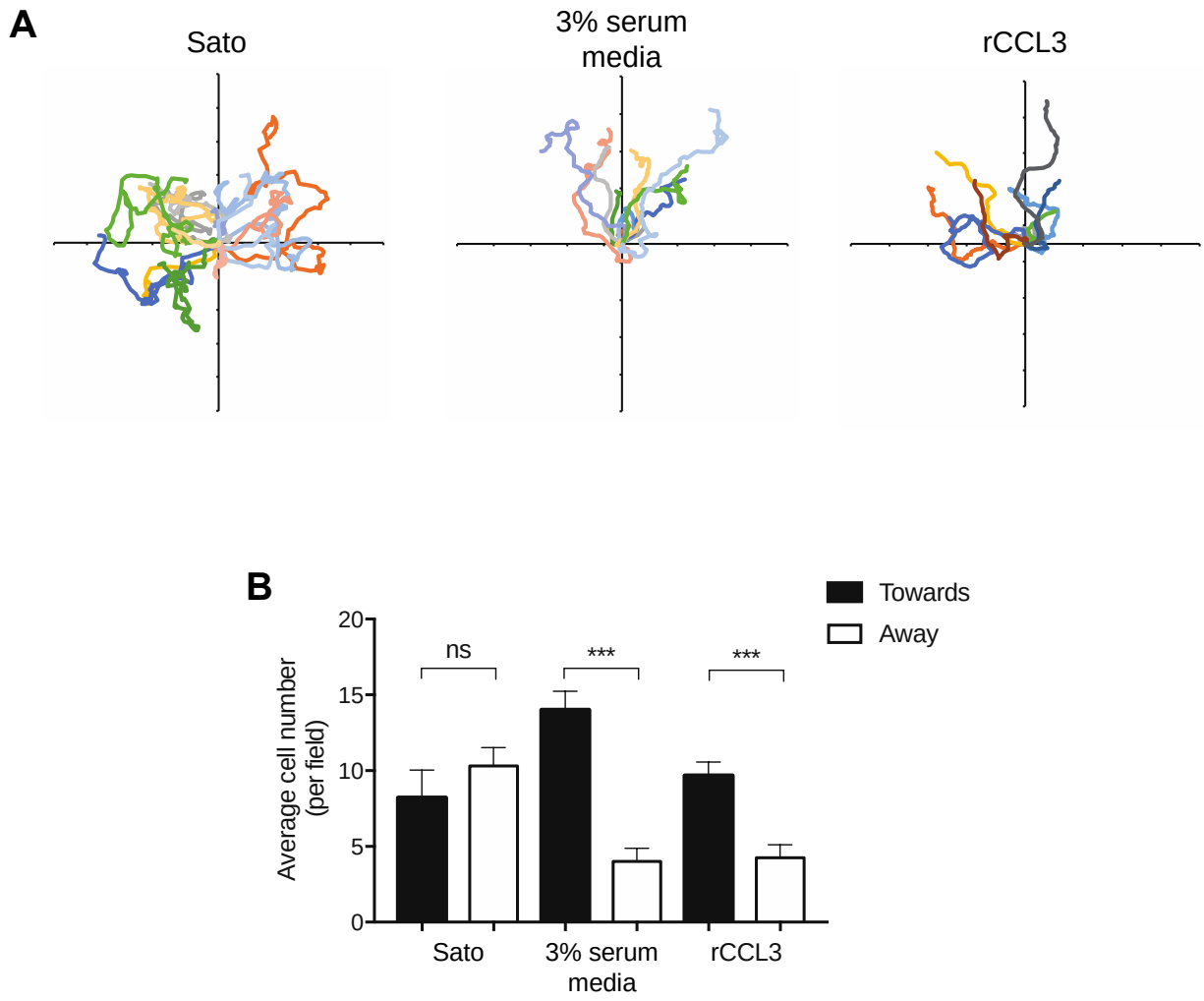

Figure 4.15 | Dunn chamber assay shows that CCL3 is able to attract Schwann cells.
A. Representative cell tracks showing Schwann migration in the response to Sato, 3% serum culture medium or 50ng/μl rCCL3. B. Quantification of Schwann cell migration towards or away from the stimulus, n=3, >60 cells counted per experiment. Graph shows mean cell number +SEM. One-way ANOVA test was used for statistical analysis.

In the Sato control condition, Schwann cells migrated in a non-directional manner (Movie 4.2 and Figure 5.17A, left panel) and there were approximately the same number of cells migrating towards and away from the outer well containing Sato (ns $p>0.05$, Figure 4.15B). In the positive control using 3% serum culture media, the majority of Schwann cells migrated in a directional manner (Movie 4.2 and Figure 4.15A, middle panel) towards the stimulus (***$p<0.001$, Figure 4.15B). In the rCCL3 condition, Schwann cells also migrated in a directional manner towards the outer well (Movie 4.2 and Figure 4.15A, right panel) and there was a significant increase in cells migrating towards the stimulus compared to migrating away from it (***$p<0.001$, Figure 4.15B). This experiment showed that in response to CCL3, Schwann cells migrated in a more directional manner, preferentially migrating towards the factor.

This result, combined with the data from the Boyden chamber experiments confirmed that CCL3 could induce Schwann cell migration. Moreover, these Dunn chamber experiments showed that CCL3 acts as a directional migration factor for Schwann cells, as we did not observe an increase in cell migration speed.

4.12. Knockdown of CCL3 in J774A.1 cells prevents Schwann cell migration

We have established that the J774A.1 cell line expresses CCL3 following incubation in hypoxia (1.5% O_2) by RNA expression analysis and Western blot. We have also observed using two migration assays, Boyden and Dunn chambers, that recombinant CCL3 is able to recruit Schwann cells. To determine whether CCL3 was the major chemokine secreted by macrophages we tested whether the knockdown of CCL3 using short interfering (si) RNAs in hypoxic J774A.1 cells inhibited the ability of these cells to increase the migration of Schwann cells.

Initially, we optimised the siRNA knockdown in J774A.1 cells. 200,000 cells/well were seeded in a 6 well plate before incubating overnight at 20% O_2 in normal culture media containing 10% serum. The following morning, cells were washed with Sato and siRNAs (62.5nM) against CCL3 (si 1-3) or the Scrambled (Scr) negative control was added, and cells were incubated with the siRNA complexes for 48 hours before harvesting for RNA or protein analysis. The efficiency of the knockdown was analysed by both RT-qPCR and Western blot analysis (Figure 4.16).

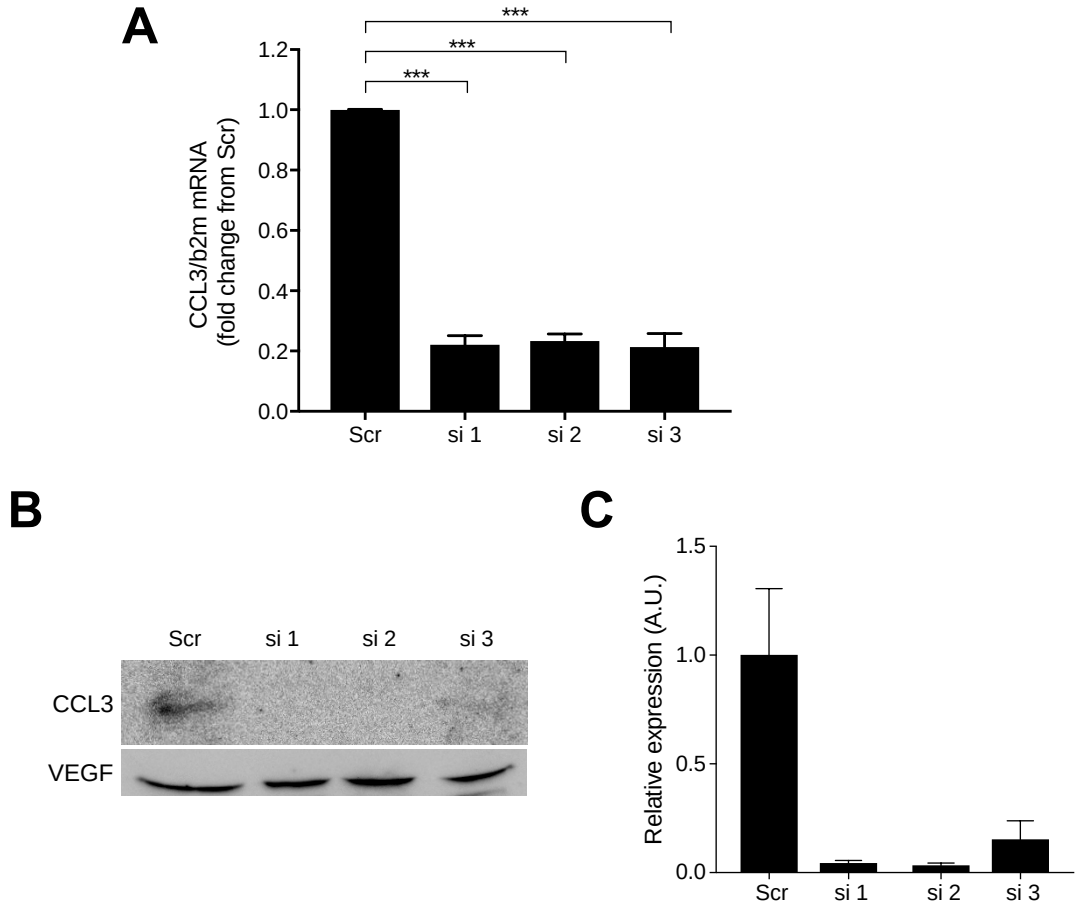

Figure 4.16 | CCL3 knockdown by siRNA

A. Graph showing RT-qPCR analysis of the mRNA expression levels of CCL3 in Scr or CCL3 knocked down cells treated with either siRNA 1, 2 or 3 for 48 hours in Sato at 1.5% O_2. Results are shown relative to the expression in Scr treated cells. (Graph shows mean cell number +SEM. n=3. Two-tailed Student's t test was used for statistical analysis.) B. Representative Western blot analysis of conditioned media from J774A.1 cells treated with Scr or siRNA against CCL3 si1, 2 or 3 for 48 hours in Sato at 1.5% O_2. C. Densitometry of Western blots, graph shows expression of CCL3 normalised to Scr. n=2.

We observed an ~80% reduction in CCL3 RNA by RT-qPCR using three independent siRNAs targeted against CCL3 compared to the Scr treated control and a ~90% reduction in CCL3 protein as measured by densitometry compared to the Scr treated control. Having optimised the siRNA knockdown in our system, the conditioned media from siRNA treated J774A.1 cells was used in the Boyden and Dunn chamber assays.

As before, J774A.1 cells were seeded and siRNA knockdown of CCL3 using three independent siRNA oligos or Scr control was carried out for 48 hours. The conditioned media from each condition was then harvested and filtered to remove cell debris. Firstly, we used the Boyden chamber assay to assess Schwann cell migration. 75,000 Schwann cells were seeded into the upper compartment of a Boyden chamber, and allowed to migrate for 4 hours in normoxia in response to Sato, 3% serum culture media, the conditioned media from Scr or siCCL3 treated J774A.1 or recombinant rat CCL3 protein. The migratory cells were then quantified and normalised to basal migration in Sato (Figure 4.17). We observed that similar to previous Boyden chamber experiments, there was an approximate 3-fold increase in Schwann cell migration in response to 3% serum culture media (***$p<0.001$) and close to 3-fold increase in response to recombinant CCL3 protein (***$p<0.001$) (Figure 4.17). We also saw that in response to the conditioned media from Scr treated J774A.1 cells, there was a similar increase in Schwann cell migration to the positive control. In response to the siCCL3 treated J774A.1 cell conditioned media, Schwann cell migration was reduced to basal levels, a significant decrease compared to the Scr control (***$p<0.001$).

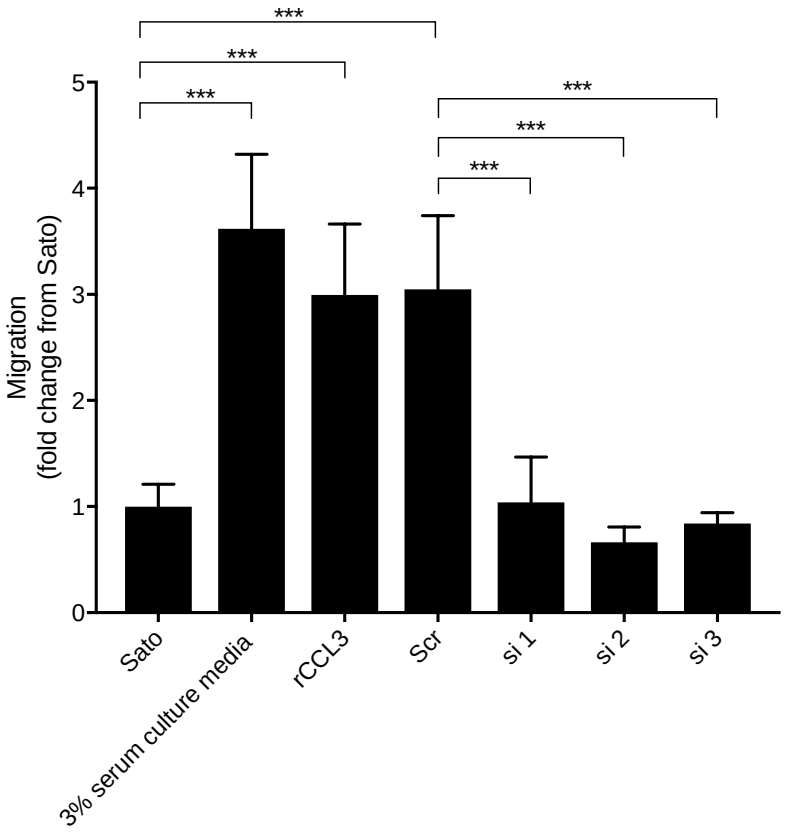

Figure 4.17 | CCL3 KD in macrophages prevents Schwann cell migration
Schwann cells were placed in the upper compartment of Boyden chambers and allowed to migrate for 4 hours into the lower chamber containing Sato, 3% serum culture media, conditioned media from Scr or siCCL3 (1-3) treated J774A.1 cells or 50ng/μl recombinant CCL3. Bars show average fold change in migration from control from 3 experiments ±SEM. One-way ANOVA test was used for statistical analysis.

Secondly, to investigate the directionality of Schwann cell migration in the absence of CCL3 following siRNA treatment we used the Dunn chamber assay and carried out the protocol as previously described, using conditioned media from the Scr or siCCL3 treated J774A.1 cells in the outer well.

In the Scr control condition, Schwann cells migrated in a preferential manner towards the outer well of the chamber (Movie 4.3 and Figure 4.18A, left panel), and quantification of the cells showed that a significant majority of cells migrated towards the stimulus compared to away (*$p<0.05$) (Figure 4.18B). When CCL3 was knocked down in J774A.1 cells using three independent oligos, Schwann cells lost their directional migration in response to the conditioned media and cells were observed to migrate in multiple, random directions (Movie 4.3 and Figure 4.18A, right panel). When cell migration was quantified, we saw that similar numbers of cells (ns $p>0.05$) migrated both towards and away from the outer well in each of the siCCL3 treated conditions.

Together, the Boyden and Dunn chamber data showed that within the conditioned media of hypoxic J774A.1 cells, CCL3 was either the only Schwann cell chemoattractant factor present, or was essential for synergy with another factor. Moreover, by using three independent oligos to specifically knock down CCL3, we showed that this was not an off-target effect. This was a particularly exciting result, as a macrophage-derived Schwann cell chemoattractant factor has not previously been described, and this chemotaxis assay showed strong evidence that Schwann cell migration could be mediated by macrophages and furthermore that CCL3 was the sole factor responsible for the increase in migration.

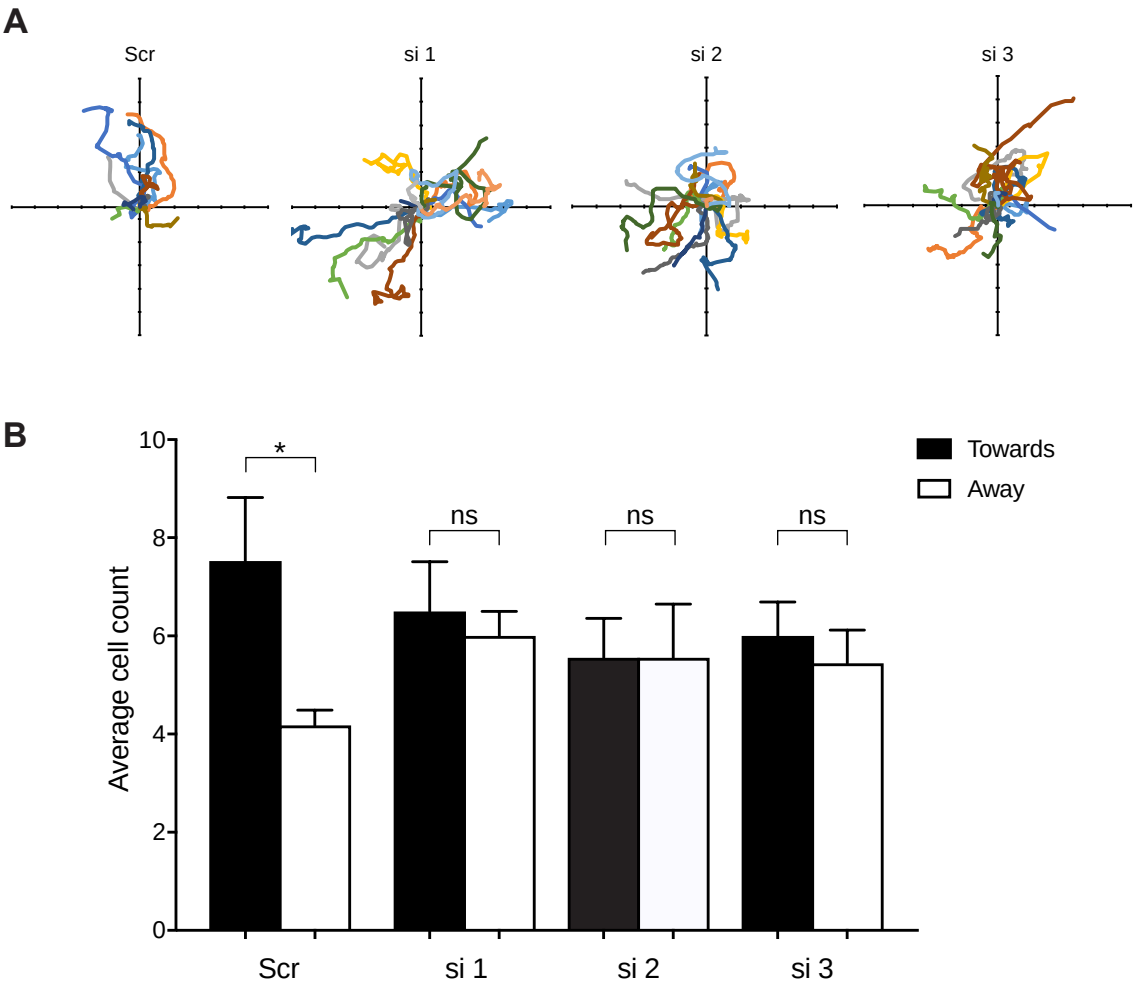

Figure 4.18 | CCL3 KD in macrophages prevents directional Schwann cell migration
A. Representative cell tracks showing Schwann migration in response to conditioned media from Scr or siCCL3 (1-3) J774A.1 cells. B. Quantification of Schwann cell migration towards or away from the stimulus, n=3, >60 cells counted per experiment. Graph shows mean cell number ±SEM. Student's t-test was used for statistical analysis.

4.13. Chapter conclusion

In this chapter, we have shown that there is a hypoxia-inducible factor in the nerve bridge, which is able to attract Schwann cells. Moreover, we have identified that the cell type responsible for the increase in Schwann cell migration is macrophages, specifically when they are hypoxic. We have also identified a potential Schwann cell chemoattractant, CCL3 using an unbiased cytokine screen. CCL3 is upregulated in both our *in vitro* and *in vivo* systems, and our data is consistent with a previous study which identified an increase of CCL3 'near' to the sciatic nerve lesion site (i.e. in the bridge) as well as 'far' (i.e. in the distal stump) following injury (Perrin et al., 2005).

Interestingly, CCL3 has previously been reported to play a role in nerve regeneration, by recruiting macrophages to the site of injury following a full transection (Perrin et al., 2005, Taskinen and Röyttä, 2000, Kiguchi et al., 2010). Levels of CCL3 were found to be increased following injury, and additionally the use of a CCL3 blocking antibody reduced the number of macrophages recruited to the injury site by 78%, as well as slowing the rates of Wallerian degeneration (Perrin et al., 2005).

Following sciatic nerve injury, Schwann cells *in vivo* were also observed to express the receptors for CCL3, CCR1 and CCR5, which suggests that CCL3 could also potentially have a chemotactic effect on Schwann cell migration (Kiguchi et al., 2010). There has also been research which suggests a link between CCL3 and neuropathic pain, as perineural injection of CCL3 induced tactile allodynia as well as thermal hyperalgesia, and anti-CCL3 antibodies were found to alleviate pain hypersensitivity in models of neuropathic pain (Kiguchi et al., 2010, Sun et al., 2016). Together this makes CCL3 an interesting potential Schwann cell chemoattractant factor within the model of peripheral nerve injury, as well as a mediator in neuropathic pain.

Importantly, we found that CCL3 was present in the nerve bridge at Day 5 following injury in mice. At this stage in the regeneration process, hypoxia has mostly been resolved due to the formation of blood vessels in this region. As CCL3 is still expressed by macrophages in the nerve bridge at this time point, this indicates that it can act as a chemoattractant factor for Schwann cells as we have observed in our *in vitro* assays. This is also consistent with our data showing that macrophages isolated from the bridge and cultured at ambient oxygen concentrations are able to attract Schwann cells in the Boyden chamber assay, indicating that they are continuing to express CCL3.

Specific knockdown of CCL3 in J774A.1 cells also showed that it was the only Schwann cell chemoattractant present in the conditioned media, which was able to induce directional migration. Using

two independent chemotaxis assays we saw that Schwann cell migration was inhibited following knockdown using three independent oligos, which demonstrated that the inhibition we observed was specific to the knockdown of CCL3 and not off target effects.

Together, these results provide compelling evidence for a Schwann cell chemoattractant factor expressed by macrophages in the bridge and provides evidence for a novel role of macrophages in inducing Schwann cell migration following injury. The following chapter will investigate the role of CCL3 following injury *in vivo* and its function during nerve regeneration.

Chapter Five: CCL3 as a therapeutic agent to aid nerve repair following injury

5.1. Chapter introduction

In the previous chapter we showed that hypoxic macrophages in the bridge of a regenerating nerve secrete a chemoattractant which is able to attract Schwann cells and identified this factor as CCL3. Whilst we have identified CCL3 as an important *in vitro* modulator of Schwann cell migration, we have not yet determined the role that CCL3 plays *in vivo* following sciatic nerve injury. The identification of factors that are able to modulate or promote nerve regeneration following injury have the potential to be therapeutically beneficial.

The specific knockdown of CCL3 in J774A.1 cells established that it was the only macrophage-derived factor which was able to induce Schwann cell migration. To replicate these studies *in vivo* we intend to use CCL3 knockout mice to provide a powerful *in vivo* model in which to test the effects of this factor on Schwann cell migration. Prior to the arrival of these mice however, we decided to perform complementary *in vivo* Schwann cell migration experiments. In one model, we overexpressed CCL3 in an attempt to disrupt the gradient of CCL3 within the bridge following injury. In a second model, we used CCL3 in an established pre-clinical model of nerve repair using an artificial conduit and tested the ability of CCL3 to induce Schwann cell migration following injury.

5.2. Testing the role of CCL3 in nerve regeneration

To investigate the role of CCL3 in directing Schwann cell migration during nerve regeneration, we decided to attempt to disrupt the gradient of CCL3 in the bridge. We hypothesised that the injection of CCL3 into both nerve stumps might prevent Schwann cell migration into the bridge by blocking the physiological gradient of CCL3 from the bridge which is sensed by Schwann cells (Figure 5.1A).

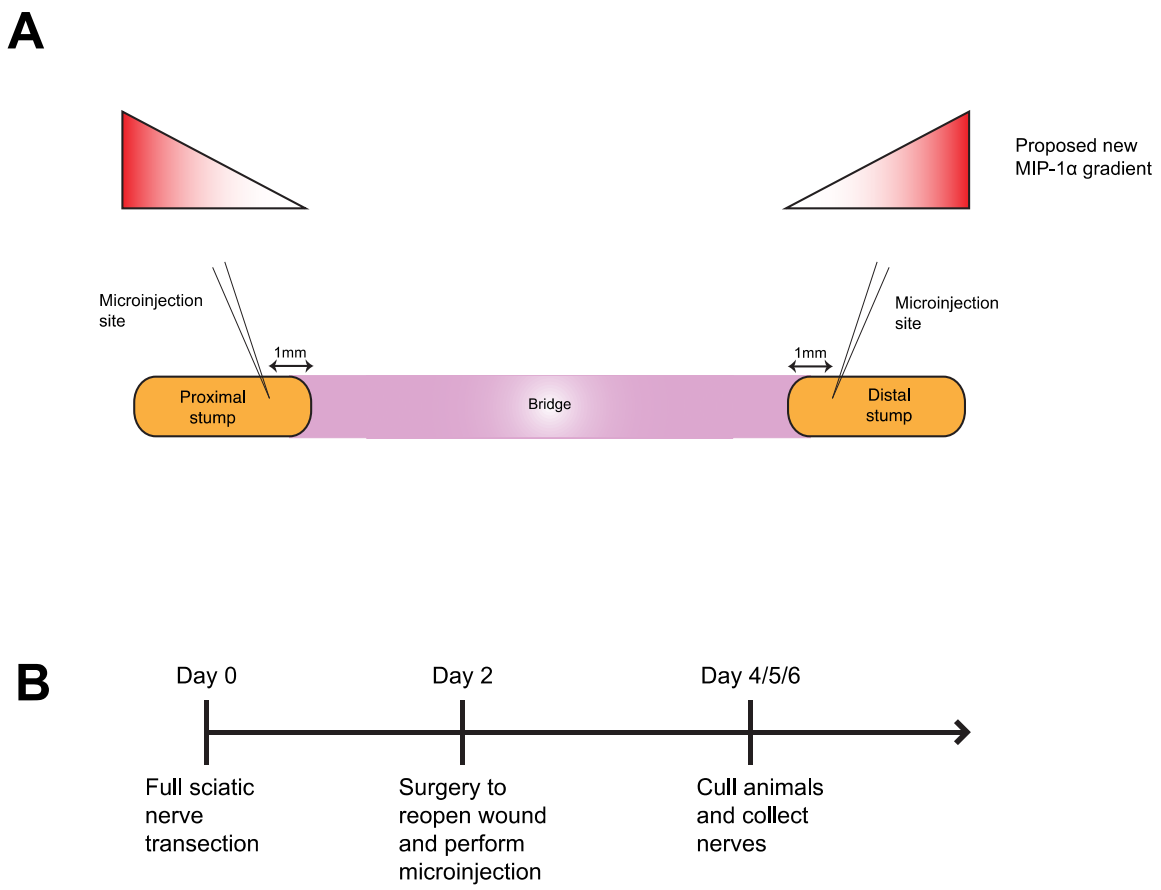

Figure 5.1 | Protocol for sciatic nerve microinjection experiment
A. Schematic indicating microinjection sites in the sciatic nerve following injury and the proposed new CCL3 gradients. B. Proposed time line of injection protocol detailing surgery and nerve harvesting time points.

In initial experiments, we performed full sciatic nerve transections in adult rats and allowed them to recover before on Day 3 following surgery, reopening the surgical wound under anaesthetic to expose the injured sciatic nerve. We chose this time point as we have previously shown that at Day 3 following injury the bridge has been vascularised, and Schwann cells are just beginning to migrate out of the nerve stumps. Therefore by injecting CCL3 at this time point, we aimed to disrupt the physiological gradient observed in the bridge (Figure 4.9A). To do this, we slowly microinjected 5μl of 50μg/ml rCCL3 at a 1mm distance from the bridge into both the proximal and distal stumps (Figure 5.1A) using a glass capillary needle and injection system. In control rats, we microinjected 5μl of sterile PBS into each stump. The wound was then closed using wound clips, and the animals were allowed to recover.

On Day 4 following the initial sciatic nerve transection surgery, the animals were culled and the injured nerves were collected (Figure 5.1B). At this time point, we would normally expect the Schwann cell cords to have entered the bridge. The nerves were fixed in PFA and prepared for cryosectioning through successive incubations in 30% sucrose and a 50:50 (w/v) solution of 30% sucrose and OCT, and freezing in OCT. Thick (50μm) longitudinal sections from the nerve were cut and stained using immunofluorescence to detect Schwann cells (S100), blood vessels (lectin), axons (neurofilament) and nuclei (Hoechst). Confocal images of the nerve were taken using a 10X objective, and reconstructed using ImageJ and Photoshop. To quantify Schwann cell growth, the furthest distance migrated by Schwann cells (as denoted by green staining) from the proximal and distal stump in each animal was measured using ImageJ.

When the nerves were harvested, there appeared to be a difference in the gross anatomy of the nerves between the CCL3 and PBS injected animals; the bridge regions of the CCL3 injected nerves seemed to be more opaque suggesting that there had been an increase in migration in these animals compared to the controls. However, when we examined the sections from the control animals, we observed that although the bridge has been vascularised, there was minimal Schwann cell migration out of either the proximal or distal stump. Moreover, there was a lot of variability between animals which correlated with variability in bridge length between animals (Figure 5.2A and quantified in Figure 5.3). In the CCL3 injected animals, we also only observed a small amount of Schwann cell migration, which also varied between animals (Figure 5.2B and quantified in Figure 5.3). As such, there was no statistical difference between the CCL3 injected and PBS controls. The lack of migration in the control animals made the experiment difficult to interpret.

As previously discussed, we chose to harvest the nerves at a time point when Schwann cell migration into the bridge should have occurred during normal nerve regeneration (Day 4). The lack of Schwann cell migration into the bridge in control animals suggested that the process of reopening the wound may have disturbed bridge formation. Additionally, the process of microinjecting into the nerve stumps may have caused an additional injury and/or inflammatory response, which could have prevented normal nerve regeneration.

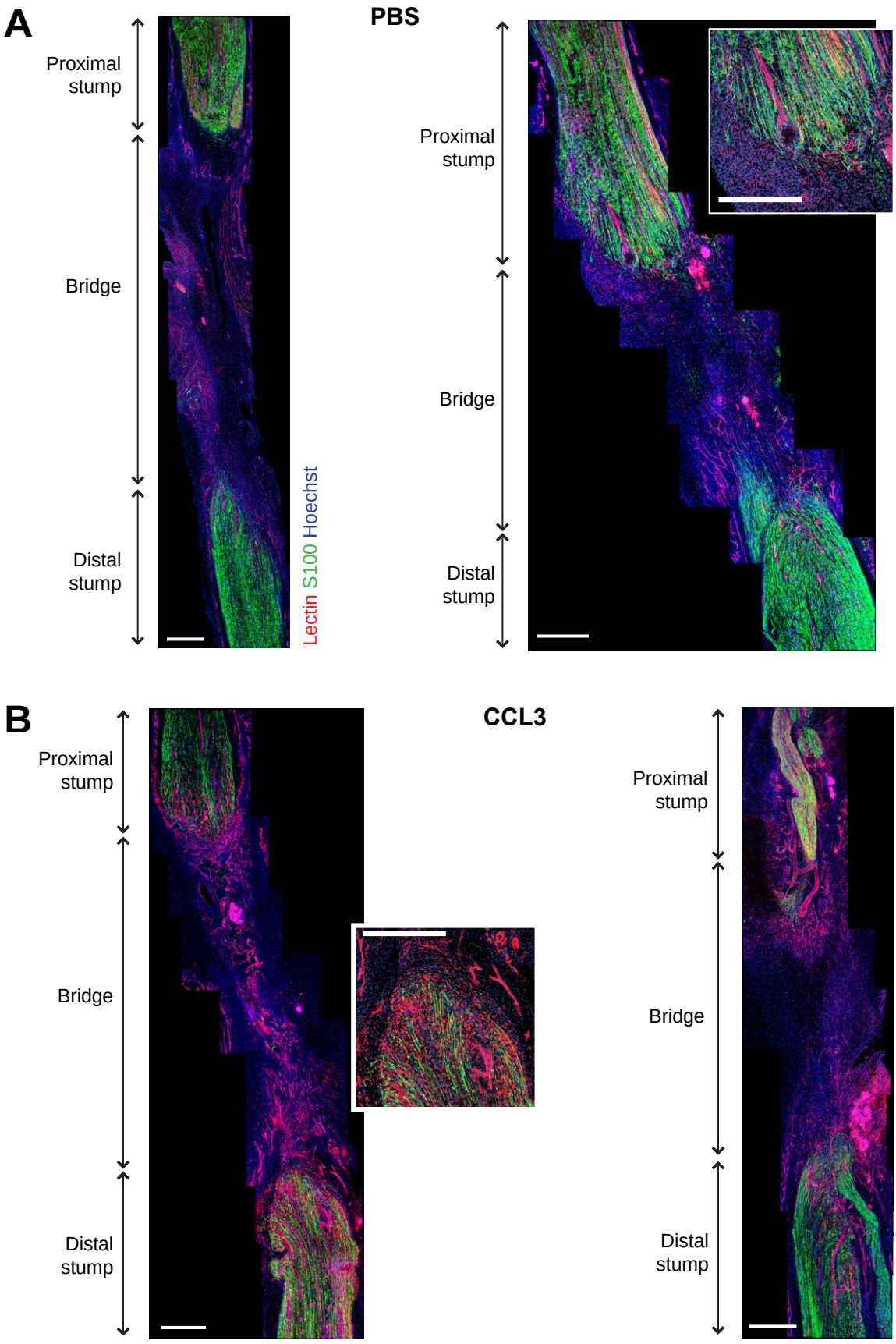

Figure 5.2 | CCL3 injection proximal and distal representative confocal images
(Legend continues on next page)

Figure 5.2 | CCL3 injection proximal and distal representative confocal images (contd)
Representative reconstructed confocal images of PBS (A) and CCL3 (B) injected sciatic nerves harvested on Day 4 following initial injury. Nerves immunostained to detect Schwann cells (S100, green), blood vessels (lectin, red) and nuclei counterstained with Hoechst (blue). The bridge and proximal and distal stumps are indicated by arrows. Inset images show higher magnification of leading Schwann cell migration edge. Scale bars = 500μm, n=2 (3 animals per condition).

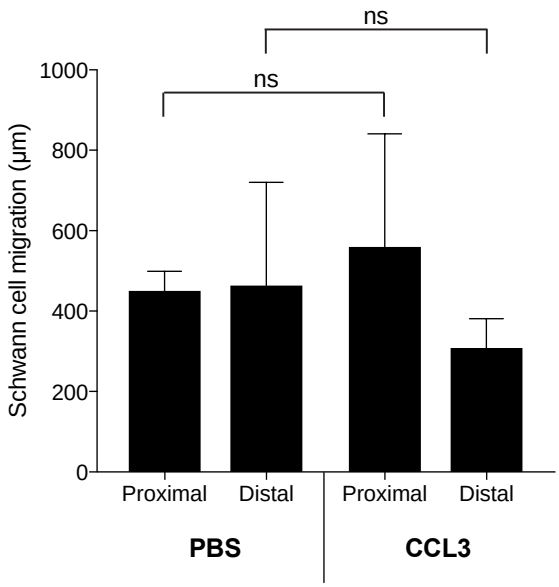

Figure 5.3 | CCL3 injection into nerve stumps did not affect Schwann cell migration into the nerve bridge
Quantifications of distance migrated (μm) by Schwann cells following nerve injury and subsequent microinjection of PBS or CCL3 into both the proximal and distal stump. n=2 (3 animals per condition), graph shows mean ±SD.

To optimise the protocol therefore, we made two changes: firstly, we harvested the animals at a later time point (Day 6) so that the nerve would have longer to regenerate, and allow Schwann cells to migrate further into the bridge. Secondly, we realised that injecting CCL3 into both stumps may have resulted in the creation of gradients from each stump which the Schwann cells at the opposite stump might sense (due to the factor diffusing away from the injection site) and respond to, i.e. the injection of CCL3 into the distal stump may have created a gradient which could be sensed by Schwann cells at the proximal stump and induced migration into the bridge and vice versa.

We therefore decided to inject CCL3 into one nerve stump only, in an attempt to block the gradient from only one of the stumps. We chose to inject into the distal stump, as injection into the proximal stump may cause an additional injury to the axons which could affect regeneration. We hypothesised that by only injecting CCL3 into the distal stump we would only prevent migration into the bridge from this stump, whereas at the proximal stump we would potentially observe normal or increased Schwann cell migration. Following the injection, the nerves were harvested at Day 6 after initial injury and processed as previously described.

In these experiments, we observed that in the PBS injected control animals, Schwann cells migrated further into the bridge from both the proximal and distal stump, compared to the previous experiments (Figure 5.4A and quantified in Figure 5.5). Encouragingly, we also saw that the variability between the animals was reduced. There also appeared to be slightly more Schwann cell migration from the proximal stump compared to the distal stump, however this was not significant.

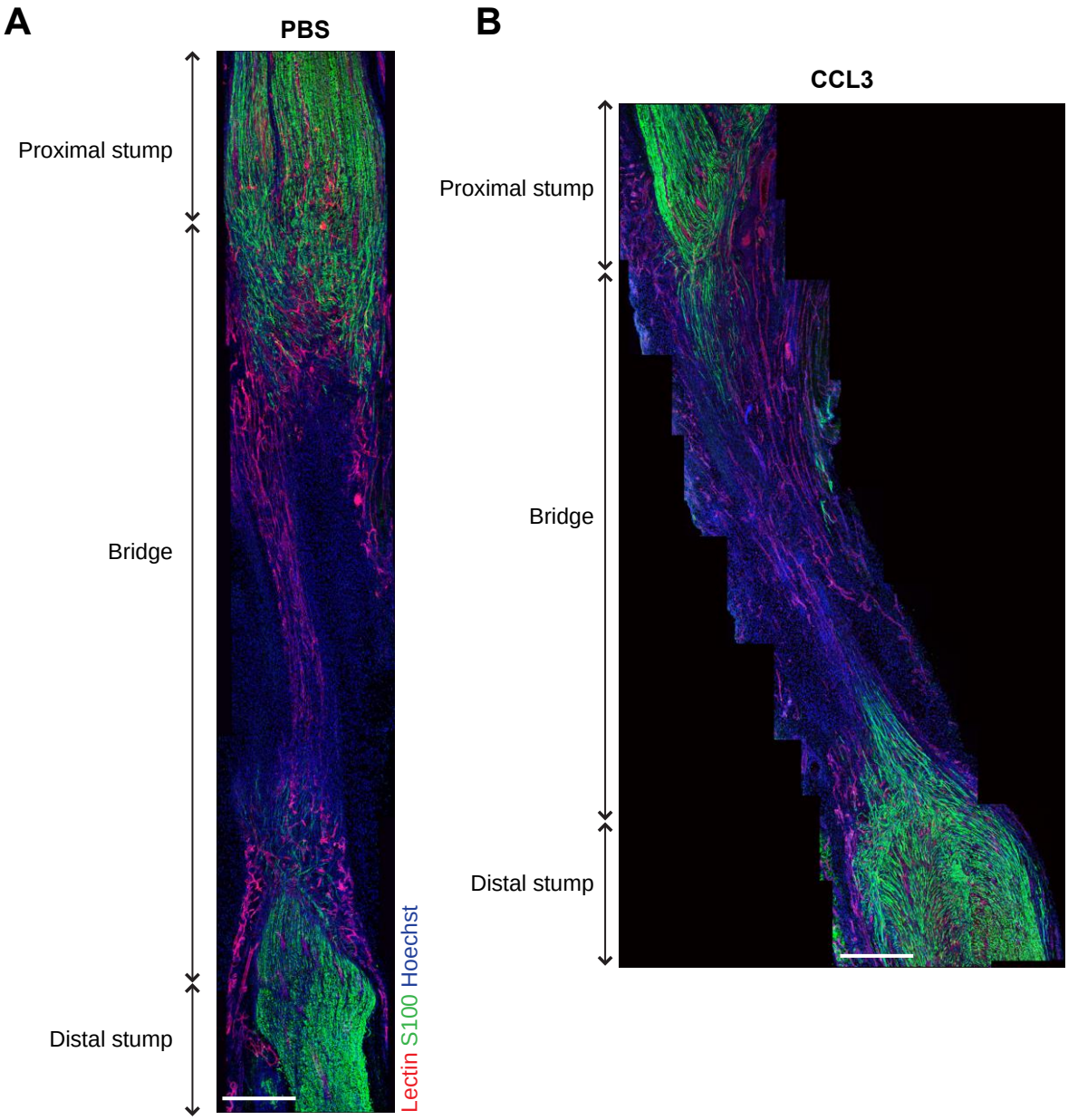

Figure 5.4 | CCL3 injection into the distal stump had no significant effect on the rate of Schwann cell migration

Representative reconstructed confocal images of PBS (A) and CCL3 (B) microinjected (into distal stump only) sciatic nerves harvested on Day 7 following the initial injury. Nerves immunostained to detect Schwann cells (S100, green), blood vessels (lectin, red) and nuclei counterstained with Hoechst (blue). The bridge and proximal and distal stumps are indicated by arrows. Scale bar = 500μm. n=2 (3 animals per condition).

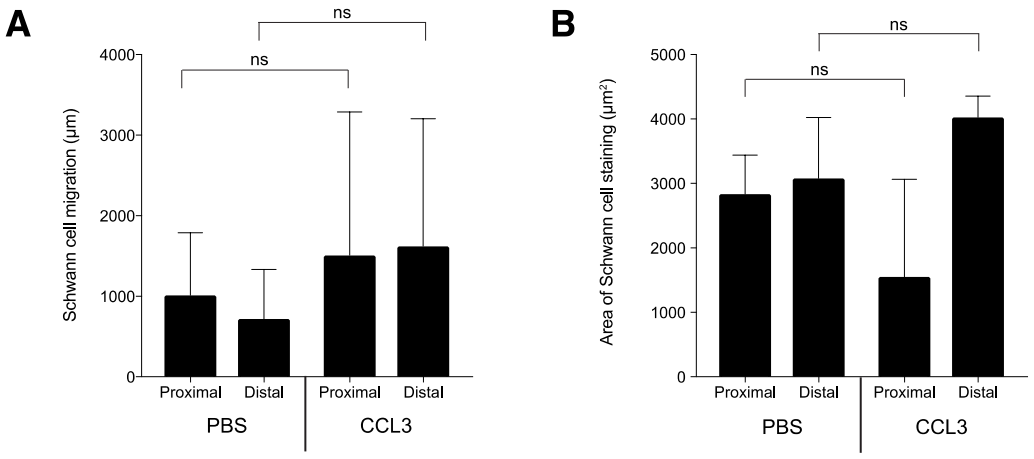

Figure 5.5 | CCL3 injection into the distal stump showed no significant effect on Schwann cell migration

A. Quantification of the distance migrated by Schwann cells (µm) following nerve injury and subsequent microinjection of PBS or CCL3 into the distal stump only. Data expressed as total distance travelled into the bridge from tip of stump, graph shows mean ±SD. n=2 (3 animals per condition). B. Quantification of area migrated by Schwann cells (μm^2) following nerve injury and subsequent microinjection of PBS or CCL3 into the distal stump only. Data expressed as total area of positive Schwann cell staining in the bridge, graph shows mean ±SD. n=2 (3 animals per condition).

In the CCL3 injected animals we found that there appeared to be an increase in Schwann cell migration from both the proximal and distal stumps compared to the PBS controls, however this was not significant (Figure 5.4B and quantified in Figure 5.5). These results were promising, suggesting that perhaps there was an increase of Schwann cell migration in the CCL3 injected animals. However, the increase of Schwann cell migration from the distal stump was unexpected as we hypothesised that the injection here would block the gradient of CCL3 from the bridge, indicating it is difficult to predict the effects of CCL3 in this *in vivo* system.

The experiments when CCL3 was only injected into the distal stump showed that there appeared to be a slight trend for an increase in migration in the rCCL3 injected animals. However, the extent of Schwann cell migration occurring in the PBS injected controls was still less than expected. To improve the level of Schwann cell migration, we decided in future experiments to harvest at a later time point (Day 8) to ensure baseline Schwann cell migration in the PBS controls was sufficient, which would allow us to determine if there was any significant change in Schwann cell migration between the PBS and CCL3 injected animals.

We set up a further experiment, however due to the small size of the animals compared to what we had previously used, we decided to harvest the experiment at Day 7, to account for an increase in regeneration speed. In the PBS controls, we saw that the bridge was well vascularised, and that cords of Schwann cells had migrated out of the nerve stumps into the nerve bridge until they almost made contact (Figure 5.6). These animals therefore represent suitable baseline controls for the analysis of any inhibitory effects of CCL3 on Schwann cell migration. We also injected CCL3 into test animals, however due to an error with the staining protocol we were unable to quantify Schwann cell migration (data not shown). We were able to observe axonal migration due to the positive neurofilament staining (data not shown), which could act as a surrogate marker for Schwann cell migration from the proximal stump. However, there did not appear to be any difference between the PBS and CCL3 injected animals.

Therefore, in the future, we will use these optimised conditions to further test the effect of CCL3 gradient blockade following injury, as well as investigating alternative methods of CCL3 delivery, as well as genetic and pharmacological blockade of CCL3 signalling.

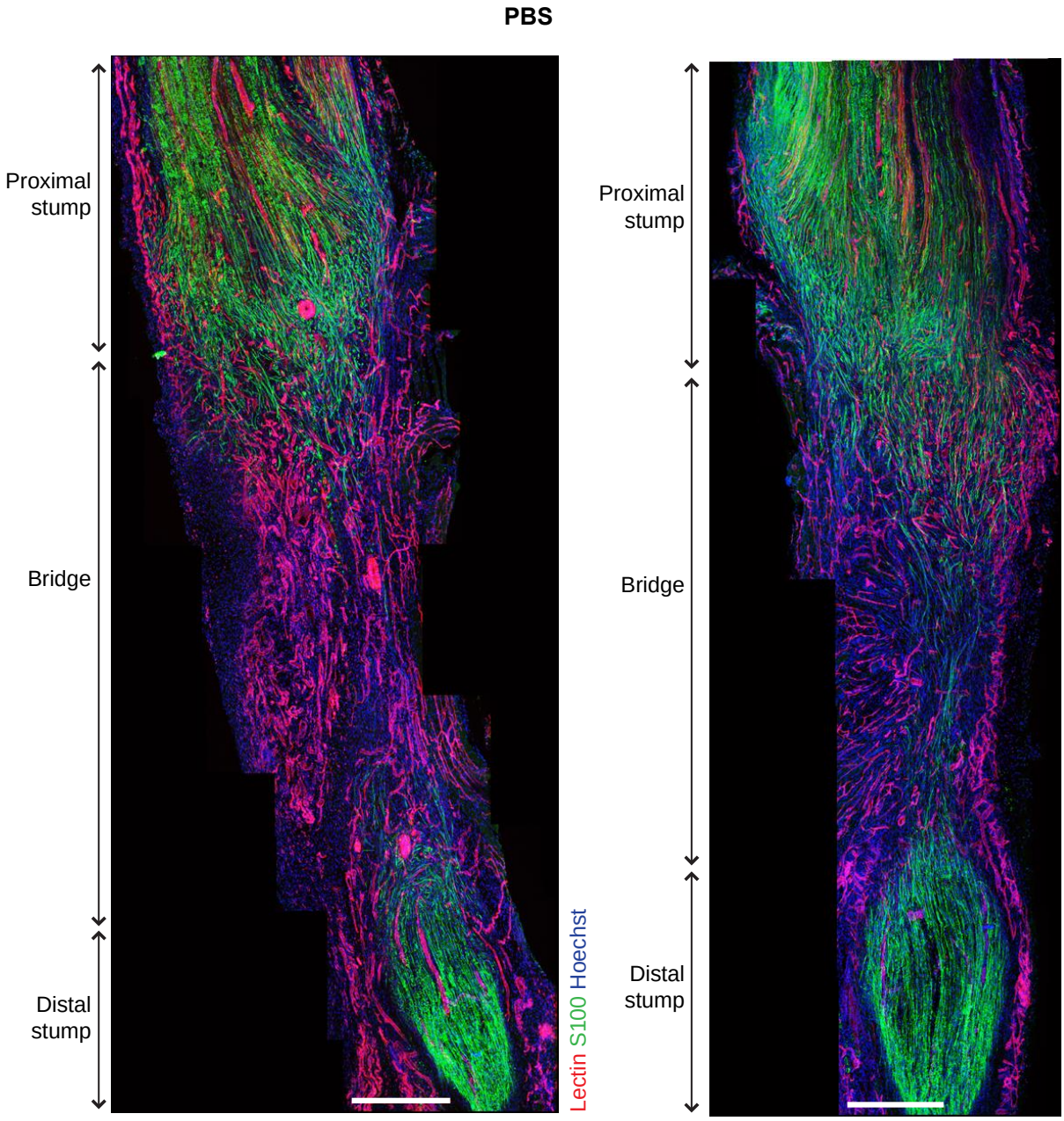

Figure 5.6 | Under optimal injection conditions cords of Schwann cells meet in the middle of nerve bridge

Representative reconstructed confocal images of PBS microinjected (into distal stump only) sciatic nerves harvested on Day 7 following initial injury. Nerves immunostained to detect Schwann cells (S100, green), blood vessels (lectin, red) with nuclei counterstained with Hoechst (blue). The bridge and proximal and distal stumps are indicated by arrows. Scale bar = 500μm. n=1 (4 animals per experimental group).

5.3. Testing the role of CCL3 in a pre-clinical model of nerve repair

The identification of a factor which is able to induce Schwann cell migration during nerve regeneration has potential therapeutic implications for those suffering from peripheral nerve injuries. Peripheral nerve damage can result from multiple causes such as injury, surgery, chemotherapy or metabolic disorders and affects approximately 300,000 people in the USA every year (Grinsell and Keating, 2014, Campbell and Meyer, 2006). Nerve injuries can have a significant effect on patients' lives and symptoms of nerve injury can include loss of sensory and motor nerve function, which in severe cases may lead to paralysis in the damaged limb, neuroma and neuropathic pain (Costigan et al., 2009, Grinsell and Keating, 2014). Despite advances in surgical techniques, as well as an increasingly large body of research investigating the molecular mechanisms of nerve regeneration, the successful repair of many of these injuries remains a major clinical challenge (Grinsell and Keating, 2014, Campbell and Meyer, 2006, Costigan et al., 2009, Scheib and Hoke, 2013).

The level of regeneration following a transection injury is dependent on many factors, such as the length of the gap between the nerve ends caused by the injury, the anatomical location of the injury, and the level and speed of clinical intervention. In some cases, the damaged nerve may simply be re-joined using sutures if this is possible without causing excess tension in the nerve. However, when the gap length increases above a 'critical gap size' (30 mm in humans, 10mm in rats), this is no longer a suitable option and an alternative repair procedure must be conducted (Mokarram et al., 2017).

To repair a nerve and to promote successful nerve regeneration, there are many different strategies which have been tested and used clinically and shown to improve the ability of axons to regenerate (Park, 2008). These different strategies create an environment more permissive to regeneration by preventing neuronal apoptosis (Terenghi et al., 2011), modifying the immunogenic profile (Mokarram et al., 2012) or through the insertion of a nerve conduit (autograft or artificial) which provides structural support for the regrowing nerve (Bell and Haycock, 2012, Heine et al., 2004). Ultimately, the aim is to create a microenvironment which is conducive and supportive for successful axonal regrowth, so that it may occur in a timely manner. Ideally, nerve regeneration should begin as soon as possible following injury to reduce the length of time the target tissue is left dennervated, which if left to become chronically dennervated can both lead to the apoptosis of neurons and contribute to the development of a hostile environment which is less conducive for axonal regrowth (Fu and Gordon, 1995). The dennervated distal stump and target tissue become less able to support axonal regrowth,

due to tissue atrophy and Schwann cell death from 8 weeks after injury, and at 6 months regeneration becomes nearly impossible (Sulaiman and Gordon, 2000, Fu and Gordon, 1995). This highlights the importance of efficient nerve repair to be initiated as soon as possible to ensure that regeneration occurs within the critical window for successful clinical outcome.

The current gold standard for repairing severe peripheral nerve injuries remains the autograft of a nerve from an alternative location to the injury site (Bhangra et al., 2016, Scheib and Hoke, 2013). The nerve to be transplanted is taken from a healthy, non-critical alternative location within the body. Commonly a sensory nerve such as the sural nerve is taken, although recently allografts from a cadaver donor have shown promise (Mokarram et al., 2017). There are many advantages to the use of autografts in nerve repair, such as the absence of tissue rejection, the ability to successfully bridge large gaps and the intact nerve structure which is retained (Grinsell and Keating, 2014). Following implantation, nerve regeneration may proceed due to the insertion of nerve tissue which is Schwann cell rich, and contains an intact and organised tissue structure which can function to guide the damaged axons as they regrow. The autograft may also contain many of the neurotrophic factors and adhesion molecules needed by axons to regenerate. There are drawbacks to this approach however, particularly for the patient, who would require an additional surgery, as well as the loss of sensory nerve function, scarring and the potential for neuroma formation at the donor site (Johnson et al., 2013). Additionally, at the implant site there may be scarring and fibrosis, as well as a size discrepancy between the donor and recipient nerve which could contribute to poor regeneration. Moreover, even if the autograft is successfully implanted, only 40% of patients will regain functionality in the damaged tissue (Scheib and Hoke, 2013).

Because of these issues, alternative methods of nerve repair are being investigated, and used in pre-clinical trials, including the implantation of artificial nerve conduits at the injury site (Gao et al., 2015, Georgiou et al., 2015, Bell and Haycock, 2012). Multiple studies have shown the effectiveness of nerve conduits in treating peripheral nerve injury (Johnson et al., 2013, Hobson et al., 2000, Gao et al., 2015). The development of such technologies is potentially of great patient benefit if the conduits were able to perform as well as, or better than, an autograft (Campbell and Meyer, 2006, Costigan et al., 2009, Houschyar et al., 2016). Current commercially available products for clinical use include nerve wraps and nerve guides, and there have been many pre-clinical trials investigating constructs which

use transplanted cells such as stem cells or Schwann cells and their precursors (Bhangra et al., 2016, Grinsell and Keating, 2014).

Many of the conduits which have been developed often use an extracellular matrix gel to provide physical support for the re-growing axons. Extracellular matrix proteins such as laminin and fibronectin are conducive for nerve regeneration, and therefore the addition of these proteins to a nerve conduit provides an environment that better promotes axonal growth. It is also important to assess the stiffness of the gel as well as the matrix net which is formed, as this can also affect the ability of cells to migrate efficiently (Liu et al., 2015). Previous experiments from our lab have shown that Schwann cells are able to migrate well within a fibrin gel matrix when in contact with a blood vessel scaffold (Cattin et al., 2015). The fibrin gels that we used consisted of low density fibrinogen and could support blood vessel formation and Schwann cell migration, which hints at the suitability of this system for use in a nerve conduit (Nakatsu et al., 2003). The finding that blood vessels are required for efficient Schwann cell migration also implies that it is likely to be important for artificial nerve conduits to be able to support vascularisation.

The inclusion of the macrophage-derived factor CCL3 in an artificial nerve conduit therefore has the potential to increase Schwann cell migration, and thus promote efficient nerve regeneration. To test whether CCL3 could improve nerve regeneration across an artificial conduit we collaborated with Dr James Phillips who has extensive experience working with artificial nerve conduits to repair peripheral nerve injury which have been previously described (Georgiou et al., 2015) and shown in a schematic in Figure 5.6A. Using a nerve conduit consisting of a silicone tube filled with fibrin gel to repair a sciatic nerve transection, we wanted to test whether the addition of CCL3 in the conduit increased Schwann cell migration and therefore promote nerve regeneration.

In the first instance, we conducted a trial experiment to test whether we could observe Schwann cell migration into the conduit. For the preliminary experiment, we implanted a 10mm long silicone tube containing fibrin gel including 500ng/ml VEGF. To make the fibrin gel, we used a low density of fibrinogen (2.9mg/ml) as our previous *in vitro* experiments had demonstrated that this concentration successfully supported blood vessel outgrowth and Schwann cell migration (Cattin et al., 2015). Following complete nerve transection the silicone tube was attached to the nerve by a single suture at the proximal and distal stumps (Dr James Phillips conducted the surgery). The animal was then allowed to recover, and the repaired nerve was harvested at Day 6 following surgery (Figure 5.7B). The nerve

was then fixed in PFA (at this point the silicone tubing was removed) and prepared for cryosectioning as previously described. The nerve was cut into thick (50μm) sections and immunostained to detect Schwann cells (S100), blood vessels (lectin) and axons (neurofilament). The nerve was imaged using confocal microscopy and merged to create a composite image and the migration of Schwann cells (longitudinal distance and staining area) was quantified using ImageJ.

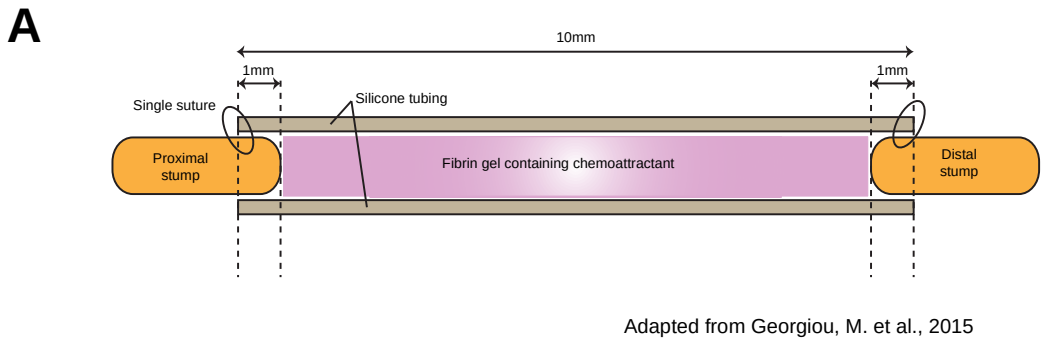

Figure 5.7 | Artificial nerve conduit repair following injury
A. Schematic of artificial nerve conduit used and method of implantation. B. Representative image of sciatic nerve after harvesting on Day 7 with the silicone tube still attached (left panel) and after removal (right panel). Scale bar = 1mm.

In this preliminary experiment, we observed that there was almost no Schwann cell migration into the conduit, and poor vascularisation of the conduit (Figure 5.8). Under normal regeneration conditions we would expect to see blood vessels migrating into the bridge at Day 2, and Schwann cells migrating into the bridge after this. This experiment showed us that compared to a naturally forming nerve bridge, the artificial conduit was inefficient at promoting nerve regeneration, as migration of all cell types was delayed. In view of this, we decided to increase the length of time the conduit was implanted, and also to shorten the tube length to assess whether detectable regeneration occurred normally but in a delayed manner.

In the second experiment, the length of tube was reduced to 8mm, and the time the tube was left in situ before harvesting was increased to 7 days. The tubes were filled with fibrin gel containing 500ng/ml VEGF only or a combination of 500ng/ml VEGF and 50μg/ml CCL3. In this experiment, we decided to use the same concentration of CCL3 that was used in the injection experiments in which we had seen a slight trend for an increase in Schwann cell migration. The tubes were blinded and implanted at random into 8 adult rats so that there were 4 animals for each condition. The tubes were attached to the nerve by a single suture at the proximal and distal stumps, and the repaired nerve was harvested at Day 7 (Figure 5.9) (James Phillips conducted the surgery). The nerves were then fixed in PFA and processed to quantify cell migration as before.

In this second experiment, we observed greater cell migration of blood vessels and Schwann cells into the nerve conduit in both conditions at Day 7 following injury (Figure 5.9 and quantified in Figure 5.10), however this was still less than what we would expect in a ‘normal’ regenerating nerve.

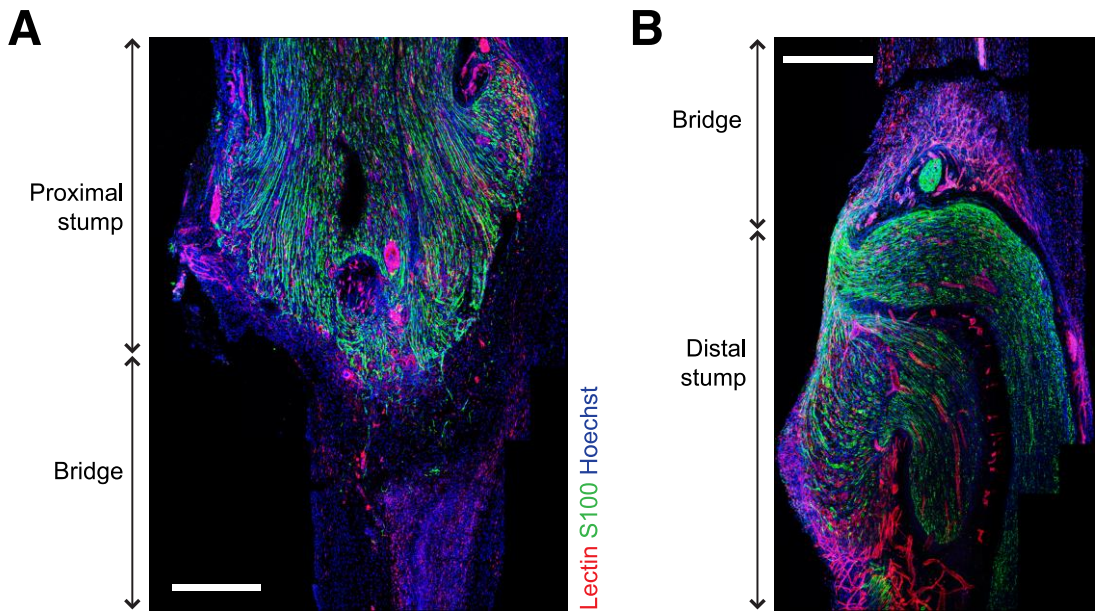

Figure 5.8 Preliminary experiment showed lack of Schwann cell migration into the nerve conduit Representative reconstructed confocal images of the proximal (A) and distal (B) stump of repaired sciatic nerves harvested on Day 6 following injury. Nerves were immunostained to detect Schwann cells (S100, green), blood vessels (lectin, red) and nuclei counterstained with Hoechst (blue). The bridge and proximal and distal stumps are indicated by arrows. Scale bar = 500μm. n=1.

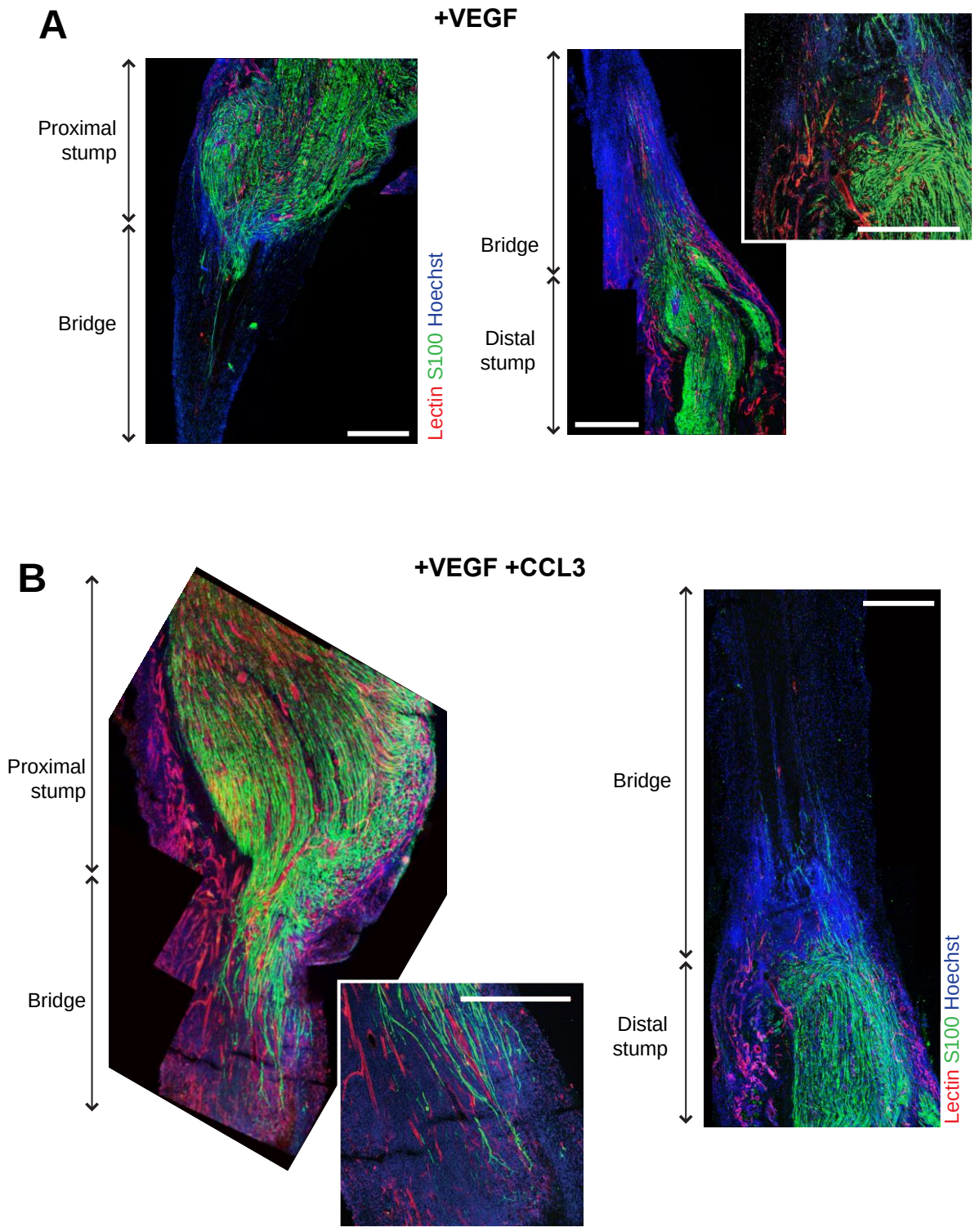

Figure 5.9 | Schwann cell migration appears limited by the poor vascularisation of the bridge
Representative reconstructed confocal images of nerve stumps from rats implanted with artificial nerve conduits containing 500ng/ml VEGF only (A) or 500ng/ml VEGF and 50μg/ml rCCL3 (B) and harvested on Day 7 following injury. Nerves were immunostained to detect Schwann cells (S100, green), blood vessels (lectin, red) and nuclei counterstained with Hoechst (blue). The bridge and proximal and distal stumps are indicated by arrows. Inset images show higher magnification of leading Schwann cell migration edge. Scale bars = 500μm. n=1 (4 animals per experimental condition).

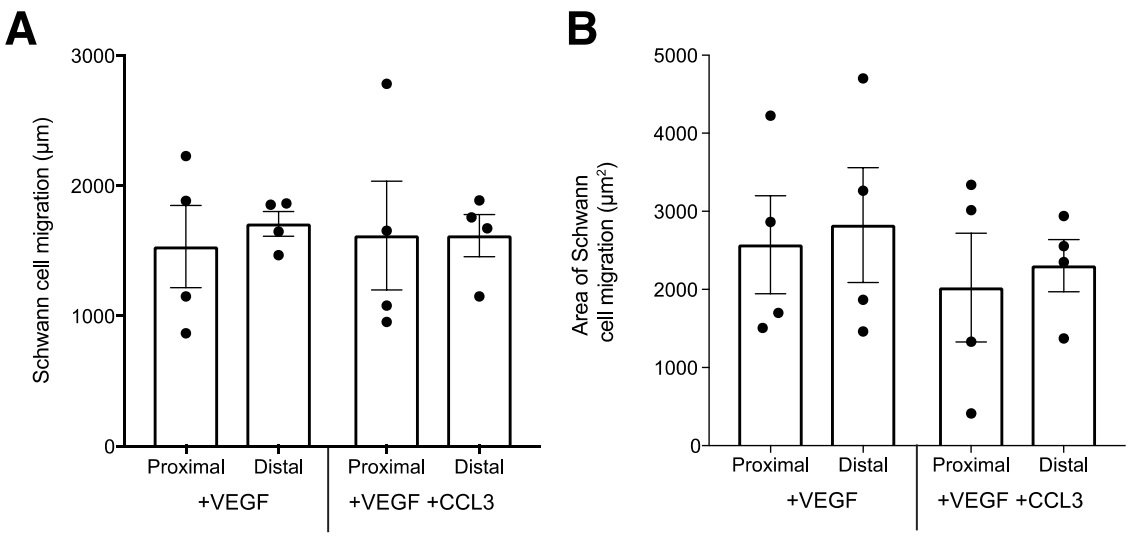

Figure 5.10 | In preliminary experiments, addition of CCL3 does not affect Schwann cell migration within nerve conduits

A. Quantification of the distance (μm) migrated by Schwann cells following nerve injury and subsequently implanted with artificial nerve conduits containing 500ng/ml VEGF only or 500ng/ml VEGF and 50μg/ml rCCL3. Data expressed as total distance travelled into bridge from tip of stump (n=1, graph shows mean of 4 animals ±SD). B. Quantification of area of positive Schwann cell staining (μm^2). Data expressed as total area of positive Schwann cell staining in the bridge (n=1, graph shows mean of 4 animals ±SD).

Quantification of Schwann cell migration into the tubes showed that there was no significant difference between the distance migrated in the presence or absence of CCL3 conditions. We did however observe that blood vessels and Schwann cells were migrating into the nerve conduit to the same extent, which is in contrast to what is observed in a 'normally' repaired nerve where blood vessels enter the bridge prior to Schwann cells. Blood vessel entry into the conduit therefore appeared to be limiting the extent of Schwann cell migration., and due to the poor vascularisation in the nerve conduit compared to what is normally observed. As the vascularisation of the conduit was poor, it was difficult to interpret whether CCL3 was having an effect on Schwann cell migration. To assess any effect of CCL3 on Schwann cell migration, it would therefore be important to improve vascularisation within the conduit.

To work towards improving the vascularisation of the nerve conduit, we tested whether the addition of VEGF in our system was acting to increase blood vessel formation as has been previously reported (Cattin et al., 2015). To do this, we tested whether VEGF stimulated vascularisation by testing conduits in the presence or absence of 500ng/ml VEGF (the same concentration used in the previous experiment). We then analysed migration into the conduits to determine whether at this concentration (Lucie Van Emmenis conducted the surgery). As an additional negative control in this experiment, we used an empty silicone tube (containing no fibrin gel) which has been reported to not support nerve regeneration (Grinsell and Keating, 2014). The tubes were attached to the nerve by a single suture at the proximal and distal stumps, and the repaired nerve was harvested at Day 7 and processed to quantify cell migration as before.

Analysis of each of the different conduit conditions showed that the vascularisation of the conduits was still poor, and showed a delay in comparison to normal nerve regeneration. The vascularisation of the conduits still appeared to be a limiting factor for Schwann cell migration as Schwann cells migrated to the front of the invading blood vessels (Figure 5.11). In the empty tube control, the least Schwann cell migration was observed (Figure 5.11A and quantified in 5.12). Despite the poor vascularisation, we did observe a slight increase in Schwann cell migration in the presence of VEGF (Figure 5.11B and C and quantified in 5.12), however this increase was not significant.

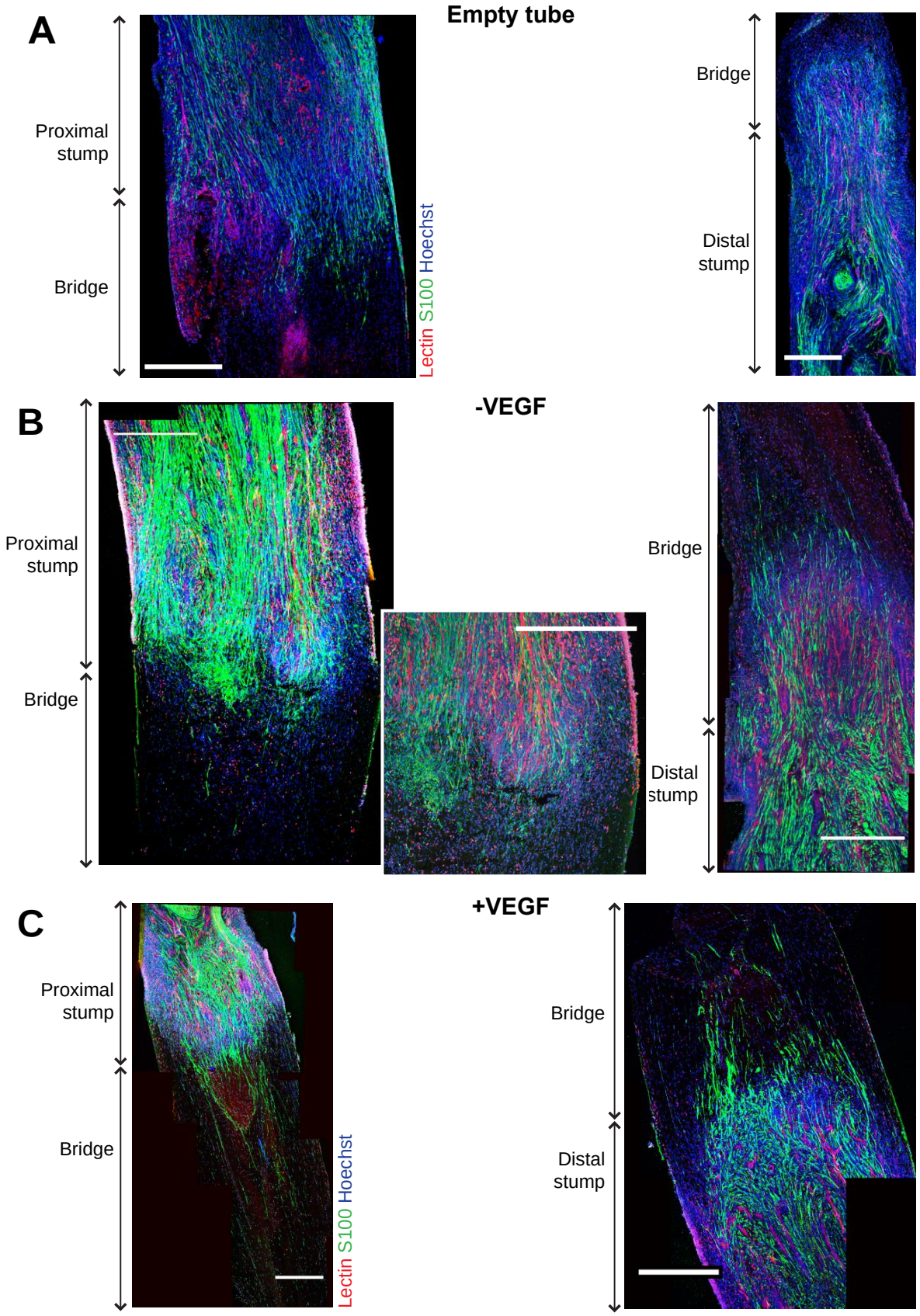

Figure 5.11 | Schwann cell migration is limited by poor vascularisation
(Legend continues overleaf.)

Figure 5.11 | Schwann cell migration is limited by poor vascularisation (contd)
Representative reconstructed confocal images of nerve stumps from rats implanted with artificial nerve conduits which were empty (A), filled with fibrin gel containing no VEGF (B) or fibrin gel containing 500ng/ml VEGF (B) and harvested on Day 7 following injury. Nerves immunostained to detect Schwann cells (S100, green), blood vessels (lectin, red) and nuclei counterstained with Hoechst (blue). The bridge and proximal and distal stumps are indicated by arrows. Inset image shows a higher magnification of the leading Schwann cells. Scale bar = 500μm. n=1.

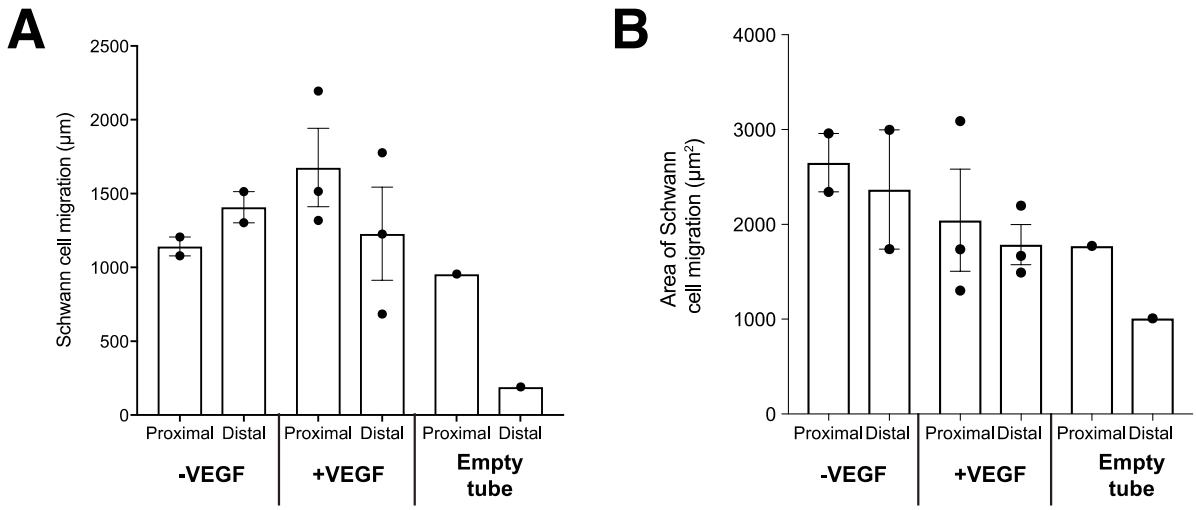

Figure 5.12 | VEGF causes a trend for an increase in Schwann cell migration
A. Quantification of the distance migrated by Schwann cells (μm) following nerve injury and subsequent implantation of artificial conduits which were empty, filled with fibrin gel -/+ 500ng/ml VEGF and harvested on Day 7. Data expressed as total distance travelled into bridge from tip of stump (n=1, graph shows mean of technical replicates ±SD). B. Quantification of area migrated by Schwann cells (μm^2) following nerve injury and subsequent implanted with artificial nerve conduits. Data expressed as total area of positive Schwann cell staining in the bridge (n=1, graph shows mean of indicated number of animals ±SD).

These results highlighted the necessity for efficient vascularisation to ensure Schwann cell migration into the conduit. Moreover, they show that our conduit conditions are not optimal to support and promote blood vessel growth. In the future, it would be advisable to conduct a larger study to test a more effective means of delivering VEGF and perhaps a modification of the other constituents of the conduit.

5.4. Chapter discussion and conclusion

Peripheral nerve injury has a high incidence and currently, few treatment options are available (Grinsell and Keating, 2014). As Schwann cells are crucial for guiding regrowing axons, the identification of a Schwann cell chemoattractant has wide therapeutic implications. We previously identified CCL3 as a factor capable of promoting Schwann cell migration *in vitro*, and in this chapter we performed preliminary experiments to address the role that CCL3 plays following nerve injury *in vivo*, as well as its potential use in promoting nerve regeneration within an artificial nerve conduit.

These experiments attempted to determine the role of CCL3 in nerve regeneration by disturbing the physiological gradient of CCL3 in the nerve bridge, and creating an additional, stronger gradient of CCL3 in the nerve stumps. By injecting CCL3 into the distal stump we hypothesised that we would create an additional gradient of CCL3 which would be sensed by the Schwann cells and thereby inhibit their migration into the nerve bridge. In our experiments, following injection of CCL3 into the distal stump, we observed instead a trend for an increase in Schwann cell migration into the bridge from both the proximal and distal stumps. This result was not significant and so must be repeated, but it suggests that CCL3 increased Schwann cell migration. It is likely that the method of microinjecting into the nerve may not be the most robust method of delivering CCL3 to the regenerating nerve due to the substance possibly diffusing away from the injection site. The injection of substances also does not provide sustained release which is likely to be necessary to induce Schwann cell migration. In future experiments, it may be advisable to use alternative delivery methods such as osmotic pumps or the implantation of cells over-expressing CCL3 to the injury site, which would allow us to control variables such as concentration and the duration of chemoattractant delivery. Additionally, it may be beneficial to establish the diffusion coefficients as well as the *in vivo* half-life of CCL3 in order to develop efficient methods of delivery of CCL3 to tissues.

One of the major issues that we had with these injection experiments was the variability in the length of the bridge, which formed following sciatic nerve surgery. In future experiments, to attempt to counter this issue it may be better to perform a half-cut surgery leaving a fascicle intact thereby providing a physical support to the cut nerve, which should reduce the level of variability of bridge lengths between animals. This approach has been used successfully by our lab in previous experiments and provides a robust method for causing a more consistent nerve injury (Parrinello et al., 2010).

The experiments shown here investigated the overexpression of CCL3 and how this affects nerve regeneration. In future experiments, we would explore how inhibition of endogenous CCL3 affects Schwann cell migration and nerve regeneration. To do this we would use a CCL3 knockout mouse, and/or administer pharmacological CCL3 receptor inhibitors. These experiments may allow a more systematic assessment of the role CCL3 plays in aiding Schwann cell migration following injury and determine the potential of a pharmacological approach for the treatment of aberrant regeneration, such as in neuromas.

Following injury, under normal conditions, the bridge is vascularised rapidly (Day 2 in rats) which facilitates the oxygenation of the new tissue, delivery of nutrients, as well as providing a physical support for migrating Schwann cells. In the artificial nerve conduits used in these studies, the formation of blood vessels was slow, and full vascularisation of the conduit was not observed, even on Day 7 post-surgery. We observed that within the artificial nerve conduits, and consistent with our previous findings (Cattin et al., 2015), that Schwann cells migrated along blood vessels, however we found that incomplete vascularisation of the conduit limited Schwann cell migration as the Schwann cells did not migrate beyond the vasculature. This shows that in this scenario, Schwann cell migration is limited by the vascularisation process. This made it impossible to determine any effect of CCL3 on Schwann cell migration. To test whether CCL3 might be useful therapeutically, it is therefore essential to first improve the vascularisation or provide a surface that mimics the blood vessels.

To improve blood vessel formation within nerve conduits, the addition of VEGF into nerve conduits has previously been investigated (Hobson et al., 2000, Pola et al., 2004), and in each case, increased vascularisation resulted in improved nerve regeneration. Previous work showed that a silicone chamber containing Matrigel and VEGF implanted into a damaged nerve following injury was beneficial for nerve regeneration, due to the enhanced formation of blood vessels (Hobson et al., 2000). It was also recently found that promoting macrophage polarisation to a ‘pro-healing’ phenotype using

IL-4, caused an increase in Schwann cell recruitment, as well as improving axonal regrowth (Mokarram et al., 2012). Moreover, when a nerve conduit was embedded with a chemoattractant which specifically recruits pro-healing macrophages, fractalkine, nerve regeneration was vastly improved compared to conduits containing a control factor (Mokarram et al., 2017). This suggested that by biasing the immune microenvironment towards a healing response, a healing cascade of Schwann cell and axonal regrowth could occur. Furthermore, if circulating macrophages are depleted by clondronate injection, a significant decrease in axon regrowth is observed (Mokarram et al., 2017), highlighting the importance of macrophages in nerve regeneration. This is consistent with data from our lab which has identified that macrophages are critical for vascularisation of the bridge (Cattin et al., 2015), as well as a potential role in inducing Schwann cell migration. Together, this suggests the therapeutic potential of including macrophages, or perhaps more specifically, macrophage-released factors, in nerve conduits.

It is clear from our preliminary experiments, as well as the literature, that vascularisation within nerve conduits must be improved, prior to investigating the role of CCL3 on Schwann cell migration. In the future, to optimise rapid and efficient vascularistion within nerve conduits, we will improve VEGF delivery methods and alter the matrix composition within the conduit, by varying the levels of fibrin as well as testing combinations of fibrin and fibronectin to determine optimal conditions for blood vessel outgrowth. With these experiments, the aim would be to replicate the normal nerve environment and therefore promote physiological nerve regeneration processes to occur.

As well as oxygenating the conduit and providing nutrients, the physical properties of blood vessels are necessary for Schwann cell migration. As discussed in the introduction, the discontinuous surface of blood vessels appear to be important for cords of Schwann cells to migrate along (Cattin et al., 2015). It may be preferable therefore to replicate these physiological conditions in a nerve conduit to promote Schwann cell migration. There have been huge advances in microfabrication and 3D-printing techniques in recent years and this has had a beneficial impact on the bioengineering of nerve conduits. Both techniques allow for the custom design of biologically relevant structures using relatively inexpensive equipment (Hsu et al., 2009, Johnson et al., 2015, Hu et al., 2016). The ability to combine 3D printing of a biologically similar nerve construct, with the implantation of neurotrophic factors is particularly interesting as it has the potential to create a more physiological nerve conduit (Johnson et al., 2015). The challenge now is to find polymers which are structurally suitable for use in these conduits.

Chapter Six: Discussion and Conclusion

6.1. Macrophage function

Macrophages are important for the health and proper functioning of all body tissues (Varol et al., 2015). As more is discovered about their roles in homeostasis and in disease, it is becoming clear that there are complex processes which govern their origin, turnover and function (Das et al., 2015, Mass et al., 2016, Soucie et al., 2016, Scott et al., 2016, O'Koren et al., 2016, Guilliams and Scott, 2017). Many different tissues contain specialised populations of resident macrophages (Davies et al., 2013, Epelman et al., 2014, Ginhoux and Guilliams, 2016), and the PNS is no exception. Here, macrophages make up approximately a tenth of the cell population; however the functions of this population during health and disease remain poorly understood.

Many tissues such as the brain and the liver have well characterised resident macrophage populations, known as microglia and Kupffer cells respectively. The origin of these resident macrophages has been determined through the use of fate mapping studies (Ginhoux et al., 2010, Ginhoux and Guilliams, 2016), and the functions which the macrophages carry out to maintain tissue homeostasis and following disease have been well described (Scott et al., 2016, Hong and Stevens, 2016, O'Koren et al., 2016). In the work presented here, we have shown, following preliminary experiments, that there appear to be two distinct resident macrophages within the PNS which can be distinguished by physiological location, as well as CX_3CR1 expression. Additionally, preliminary analysis to compare nerve resident macrophages with other tissue populations showed they have a distinct transcriptional profile, which may reflect the differences in origin and/or function of the populations. It is still unclear however what role(s) the resident macrophages within the PNS carry out under normal conditions. Moreover, following injury we have observed that there is only minimal proliferation of resident macrophages which become outnumbered following the entry of monocyte-derived cells. Therefore, it is not clear whether, or how, this relatively minor population contributes to the regenerative process in the distal stump, or indeed how the resident population behaves following injury.

As well as providing information on resident macrophages in the PNS, our experiments showed that following injury the vast majority of cells in the bridge and the distal stump were monocyte-derived, which confirmed our previous findings (Cattin et al., 2015). Further contributing to this exciting and

dynamic field of research, we have found novel roles for macrophages in the process of nerve regeneration both in stimulating blood vessel formation (Cattin et al., 2015), as well as promoting directional Schwann cell migration through the release of VEGF and CCL3 respectively. We also determined that macrophages within the nerve bridge exhibit an intrinsic differential response to the hypoxic environment, which enabled them to carry out this crucial function in nerve regeneration. The macrophage cell line J774A.1 also displayed this characteristic which strongly implied that this is a property which is common to all macrophages. Macrophages have previously been observed to adapt their phenotype and function in response to hypoxia (Lin and Simon, 2016) and so to possess a differential response to hypoxia fits with the current literature.

Macrophages are a key cell type which have crucial roles in maintaining tissue homeostasis, as well as contributing towards the initiation and resolution of inflammation. It is therefore important that the resident population of macrophages in the peripheral nerve is characterised further to understand the roles that they play during health and disease, as this may lead to the ability to target and manipulate these populations for therapeutic benefit. In particular, as the extent of macrophage involvement in facilitating nerve regeneration is realised, the ability to modulate macrophage phenotype (Mokarram et al., 2017) or to mimic the conditions of a normally regenerating nerve are becoming attractive subjects for further investigation.

6.2. PNS macrophage characterisation

Other tissues have macrophage populations, which are often specialised morphologically and functionally in order to carry out tissue specific roles. Within the healthy nerve, it is unclear what that role may be. In the brain, it is clear that the microglia have important roles not only in scanning for and clearing debris (Hong and Stevens, 2016), but also in maintaining tissue integrity (Frost and Schafer, 2016) and even pruning synapses (Hong et al., 2016, Tremblay et al., 2010). Because of these well characterised resident populations, we might assume that macrophages in the normal nerve function to scan the environment for pathogens (Rosenberg et al., 2012), as well as contributing towards the integrity of the homeostatic tissue. Additionally, based on the role of microglia, we might speculate that macrophages in the nerve play a role in maintaining axonal health and ensuring correct axonal growth during development and following injury.

One important unanswered question concerning macrophages in the nerve centres around the origin of this tissue population. It is important to characterise the origin of this population as the tools to determine this may lead to defining other macrophage variables such as how the cells turnover, and whether they require input from monocyte populations, as well as how the resident population behaves following injury. Whilst the origin of this resident population may not necessarily contribute towards the specific macrophage phenotype (the nerve tissue environment is more likely to influence many macrophage characteristics), this knowledge will enable us to establish additional mouse models to allow us to further characterise the understudied PNS macrophage population.

Within the PNS, we found that there appears to be two distinct populations of resident macrophages which are defined by their physiological location in the nerve and CX_3CR1 expression, which was also hinted at by the flow cytometry data which identified monocyte-derived cells as well as a mixed population of mature macrophages. This difference in CX_3CR1 gene expression suggests different homeostatic roles for these macrophages in the normal nerve, related to their location. Macrophages are a highly plastic cell type, and this is due in large part to their tissue environment, with resident tissue populations distinguishable by their gene expression profiles (Lavin et al., 2014, Mass et al., 2016). The different tissue environments, or 'niches', of the endoneurium or the perineurium therefore may contribute to the specific phenotype and function of the distinct resident macrophage populations found here. We have observed different expression of CX_3CR1, and it is likely that the two populations also display different transcriptional profiles related to their function.

PNS macrophages may be similar to microglia, the resident macrophage population in the nerve, which originate solely from the yolk sac and do not have contributions from circulating monocytes to maintain populations (Hong and Stevens, 2016, O'Koren et al., 2016), or they may be similar to other tissue populations which have dual embryonic origins and require contributions from monocytes to maintain numbers (Ginhoux and Jung, 2014). We have shown using the CX_3CR1^{GFP} mouse that resident macrophages within the endoneurium constitutively express CX_3CR1, indicating that similar to microglia, this population of macrophages is likely established prenatally by yolk-sac progenitors, are long lived and able to self-renew, and constitutively express CX_3CR1 (Jung et al., 2000, Yona et al., 2013). In contrast, the resident macrophage population within the epineurium have lost CX_3CR1 expression indicating that this population is unlike microglia, and perhaps more similar to macrophage populations in the lung or spleen. It would be desirable therefore to conduct a full transcriptomic analysis

of these two distinct populations, using the CX_3CR1^{GFP} mouse to allow us to sort these two subsets of cells.

We have also explored the role of macrophages following injury, however in the studies presented in this thesis we have only studied the role of macrophages in the early stages of nerve repair. Questions remain about what happens to the recruited macrophages following injury resolution, if and how they are cleared from the nerve, or whether the recruited cells remain in the nerve long term and differentiate into functional resident macrophages. Such studies could be completed with the use of fate mapping and lineage tracing analysis, as well as RNA-seq analysis, to build up a detailed overview of what is occurring. How these recruited cells behave post-injury may also indicate how resident nerve macrophages self-maintain as well as further characterising this understudied macrophage population.

6.3. PNS regeneration

Regeneration in the PNS is a complex and multicellular process which requires the coordination of multiple processes in order to achieve successful injury resolution (Boilly et al., 2017, Fawcett and Keynes, 1990, Fex Svennigsen and Dahlin, 2013, Jessen and Mirsky, 2016, Napoli et al., 2012, Cattin and Lloyd, 2016). Macrophages are key players in the nerve regeneration process and have multiple important roles in discrete regions of the regenerating nerve (Rosenberg et al., 2012, Ydens et al., 2012, Niemi et al., 2013, Chen et al., 2015, Zhan et al., 2015). Recently, we have identified a novel role for macrophages in nerve regeneration, selectively sensing hypoxia and causing the release of VEGF to promote vascularisation (Cattin et al., 2015). This a crucial process which facilitates Schwann cell migration and subsequent axonal regrowth across the injury site.

6.3.1. Distal stump

Macrophages in the distal stump are thought to be recruited through the release of Schwann cell-derived CCL2 (Jessen and Mirsky, 2016). Here, macrophages carry out a predominantly phagocytic role and assist Schwann cells with clearing myelin debris, and remodelling the environment to permit axonal regrowth (Kang and Lichtman, 2013, Klein and Martini, 2016). We have shown that following injury, the majority of macrophages within the distal stump are monocyte-derived and exhibit temporal changes in phenotype following injury. There appears to be a minimal contribution from resident

macrophages, as determined by flow cytometry and CCR2 expression, however it is likely they have a role. To address this, we could make use of the $CX_3CR1^{YFP-CreER/wt}$:$R26^{RFP}$ mouse (O'Koren et al., 2016) which, following a pulse dose of tamoxifen and a subsequent wash out period, would result in monocytes and monocyte-derived cells being YFP^+, resident macrophages inside the fascicles being RFP+ and resident macrophages surrounding the endoneurium being YFP^-. By immunofluorescent staining and/or flow cytometry it should be possible to confirm the contribution of resident macrophages and also analyse macrophages from both inside and outside the BNB. By staining it should also be possible to determine whether resident macrophages within the distal stump have a phagocytic role, as during this process macrophages take on a characteristic 'foamy' appearance.

Following injury resolution, it is unclear what happens to the large number of recruited macrophages to the region. In previous studies in alternative injury models in different tissues, infiltrating macrophages have been observed to modulate their phenotype to mimic the established resident population (Scott et al., 2016). However, in the case of the brain, infiltrating monocyte-derived cells do not fully assimilate and instead leave the brain following resolution, leaving the microglia population to repopulate the tissue (O'Koren et al., 2016). We have found that within the nerve there are two populations of resident macrophages, as determined by their CX_3CR1 expression and physiological location. It would therefore be interesting to see how these discrete populations recover following injury, whether the recruited monocyte-derived cells are distinguishable from nerve resident macrophages, and whether there are differences between the CX_3CR1^+/ CX_3CR1^- nerve populations. To do this we would again use the $CX_3CR1^{YFP-CreER/wt}$:$R26^{RFP}$ mouse, which would allow us to distinguish between the two resident populations, as well as the infiltrating monocytes. Following injury, we could then conduct a time course of up to 6 months to analyse how the macrophage populations behave. It would also be desirable to conduct an RNA-seq on the resident macrophages prior to injury, and then at various points during recovery to see how the expression profile of the different populations change and adapt during regeneration. This analysis would also allow us to determine whether the PNS resident macrophage population behave more like microglia or macrophages from other tissues.

6.3.2. Formation of a nerve bridge is essential to ensure successful nerve regeneration

One challenge during nerve regeneration is how to initiate directional cell migration and growth in mature, quiescent tissues when there is a lack of directionality signals. In contrast, during

development there is an abundance of attractive and repulsive signals which guide migrating cells and facilitate the formation of multiple tissues (Frost and Schafer, 2016, Scarpa and Mayor, 2016, Theveneau et al., 2010). Within the nerve bridge, we have found that chemotactic signals are released to facilitate cell migration and promote regeneration. We have previously determined a role for macrophages in inducing blood vessel formation in the bridge through the release of hypoxia-induced VEGF (Cattin et al., 2015).

In addition, work presented here has found a further novel role for macrophages in promoting Schwann cell migration, through the release of CCL3. This chemokine has previously been described as a macrophage chemoattractant (Perrin et al., 2005, Taskinen and Röyttä, 2000) and we have observed that CCL3 is upregulated within the monocyte-derived macrophage population in the bridge compared to the distal stump, creating a gradient which may induce Schwann cell migration. *In vitro* chemotaxis assays have confirmed the ability of CCL3 to induce directional Schwann cell migration, which provides compelling evidence for this factor playing a role in regeneration. To test the role of CCL3 in the future, it will be necessary to use a CCL3 knockout mouse or pharmacological inhibitors of CCR1 and CCR5 to determine the effect that blocking CCL3 signalling has on Schwann cell migration and nerve regeneration. Additionally, we could test alternative delivery methods for CCL3 to test whether this factor is able to promote Schwann cell migration following injury and improve regeneration outcomes.

6.3.3.Key factors to ensure fast and successful regeneration outcomes

Despite the remarkable ability of the PNS to regenerate following injury, this process does not always work perfectly, and multiple factors such as time, length of nerve defect and age can negatively affect the regenerative process (Grinsell and Keating, 2014, Kang and Lichtman, 2013). In particular in humans, these factors will influence the success of normal nerve repair, as well as affecting the efficiency of artificial conduits or nerve transplants to restore nerve function (Rodrigues et al., 2012, Scheib and Hoke, 2013, Houschyar et al., 2016).

The longer that a distal stump and target tissue are denervated, the less likely it is that repair will be successful, as Schwann cells become less able to support axonal regrowth (Grinsell and Keating, 2014, Boilly et al., 2017). Furthermore, severed axons must traverse the newly formed bridge tissue. In mammals, a ‘critical nerve gap’ length is defined as a distance over which no recovery can occur without

assistance from a nerve graft or artificial bridging structure (Daly et al., 2012). In rats this length is ~1.5cm and in humans ~4cm (Grinsell and Keating, 2014). It is therefore important that any therapeutic strategies are able to assist nerve regeneration across these larger distances to ensure maximal patient benefit. Also as mammals age, the clearance of myelin is delayed, and upon contact with remaining debris, axonal growth is stunted and regeneration is delayed (Kang and Lichtman, 2013). In adults, nerve injury is also more likely to result in neuropathic pain compared to younger animals (Fitzgerald and McKelvey, 2016).

Despite these difficulties however, regeneration in the PNS is possible and function can be restored. Our findings have contributed to the vast field of nerve regeneration, and the identification of a Schwann cell migratory factor could help to overcome some of the complications which impede nerve recovery, as Schwann cell migration is crucial for axonal regrowth in bridge structures. We have conducted preliminary experiments investigating the role of CCL3 *in vivo*, however issues with the delivery meant that the impact of CCL3 was difficult to interpret. To overcome this problem, it would be advisable to use alternative methods. For example, using the CCL3 knockout mouse, the rates of Schwann cell migration and nerve regeneration could be compared to controls over a time course to determine the effect of CCL3. Alternatively, slow release osmotic pumps could be used which would allow the sustained delivery of CCL3 to the injured nerve and potentially promote faster nerve regeneration. We also tested CCL3 in an artificial conduit model of nerve repair, however difficulties with conduit vascularisation meant it was difficult to determine the effect of CCL3 on nerve growth. Out strategies for improving this model of nerve repair will be discussed in subsequent sections.

6.3.4. Other tissue regeneration mechanisms

The PNS is not the only tissue in the adult which is able to regenerate, regeneration has been observed in mammalian digit tips (Han et al., 2008, Johnston et al., 2016), and it is well documented that the liver (Taub, 2004, Riehle et al., 2011) and the endometrium (Evans et al., 2016) are able to naturally regenerate. The ability of digit tips to regenerate is particularly remarkable due to the multiple tissues which must be coordinated to form the bone, skin, muscle and nail components. Additionally, within the digit tip, it has recently been determined that there is a specific requirement for Schwann cells within this process to support successful tissue regeneration (Johnston et al., 2016). Other animals also exhibit regeneration on a larger scale; amphibians such as newts are able to regenerate entire

appendages. This is possible following the formation of a blastema, which is an area of progenitor cells adjacent to the wound site that promotes limb growth (Kumar and Brockes, 2012). This is similar to human PNS and digit regeneration, where Schwann cell migration is key for this process (Johnston et al., 2016, Kumar et al., 2007, Kumar and Brockes, 2012). Importantly, following amputation, damage to local nerves leads to the dedifferentiation of associated Schwann cells (similar to what is observed following PNS transection) and crucially, these Schwann cells migrate towards the injury site and promote the expansion of mesenchymal precursors to facilitate tissue regeneration (Johnston et al., 2013, Johnston et al., 2016).

In our model of nerve injury we have determined that CCL3 is able to induce Schwann cell migration. It is not clear however in the digit model of regeneration whether there is a specific Schwann cell chemoattractant which is able to induce migration. It is conceivable however, that due to the injury and associated inflammatory response, CCL3 is present and aids the directional migration of Schwann cells. It would therefore be interesting in the future to investigate whether CCL3 is present in the digit tip, and whether CCL3 would be able to promote the wound healing and regenerative function of dedifferentiated Schwann cells within this situation.

6.4. The clinical implications of identifying a chemotactic factor for Schwann cells

In order for cells to collectively migrate during development or in regeneration or tissue formation, there is often a known chemokine which directs migration and ensures efficient migration towards a defined location (Trepat et al., 2012, Mayor and Etienne-Manneville, 2016, Scarpa and Mayor, 2016). In our *in vivo* model of migration we determined that for Schwann cells to migrate into the bridge, blood vessels were required to provide structural support (Cattin et al., 2015). It was less clear at that point whether there was an additional chemotactic factor present in the bridge which was able to promote Schwann cell migration. However given the reliance of collective cell migration on a guiding signal, it was likely that Schwann cells were responding to a molecular cue. *In vitro* work presented here has shown strong evidence for macrophage induced CCL3 in promoting directional Schwann cell migration. This is a novel role for macrophages in nerve regeneration, as a specific Schwann cell chemoattractant in nerve regeneration has not previously been described. The absolute requirement of CCL3 to induce Schwann cell migration following injury remains to be determined. In the future, we could model Schwann cell behaviour and how it responds to the gradient of CCL3 in the

bridge, as we gather more information on CCL3, for example cellular source(s), duration of release, as well as diffusion coefficients. Although further work must be carried out to fully characterise the role of CCL3 in nerve regeneration, these preliminary results are interesting and have the possibility to be employed in many different therapeutic settings.

Millions of people suffer from nerve injuries every year, and the current treatment options are often ineffective (Johnson et al., 2013, Scheib and Hoke, 2013). The current gold standard for repair is the use of an autograft, however there has been growing interest and research into the use of artificial nerve conduits to bridge nerve gaps and to aid regeneration (Johnson et al., 2013, Scheib and Hoke, 2013, Houschyar et al., 2016). Artificial conduits often fail because of the poor efficiency of the regeneration process through the environment of these structures (Houschyar et al., 2016). In contrast, the regrowth of axons across naturally occurring nerve bridges of similar length is more efficient. We therefore reasoned that the current design of conduits could be improved by mimicking the aspects of the physiological nerve bridge that promote the regenerative process.

In the first instance, due to our findings (Cattin et al., 2015) as well as the work presented in this thesis, we believe that the formation of a polarised vasculature, together with a gradient of CCL3 could be a promising strategy to promote nerve regeneration. Our *in vivo* studies have shown that the nerve bridge is mostly composed of fibrin and fibronectin, and therefore the artificial conduit should replicate the *in vivo* environment, particularly when molecular mediators of nerve regeneration (e.g. VEGF and CCL3) are added. To enable us to determine the therapeutic use of CCL3 in nerve conduits therefore, the nerve conduit must be efficiently vascularised in order to support Schwann cell migration.

As a second approach to mimic the nerve environment within an artificial nerve conduit, the use of microfabrication could enable the production of structures which are similar to those found in the regenerating nerve, i.e. blood vessels, which are crucial to allow regeneration to occur (Cattin et al., 2015). The use of micropatterning and 3D printing in a therapeutic setting, to aid tissue regeneration and provide tissue scaffolds is currently being explored by a number of groups (Johnson et al., 2015, Hu et al., 2016, Wu and Hsu, 2015, Hsu et al., 2009). To aid nerve regeneration, it would be desirable to replicate the discontinuous surface of blood vessels which we have previously shown are necessary for the amoeboid-like migration of Schwann cells (Cattin et al., 2015). Using micropatterning techniques it may be possible to create tubes of 3-20μm in diameter to mimic the surface of the blood vessels. We would coat these tubes with matrix components in the presence or absence of CCL3 and test first *in*

vitro and then *in vivo* whether they can support efficient Schwann cell migration and act as a viable therapeutic aid. Similar types of tethered tubes have been previously used to study epithelial cell migration (Yevick et al., 2015) which suggests that within the context of the regenerating nerve this technique may also be suitable.

More recently, conduits using living cells have been investigated in pre-clinical trials. Stem cells have been extensively tested due to their abilities to both self-renew and to differentiate into multiple cell lineages (Ren et al., 2012, Bell and Haycock, 2012, Bhangra et al., 2016). In particular, the differentiation of adipose stem cells into a Schwann cell-like phenotype and subsequent alignment in a stabilised collagen gel has proved successful in promoting neurite extension and regeneration in critical sized gaps *in vivo* (Georgiou et al., 2015, Hu et al., 2016, Wang et al., 2017). Schwann cells, Schwann cell precursors or Schwann cell-like cells are also being trialled for use in nerve conduits *in vivo*, however there is still a lot more work to be done before these treatments would reach a clinical setting (Wang et al., 2017, Rodrigues et al., 2012). Cell based therapies are not often brought to clinical trials due to rejection issues and the ability to source autologous cells for use in the scaffold. Moreover, our previous findings (Cattin et al., 2015), as well as the work presented here suggests that artificial nerve conduits may be more successful when physiological repair mechanisms and the nerve environment are mimicked, in order to stimulate a more 'normal' regeneration response. Additionally, for practical reasons, it would be preferable to have a readily available or 'off the shelf' nerve conduit which wouldn't need critical storage conditions and could be used therapeutically in all patients without the need to extract tissue or cells. Further investigation into the alternative nerve conduits presented here may therefore help to facilitate and promote efficient nerve repair following injury, and provide significant patient benefit.

6.5. Neuroma formation and neuropathic pain relies on the nerve microenvironment and chemokine signalling

Following nerve injury, successful recovery and resolution is not always possible, and subsequently, aberrant nerve regeneration can occur which can lead to the formation of neuromas and a severe pain response (Scholz and Woolf, 2007, Campbell and Meyer, 2006, Costigan et al., 2009). Neuropathic pain can be characterised by a burning, raw or stabbing sensation and hypersensitivity to light touch, which originates from a nervous tissue lesion (White et al., 2009, Campbell and Meyer,

2006). There are many different methods for the treatment of neuropathic pain such as electrical stimulation, massage and surgery which may involve redirecting the proximal nerve or even capping the nerve ends to prevent further pain transmission (Costigan et al., 2009).

Macrophages and the nerve microenvironment have been implicated in the development of neuroma and neuropathic pain (Abbadie et al., 2003, Scholz and Woolf, 2007, White et al., 2009). CCL3 has previously been reported to mediate neuropathic pain in models of PNS injury (Kiguchi et al., 2010), however the association between CCL3 and Schwann cell migration was not explored.

To prevent aberrant nerve growth and neuropathic pain following injury therefore, we hypothesise that by inhibiting the migration of Schwann cells, which guide the regrowing axons, we may see a therapeutic effect. We have found that Schwann cell migration can be directed by CCL3, and therefore could be prevented by the inhibition of CCL3 signalling. We could investigate this using a number of different approaches. Initially, using the CCL3 knockout mouse and causing nerve injury we could analyse the pain response of these animals to see whether a decrease is observed. As an additional method, we could use pharmacological inhibitors of the receptors for CCL3, CCR1 and CCR5, following injury to attempt to curtail aberrant migration. We could trial both systemic, as well as targeted inhibitor delivery to see whether this has an effect on aberrant nerve growth. The effect on neuropathic pain, as well as functional recovery could be determined to see whether CCL3 is able to successfully block neuropathic pain.

6.6. Cancer

The processes involved in nerve repair and tumourigenesis have many similarities. They involve the complex coordination of multiple cell types to make a new tissue, and upregulate multiple cytokines and chemokines to promote cell migration, matrix formation and the remodelling of the local environment (Amit et al., 2016, Cole et al., 2015, Murdoch et al., 2008, Bunimovich et al., 2017).

6.6.1. Microenvironment remodelling to promote migration and growth

Tissue regeneration in the nerve or digit tip, and tumour formation are some of the few examples of the ability to form new tissue within adult mammals. Within new tissue, the specific microenvironment is influential in ensuring either injury resolution or tumourigenesis.

Macrophages play important roles, both within tissue regeneration and tumourigenesis. The hypoxic environment of tumours has previously been shown to affect the function of tumour associated macrophages (TAMs) and is associated with poor prognosis (Henze and Mazzone, 2016, Laoui et al., 2014). The accumulation of TAMs in areas of hypoxia is also being exploited as a mechanism to treat some cancer types (Muthana et al., 2011). Following nerve injury, monocyte-derived macrophages accumulate in both the bridge and the distal stump (Cattin et al., 2015, Rosenberg et al., 2012), and similarly, macrophages accumulate at the sites of tumours (Roussos et al., 2011). We have also observed that macrophages in distinct areas of the regenerating nerve have specific functions, and this may also be the case in tumours. In particular, neurofibromas in NF1 patients are known to contain large populations of macrophages (Prada et al., 2013). A recent study showed that macrophages within the neurofibromas are distinct from those in the circulation which indicates that the tumour microenvironment alters the phenotype and function of these TAMs (Choi et al., 2017). Paracrine, chemokine and cytokine loops were also identified between the macrophage and Schwann cell populations within the tumours, which suggests that the mechanisms of interactions between these cell types may be similar to those observed following nerve injury. In addition, this highlights the similarities between tissue regeneration and tumourigenesis.

6.6.2. Tumour innervation

Tumour innervation has currently only been described for a few cancer types, but it is likely to be important in many more types of tumour. There is evidence to suggest that Schwann cells may play a role in mechanisms relating to cancer such as tumour innervation (Boilly et al., 2017, Deborde and Wong, 2017) as well as shaping the tumour microenvironment (Bunimovich et al., 2017). Schwann cells have been observed to closely associate with tumour cells in some *in vivo* models as well as being located in early prostate tumour lesions suggesting a role in early tumour development (Ayala et al., 2001, Magnon et al., 2013). Interactions between Schwann cells and tumour cells during early stages of tumourigenesis may provide tumours with access to nerves and therefore lead to additional influences on the tumour microenvironment as well as contributing towards tumour innervation (Amit et al., 2016). In pancreatic cancer, Schwann cell invasion has been observed to occur prior to nerve innervation which heavily hints at their role in this process (Deborde et al., 2016, Demir et al., 2014). It has been observed that in the adult, mature Schwann cells can dissociate from axons, dedifferentiate

into a progenitor phenotype and regain the ability to migrate following injury. Perhaps by a similar mechanism, and possibly as a result of the inflammation caused when tumour cells invade into a tissue, Schwann cells from nerves adjacent to a tumour site may dissociate and migrate toward the injury site and proliferate (Demir et al., 2014, Ayala et al., 2008). Due to the known role Schwann cells have in guiding axonal regrowth following injury, it is possible that Schwann cells also contribute to the migration and directionality of nerves towards tumours.

In *in vitro* experiments, Schwann cells, colon and glioblastoma cancer cells, as well as non-malignant cell types fibroblasts and pancreatic stellate cells were co-cultured, and Schwann cell migration towards the different cell types was analysed (Demir et al., 2014). Schwann cells were observed to preferentially migrate towards the cancer cells compared to the benign cells, which suggests that Schwann cells are attracted to cancer cells. The proposed model was that nerve-independent Schwann cells migrate towards precursor cancer cells through the NGF-p75NTR signalling axis, which then induces nerve innervation of the tumour (Demir et al., 2014). It is not currently known whether there is an additional chemoattractant in the nerve bridge which is able to induce Schwann cell migration, however due to the similarities between regeneration and tumourigenesis, it is possible that there is a common factor present in both conditions which may promote migration, and that CCL3 is a good potential candidate.

Although nerve innervation has recently been described in prostate, colorectal, pancreatic and head and neck cancers, there is still little known about the clinical relevance of this process. In pre-clinical tumour models, the alteration of nervous connectivity to tumours has proven to be effective at reducing tumour progression and spread (Cole et al., 2015, Magnon et al., 2013). Due to the clinical severity associated with tumours which exhibit innervation, there may be great patient benefit from investigating the significance of preventing innervation as a therapeutic tool. The neurobiology of cancer is an emerging field and there is still much to be discovered about this process and its clinical effects.

The tumour microenvironment contains a huge chemokine network which contributes towards chemotaxis, which aids cell:cell communication within the tumour microenvironment, angiogenesis, immune evasion as well as the invasion and dissemination of tumour cells (Roussos et al., 2011, Cole et al., 2015, Murdoch et al., 2008). As previously stated, macrophages and tumours have a well described relationship, and in patients with pancreatic ductal adeno carcinoma, high levels of infiltration by macrophages, T cells and mast cells into nerves is observed (Cavel et al., 2012). In light of the work

presented in this thesis, we might ask whether these inflammatory cells contribute to PNI by recruiting Schwann cells. As we have found in nerve regeneration, there may be a macrophage induced signal (CCL3?) which can induce Schwann cell migration.

The mechanism of tumour spread via the nerves, known as perineural invasion (PNI) is not well characterised, and this process needs more investigation to fully elucidate the role that macrophages play in PNI and tumour spread. Elucidating the mechanism by which Schwann cells migrate along blood vessels is important not only to increase our understanding of regeneration within the PNS but also to see how this mechanism of migration may be relevant to tumour cells. This highlights the impact of identifying a chemoattractant, or chemoattractants, for Schwann cells, as the therapeutic implications are wide ranging. Characterising this process may therefore help to understand how these tumours metastasise and could ultimately lead to therapeutic agents which may halt the metastatic process.

Tumour invasion into the nerve sheath also resembles a damaged or dying nerve by causing a nerve injury which may promote the inflammatory response which is normally associated with nerve injury and regeneration (Amit et al., 2016). It is possible therefore that the same critical growth and proliferation signals which are important in nerve regeneration are also crucial for PNI and tumour dissemination, especially as reciprocal signalling between tumour cells and nerves has been observed (Amit et al., 2016).

6.6.3. Injury resolution and consequences of failure to resolve

In every case of regeneration or tissue formation, there must be resolution. When we talk about resolution in a tissue, this involves many different processes; inflammation must cease, the tissue must be remodelled and normal function must be resumed (Forbes and Rosenthal, 2014). To achieve this, many different cell types and mechanisms must be employed and coordinated to result in a fully functioning tissue. Failure to resolve following injury can lead to pathologies such as aberrant nerve growth, leading to the formation or neuromas as well as neuropathic pain which has negative patient outcomes (Costigan et al., 2009). In the case of the endometrium, failure to remodel following regeneration may lead to infertility and endometriosis (Evans et al., 2016). The ability to repair and regenerate this tissue in a ‘scar-free’ manner is particularly relevant to the study of wound healing, and parallels could be drawn between this process and other forms of regeneration.

The process of tissue and tumour formation are similar in many ways. A new tissue is formed which is comprised of multiple different cell types, there is an upregulation of genes relating to chemokine release, vascularisation, cell migration and matrix formation as well as innervation (Cole et al., 2015, Jin et al., 2008, Murdoch et al., 2008, Qian and Pollard, 2010, Roussos et al., 2011). We have observed in PNS injury that for successful regeneration to occur, blood vessels are formed in direct response to hypoxia, which is initiated by macrophages (Cattin et al., 2015). Similarly, tumours exhibit hypoxia, and here too, TAMs induce the formation of blood vessels to ensure oxygenation and nutrient delivery to the tumours (Roussos et al., 2011, Semenza, 2012, Henze and Mazzone, 2016).

One of the major differences between these two processes however is the lack of resolution. Tumours contain high numbers of inflammatory mediators (Qian and Pollard, 2010, Mantovani et al., 2017), and some tumours resemble unrepaired wounds (i.e. NF1 tumours) (Parrinello and Lloyd, 2009). Without resolution, tumours remain a disorganised, chaotic mass of cells and matrix, and networks of vasculature and nerves. This is in stark contrast to what happens following nerve injury, initially the newly formed nerve bridge is also an unorganised structure with no directionality cues or signals, however as regeneration progresses, order emerges from this structure as blood vessels form, matrix is deposited and polarised axons are lead back to their targets by Schwann cells (Cattin and Lloyd, 2016). To treat tumours therefore it may be desirable to promote the 'resolution' of tumour tissue to promote healing and a return to normal tissue function, which could be achieved by targeting aspects of the tumour microenvironment such as macrophage populations (Mantovani et al., 2017).

6.7. Closing remarks

We have identified a novel, macrophage-secreted Schwann cell chemokine, CCL3, which may have important roles in nerve regeneration. Further characterisation of the macrophages which initiate and mediate PNS regeneration, as well as the role of CCL3 in promoting Schwann cell migration, has wide ranging therapeutic potential. Future work should aim to determine the therapeutic use of CCL3 for both improving nerve regeneration following injury and as a potential target to inhibit the aberrant regenerative process associated with pain. The completion of crucial *in vivo* experiments should determine the clinical potential of CCL3 and serve as groundwork for future studies to improve the treatment of multiple disorders.

References

ABBADIE, C., LINDIA, J. A., CUMISKEY, A. M., PETERSON, L. B., MUDGETT, J. S., BAYNE, E. K., DEMARTINO, J. A., MACINTYRE, D. E. & FORREST, M. J. 2003. Impaired neuropathic pain responses in mice lacking the chemokine receptor CCR2. *Proceedings of the National Academy of Sciences,* 100**,** 7947-7952.

ADAMEYKO, I., LALLEMEND, F., AQUINO, J. B., PEREIRA, J. A., TOPILKO, P., MÜLLER, T., FRITZ, N., BELJAJEVA, A., MOCHII, M., LISTE, I., USOSKIN, D., SUTER, U., BIRCHMEIER, C. & ERNFORS, P. 2009. Schwann Cell Precursors from Nerve Innervation Are a Cellular Origin of Melanocytes in Skin. *Cell,* 139**,** 366-379.

AFSHARI, F. T., KWOK, J. C., WHITE, L. & FAWCETT, J. W. 2010. Schwann cell migration is integrin-dependent and inhibited by astrocyte-produced aggrecan. *Glia,* 58**,** 857-869.

AJAMI, B., BENNETT, J. L., KRIEGER, C., MCNAGNY, K. M. & ROSSI, F. M. V. 2011. Infiltrating monocytes trigger EAE progression, but do not contribute to the resident microglia pool. *Nat Neurosci,* 14**,** 1142-1149.

AMIT, M., NA'ARA, S. & GIL, Z. 2016. Mechanisms of cancer dissemination along nerves. *Nat Rev Cancer,* 16**,** 399-408.

ARMATI, P. J. & MATHEY, E. K. 2013. An update on Schwann cell biology — Immunomodulation, neural regulation and other surprises. *Journal of the Neurological Sciences,* 333**,** 68-72.

ARTHUR-FARRAJ, P. J. 2012. c-Jun reprograms Schwann cells of injured nerves to generate a repair cell essential for regeneration. *Neuron,* 75**,** 633-647.

AYALA, G. E., DAI, H., POWELL, M., LI, R., DING, Y., WHEELER, T. M., SHINE, D., KADMON, D., THOMPSON, T., MILES, B. J., ITTMANN, M. M. & ROWLEY, D. 2008. Cancer-Related Axonogenesis and Neurogenesis in Prostate Cancer. *Clinical Cancer Research,* 14**,** 7593.

AYALA, G. E., WHEELER, T. M., SHINE, H. D., SCHMELZ, M., FROLOV, A., CHAKRABORTY, S. & ROWLEY, D. 2001. In vitro dorsal root ganglia and human prostate cell line interaction: Redefining perineural invasion in prostate cancer. *The Prostate,* 49**,** 213-223.

BAETS, J., DE JONGHE, P. & TIMMERMAN, V. 2014. Recent advances in Charcot–Marie–Tooth disease. *Current Opinion in Neurology,* 27.

BAIN, C. C., BRAVO-BLAS, A., SCOTT, C. L., GOMEZ PERDIGUERO, E., GEISSMANN, F., HENRI, S., MALISSEN, B., OSBORNE, L. C., ARTIS, D. & MOWAT, A. M. 2014. Constant replenishment from circulating monocytes maintains the macrophage pool in the intestine of adult mice. *Nat Immunol,* 15**,** 929-937.

BAIN, C. C., HAWLEY, C. A., GARNER, H., SCOTT, C. L., SCHRIDDE, A., STEERS, N. J., MACK, M., JOSHI, A., GUILLIAMS, M., MOWAT, A. M. I., GEISSMANN, F. & JENKINS, S. J. 2016. Long-lived self-renewing bone marrow-derived macrophages displace embryo-derived cells to inhabit adult serous cavities. *Nature Communications,* 7**,** ncomms11852.

BARNETT, M. W. & LARKMAN, P. M. 2007. The action potential. *Practical Neurology,* 7**,** 192.

BARRETTE, B., NAVE, K. A. & EDGAR, J. M. 2013. Molecular triggers of neuroinflammation in mouse models of demyelinating diseases. *Biol Chem,* 394**,** 1571-81.

BARTON, M. J., JOHN, J. S., CLARKE, M., WRIGHT, A. & EKBERG, J. 2017. The Glia Response after Peripheral Nerve Injury: A Comparison between Schwann Cells and Olfactory Ensheathing Cells and Their Uses for Neural Regenerative Therapies. *Int J Mol Sci,* 18.

BELL, J. H. & HAYCOCK, J. W. 2012. Next generation nerve guides: materials, fabrication, growth factors, and cell delivery. *Tissue Eng. Part B Rev.,* 18**,** 116-128.

BERGERT, M., ERZBERGER, A., DESAI, R. A., ASPALTER, I. M., OATES, A. C., CHARRAS, G., SALBREUX, G. & PALUCH, E. K. 2015. Force transmission during adhesion-independent migration. *Nat Cell Biol,* 17**,** 524-9.

BHANGOO, S. K., REN, D., MILLER, R. J., CHAN, D. M., RIPSCH, M. S., WEISS, C., MCGINNIS, C. & WHITE, F. A. 2007. CXCR4 chemokine receptor signaling mediates pain hypersensitivity in association with antiretroviral toxic neuropathy. *Brain, behavior, and immunity,* 21**,** 581-591.

BHANGRA, K. S., BUSUTTIL, F., PHILLIPS, J. B. & RAHIM, A. A. 2016. Using Stem Cells to Grow Artificial Tissue for Peripheral Nerve Repair. *Stem Cells International,* 2016**,** 18.

BHATHEJA, K. & FIELD, J. 2006. Schwann cells: Origins and role in axonal maintenance and regeneration. *The International Journal of Biochemistry & Cell Biology,* 38**,** 1995-1999.

BOERBOOM, A., DION, V., CHARIOT, A. & FRANZEN, R. 2017. Molecular Mechanisms Involved in Schwann Cell Plasticity. *Frontiers in Molecular Neuroscience,* 10**,** 38.

BOILLY, B., FAULKNER, S., JOBLING, P. & HONDERMARCK, H. 2017. Nerve Dependence: From Regeneration to Cancer. *Cancer Cell,* 31**,** 342-354.

BOLLAG, G., CLAPP, D. W., SHIH, S., ADLER, F., ZHANG, Y. Y., THOMPSON, P., LANGE, B. J., FREEDMAN, M. H., MCCORMICK, F., JACKS, T. & SHANNON, K. 1996. Loss of NF1 results in activation of the Ras signaling pathway and leads to aberrant growth in haematopoietic cells. *Nat Genet,* 12**,** 144-8.

BONNER, J. T. 1947. Evidence for the formation of cell aggregates by chemotaxis in the development of the slime mold Dictyostelium discoideum. *J Exp Zool,* 106**,** 1-26.

BORING, L., GOSLING, J., CHENSUE, S. W., KUNKEL, S. L., FARESE, R. V., BROXMEYER, H. E. & CHARO, I. F. 1997. Impaired monocyte migration and reduced type 1 (Th1) cytokine responses in C-C chemokine receptor 2 knockout mice. *Journal of Clinical Investigation,* 100**,** 2552-2561.

BOVETTI, S., HSIEH, Y. C., BOVOLIN, P., PERROTEAU, I., KAZUNORI, T. & PUCHE, A. C. 2007. Blood vessels form a scaffold for neuroblast migration in the adult olfactory bulb. *J Neurosci,* 27**,** 5976-80.

BOYDEN, S. 1962. THE CHEMOTACTIC EFFECT OF MIXTURES OF ANTIBODY AND ANTIGEN ON POLYMORPHONUCLEAR LEUCOCYTES. *The Journal of Experimental Medicine,* 115**,** 453-466.

BUNIMOVICH, Y. L., KESKINOV, A. A., SHURIN, G. V. & SHURIN, M. R. 2017. Schwann cells: a new player in the tumor microenvironment. *Cancer Immunology, Immunotherapy,* 66**,** 959-968.

BURKE, B., GIANNOUDIS, A., CORKE, K. P., GILL, D., WELLS, M., ZIEGLER-HEITBROCK, L. & LEWIS, C. E. 2003. Hypoxia-Induced Gene Expression in Human Macrophages: Implications for Ischemic Tissues and Hypoxia-Regulated Gene Therapy. *The American Journal of Pathology,* 163**,** 1233-1243.

CAI, Z., JITKAEW, S., ZHAO, J., CHIANG, H.-C., CHOKSI, S., LIU, J., WARD, Y., WU, L.-G. & LIU, Z.-G. 2014. Plasma membrane translocation of trimerized MLKL protein is required for TNF-induced necroptosis. *Nat Cell Biol,* 16**,** 55-65.

CAMPBELL, J. N. & MEYER, R. A. 2006. Mechanisms of Neuropathic Pain. *Neuron,* 52**,** 77-92.

CATALA, M. & KUBIS, N. 2013. Gross anatomy and development of the peripheral nervous system. *Handbook of Clinical Neurology,* 115**,** 29-41.

CATTIN, A.-L., BURDEN, JEMIMA J., VAN EMMENIS, L., MACKENZIE, FRANCESCA E., HOVING, JULIAN J. A., GARCIA CALAVIA, N., GUO, Y., MCLAUGHLIN, M., ROSENBERG, LAURA H., QUEREDA, V., JAMECNA, D., NAPOLI, I., PARRINELLO, S., ENVER, T., RUHRBERG, C. & LLOYD, ALISON C. 2015. Macrophage-Induced Blood Vessels Guide Schwann Cell-Mediated Regeneration of Peripheral Nerves. *Cell,* 162**,** 1127-1139.

CATTIN, A.-L. & LLOYD, A. C. 2016. The multicellular complexity of peripheral nerve regeneration. *Current Opinion in Neurobiology,* 39**,** 38-46.

CAUX, C., RAMOS, R. N., PRENDERGAST, G. C., BENDRISS-VERMARE, N. & MÉNÉTRIER-CAUX, C. 2016. A Milestone Review on How Macrophages Affect Tumor Growth. *Cancer Research,* 76**,** 6439.

CAVEL, O., SHOMRON, O., SHABTAY, A., VITAL, J., TREJO-LEIDER, L., WEIZMAN, N., KRELIN, Y., FONG, Y., WONG, R. J., AMIT, M. & GIL, Z. 2012. Endoneurial Macrophages Induce Perineural Invasion of Pancreatic Cancer Cells by Secretion of GDNF and Activation of RET Tyrosine Kinase Receptor. *Cancer Research,* 72**,** 5733.

CHARRAS, G. & SAHAI, E. 2014. Physical influences of the extracellular environment on cell migration. *Nat Rev Mol Cell Biol,* 15**,** 813-824.

CHAWLA, A. 2010. Control of macrophage activation and function by PPARs. *Circulation research,* 106**,** 1559-1569.

CHEN, P., PIAO, X. & BONALDO, P. 2015. Role of macrophages in Wallerian degeneration and axonal regeneration after peripheral nerve injury. *Acta Neuropathologica,* 130**,** 605-618.

CHEN, Z. L., YU, W. M. & STRICKLAND, S. 2007. Peripheral regeneration. *Annu. Rev. Neurosci.,* 30**,** 209-233.

CHO, N.-H., SEONG, S.-Y., HUH, M.-S., HAN, T.-H., KOH, Y.-S., CHOI, M.-S. & KIM, I.-S. 2000. Expression of Chemokine Genes in Murine Macrophages Infected with Orientia tsutsugamushi. *Infection and Immunity,* 68**,** 594-602.

CHOI, K., KOMUROV, K., FLETCHER, J. S., JOUSMA, E., CANCELAS, J. A., WU, J. & RATNER, N. 2017. An inflammatory gene signature distinguishes neurofibroma Schwann cells and macrophages from cells in the normal peripheral nervous system. *Scientific Reports,* 7**,** 43315.

CITTERA, E., LEIDI, M., BURACCHI, C., PASQUALINI, F., SOZZANI, S., VECCHI, A., WATERFIELD, J. D., INTRONA, M. & GOLAY, J. 2007. The CCL3 Family of Chemokines and Innate Immunity Cooperate In Vivo in the Eradication of an Established Lymphoma Xenograft by Rituximab. *The Journal of Immunology,* 178**,** 6616.

CLARK, A. G. & VIGNJEVIC, D. M. 2015. Modes of cancer cell invasion and the role of the microenvironment. *Current Opinion in Cell Biology,* 36**,** 13-22.

COLE, S. W., NAGARAJA, A. S., LUTGENDORF, S. K., GREEN, P. A. & SOOD, A. K. 2015. Sympathetic nervous system regulation of the tumour microenvironment. *Nat Rev Cancer,* 15**,** 563-572.

COOK, D. N., BECK, M. A., COFFMAN, T. M., KIRBY, S. L., SHERIDAN, J. F., PRAGNELL, I. B. & SMITHIES, O. 1995. Requirement of MIP-1 alpha for an inflammatory response to viral infection. *Science,* 269**,** 1583.

COPP, A. J., GREENE, N. D. E. & MURDOCH, J. N. 2003. The genetic basis of mammalian neurulation. *Nat Rev Genet,* 4**,** 784-793.

COSTIGAN, M., SCHOLZ, J. & WOOLF, C. J. 2009. Neuropathic Pain: A Maladaptive Response of the Nervous System to Damage. *Annual Review of Neuroscience,* 32**,** 1-32.

CRUVEILHEIR, J. 1835. *Maladies Des Nerfs Anatomie Pathologique Du Corps Humain* . Paris, France, JB Bailliere.

CUDDAPAH, V. A., ROBEL, S., WATKINS, S. & SONTHEIMER, H. 2014. A neurocentric perspective on glioma invasion. *Nat Rev Neurosci,* 15**,** 455-465.

DALY, W., YAO, L., ZEUGOLIS, D., WINDEBANK, A. & PANDIT, A. 2012. A biomaterials approach to peripheral nerve regeneration: bridging the peripheral nerve gap and enhancing functional recovery. *Journal of the Royal Society Interface,* 9**,** 202-221.

DAS, A., SINHA, M., DATTA, S., ABAS, M., CHAFFEE, S., SEN, C. K. & ROY, S. 2015. Monocyte and Macrophage Plasticity in Tissue Repair and Regeneration. *The American Journal of Pathology,* 185**,** 2596-2606.

DAVATELIS G, T.-O. P., WOLPE S D, HERMSEN K, LUEDKE C, GALLEGOS C, COIT D, MERRYWEATHER J, CERAMI A 1988. Cloning and characterization of a cDNA for murine macrophage inflammatory protein (MIP), a novel monokine with inflammatory and chemokinetic properties [published erratum appears in J Exp Med 1989 Dec 1;170(6):2189]. *The Journal of Experimental Medicine,* 167**,** 1939-1944.

DAVIES, L. C., JENKINS, S. J., ALLEN, J. E. & TAYLOR, P. R. 2013. Tissue-resident macrophages. *Nature immunology,* 14**,** 986-995.

DAVIES, L. C., ROSAS, M., SMITH, P. J., FRASER, D. J., JONES, S. A. & TAYLOR, P. R. 2011. A quantifiable proliferative burst of tissue macrophages restores homeostatic macrophage populations after acute inflammation. *European Journal of Immunology,* 41**,** 2155-2164.

DAVIES, L. C. & TAYLOR, P. R. 2015. Tissue-resident macrophages: then and now. *Immunology,* 144**,** 541-548.

DEBORDE, S., OMELCHENKO, T., LYUBCHIK, A., ZHOU, Y., HE, S., MCNAMARA, W. F., CHERNICHENKO, N., LEE, S.-Y., BARAJAS, F., CHEN, C.-H., BAKST, R. L., VAKIANI, E., HE, S., HALL, A. & WONG, R. J. 2016. Schwann cells induce cancer cell dispersion and invasion. *The Journal of Clinical Investigation,* 126**,** 1538-1554.

DEBORDE, S. & WONG, R. J. 2017. How Schwann cells facilitate cancer progression in nerves. *Cellular and Molecular Life Sciences*.

DEMIR, I. E., BOLDIS, A., PFITZINGER, P. L., TELLER, S., BRUNNER, E., KLOSE, N., KEHL, T., MAAK, M., LESINA, M., LASCHINGER, M., JANSSEN, K.-P., ALGÜL, H., FRIESS, H. & CEYHAN, G. O. 2014. Investigation of Schwann Cells at Neoplastic Cell Sites Before the Onset of Cancer Invasion. *JNCI: Journal of the National Cancer Institute,* 106**,** dju184-dju184.

DEMIR, I. E., KUJUNDZIC, K., PFITZINGER, P. L., SARICAOGLU, Ö. C., TELLER, S., KEHL, T., REYES, C. M., ERTL, L. S., MIAO, Z., SCHALL, T. J., TIEFTRUNK, E., HALLER, B., DIAKOPOULOS, K. N., KURKOWSKI, M. U., LESINA, M., KRÜGER, A., ALGÜL, H., FRIESS, H. & CEYHAN, G. O. 2017. Early pancreatic cancer lesions suppress pain through CXCL12-mediated chemoattraction of Schwann cells. *Proceedings of the National Academy of Sciences,* 114**,** E85-E94.

DOLENC, V. & JANKO, M. 1976. Nerve regeneration following primary repair. *Acta Neurochir.,* 34**,** 223-234.

EPELMAN, S., LAVINE, K. J. & RANDOLPH, G. J. 2014. Origin and Functions of Tissue Macrophages. *Immunity,* 41**,** 21-35.

EVANS, J., SALAMONSEN, L. A., WINSHIP, A., MENKHORST, E., NIE, G., GARGETT, C. E. & DIMITRIADIS, E. 2016. Fertile ground: human endometrial programming and lessons in health and disease. *Nat Rev Endocrinol,* 12**,** 654-667.

FAWCETT, J. W. & KEYNES, R. J. 1990. Peripheral nerve regeneration. *Annu Rev Neurosci,* 13**,** 43-60.

FELDMAN, E. L., NAVE, K.-A., JENSEN, T. S. & BENNETT, D. L. H. 2017. New Horizons in Diabetic Neuropathy: Mechanisms, Bioenergetics, and Pain. *Neuron,* 93**,** 1296-1313.

FELTRI, L. M., POITELON, Y. & PREVITALI STEFANO, C. 2016. How Schwann Cells Sort Axons: New Concepts. *The Neuroscientist : a review journal bringing neurobiology, neurology and psychiatry,* 22**,** 252-265.

FEX SVENNIGSEN, Å. & DAHLIN, L. B. 2013. Repair of the Peripheral Nerve—Remyelination that Works. *Brain Sciences,* 3**,** 1182-1197.

FINZSCH, M., SCHREINER, S., KICHKO, T., REEH, P., TAMM, E. R., BÖSL, M. R., MEIJER, D. & WEGNER, M. 2010. Sox10 is required for Schwann cell identity and progression beyond the immature Schwann cell stage. *The Journal of Cell Biology,* 189**,** 701-712.

FITZGERALD, M. & MCKELVEY, R. 2016. Nerve injury and neuropathic pain - A question of age. *Exp Neurol,* 275 Pt 2**,** 296-302.

FONTANA, X., HRISTOVA, M., DA COSTA, C., PATODIA, S., THEI, L., MAKWANA, M., SPENCER-DENE, B., LATOUCHE, M., MIRSKY, R., JESSEN, K. R., KLEIN, R., RAIVICH, G. & BEHRENS, A. 2012. c-Jun in Schwann cells promotes axonal regeneration and motoneuron survival via paracrine signaling. *The Journal of Cell Biology,* 198**,** 127-141.

FORBES, S. J. & ROSENTHAL, N. 2014. Preparing the ground for tissue regeneration: from mechanism to therapy. *Nat Med,* 20**,** 857-869.

FRANCO, R. & FERNÁNDEZ-SUÁREZ, D. 2015. Alternatively activated microglia and macrophages in the central nervous system. *Progress in Neurobiology,* 131**,** 65-86.

FRICKER, F. R., ZHU, N., TSANTOULAS, C., ABRAHAMSEN, B., NASSAR, M. A., THAKUR, M., GARRATT, A. N., BIRCHMEIER, C., MCMAHON, S. B., WOOD, J. N. & BENNETT, D. L. 2009. Sensory axon-derived neuregulin-1 is required for axoglial signaling and normal sensory function but not for long-term axon maintenance. *J Neurosci,* 29**,** 7667-78.

FRIEDL, P. & WOLF, K. 2010. Plasticity of cell migration: a multiscale tuning model. *The Journal of Cell Biology,* 188**,** 11-19.

FROST, J. L. & SCHAFER, D. P. 2016. Microglia: Architects of the Developing Nervous System. *Trends in Cell Biology,* 26**,** 587-597.

FU, S. Y. & GORDON, T. 1995. Contributing factors to poor functional recovery after delayed nerve repair: prolonged axotomy. *J. Neurosci.,* 15**,** 3876-3885.

GAO, Y., WANG, Y.-L., KONG, D., QU, B., SU, X.-J., LI, H. & PI, H.-Y. 2015. Nerve autografts and tissue-engineered materials for the repair of peripheral nerve injuries: a 5-year bibliometric analysis. *Neural Regeneration Research,* 10**,** 1003-1008.

GAUTIER, E. L., SHAY, T., MILLER, J., GRETER, M., JAKUBZICK, C., IVANOV, S., HELFT, J., CHOW, A., ELPEK, K. G., GORDONOV, S., MAZLOOM, A. R., MA'AYAN, A., CHUA, W.-J., HANSEN, T. H., TURLEY, S. J., MERAD, M., RANDOLPH, G. J. & THE IMMUNOLOGICAL GENOME, C. 2012. Gene expression profiles and transcriptional regulatory pathways underlying mouse tissue macrophage identity and diversity. *Nature immunology,* 13**,** 1118-1128.

GEIGER, B., SPATZ, J. P. & BERSHADSKY, A. D. 2009. Environmental sensing through focal adhesions. *Nat Rev Mol Cell Biol,* 10**,** 21-33.

GEORGIOU, M., GOLDING, J. P., LOUGHLIN, A. J., KINGHAM, P. J. & PHILLIPS, J. B. 2015. Engineered neural tissue with aligned, differentiated adipose-derived stem cells promotes peripheral nerve regeneration across a critical sized defect in rat sciatic nerve. *Biomaterials,* 37**,** 242-251.

GEUNA, S. 2015. The sciatic nerve injury model in pre-clinical research. *Journal of Neuroscience Methods,* 243**,** 39-46.

GINHOUX, F., GRETER, M., LEBOEUF, M., NANDI, S., SEE, P., GOKHAN, S., MEHLER, M. F., CONWAY, S. J., NG, L. G., STANLEY, E. R., SAMOKHVALOV, I. M. & MERAD, M. 2010. Fate Mapping Analysis Reveals That Adult Microglia Derive from Primitive Macrophages. *Science (New York, N.Y.),* 330**,** 841-845.

GINHOUX, F. & GUILLIAMS, M. 2016. Tissue-Resident Macrophage Ontogeny and Homeostasis. *Immunity,* 44**,** 439-449.

GINHOUX, F. & JUNG, S. 2014. Monocytes and macrophages: developmental pathways and tissue homeostasis. *Nat Rev Immunol,* 14**,** 392-404.

GOMEZ-SANCHEZ, J. A., CARTY, L., IRUARRIZAGA-LEJARRETA, M., PALOMO-IRIGOYEN, M., VARELA-REY, M., GRIFFITH, M., HANTKE, J., MACIAS-CAMARA, N., AZKARGORTA, M., AURREKOETXEA, I., DE JUAN, V. G., JEFFERIES, H. B. J., ASPICHUETA, P., ELORTZA, F., ARANSAY, A. M., MARTÍNEZ-CHANTAR, M. L., BAAS, F., MATO, J. M., MIRSKY, R., WOODHOO, A. & JESSEN, K. R. 2015. Schwann cell autophagy, myelinophagy, initiates myelin clearance from injured nerves. *The Journal of Cell Biology,* 210**,** 153-168.

GORELIK, R. & GAUTREAU, A. 2014. Quantitative and unbiased analysis of directional persistence in cell migration. *Nat. Protocols,* 9**,** 1931-1943.

GRIFFIN, J. W., GEORGE, R. & HO, T. 1993. Macrophage systems in peripheral nerves. A review. *J. Neuropathol. Exp. Neurol.,* 52**,** 553-560.

GRINSELL, D. & KEATING, C. P. 2014. Peripheral Nerve Reconstruction after Injury: A Review of Clinical and Experimental Therapies. *BioMed Research International,* 2014**,** 13.

GROH, J., KLEIN, I., HOLLMANN, C., WETTMARSHAUSEN, J., KLEIN, D. & MARTINI, R. 2015. CSF-1-activated macrophages are target-directed and essential mediators of schwann cell dedifferentiation and dysfunction in Cx32-deficient mice. *Glia,* 63**,** 977-986.

GUILLIAMS, M., BRUHNS, P., SAEYS, Y., HAMMAD, H. & LAMBRECHT, B. N. 2014. The function of Fc[gamma] receptors in dendritic cells and macrophages. *Nat Rev Immunol,* 14**,** 94-108.

GUILLIAMS, M. & SCOTT, C. L. 2017. Does niche competition determine the origin of tissue-resident macrophages? *Nat Rev Immunol,* advance online publication.

GUTMANN, D. H., FERNER, R. E., LISTERNICK, R. H., KORF, B. R., WOLTERS, P. L. & JOHNSON, K. J. 2017. Neurofibromatosis type 1. 3**,** 17004.

HAN, M., YANG, X., LEE, J., ALLAN, C. H. & MUNEOKA, K. 2008. Development and regeneration of the neonatal digit tip in mice. *Developmental Biology,* 315**,** 125-135.

HANEWINCKEL, R., VAN OIJEN, M., IKRAM, M. A. & VAN DOORN, P. A. 2016. The epidemiology and risk factors of chronic polyneuropathy. *European Journal of Epidemiology,* 31**,** 5-20.

HARRISINGH, M. C., PEREZ-NADALES, E., PARKINSON, D. B., MALCOLM, D. S., MUDGE, A. W. & LLOYD, A. C. 2004. The Ras/Raf/ERK signalling pathway drives Schwann cell dedifferentiation. *The EMBO Journal,* 23**,** 3061-3071.

HASHIMOTO, D., CHOW, A., NOIZAT, C., TEO, P., BEASLEY, M. B., LEBOEUF, M., BECKER, C. D., SEE, P., PRICE, J., LUCAS, D., GRETER, M., MORTHA, A., BOYER, S. W., FORSBERG, E. C., TANAKA, M., VAN ROOIJEN, N., GARCÍA-SASTRE, A., STANLEY, E. R., GINHOUX, F., FRENETTE, P. S. & MERAD, M. 2013. Tissue-resident macrophages self-maintain locally throughout adult life with minimal contribution from circulating monocytes. *Immunity,* 38**,** 792-804.

HE, S., HE, S., CHEN, C.-H., DEBORDE, S., BAKST, R. L., CHERNICHENKO, N., MCNAMARA, W. F., LEE, S. Y., BARAJAS, F., YU, Z., AL-AHMADIE, H. A. & WONG, R. J. 2015. The chemokine (CCL2-CCR2) signaling axis mediates perineural invasion. *Molecular cancer research : MCR,* 13**,** 380-390.

HEINE, W., CONANT, K., GRIFFIN, J. W. & HOKE, A. 2004. Transplanted neural stem cells promote axonal regeneration through chronically denervated peripheral nerves. *Exp. Neurol.,* 189**,** 231-240.

HENZE, A.-T. & MAZZONE, M. 2016. The impact of hypoxia on tumor-associated macrophages. *The Journal of Clinical Investigation,* 126**,** 3672-3679.

HOBSON, M. I., GREEN, C. J. & TERENGHI, G. 2000. VEGF enhances intraneural angiogenesis and improves nerve regeneration after axotomy. *Journal of Anatomy,* 197**,** 591-605.

HODGKIN, A. L. & HUXLEY, A. F. 1952. A quantitative description of membrane current and its application to conduction and excitation in nerve. *The Journal of Physiology,* 117**,** 500-544.

HONG, S., BEJA-GLASSER, V. F., NFONOYIM, B. M., FROUIN, A., LI, S., RAMAKRISHNAN, S., MERRY, K. M., SHI, Q., ROSENTHAL, A., BARRES, B. A., LEMERE, C. A., SELKOE, D. J. & STEVENS, B. 2016. Complement and Microglia Mediate Early Synapse Loss in Alzheimer Mouse Models. *Science (New York, N.Y.),* 352**,** 712-716.

HONG, S. & STEVENS, B. 2016. Microglia: Phagocytosing to Clear, Sculpt, and Eliminate. *Developmental Cell,* 38**,** 126-128.

HOUSCHYAR, K. S., MOMENI, A., PYLES, M. N., CHA, J. Y., MAAN, Z. N., DUSCHER, D., JEW, O. S., SIEMERS, F. & SCHOONHOVEN, J. V. 2016. The Role of Current Techniques and Concepts in Peripheral Nerve Repair. *Plastic Surgery International,* 2016**,** 8.

HSU, S.-H., SU, C.-H. & CHIU, I.-M. 2009. A Novel Approach to Align Adult Neural Stem Cells on Micropatterned Conduits for Peripheral Nerve Regeneration: A Feasibility Study. *Artificial Organs,* 33**,** 26-35.

HU, Y., WU, Y., GOU, Z., TAO, J., ZHANG, J., LIU, Q., KANG, T., JIANG, S., HUANG, S., HE, J., CHEN, S., DU, Y. & GOU, M. 2016. 3D-engineering of Cellularized Conduits for Peripheral Nerve Regeneration. 6**,** 32184.

HUEBNER, E. A. & STRITTMATTER, S. M. 2009. Axon regeneration in the peripheral and central nervous systems. *Results Probl. Cell Differ.,* 48**,** 339-351.

HUGHES, R. A. C. 2002. Peripheral neuropathy. *BMJ : British Medical Journal,* 324**,** 466-469.

HUME, D. A. 2006. The mononuclear phagocyte system. *Current Opinion in Immunology,* 18**,** 49-53.

IDE, C. 1996. Peripheral nerve regeneration. *Neurosci. Res.,* 25**,** 101-121.

ISKRATSCH, T., WOLFENSON, H. & SHEETZ, M. P. 2014. Appreciating force and shape [mdash] the rise of mechanotransduction in cell biology. *Nat Rev Mol Cell Biol,* 15**,** 825-833.

JACOB, C., LÖTSCHER, P., ENGLER, S., BAGGIOLINI, A., VARUM TAVARES, S., BRÜGGER, V., JOHN, N., BÜCHMANN-MØLLER, S., SNIDER, P. L., CONWAY, S. J., YAMAGUCHI, T., MATTHIAS, P., SOMMER, L., MANTEI, N. & SUTER, U. 2014. HDAC1 and HDAC2 control the specification of neural crest cells into peripheral glia. *J Neurosci,* 34**,** 6112-22.

JAENSSON, E., URONEN-HANSSON, H., PABST, O., EKSTEEN, B., TIAN, J., COOMBES, J. L., BERG, P. L., DAVIDSSON, T., POWRIE, F., JOHANSSON-LINDBOM, B. & AGACE, W. W. 2008. Small intestinal CD103+ dendritic cells display unique functional properties that are conserved between mice and humans. *J Exp Med,* 205**,** 2139-49.

JAKUBZICK, C., GAUTIER, E. L., GIBBINGS, S. L., SOJKA, D. K., SCHLITZER, A., JOHNSON, T. E., IVANOV, S., DUAN, Q., BALA, S., CONDON, T., VAN ROOIJEN, N., GRAINGER, J. R., BELKAID, Y., MA'AYAN, A., RICHES, D. W., YOKOYAMA, W. M., GINHOUX, F., HENSON, P. M. & RANDOLPH, G. J. 2013. Minimal differentiation of classical monocytes as they survey steady-state tissues and transport antigen to lymph nodes. *Immunity,* 39**,** 599-610.

JESSEN, K. R. & MIRSKY, R. 2005. The origin and development of glial cells in peripheral nerves. *Nat Rev Neurosci,* 6**,** 671-682.

JESSEN, K. R. & MIRSKY, R. 2008. Negative regulation of myelination: relevance for development, injury, and demyelinating disease. *Glia,* 56**,** 1552-1565.

JESSEN, K. R. & MIRSKY, R. 2016. The repair Schwann cell and its function in regenerating nerves. *The Journal of Physiology,* 594**,** 3521-3531.

JESSEN, KRISTJAN R., MIRSKY, R. & ARTHUR-FARRAJ, P. 2015. The Role of Cell Plasticity in Tissue Repair: Adaptive Cellular Reprogramming. *Developmental Cell,* 34**,** 613-620.

JETT, K. & FRIEDMAN, J. M. 2010. Clinical and genetic aspects of neurofibromatosis 1. *Genet Med,* 12**,** 1-11.

JETTEN, N., VERBRUGGEN, S., GIJBELS, M. J., POST, M. J., DE WINTHER, M. P. & DONNERS, M. M. 2014. Anti-inflammatory M2, but not pro-inflammatory M1 macrophages promote angiogenesis in vivo. *Angiogenesis,* 17**,** 109-18.

JIN, T., XU, X. & HERELD, D. 2008. Chemotaxis, chemokine receptors and human disease. *Cytokine,* 44**,** 1-8.

JOHNSON, B. N., LANCASTER, K. Z., ZHEN, G., HE, J., GUPTA, M. K., KONG, Y. L., ENGEL, E. A., KRICK, K. D., JU, A., MENG, F., ENQUIST, L. W., JIA, X. & MCALPINE, M. C. 2015. 3D Printed Anatomical Nerve Regeneration Pathways. *Advanced Functional Materials,* 25**,** 6205-6217.

JOHNSON, P. J., WOOD, M. D., MOORE, A. M. & MACKINNON, S. E. 2013. Tissue engineered constructs for peripheral nerve surgery. *European surgery : ACA : Acta chirurgica Austriaca,* 45**,** 10.1007/s10353-013-0205-0.

JOHNSTON, ADAM P. W., NASKA, S., JONES, K., JINNO, H., KAPLAN, DAVID R. & MILLER, FREDA D. 2013. Sox2-Mediated Regulation of Adult Neural Crest Precursors and Skin Repair. *Stem Cell Reports,* 1**,** 38-45.

JOHNSTON, ADAM P. W., YUZWA, SCOTT A., CARR, MATTHEW J., MAHMUD, N., STORER, MEKAYLA A., KRAUSE, MATTHEW P., JONES, K., PAUL, S., KAPLAN, DAVID R. & MILLER, FREDA D. 2016. Dedifferentiated Schwann Cell Precursors Secreting Paracrine Factors Are Required for Regeneration of the Mammalian Digit Tip. *Cell Stem Cell,* 19**,** 433-448.

JUAREZ, P. & PALAU, F. 2012. Neural and Molecular Features on Charcot-Marie-Tooth Disease Plasticity and Therapy. *Neural Plasticity,* 2012**,** 11.

JUNG, S., ALIBERTI, J., GRAEMMEL, P., SUNSHINE, M. J., KREUTZBERG, G. W., SHER, A. & LITTMAN, D. R. 2000. Analysis of Fractalkine Receptor CX3CR1 Function by Targeted Deletion and Green Fluorescent Protein Reporter Gene Insertion. *Molecular and Cellular Biology,* 20**,** 4106-4114.

KANG, H. & LICHTMAN, J. W. 2013. Motor Axon Regeneration and Muscle Reinnervation in Young Adult and Aged Animals. *The Journal of Neuroscience,* 33**,** 19480.

KAY, R. R., LANGRIDGE, P., TRAYNOR, D. & HOELLER, O. 2008. Changing directions in the study of chemotaxis. *Nat Rev Mol Cell Biol,* 9**,** 455-463.

KIDD, G. J., OHNO, N. & TRAPP, B. D. 2013. Biology of Schwann cells. *Handbook of Clinical Neurology,* 115**,** 55-79.

KIERDORF, K. & DIONNE, MARC S. 2016. The Software and Hardware of Macrophages: A Diversity of Options. *Developmental Cell,* 38**,** 122-125.

KIESEIER, B. C., HARTUNG, H. P. & WIENDL, H. 2006. Immune circuitry in the peripheral nervous system. *Curr Opin Neurol,* 19**,** 437-45.

KIGUCHI, N., MAEDA, T., KOBAYASHI, Y., FUKAZAWA, Y. & KISHIOKA, S. 2010. Macrophage inflammatory protein-1alpha mediates the development of neuropathic pain following peripheral nerve injury through interleukin-1beta up-regulation. *Pain,* 149**,** 305-15.

KISNER, C. & COLBY, L. A. 2012. *Therapeutic Exercise: Foundations and Techniques*, F.A. Davis Company.

KLEIN, D. & MARTINI, R. 2016. Myelin and macrophages in the PNS: An intimate relationship in trauma and disease. *Brain Research,* 1641**,** 130-138.

KRAGL, M., KNAPP, D., NACU, E., KHATTAK, S., MADEN, M., EPPERLEIN, H. H. & TANAKA, E. M. 2009. Cells keep a memory of their tissue origin during axolotl limb regeneration. *Nature,* 460**,** 60-65.

KRAMES, E. S. 2014. The Role of the Dorsal Root Ganglion in the Development of Neuropathic Pain. *Pain Medicine,* 15**,** 1669-1685.

KRENKEL, O. & TACKE, F. 2017. Liver macrophages in tissue homeostasis and disease. *Nat Rev Immunol,* 17**,** 306-321.

KRESS, G. J. & MENNERICK, S. 2009. Action potential initiation and propagation: upstream influences on neurotransmission. *Neuroscience,* 158**,** 211-222.

KUMAR, A. & BROCKES, J. P. 2012. Nerve dependence in tissue, organ, and appendage regeneration. *Trends in Neurosciences,* 35**,** 691-699.

KUMAR, A., GODWIN, J. W., GATES, P. B., GARZA-GARCIA, A. A. & BROCKES, J. P. 2007. Molecular Basis for the Nerve Dependence of Limb Regeneration in an Adult Vertebrate. *Science (New York, N.Y.),* 318**,** 772-777.

KWON, M. J., KIM, J., SHIN, H., JEONG, S. R., KANG, Y. M., CHOI, J. Y., HWANG, D. H. & KIM, B. G. 2013. Contribution of macrophages to enhanced regenerative capacity of dorsal root ganglia sensory neurons by conditioning injury. *J Neurosci,* 33**,** 15095-108.

KWON, M. J., SHIN, H. Y., CUI, Y., KIM, H., THI, A. H., CHOI, J. Y., KIM, E. Y., HWANG, D. H. & KIM, B. G. 2015. CCL2 Mediates Neuron-Macrophage Interactions to Drive Proregenerative Macrophage Activation Following Preconditioning Injury. *J Neurosci,* 35**,** 15934-47.

LÄMMERMANN, T., BADER, B. L., MONKLEY, S. J., WORBS, T., WEDLICH-SÖLDNER, R., HIRSCH, K., KELLER, M., FÖRSTER, R., CRITCHLEY, D. R., FÄSSLER, R. & SIXT, M. 2008. Rapid leukocyte migration by integrin-independent flowing and squeezing. *Nature,* 453**,** 51-5.

LAOUI, D., VAN OVERMEIRE E FAU - DI CONZA, G., DI CONZA G FAU - ALDENI, C., ALDENI C FAU - KEIRSSE, J., KEIRSSE J FAU - MORIAS, Y., MORIAS Y FAU - MOVAHEDI, K., MOVAHEDI K FAU - HOUBRACKEN, I., HOUBRACKEN I FAU - SCHOUPPE, E., SCHOUPPE E FAU - ELKRIM, Y., ELKRIM Y FAU - KARROUM, O., KARROUM O FAU - JORDAN, B., JORDAN B FAU - CARMELIET, P., CARMELIET P FAU - GYSEMANS, C., GYSEMANS C FAU - DE BAETSELIER, P., DE BAETSELIER P FAU - MAZZONE, M., MAZZONE M FAU - VAN GINDERACHTER, J. A. & VAN GINDERACHTER, J. A. 2014. Tumor hypoxia does not drive differentiation of tumor-associated macrophages but rather fine-tunes the M2-like macrophage population.

LAVIN, Y., WINTER, D., BLECHER-GONEN, R., DAVID, E., KEREN-SHAUL, H., MERAD, M., JUNG, S. & AMIT, I. 2014. Tissue-Resident Macrophage Enhancer Landscapes Are Shaped by the Local Microenvironment. *Cell,* 159**,** 1312-1326.

LEBER, T. 1888. Über die Entstehung der Entzündung und die Wirkung der entzündungserregenden Schädlichkeiten. Fortschritte der Medizin.

LIEBIG, C., AYALA, G., WILKS, J. A., BERGER, D. H. & ALBO, D. 2009. Perineural invasion in cancer. *Cancer,* 115**,** 3379-3391.

LIEBSCHER, I., SCHÖN, J., PETERSEN, S. C., FISCHER, L., AUERBACH, N., DEMBERG, L. M., MOGHA, A., CÖSTER, M., SIMON, K. U., ROTHEMUND, S., MONK, K. R. & SCHÖNEBERG, T. 2014. A tethered agonist within the ectodomain activates the adhesion G protein-coupled receptors GPR126 and GPR133. *Cell Rep,* 9**,** 2018-26.

LIN, N. & SIMON, M. C. 2016. Hypoxia-inducible factors: key regulators of myeloid cells during inflammation. *The Journal of Clinical Investigation,* 126.

LINDBORG, J. A., MACK, M. & ZIGMOND, R. E. 2017. Neutrophils are critical for myelin removal in a peripheral nerve injury model of Wallerian degeneration. *The Journal of Neuroscience*.

LIU, Y. J., LE BERRE, M., LAUTENSCHLAEGER, F., MAIURI, P., CALLAN-JONES, A., HEUZÉ, M., TAKAKI, T., VOITURIEZ, R. & PIEL, M. 2015. Confinement and low adhesion induce fast amoeboid migration of slow mesenchymal cells. *Cell,* 160**,** 659-72.

LUNDBORG, G. 2003. Nerve injury and repair – a challenge to the plastic brain. *Journal of the Peripheral Nervous System,* 8**,** 209-226.

LUPSKI, J. R., DE OCA-LUNA, R. M., SLAUGENHAUPT, S., PENTAO, L., GUZZETTA, V., TRASK, B. J., SAUCEDO-CARDENAS, O., BARKER, D. F., KILLIAN, J. M., GARCIA, C. A., CHAKRAVARTI, A. & PATEL, P. I. 1991. DNA duplication associated with Charcot-Marie-Tooth disease type 1A. *Cell,* 66**,** 219-32.

MA, W., ZHANG, Y., GAO, C., FARISS, R. N., TAM, J. & WONG, W. T. 2017. Monocyte infiltration and proliferation reestablish myeloid cell homeostasis in the mouse retina following retinal pigment epithelial cell injury. *Sci Rep,* 7**,** 8433.

MAGNON, C. 2015. Role of the autonomic nervous system in tumorigenesis and metastasis. *Molecular & Cellular Oncology,* 2**,** e975643.

MAGNON, C., HALL, S. J., LIN, J., XUE, X., GERBER, L., FREEDLAND, S. J. & FRENETTE, P. S. 2013. Autonomic Nerve Development Contributes to Prostate Cancer Progression. *Science,* 341.

MANTOVANI, A., MARCHESI, F., MALESCI, A., LAGHI, L. & ALLAVENA, P. 2017. Tumour-associated macrophages as treatment targets in oncology. *Nat Rev Clin Oncol,* 14**,** 399-416.

MARTIN, G. A., VISKOCHIL, D., BOLLAG, G., MCCABE, P. C., CROSIER, W. J., HAUBRUCK, H., CONROY, L., CLARK, R., O'CONNELL, P. & CAWTHON, R. M. 1990. The GAP-related domain of the neurofibromatosis type 1 gene product interacts with ras p21. *Cell,* 63**,** 843-9.

MARTINEZ, F. O. & GORDON, S. 2014. The M1 and M2 paradigm of macrophage activation: time for reassessment. *F1000Prime Reports,* 6**,** 13.

MASS, E., BALLESTEROS, I., FARLIK, M., HALBRITTER, F., GÜNTHER, P., CROZET, L., JACOME-GALARZA, C. E., HÄNDLER, K., KLUGHAMMER, J., KOBAYASHI, Y., GOMEZ-PERDIGUERO, E., SCHULTZE, J. L., BEYER, M., BOCK, C. & GEISSMANN, F. 2016. Specification of tissue-resident macrophages during organogenesis. *Science*.

MATHON, N. F., MALCOLM, D. S., HARRISINGH, M. C., CHENG, L. & LLOYD, A. C. 2001. Lack of replicative senescence in normal rodent glia. *Science,* 291**,** 872-5.

MAUS, U. A., KOAY, M. A., DELBECK, T., MACK, M., ERMERT, M., ERMERT, L., BLACKWELL, T. S., CHRISTMAN, J. W., SCHLÖNDORFF, D., SEEGER, W. & LOHMEYER, J. 2002. Role of resident

alveolar macrophages in leukocyte traffic into the alveolar air space of intact mice. *American Journal of Physiology - Lung Cellular and Molecular Physiology,* 282**,** L1245.

MAYOR, R. & ETIENNE-MANNEVILLE, S. 2016. The front and rear of collective cell migration. *Nat Rev Mol Cell Biol,* 17**,** 97-109.

MCDONALD, D., CHENG, C., CHEN, Y. & ZOCHODNE, D. 2006. Early events of peripheral nerve regeneration. *Neuron Glia Biol,* 2**,** 139-47.

MEI, L. & XIONG, W. C. 2008. Neuregulin 1 in neural development, synaptic plasticity and schizophrenia. *Nat. Rev. Neurosci.,* 9**,** 437-452.

MENDELSON, A. & FRENETTE, P. S. 2014. Hematopoietic stem cell niche maintenance during homeostasis and regeneration. *Nat Med,* 20**,** 833-846.

MENTEN, P., WUYTS, A. & VAN DAMME, J. 2002. Macrophage inflammatory protein-1. *Cytokine & Growth Factor Reviews,* 13**,** 455-481.

MERAD, M., MANZ, M. G., KARSUNKY, H., WAGERS, A., PETERS, W., CHARO, I., WEISSMAN, I. L., CYSTER, J. G. & ENGLEMAN, E. G. 2002. Langerhans cells renew in the skin throughout life under steady-state conditions. *Nat Immunol,* 3**,** 1135-41.

MOGHA, A., BENESH, A. E., PATRA, C., ENGEL, F. B., SCHÖNEBERG, T., LIEBSCHER, I. & MONK, K. R. 2013. Gpr126 Functions in Schwann Cells to Control Differentiation and Myelination via G-Protein Activation. *The Journal of Neuroscience,* 33**,** 17976-17985.

MOKARRAM, N., DYMANUS, K., SRINIVASAN, A., LYON, J. G., TIPTON, J., CHU, J., ENGLISH, A. W. & BELLAMKONDA, R. V. 2017. Immunoengineering nerve repair. *Proceedings of the National Academy of Sciences,* 114**,** E5077-E5084.

MOKARRAM, N., MERCHANT, A., MUKHATYAR, V., PATEL, G. & BELLAMKONDA, R. V. 2012. Effect of modulating macrophage phenotype on peripheral nerve repair. *Biomaterials,* 33**,** 8793-8801.

MONK, K. R., FELTRI, M. L. & TAVEGGIA, C. 2015. New insights on Schwann cell development. *Glia,* 63**,** 1376-93.

MORRISON, S. J. & SCADDEN, D. T. 2014. The bone marrow niche for haematopoietic stem cells. *Nature,* 505**,** 327-334.

MUELLER, M. 2001. Rapid response of identified resident endoneurial macrophages to nerve injury. *Am. J. Pathol.,* 159**,** 2187-2197.

MUELLER, M. 2003. Macrophage response to peripheral nerve injury: the quantitative contribution of resident and hematogenous macrophages. *Lab. Invest.,* 83**,** 175-185.

MÜLLER, M., LEONHARD, C., KRAUTHAUSEN, M., WACKER, K. & KIEFER, R. 2010. On the longevity of resident endoneurial macrophages in the peripheral nervous system: a study of physiological macrophage turnover in bone marrow chimeric mice. *Journal of the Peripheral Nervous System,* 15**,** 357-365.

MURDOCH, C., MUTHANA, M., COFFELT, S. B. & LEWIS, C. E. 2008. The role of myeloid cells in the promotion of tumour angiogenesis. *Nat Rev Cancer,* 8**,** 618-31.

MURRAY, P. J. 2017. Macrophage Polarization. *Annual Review of Physiology,* 79**,** 541-566.

MURRAY, P. J., ALLEN, J. E., BISWAS, S. K., FISHER, E. A., GILROY, D. W., GOERDT, S., GORDON, S., HAMILTON, J. A., IVASHKIV, L. B., LAWRENCE, T., LOCATI, M., MANTOVANI, A., MARTINEZ, F. O., MEGE, J. L., MOSSER, D. M., NATOLI, G., SAEIJ, J. P., SCHULTZE, J. L., SHIREY, K. A., SICA, A., SUTTLES, J., UDALOVA, I., VAN GINDERACHTER, J. A., VOGEL, S. N. & WYNN, T.

A. 2014. Macrophage activation and polarization: nomenclature and experimental guidelines. *Immunity,* 41**,** 14-20.

MUTHANA, M., GIANNOUDIS, A., SCOTT, S. D., FANG, H. Y., COFFELT, S. B., MORROW, F. J., MURDOCH, C., BURTON, J., CROSS, N., BURKE, B., MISTRY, R., HAMDY, F., BROWN, N. J., GEORGOPOULOS, L., HOSKIN, P., ESSAND, M., LEWIS, C. E. & MAITLAND, N. J. 2011. Use of macrophages to target therapeutic adenovirus to human prostate tumors. *Cancer Res,* 71**,** 1805-15.

NAKATSU, M. N., SAINSON, R. C. A., AOTO, J. N., TAYLOR, K. L., AITKENHEAD, M., PÉREZ-DEL-PULGAR, S., CARPENTER, P. M. & HUGHES, C. C. W. 2003. Angiogenic sprouting and capillary lumen formation modeled by human umbilical vein endothelial cells (HUVEC) in fibrin gels: the role of fibroblasts and Angiopoietin-1. *Microvascular Research,* 66**,** 102-112.

NAKATSUJI, Y. 2017. What is the difference between the blood–nerve barrier and blood–brain barrier? *Clinical and Experimental Neuroimmunology,* 8**,** 13-14.

NAPOLI, I., NOON, L. A., RIBEIRO, S., KERAI, A. P., PARRINELLO, S., ROSENBERG, L. H., COLLINS, M. J., HARRISINGH, M. C., WHITE, I. J., WOODHOO, A. & LLOYD, A. C. 2012. A central role for the ERK-signaling pathway in controlling Schwann cell plasticity and peripheral nerve regeneration in vivo. *Neuron,* 73**,** 729-42.

NAVE, K.-A. 2010. Myelination and support of axonal integrity by glia. *Nature,* 468**,** 244-252.

NAVE, K.-A. & WERNER, H. B. 2014. Myelination of the Nervous System: Mechanisms and Functions. *Annual Review of Cell and Developmental Biology,* 30**,** 503-533.

NEWBERN, J. & BIRCHMEIER, C. 2010. Nrg1/ErbB signaling networks in Schwann cell development and myelination. *Semin Cell Dev Biol,* 21**,** 922-8.

NICHOLSON, G. & MYERS, S. 2006. Intermediate forms of Charcot-Marie-Tooth neuropathy. *NeuroMolecular Medicine,* 8**,** 123-130.

NIEMI, J. P., DEFRANCESCO-LISOWITZ, A., ROLDÁN-HERNÁNDEZ, L., LINDBORG, J. A., MANDELL, D. & ZIGMOND, R. E. 2013. A Critical Role for Macrophages Near Axotomized Neuronal Cell Bodies in Stimulating Nerve Regeneration. *The Journal of Neuroscience,* 33**,** 16236.

O'KOREN, E. G., MATHEW, R. & SABAN, D. R. 2016. Fate mapping reveals that microglia and recruited monocyte-derived macrophages are definitively distinguishable by phenotype in the retina. *Scientific Reports,* 6**,** 20636.

ÖDEMIS, V., BOOSMANN, K., HEINEN, A., KÜRY, P. & ENGELE, J. 2010. CXCR7 is an active component of SDF-1 signalling in astrocytes and Schwann cells. *Journal of Cell Science,* 123**,** 1081-1088.

OKADA, Y., EIBL, G., GUHA, S., DUFFY, J. P., REBER, H. A. & HINES, O. J. 2004. Nerve growth factor stimulates MMP-2 expression and activity and increases invasion by human pancreatic cancer cells. *Clinical & Experimental Metastasis,* 21**,** 285.

PARK, K. K. 2008. Promoting axon regeneration in the adult CNS by modulation of the PTEN/mTOR pathway. *Science,* 322**,** 963-966.

PARKINSON, D. B., BHASKARAN, A., DROGGITI, A., DICKINSON, S., D'ANTONIO, M., MIRSKY, R. & JESSEN, K. R. 2004. Krox-20 inhibits Jun-NH2-terminal kinase/c-Jun to control Schwann cell proliferation and death. *J Cell Biol,* 164**,** 385-94.

PARRA, B., LIZARAZO, J., JIMÉNEZ-ARANGO, J. A., ZEA-VERA, A. F., GONZÁLEZ-MANRIQUE, G., VARGAS, J., ANGARITA, J. A., ZUÑIGA, G., LOPEZ-GONZALEZ, R., BELTRAN, C. L., RIZCALA, K. H., MORALES, M. T., PACHECO, O., OSPINA, M. L., KUMAR, A., CORNBLATH, D. R., MUÑOZ, L. S., OSORIO, L., BARRERAS, P. & PARDO, C. A. 2016. Guillain-Barré Syndrome Associated with Zika Virus Infection in Colombia. *N Engl J Med,* 375**,** 1513-1523.

PARRINELLO, S. & LLOYD, A. C. 2009. Neurofibroma development in NF1 – insights into tumour initiation. *Trends in Cell Biology,* 19**,** 395-403.

PARRINELLO, S., NAPOLI, I., RIBEIRO, S., WINGFIELD DIGBY, P., FEDOROVA, M., PARKINSON, D. B., DODDRELL, R. D., NAKAYAMA, M., ADAMS, R. H. & LLOYD, A. C. 2010. EphB signaling directs peripheral nerve regeneration through Sox2-dependent Schwann cell sorting. *Cell,* 143**,** 145-55.

PATEL, A. A., ZHANG, Y., FULLERTON, J. N., BOELEN, L., RONGVAUX, A., MAINI, A. A., BIGLEY, V., FLAVELL, R. A., GILROY, D. W., ASQUITH, B., MACALLAN, D. & YONA, S. 2017. The fate and lifespan of human monocyte subsets in steady state and systemic inflammation. *The Journal of Experimental Medicine,* 214**,** 1913-1923.

PAUL, C. D., MISTRIOTIS, P. & KONSTANTOPOULOS, K. 2017. Cancer cell motility: lessons from migration in confined spaces. *Nat Rev Cancer,* 17**,** 131-140.

PERRIN, F. E., LACROIX, S., AVILÉS-TRIGUEROS, M. & DAVID, S. 2005. Involvement of monocyte chemoattractant protein-1, macrophage inflammatory protein-1alpha and interleukin-1beta in Wallerian degeneration. *Brain,* 128**,** 854-66.

PFEFFER, W. 1884. Locomotorische Richtungsbewegungen durch chemische Reise. Untersuch. Bot. Inst. Tübingen.

POLA, R., APRAHAMIAN, T. R., BOSCH-MARCÉ, M., CURRY, C., GAETANI, E., FLEX, A., SMITH, R. C., ISNER, J. M. & LOSORDO, D. W. 2004. Age-dependent VEGF expression and intraneural neovascularization during regeneration of peripheral nerves. *Neurobiology of Aging,* 25**,** 1361-1368.

PRADA, C. E., JOUSMA, E., RIZVI, T. A., WU, J., DUNN, R. S., MAYES, D. A., CANCELAS, J. A., DOMBI, E., KIM, M.-O., WEST, B. L., BOLLAG, G. & RATNER, N. 2013. Neurofibroma-associated macrophages play roles in tumor growth and response to pharmacological inhibition. *Acta neuropathologica,* 125**,** 159-168.

QIAN, B.-Z. & POLLARD, J. W. 2010. Macrophage Diversity Enhances Tumor Progression and Metastasis. *Cell,* 141**,** 39-51.

RANTAKARI, P., JÄPPINEN, N., LOKKA, E., MOKKALA, E., GERKE, H., PEUHU, E., IVASKA, J., ELIMA, K., AUVINEN, K. & SALMI, M. 2016. Fetal liver endothelium regulates the seeding of tissue-resident macrophages. *Nature,* 538**,** 392-396.

RAPHAEL, A. R. & TALBOT, W. S. 2011. New insights into signaling during myelination in zebrafish. *Curr Top Dev Biol,* 97**,** 1-19.

RATNER, N. & MILLER, S. J. 2015. A RASopathy gene commonly mutated in cancer: the neurofibromatosis type 1 tumour suppressor. *Nature reviews. Cancer,* 15**,** 290-301.

REN, Z., WANG, Y., PENG, J., ZHAO, Q. & LU, S. 2012. Role of stem cells in the regeneration and repair of peripheral nerves. *Rev. Neurosci.,* 23**,** 135-143.

RIBEIRO, S., NAPOLI, I., WHITE, I. J., PARRINELLO, S., FLANAGAN, A. M., SUTER, U., PARADA, L. F. & LLOYD, A. C. 2013. Injury signals cooperate with Nf1 loss to relieve the tumor-suppressive environment of adult peripheral nerve. *Cell Rep,* 5**,** 126-36.

RIBOLDI, E., PORTA, C., MORLACCHI, S., VIOLA, A., MANTOVANI, A. & SICA, A. 2012. Hypoxia-mediated regulation of macrophage functions in pathophysiology. *International Immunology*.

RICHARDSON, R. B., ALLAN, D. S. & LE, Y. 2014. Greater organ involution in highly proliferative tissues associated with the early onset and acceleration of ageing in humans. *Experimental Gerontology,* 55**,** 80-91.

RIEHLE, K. J., DAN, Y. Y., CAMPBELL, J. S. & FAUSTO, N. 2011. New Concepts in Liver Regeneration. *Journal of gastroenterology and hepatology,* 26**,** 203-212.

RODRIGUES, M. C., RODRIGUES JR, A. A., GLOVER, L. E., VOLTARELLI, J. & BORLONGAN, C. V. 2012. Peripheral nerve repair with cultured Schwann cells: getting closer to the clinics. *ScientificWorldJournal,* 2012**,** 413091.

ROSENBERG, A. F., WOLMAN, M. A., FRANZINI-ARMSTRONG, C. & GRANATO, M. 2012. In vivo nerve-macrophage interactions following peripheral nerve injury. *J. Neurosci.,* 32**,** 3898-3909.

ROUSSOS, E. T., CONDEELIS, J. S. & PATSIALOU, A. 2011. Chemotaxis in cancer. *Nat Rev Cancer,* 11**,** 573-587.

RUBIN, J. B. & GUTMANN, D. H. 2005. Neurofibromatosis type 1 - a model for nervous system tumour formation? *Nat Rev Cancer,* 5**,** 557-564.

SALONEN, V., AHO, H., RÖYTTÄ, M. & PELTONEN, J. 1988. Quantitation of Schwann cells and endoneurial fibroblast-like cells after experimental nerve trauma. *Acta Neuropathologica,* 7**5,** 331-336.

SCARPA, E. & MAYOR, R. 2016. Collective cell migration in development. *The Journal of Cell Biology,* 212**,** 143-155.

SCHEIB, J. & HOKE, A. 2013. Advances in peripheral nerve regeneration. *Nat Rev Neurol,* 9**,** 668-676.

SCHOLZ, J. & WOOLF, C. J. 2007. The neuropathic pain triad: neurons, immune cells and glia. 10**,** 1361.

SCOTT, C. L., ZHENG, F., DE BAETSELIER, P., MARTENS, L., SAEYS, Y., DE PRIJCK, S., LIPPENS, S., ABELS, C., SCHOONOOGHE, S., RAES, G., DEVOOGDT, N., LAMBRECHT, B. N., BESCHIN, A. & GUILLIAMS, M. 2016. Bone marrow-derived monocytes give rise to self-renewing and fully differentiated Kupffer cells. *Nature Communications,* 7**,** 10321.

SEMENZA, G. L. 2001. HIF-1, O(2), and the 3 PHDs: how animal cells signal hypoxia to the nucleus. *Cell,* 107**,** 1-3.

SEMENZA, G. L. 2012. Hypoxia-inducible factors: mediators of cancer progression and targets for cancer therapy. *Trends in Pharmacological Sciences,* 33**,** 207-214.

SHEU, J. Y., KULHANEK, D. J. & ECKENSTEIN, F. P. 2000. Differential Patterns of ERK and STAT3 Phosphorylation after Sciatic Nerve Transection in the Rat. *Experimental Neurology,* 166**,** 392-402.

SIEBERT, H., SACHSE, A., KUZIEL, W. A., MAEDA, N. & BRÜCK, W. 2000. The chemokine receptor CCR2 is involved in macrophage recruitment to the injured peripheral nervous system. *Journal of Neuroimmunology,* 110**,** 177-185.

SIQUEIRA MIETTO, B., KRONER, A., GIROLAMI, E. I., SANTOS-NOGUEIRA, E., ZHANG, J. & DAVID, S. 2015. Role of IL-10 in Resolution of Inflammation and Functional Recovery after Peripheral Nerve Injury. *J Neurosci,* 35**,** 16431-42.

SLOAN, E. K., PRICEMAN, S. J., COX, B. F., YU, S., PIMENTEL, M. A., TANGKANANGNUKUL, V., AREVALO, J. M., MORIZONO, K., KARANIKOLAS, B. D., WU, L., SOOD, A. K. & COLE, S. W. 2010. The sympathetic nervous system induces a metastatic switch in primary breast cancer. *Cancer Res,* 70**,** 7042-52.

SOUCIE, E. L., WENG, Z., GEIRSDÓTTIR, L., MOLAWI, K., MAURIZIO, J., FENOUIL, R., MOSSADEGH-KELLER, N., GIMENEZ, G., VANHILLE, L., BENIAZZA, M., FAVRET, J., BERRUYER, C., PERRIN, P., HACOHEN, N., ANDRAU, J. C., FERRIER, P., DUBREUIL, P., SIDOW, A. & SIEWEKE, M. H. 2016. Lineage-specific enhancers activate self-renewal genes in macrophages and embryonic stem cells. *Science,* 351.

STASER, K., YANG, F.-C. & CLAPP, D. W. 2012. Pathogenesis of Plexiform Neurofibroma: Tumor-Stromal/Hematopoietic Interactions in Tumor Progression. *Annual review of pathology,* 7**,** 469-495.

STASSART, R. M., FLEDRICH, R., VELANAC, V., BRINKMANN, B. G., SCHWAB, M. H., MEIJER, D., SEREDA, M. W. & NAVE, K. A. 2013. A role for Schwann cell-derived neuregulin-1 in remyelination. *Nat Neurosci,* 16**,** 48-54.

STEEG, P. S. 2016. Targeting metastasis. *Nat Rev Cancer,* 16**,** 201-218.

STOLINSKI, C. 1995. Structure and composition of the outer connective tissue sheaths of peripheral nerve. *Journal of Anatomy,* 186**,** 123-130.

SULAIMAN, O. A. & GORDON, T. 2000. Effects of short- and long-term Schwann cell denervation on peripheral nerve regeneration, myelination, and size. *Glia,* 32**,** 234-246.

SUN, S., CHEN, D., LIN, F., CHEN, M., YU, H., HOU, L. & LI, C. 2016. Role of interleukin-4, the chemokine CCL3 and its receptor CCR5 in neuropathic pain. *Molecular Immunology,* 77**,** 184-192.

SUWANICHKUL, A. & WENDERFER, S. E. 2013. Differential Expression of Functional Fc-Receptors and Additional Immune Complex Receptors on Mouse Kidney Cells. *Molecular immunology,* 56**,** 369-379.

TAMOUTOUNOUR, S., GUILLIAMS, M., MONTANANA SANCHIS, F., LIU, H., TERHORST, D., MALOSSE, C., POLLET, E., ARDOUIN, L., LUCHE, H., SANCHEZ, C., DALOD, M., MALISSEN, B. & HENRI, S. 2013. Origins and Functional Specialization of Macrophages and of Conventional and Monocyte-Derived Dendritic Cells in Mouse Skin. *Immunity,* 39**,** 925-938.

TASKINEN, H.-S. & RÖYTTÄ, M. 2000. Increased expression of chemokines (MCP-1, MIP-1α, RANTES) after peripheral nerve transection. *Journal of the Peripheral Nervous System,* 5**,** 75-81.

TAUB, R. 2004. Liver regeneration: from myth to mechanism. *Nat Rev Mol Cell Biol,* 5**,** 836-847.

TAVEGGIA, C., ZANAZZI, G., PETRYLAK, A., YANO, H., ROSENBLUTH, J., EINHEBER, S., XU, X., ESPER, R. M., LOEB, J. A., SHRAGER, P., CHAO, M. V., FALLS, D. L., ROLE, L. & SALZER, J. L. 2005. Neuregulin-1 type III determines the ensheathment fate of axons. *Neuron,* 47**,** 681-94.

TAYLOR, C. T., DOHERTY, G., FALLON, P. G. & CUMMINS, E. P. 2016. Hypoxia-dependent regulation of inflammatory pathways in immune cells. *The Journal of Clinical Investigation,* 126**,** 3716-3724.

TE BOEKHORST, V., PREZIOSI, L. & FRIEDL, P. 2016. Plasticity of Cell Migration In Vivo and In Silico. *Annual Review of Cell and Developmental Biology,* 32**,** 491-526.

TERENGHI, G., HART, A. & WIBERG, M. 2011. The nerve injury and the dying neurons: diagnosis and prevention. *J. Hand Surg. Eur.,* 36**,** 730-734.

THEVENEAU, E., MARCHANT, L., KURIYAMA, S., GULL, M., MOEPPS, B., PARSONS, M. & MAYOR, R. 2010. Collective chemotaxis requires contact-dependent cell polarity. *Dev Cell,* 19**,** 39-53.

TOPILKO, P., SCHNEIDER-MAUNOURY, S., LEVI, G., BARON-VAN 					EVERCOOREN, A., CHENNOUFI, A. B. Y., SEITANIDOU, T., BABINET, C. & CHARNAY, P. 1994. Krox-20 controls myelination in the peripheral nervous system. *Nature,* 371**,** 796-799.

TOZLUOĞLU, M., TOURNIER, A. L., JENKINS, R. P., HOOPER, S., BATES, P. A. & SAHAI, E. 2013. Matrix geometry determines optimal cancer cell migration strategy and modulates response to interventions. *Nat Cell Biol,* 15**,** 751-62.

TREMBLAY, M.-È., LOWERY, R. L. & MAJEWSKA, A. K. 2010. Microglial Interactions with Synapses Are Modulated by Visual Experience. *PLOS Biology,* 8**,** e1000527.

TREPAT, X., CHEN, Z. & JACOBSON, K. 2012. Cell Migration. *Comprehensive Physiology,* 2**,** 2369-2392.

TRIFILO, M. J., BERGMANN, C. C., KUZIEL, W. A. & LANE, T. E. 2003. CC chemokine ligand 3 (CCL3) regulates CD8(+)-T-cell effector function and migration following viral infection. *J Virol,* 77**,** 4004-14.

TWEEDY, L., KNECHT, D. A., MACKAY, G. M. & INSALL, R. H. 2016. Self-Generated Chemoattractant Gradients: Attractant Depletion Extends the Range and Robustness of Chemotaxis. *PLoS Biology,* 14**,** e1002404.

VAN FURTH, R. & COHN, Z. A. 1968. The origin and kinetics of mononuclear phagocytes. *J Exp Med,* 128**,** 415-35.

VAN HAASTERT, P. J. M. & DEVREOTES, P. N. 2004. Chemotaxis: signalling the way forward. *Nat Rev Mol Cell Biol,* 5**,** 626-634.

VAROL, C., MILDNER, A. & JUNG, S. 2015. Macrophages: Development and Tissue Specialization. *Annual Review of Immunology,* 33**,** 643-675.

VASS, K., HICKEY, W. F., SCHMIDT, R. E. & LASSMANN, H. 1993. Bone marrow-derived elements in the peripheral nervous system. An immunohistochemical and ultrastructural investigation in chimeric rats. *Lab Invest,* 69**,** 275-82.

WAKERLEY, B. R. & YUKI, N. 2013. Infectious and noninfectious triggers in Guillain-Barré syndrome. *Expert Rev Clin Immunol,* 9**,** 627-39.

WANG, G., CAO, L., WANG, Y., HUA, Y., CAI, Z., CHEN, J., CHEN, L., JIN, Y., NIU, L., SHEN, H., LU, Y. & SHEN, Z. 2017. Human eyelid adipose tissue-derived Schwann cells promote regeneration of a transected sciatic nerve. 7**,** 43248.

WANG, Y., TENG, H.-L. & HUANG, Z.-H. 2012. Intrinsic Migratory Properties of Cultured Schwann Cells Based on Single-Cell Migration Assay. *PLOS ONE,* 7**,** e51824.

WEAVERS, H., LIEPE, J., SIM, A., WOOD, W., MARTIN, P. & STUMPF, MICHAEL P. H. 2016. Systems Analysis of the Dynamic Inflammatory Response to Tissue Damage Reveals Spatiotemporal Properties of the Wound Attractant Gradient. *Current Biology,* 26**,** 1975-1989.

WEERASURIYA, A. & MIZISIN, A. P. 2011. The Blood-Nerve Barrier: Structure and Functional Significance. *In:* NAG, S. (ed.) *The Blood-Brain and Other Neural Barriers: Reviews and Protocols.* Totowa, NJ: Humana Press.

WHITE, F. A., FELDMAN, P. & MILLER, R. J. 2009. Chemokine Signaling and the Management of Neuropathic Pain. *Molecular Interventions,* 9**,** 188-195.

WOODHOO, A., ALONSO, M. B. D., DROGGITI, A., TURMAINE, M., D'ANTONIO, M., PARKINSON, D. B., WILTON, D. K., AL-SHAWI, R., SIMONS, P., SHEN, J., GUILLEMOT, F., RADTKE, F., MEIJER, D., FELTRI, M. L., WRABETZ, L., MIRSKY, R. & JESSEN, K. R. 2009. Notch controls embryonic Schwann cell differentiation, postnatal myelination and adult plasticity. *Nature neuroscience,* 12**,** 839-847.

WU, C., ASOKAN, SREEJA B., BERGINSKI, MATTHEW E., HAYNES, ELIZABETH M., SHARPLESS, NORMAN E., GRIFFITH, JACK D., GOMEZ, SHAWN M. & BEAR, JAMES E. 2012. Arp2/3 Is Critical for Lamellipodia and Response to Extracellular Matrix Cues but Is Dispensable for Chemotaxis. *Cell,* 148**,** 973-987.

WU, G.-H. & HSU, S.-H. 2015. Review: Polymeric-Based 3D Printing for Tissue Engineering. *Journal of Medical and Biological Engineering,* 35**,** 285-292.

WYNN, T. A., CHAWLA, A. & POLLARD, J. W. 2013. Origins and Hallmarks of Macrophages: Development, Homeostasis, and Disease. *Nature,* 496**,** 445-455.

WYNN, THOMAS A. & VANNELLA, KEVIN M. 2016. Macrophages in Tissue Repair, Regeneration, and Fibrosis. *Immunity,* 44**,** 450-462.

YAMAUCHI, J., CHAN, J. R. & SHOOTER, E. M. 2004. Neurotrophins regulate Schwann cell migration by activating divergent signaling pathways dependent on Rho GTPases. *Proc Natl Acad Sci U S A,* 101**,** 8774-9.

YDENS, E., CAUWELS, A., ASSELBERGH, B., GOETHALS, S., PEERAER, L., LORNET, G., ALMEIDA-SOUZA, L., VAN GINDERACHTER, J. A., TIMMERMAN, V. & JANSSENS, S. 2012. Acute injury in the peripheral nervous system triggers an alternative macrophage response. *J Neuroinflammation,* 9**,** 176.

YEVICK, H. G., DUCLOS, G., BONNET, I. & SILBERZAN, P. 2015. Architecture and migration of an epithelium on a cylindrical wire. *Proc Natl Acad Sci U S A,* 112**,** 5944-9.

YONA, S., KIM, K.-W., WOLF, Y., MILDNER, A., VAROL, D., BREKER, M., STRAUSS-AYALI, D., VIUKOV, S., GUILLIAMS, M., MISHARIN, A., HUME, DAVID A., PERLMAN, H., MALISSEN, B., ZELZER, E. & JUNG, S. 2013. Fate Mapping Reveals Origins and Dynamics of Monocytes and Tissue Macrophages under Homeostasis. *Immunity,* 38**,** 79-91.

ZHAN, C., MA, C.-B., YUAN, H.-M., CAO, B.-Y. & ZHU, J.-J. 2015. Macrophage-derived microvesicles promote proliferation and migration of Schwann cell on peripheral nerve repair. *Biochemical and Biophysical Research Communications*.

ZHANG, H., LI, Y., DE CARVALHO-BARBOSA, M., KAVELAARS, A., HEIJNEN, C. J., ALBRECHT, P. J. & DOUGHERTY, P. M. 2016. Dorsal Root Ganglion Infiltration by Macrophages Contributes to Paclitaxel Chemotherapy-Induced Peripheral Neuropathy. *The Journal of Pain,* 17**,** 775-786.

ZHAO, C.-M., HAYAKAWA, Y., KODAMA, Y., MUTHUPALANI, S., WESTPHALEN, C. B., ANDERSEN, G. T., FLATBERG, A., JOHANNESSEN, H., FRIEDMAN, R. A., RENZ, B. W., SANDVIK, A. K., BEISVAG, V., TOMITA, H., HARA, A., QUANTE, M., LI, Z., GERSHON, M. D., KANEKO, K., FOX, J. G., WANG, T. C. & CHEN, D. 2014. Denervation suppresses gastric tumorigenesis. *Science translational medicine,* 6**,** 250ra115-250ra115.

ZICHA, D., DUNN, G. A. & BROWN, A. F. 1991. A new direct-viewing chemotaxis chamber. *Journal of Cell Science,* 99**,** 769.

ZIGMOND, E., SAMIA-GRINBERG, S., PASMANIK-CHOR, M., BRAZOWSKI, E., SHIBOLET, O., HALPERN, Z. & VAROL, C. 2014. Infiltrating Monocyte-Derived Macrophages and Resident Kupffer Cells Display Different Ontogeny and Functions in Acute Liver Injury. *The Journal of Immunology,* 193**,** 344.

ZOCHODNE, D. W. 2012. The challenges and beauty of peripheral nerve regrowth. *Journal of the Peripheral Nervous System,* 17**,** 1-18.